

Topological Aspects of Linear Dynamic Networks: Identifiability and Identification

Citation for published version (APA):

Shi, S. (2021). *Topological Aspects of Linear Dynamic Networks: Identifiability and Identification*. [Phd Thesis 1 (Research TU/e / Graduation TU/e), Electrical Engineering]. Eindhoven University of Technology.

Document status and date:

Published: 01/09/2021

Document Version:

Publisher's PDF, also known as Version of Record (includes final page, issue and volume numbers)

Please check the document version of this publication:

- A submitted manuscript is the version of the article upon submission and before peer-review. There can be important differences between the submitted version and the official published version of record. People interested in the research are advised to contact the author for the final version of the publication, or visit the DOI to the publisher's website.
- The final author version and the galley proof are versions of the publication after peer review.
- The final published version features the final layout of the paper including the volume, issue and page numbers.

[Link to publication](#)

General rights

Copyright and moral rights for the publications made accessible in the public portal are retained by the authors and/or other copyright owners and it is a condition of accessing publications that users recognise and abide by the legal requirements associated with these rights.

- Users may download and print one copy of any publication from the public portal for the purpose of private study or research.
- You may not further distribute the material or use it for any profit-making activity or commercial gain
- You may freely distribute the URL identifying the publication in the public portal.

If the publication is distributed under the terms of Article 25fa of the Dutch Copyright Act, indicated by the "Taverne" license above, please follow below link for the End User Agreement:

www.tue.nl/taverne

Take down policy

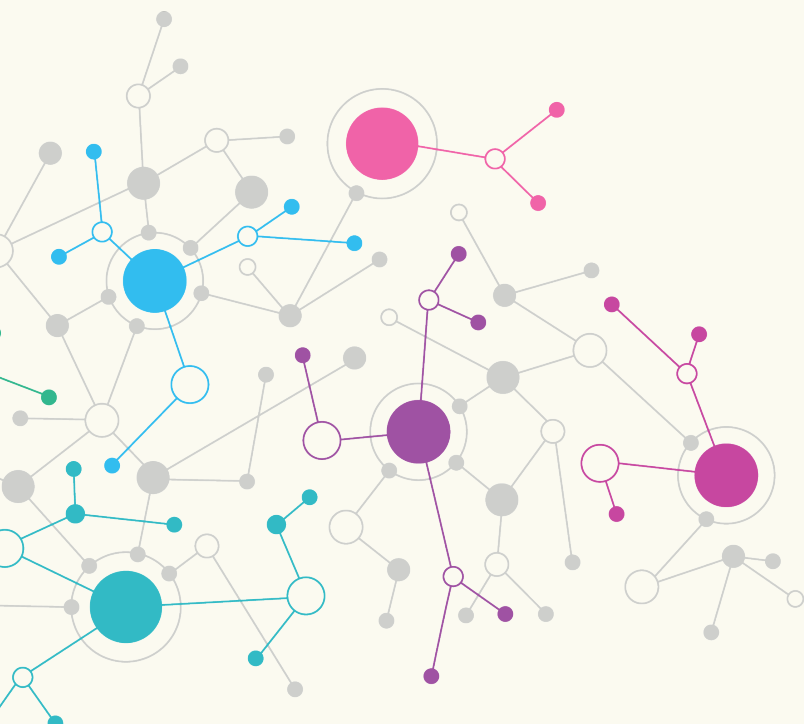
If you believe that this document breaches copyright please contact us at:

openaccess@tue.nl

providing details and we will investigate your claim.

TOPOLOGICAL ASPECTS OF LINEAR DYNAMIC NETWORKS: IDENTIFIABILITY AND IDENTIFICATION

Shengling Shi



Topological Aspects of Linear Dynamic Networks: Identifiability and Identification

PROEFSCHRIFT

ter verkrijging van de graad van doctor aan de Technische Universiteit
Eindhoven, op gezag van de rector magnificus prof.dr.ir. F.P.T. Baaijens,
voor een commissie aangewezen door het College voor Promoties, in het
openbaar te verdedigen op woensdag 1 september 2021 om 16:00 uur

door

Shengling Shi

geboren te Sichuan, China

Dit proefschrift is goedgekeurd door de promotoren en de samenstelling van de promotiecommissie is als volgt:

voorzitter: Prof. dr. ir. A. B. Smolders
promotor: Prof. dr. ir. P. M. J. Van den Hof
copromotor: Dr. X. Cheng (University of Cambridge)
leden: Prof. dr. ir. A. de Vries
Prof. dr. B. Wahlberg (KTH Royal Institute of Technology)
Prof. dr. J. Hendrickx (UC Louvain,
Ecole Polytechnique de Louvain)
Prof. dr. A.S. Bazanella (Federal University of
Rio Grande do Sul)
Prof. dr. ir. J.M.A. Scherpen (Rijksuniversiteit Groningen)

Het onderzoek of ontwerp dat in dit proefschrift wordt beschreven is uitgevoerd in overeenstemming met de TU/e Gedragscode Wetenschapsbeoefening.

Topological Aspects of Linear Dynamic Networks: Identifiability and Identification

Shengling Shi



This project has received funding from the European Research Council (ERC), Advanced Research Grant SYSDYNET, under the European Union's Horizon 2020 research and innovation programme (Grant Agreement No. 694504).



The research reported in this thesis is part of the research program of the Dutch Institute of Systems and Control (DISC). The author has successfully completed the educational program of the Graduate School DISC.

Topological Aspects of Linear Dynamic Networks: Identifiability and Identification
by Shengling Shi
Eindhoven, Technische Universiteit Eindhoven, 2021. Proefschrift.

A catalogue record is available from the Eindhoven University of Technology Library
ISBN: 978-90-386-5324-2

This thesis was prepared with the \LaTeX documentation system.

Cover design: Jiaen Wu, Shengling Shi

Reproduction: ADC Nederland, The Netherlands

Copyright © 2021 by Shengling Shi

Topological aspects of linear dynamic networks: Identifiability and identification

SUMMARY

Due to advances in current technology, many engineering systems are becoming increasingly complex and encompass numerous subsystems which are spatially interconnected and achieve sophisticated tasks via interaction. Such complex systems are typically referred to as dynamic networks, which appear in various applications such as multi-robot coordination, transportation networks, power grids, gene networks, and brain networks.

In the design, analysis, and control of dynamic networks, dynamic models are commonly used to describe their behavior. The existing network models typically consist of a mathematical expression and the corresponding graphical representation, which contains vertices and edges to encode the network topology. Considering a network as a representation of causal dependencies among manifest signals, the so-called module representation is a popular modeling framework for dynamic networks in the system identification domain. In this representation, vertices represent the internal signals, and directed edges denote transfer functions, also referred to as modules, that represent the causal relations among the internal signals. This thesis will adhere to the module framework and addresses a number of open problems in the data-driven modeling of complex dynamic networks, utilizing graph-theoretical analysis as a key enabling technique.

Identifiability is a fundamental property in network identification and deals with the question whether a network model can be uniquely identified from measured data. This uniqueness is desired, for example, when the physical interpretation of network models is important. In addition, a particular version of network identifiability, i.e. the so-called generic identifiability, is an important focus of this thesis, since it has been shown in the literature that the concept of generic identifiability allows for attractive graphical analysis based on the topological information of dynamic networks only. However, the existing graphical analysis also has several limitations. It does not consider noise information nor the possible appearance of prior known local components in the network, while these extra ingredients are of practical importance and can lead to less conservative identifiability conditions.

In this thesis, the existing graphical analysis is first extended to address the above limitations, in the special setting where all the internal signals in a network are measured. The obtained path-based conditions show that the generic identifiability of modules depends on the network topology and the location of the external signals, i.e. the measured excitation signals and the

unmeasured noises. Furthermore, while the obtained conditions are sufficient for generic identifiability in parametric model sets, they are shown to become necessary conditions when non-parametric model sets are considered. To address the necessity of the identifiability conditions for non-parametric model sets, a different notion of genericity is introduced such that the concept of generic identifiability is not limited to finite-dimensional spaces and thus can be applied to non-parametric model sets as well.

In the setting where all the internal signals are measured, the above path-based conditions show that the generic identifiability of network modules requires a sufficient number of external excitation signals. While the conditions provide efficient means to verify identifiability, they cannot be used to address the synthesis question, i.e. where to allocate additional excitation signals such that network modules become identifiable? This problem has only been considered in the literature for very particular network topologies. To address the synthesis problem in a general setting, novel graphical conditions are developed in this thesis based on the path-based condition, by exploiting the graphical concept of disconnecting sets and a novel graphical concept called pseudotrees. In these new conditions, the disconnecting sets and pseudotrees provide explicit information regarding where excitation signals should be allocated, which motivates several synthesis approaches that can allocate excitation signals to achieve generic identifiability automatically.

While the previous results are limited to the situation where all the internal signals in a network are measured, they are also extended in this thesis to the setting where not all internal signals are measured or excited, i.e. the so-called partial measurement and partial excitation setting. Novel graphical conditions for generic identifiability are developed, which show that generic identifiability depends on the network topology and the location of the external signals and the measured internal signals. The above information motivates several synthesis approaches for the allocation of additional actuators and sensors to achieve generic identifiability. In addition, the above identifiability results also lead to novel indirect identification methods that can estimate the local dynamics of the network consistently.

All the previous graphical results related to identifiability are based on a pre-specified network topology. This topological information may come from the prior knowledge or simply the modeling assumptions of the user. In many practical situations, it is desired to estimate this topological information from the data of dynamic networks. This topology identification problem itself is also important in various applications, such as in biological systems.

To address the topology identification problem, a novel Bayesian approach is developed in this thesis. In this approach, the subsystems of a network are modeled as Gaussian processes with hyperparameters, which are estimated by the expectation-maximization algorithm. Then a Bayesian model selection criterion and a forward-backward search algorithm are employed, such that a (local) optimal topology is selected. Numerical analysis shows the effectiveness of the method. The important advantage of this method is that it does not require any tuning

effort from the user.

While the above Bayesian approach estimates the network topology from a single data set, it is further extended to infer network typologies from multiple data sets. This extension is motivated by the practical situations where multiple data sets are collected from groups of subjects. More importantly, the developed method is applied to the inference of brain connectivity based on the fMRI data collected from 16 subjects, in order to reveal the topological changes in brain networks after extensively listening to Mozart's music. The above exploratory study shows the potential effects of Mozart's music on the cognitive processing of the subjects. It also demonstrates the effectiveness of the developed Bayesian approach.

With the above results on the topological analysis, synthesis for identifiability, and topology identification, there are still many challenges and open questions. In the setting with partial measurement and excitation, the synthesis problem for the generic identifiability of a full network still lacks a satisfactory solution. For the topology identification problem, how to quantify and control the errors of the topology estimate are also important open questions.

Contents

I	INTRODUCTION	1
1.1	Motivation	1
1.2	Network models	3
1.3	Identification of dynamic networks	11
1.4	Research problem	13
1.5	Formulation of sub-problems	17
1.6	Structure of thesis	19
2	PRELIMINARIES	23
2.1	Dynamic network model	23
2.2	Model set	25
2.3	Network identifiability	26
2.4	Graphical representation	29
2.5	Notations and definitions	33
2.6	Connections to other network models	34
2.7	Conclusions	38
3	IDENTIFIABILITY WITH FULL MEASUREMENT: ANALYSIS	39
3.1	Introduction	39
3.2	Existing concepts of generic identifiability and their limitations	41
3.3	Generic identifiability: revisit	44
3.4	Algebraic conditions	46
3.5	Path-based conditions	48
3.6	Conclusions	55
3.7	Appendix	56
4	IDENTIFIABILITY WITH FULL MEASUREMENT: SYNTHESIS	63
4.1	Introduction	63
4.2	Disconnecting-set-based conditions for subnetwork identifiability	64
4.3	Signal allocation for subnetwork identifiability	69

4.4	Disjoint Pseudotree Covering	74
4.5	Signal allocation for full network identifiability	78
4.6	Conclusions	83
4.7	Appendix	83
5	IDENTIFIABILITY WITH PARTIAL MEASUREMENT AND EXCITATION	89
5.1	Introduction	89
5.2	Problem formulation	91
5.3	Equivalent network for noise excitation	92
5.4	Necessary graphical conditions	95
5.5	Sufficient conditions: Both input and output measured or excited	96
5.6	Sufficient conditions: Measured input or output with indirect excitation	105
5.7	Actuator and sensor allocation for identifiability	107
5.8	Indirect identification methods	110
5.9	Conclusions	112
5.10	Appendix	112
6	BAYESIAN TOPOLOGY IDENTIFICATION	121
6.1	Introduction	121
6.2	Problem formulation	123
6.3	Bayesian model selection	124
6.4	Bayesian topology identification	125
6.5	Kernel-based group Lasso	132
6.6	Numerical results	132
6.7	Conclusions	135
6.8	Appendix	136
7	TOPOLOGY IDENTIFICATION OF BRAIN NETWORKS FOR DETECTING THE MOZART EFFECT	139
7.1	Introduction	139
7.2	Theory	142
7.3	Materials	144
7.4	Methods	149
7.5	Results	155
7.6	Discussion	161
7.7	Conclusions	163
7.8	Appendix	164
8	CONCLUSIONS AND FUTURE WORK	165

8.1	Conclusions	165
8.2	Future work	167
	REFERENCES	180
	LIST OF SYMBOLS	181
	LIST OF ABBREVIATIONS	183
	ACKNOWLEDGEMENTS	185
	CURRICULUM VITAE	186

TO MY PARENTS:

致我的父母

JUN SHI AND WEI QU

史君 和 屈伟

AND TO MY FAMILY:

和我的家人

QUANQI QU AND MINCHENG REN

屈全琦 和 任敏成

XUEMING SHI AND XIURU YAN

史学明 和 晏秀儒

JIAEN WU

吴佳恩

竹杖芒鞋轻胜马，谁怕？一蓑烟雨任平生。

苏轼（宋）

*Better than saddled horse I like sandals and cane. Oh, I would fain.
Spend a straw-cloaked life in mist and rain.*

Shi Su (Song dynasty); Translated by Yuanchong Xu

1

Introduction

I.I MOTIVATION

The scientific field of system identification concerns data-driven modeling problems of dynamic systems [90]. Since in many situations constructing models from first principles only is costly or even infeasible, the measured data collected during the operation of the system can be exploited to aid the modeling procedure. Data-driven methods can be helpful for estimating unknown parameters of the obtained physical models, i.e. grey-box identification, or models can be completely obtained from data possibly without physical interpretation, i.e. black-box identification. Then the obtained models can be used for analysis, design, and control of the considered engineering systems. The tools developed in the system identification community have been used for various applications, such as aerospace [73], vehicles [6], motion systems [111], biological networks [1], process control [184], and power grids [183].

The classical methods in system identification concern relatively simple configurations such as open-loop and closed-loop multivariate systems [90]. However, current engineering systems have increasing complexities and typically consist of a large number of subsystems that interact with each other to achieve sophisticated tasks. These so-called networked systems, or dynamic networks, appear in many domains and require developments of new data-driven modeling tools to cope with the system complexities.

Intelligent Transportation Systems (ITSs) for road transportation form representative examples of networked systems [5, 51]. Based on the advances in communication networks and computing, ITSs gather data and provide services to many entities involved in transportation, which promotes vehicle-to-vehicle and vehicle-to-infrastructure communications. In this case, a transportation network is established where vehicles and infrastructure are connected together and make decisions cooperatively. Enormous data can be collected from transportation networks, which leads to many new problems that rely on data-driven techniques, such as traffic flow prediction [146], identification of subsystems and the network [84], and the estimation of missing data from the network [9].

The power grids also form a complex network. Clean energy sources such as wind and solar energy, new loads including electric vehicles, and distributed energy storage such as batteries and ice storage are added into the power grid. These new sources and loads provide a more sustainable energy supply, but they also increase the complexity of the power grid and cause voltage fluctuations that influence system operations. Therefore, it is important to develop new technologies for control, optimization, and monitoring of the power grid to achieve sustainable energy supply, i.e. creating the so-called autonomous energy grid (AEG) [79]. AEGs rely on the decomposition of the complex power network into scalable small blocks which can form independent microgrids when isolated from the whole grid. When these blocks are interconnected, they should achieve optimal operations via information sharing and cooperation. To achieve AEGs, it is important to take advantage of the data obtained from the operation of AEGs. These data-driven techniques concern, for example, the identification of unknown parameters and network topology [8], and fault detection [22].

There are also many other networked systems that face challenging data-driven modeling problems, e.g. the topology identification of gene networks and brain networks [54, 92], and the data-driven modeling of social networks [144].

The above networked systems and the associated data-driven modeling problems require developments of new techniques in the field of system identification to go beyond the classical simple configurations. Therefore, this thesis is devoted to the data-driven modeling problems of dynamic networks. These problems concern the estimation (of characteristics) of networked models from measured data. The obtained models can then be used for the analysis [54], design [86], and control [176] of networks. Since models play central roles in these problems, different types of models for dynamic networks will first be introduced and discussed. Then a particular model type will be motivated, and the related data-driven modeling problems will be introduced.

I.2 NETWORK MODELS

I.2.1 INTRODUCTION

Analysis, monitoring, and control of dynamic networks require the knowledge of how the systems behave, and this knowledge is typically formulated into mathematical models which are inherently present in almost all fields of engineering and physics. While in the control community there are interests in the data-driven control without first obtaining a model [20, 71], the model-based control framework is still predominant.

Models for dynamic networks typically contain two components, including a graphical representation and a corresponding set of mathematical expressions. The graphical representation contains vertices that are connected by either directed or undirected edges, and the graph is used to encode the network topology, i.e. how the local entities are interconnected. Examples of network graphs can be found in Figure 1.1.

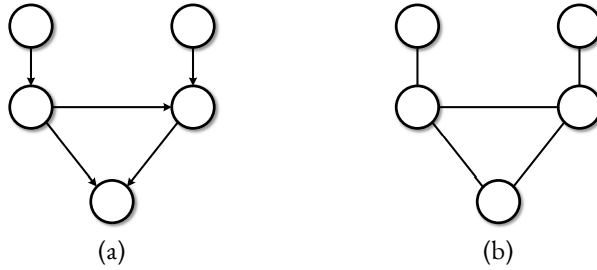


Figure 1.1: Examples of graphical representations for two dynamic networks with directed edges in (a) and undirected edges in (b).

Depending on the considered physical system and the modeling framework, the vertices and the edges in the network graphs can represent different objects, and the underlying mathematical models that describe the behavior of the network are also different. For example, a vertex in a graph can represent a time series, a random variable, or a local subsystem in different modeling frameworks. In this section, several different modeling frameworks of dynamic networks from various domains will be briefly discussed.

I.2.2 PROBABILISTIC GRAPHICAL MODELS

Probabilistic graphical models (PGMs) consist of a joint distribution and a graph, where the graph encodes the structure, typically the conditional independence and dependence, of the joint distribution [82]. One representative example of PGMs is the Bayesian network [78]. Particularly, the dynamic Bayesian network (DBN) is of interest due to its ability to model dynamic networks [104]. One example of a graph for a DBN can be found in Figure 1.2(a), where each

vertex denotes a random variable, e.g., $x(1)$ is the first time instance of the time series $x(t)$, and the edges denote the conditional dependence among the random variables.

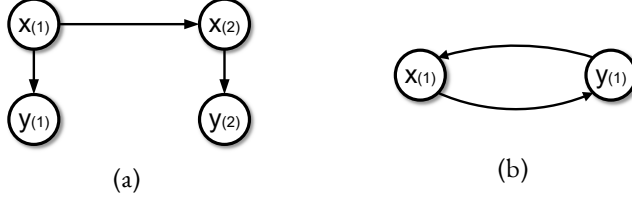


Figure 1.2: In (a), an example of a DBN is shown for two time instances of the time series $x(t)$ and $y(t)$. In (b), there is a cycle around $x(1)$ and $y(1)$.

Overall, the graph in Figure 1.2(a) represents the structure of a joint distribution of the four random variables, i.e. $\{x(1), x(2), y(1), y(2)\}$, and more importantly, the graph shows that the joint distribution has a structure of conditional independence such that

$$P(x(1), x(2), y(1), y(2)) = P(y(2)|x(2))P(x(2)|x(1))P(y(1)|x(1))P(x(1)),$$

where $P(x(2)|x(1))$ appears since only $x(1)$ has a directed edge to $x(2)$. The advantage of PGMs is that, by exploiting the graphical representation such as depicted in Figure 1.2, a complex joint distribution can be decomposed into a set of simpler conditional distributions.

In addition, graphs of Bayesian networks are typically defined to be acyclic [78], otherwise, the product of the conditional distributions represented by the graph does not lead to a joint distribution. Consider the example in Figure 1.2(b) which encodes two conditional distributions $P(y(1)|x(1))$ and $P(x(1)|y(1))$. It can be found that their product

$$P(y(1)|x(1))P(x(1)|y(1))$$

does not lead to the joint distribution of $x(1)$ and $y(1)$.

Since a PGM is essentially a joint distribution together with a graph that encodes the distribution's structure, it can be applied to a large number of real-world problems, as long as a joint distribution can serve the modeling purpose. Examples include visual tracking in the computer vision community, the navigation of robotics, speech recognition, and fault diagnosis of complex systems [78].

1.2.3 STRUCTURAL EQUATION MODELS

Structural equation models (SEMs) can also be used to model dynamic networks [113, 114]. An example of an SEM can be found in Figure 1.3, where the first two time instances of time series $x(t)$ and $y(t)$ are represented graphically, and $e(t)$ and $v(t)$ denote unmeasured noise processes. Therefore, each vertex still denotes a single time instance from a time series.

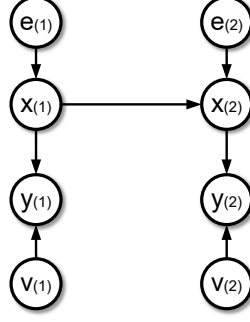


Figure 1.3: An example of SEM for time series $x(t)$ and $y(t)$ with noise processes $e(t)$ and $v(t)$.

The model corresponding to Figure 1.3 consists of four functions which describe the behavior of $x(1)$, $x(2)$, $y(1)$ and $y(2)$:

$$\begin{aligned} x(1) &= f_1(e(1)), \quad y(1) = f_2(x(1), v(1)), \\ x(2) &= f_3(x(1), e(2)), \quad y(2) = f_4(x(2), v(2)). \end{aligned} \tag{1.1}$$

It can be found that the directed edges in Figure 1.3 encode the functional dependencies among the variables, e.g., $y(2)$ is a function of $v(2)$ and $x(2)$ since there are directed edges from $v(2)$ and $x(2)$ to $y(2)$.

Compared to DBNs in a probabilistic setting, SEMs make use of functional dependencies. It can be shown that under some conditions, the SEM in Figure 1.3 can represent a joint distribution over $x(1)$, $x(2)$, $y(1)$ and $y(2)$, and the distribution satisfies the conditional independence among the four variables encoded by the graph [113, Theorem 1.4.1]. Therefore, the SEM induces a Bayesian network in this case.

1.2.4 VECTOR AUTOREGRESSIVE MODEL AND ITS VARIANTS

The vector autoregressive (VAR) model is one of the most common models for describing the evolution of the signals collected from dynamic networks [149]. Consider a vector of three time series $x(t) = [x_1(t) \ x_2(t) \ x_3(t)]^\top$, an example of a VAR model is

$$x(t) = \sum_{i=1}^n A_i x(t-i) + e(t), \tag{1.2}$$

where A_i is a matrix of real coefficients, n is a positive integer and denotes the number of time lags in the model, and $e(t)$ is a vector of uncorrelated noise processes. The above model is used to study how the present value of $x(t)$ depends on its past values, and a causal interpretation can be assigned to this model based on the so-called Granger causality, i.e. $x_3(t)$ is not caused by $x_1(t)$ if

$x_3(t)$ does not depend on the past values of $x_1(t)$ [50, 63]. In addition, a graphical representation of a VAR model can also be formulated, such as the one in Figure 1.4 [50], where each vertex denotes a time series in the vector $x(t)$, and the edges denote the dependencies among these time series. For example, there is no directed edge between x_1 and x_2 , which means that the $(1, 2)$ -th and $(2, 1)$ -th entries of A_i are zero in (1.2), for all i .

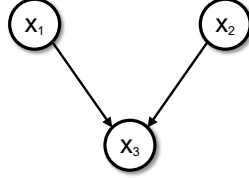


Figure 1.4: A graphical representation of a VAR model with three time series.

Compared to the graphical representations in Figures 1.2 and 1.3, a vertex in Figure 1.4 denotes a complete time series instead of one time instance of the time series. However, the above difference is simply caused by how the graphical representation is defined, and a graph like the one in Figure 1.3 can also be used to represent a VAR model. In addition, the close relationship between VAR models and SEMs can be observed by comparing (1.1) and (1.2).

The VAR model has several variants, e.g. the autoregressive moving-average model [149], and they have various applications such as in financial and economic time series analysis and biological networks [127].

1.2.5 MODULE NETWORKS

As an extension of the classical closed-loop setting in the system and control community, i.e. an interconnection of a plant and a controller in the feedback loop, networks of transfer functions, also referred to as *module networks*, have been introduced to model systems with increasing complexity [152]. This modeling framework is discussed here through a real-world example.

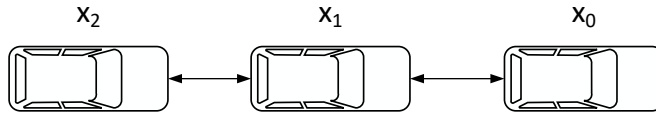


Figure 1.5: A platoon of three vehicles with x_i being the i -th vehicle's relative position. Vehicle 0 is leading the platoon and is controlled by a human driver, while the other vehicles autonomously follow its preceding vehicle with a safe distance.

In Figure 1.5, a platoon of three vehicles is shown, where vehicle 1 and vehicle 2 follow their preceding vehicles autonomously with a safe distance, while the leading vehicle is controlled by a human driver. To achieve the automatic following, each follower is equipped with sensors to measure the relative distance with respect to its preceding vehicle and then adjusts its acceleration

by using the onboard controller. The control architecture of the two followers, i.e. vehicles 1 and 2 in Figure 1.5, is shown in Figure 1.6 [107].

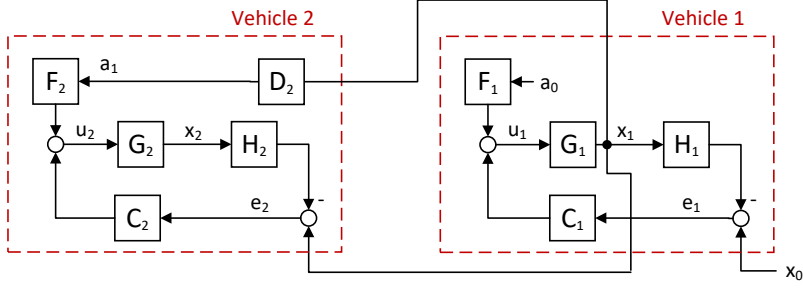


Figure 1.6: Control architecture of the two followers vehicles 1 and 2, where each block, e.g. G_1 , denotes a transfer function. The i -th vehicle receives the relative position x_{i-1} and (delayed) acceleration a_{i-1} of the preceding $(i - 1)$ -th vehicle from sensors or wireless connections. With the above information, the control input u_i is calculated by the feedforward controller F_i and the feedback controller C_i , and then u_i is applied to the vehicle dynamics G_i . H_i denotes the desired distance dynamics between two vehicles, and e_i represents the error between the current relative distance and the desired relative distance.

From the physical network in Figure 1.5 to its control architecture in Figure 1.6, a set of transfer functions is obtained and interconnected to model the evolution of the signals in the physical system. In order to model physical networks such as the vehicle platoon using transfer functions in a more compact way, a graph-based representation for networks of transfer functions is motivated [152].

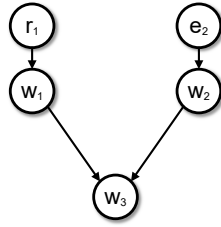


Figure 1.7: An example of a module network, where each edge denotes a transfer function and each vertex denotes a time series.

An example of a graph representation of a module network is shown in Figure 1.7, where each vertex denotes a time series, and each directed edge denotes a transfer function, also referred as to *modules*. $r_1(t)$ and $e_1(t)$ are the external reference and noise signals, respectively, while $w_i(t)$ is the so-called *internal signal* of a system. The mathematical expression corresponding to Figure 1.7 consists of three equations which model the evolution of the three internal signals:

$$w_1(t) = R_1(q)r_1(t), \quad w_2(t) = H_2(q)e_2(t), \quad w_3(t) = G_{31}(q)w_1(t) + G_{32}(q)w_2(t),$$

where $G(q)$, $R(q)$ and $H(q)$ denote the transfer operators represented by the directed edges, and q is the delay operator, i.e. $q^{-1}r(t) = r(t - 1)$. The graph in Figure 1.7 encodes the structure

of the model, e.g., $w_1(t)$ does not depend on $w_2(t)$ in the above equations because there is no directed edge from w_2 to w_1 . From the diagram in Figure 1.6 to the graph representation in Fig-

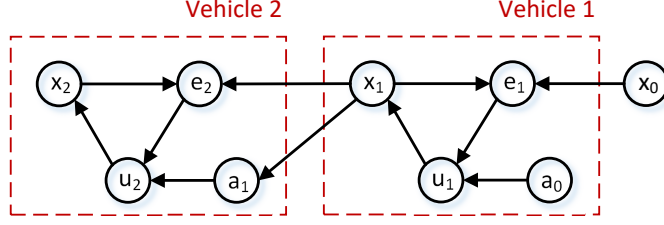


Figure 1.8: A module network representation of the control architecture in Figure 1.6.

ure 1.7, the main goal is to use a simpler and more compact graphical language to describe the structure of module networks. Figure 1.6 can be easily reformulated into a graphical representation, as shown in Figure 1.8.

1.2.6 STATE-SPACE NETWORK MODELS

A state-space network model is typically used to describe the behavior of large-scale physical systems using a set of first-order differential equations, see e.g., [29, 35, 100] for an overview. An example of a state-space model for an electric circuit is shown in Figure 1.9(a) from [100], where the capacitors and the resistors have 1 F and 1 Ω , respectively. Then according to Kirchhoff's

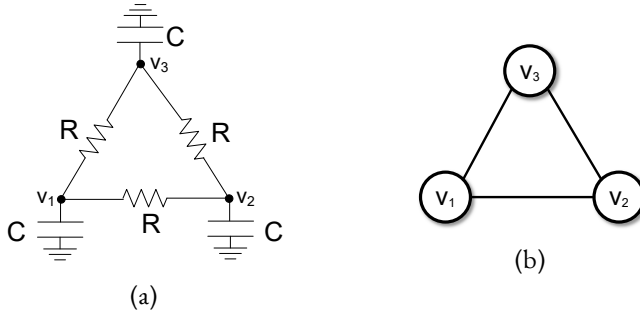


Figure 1.9: An electrical circuit in (a) with v_i denoting the voltage and its graphical representation in (b).

current law, the voltage dynamics is given as

$$\begin{bmatrix} \dot{v}_1(t) \\ \dot{v}_2(t) \\ \dot{v}_3(t) \end{bmatrix} = -L \begin{bmatrix} v_1(t) \\ v_2(t) \\ v_3(t) \end{bmatrix}, \text{ with } L = \begin{bmatrix} 2 & -1 & -1 \\ -1 & 2 & -1 \\ -1 & -1 & 2 \end{bmatrix}, \quad (1.3)$$

where the continuous-time dynamics is considered. This is a typical deterministic single-integrator network where the matrix L is the so-called Laplacian matrix representing diffusive couplings

among the state variables [100]. The nonzero pattern of L is reflected in a graph in Figure 1.9(b), where each vertex denotes a voltage value, and an undirected edge exists when there is a resistor connecting the two points. It is shown that the system (1.3) reaches consensus i.e. $\lim_{t \rightarrow \infty} (v_i(t) - v_j(t)) = 0$, for any initial conditions [85, 126].

In a more general setting, each vertex in a network represents a second-order or higher-order state-space subsystem, see e.g., [33, 34, 128, 159, 182]. This type of state-space network model has been extensively studied in the system and control community [25, 100]. Particularly, this modeling framework based on state-space models is also widely considered in the control and identification literature, see e.g., [45, 105, 153, 158, 159, 178].

1.2.7 NETWORKS OF DIFFERENTIAL EQUATIONS

Instead of resorting to first-order differential equations, there are modeling frameworks of networked systems, or interconnected systems, using possibly high-order differential equations. We discuss one example called the behavioral model here [18, 174].

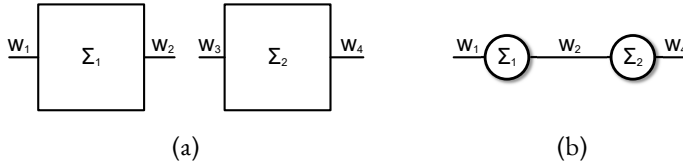


Figure 1.10: Two dynamic systems Σ_1 and Σ_2 in (a), where each of them has two ports representing two signals of the systems. They are interconnected by the constraint that $w_2 = w_3$ in (b) and then represented by a graph.

Consider two linear time invariant systems Σ_1 and Σ_2 in Figure 1.10(a), where $w_1(t)$ and $w_2(t)$ denote two trajectories that model the dynamical behavior of Σ_1 , and Σ_2 has trajectories $w_3(t)$ and $w_4(t)$. Σ_1 is modeled by a differential equation

$$A_0 \begin{bmatrix} w_1(t) \\ w_2(t) \end{bmatrix} + A_1 \frac{d}{dt} \begin{bmatrix} w_1(t) \\ w_2(t) \end{bmatrix} + \cdots + A_n \frac{d^n}{dt^n} \begin{bmatrix} w_1(t) \\ w_2(t) \end{bmatrix} = 0,$$

which can be reformulated into a compact form as

$$\begin{bmatrix} R_1(\frac{d}{dt}) & R_2(\frac{d}{dt}) \end{bmatrix} \begin{bmatrix} w_1(t) \\ w_2(t) \end{bmatrix} = 0, \quad (1.4)$$

where $R_i(\frac{d}{dt})$ is a matrix of differential operators. Similarly, Σ_2 is modeled as

$$\begin{bmatrix} Q_1(\frac{d}{dt}) & Q_2(\frac{d}{dt}) \end{bmatrix} \begin{bmatrix} w_3(t) \\ w_4(t) \end{bmatrix} = 0. \quad (1.5)$$

The goal is then to model the networked system consisting of Σ_1 and Σ_2 , where the two

subsystems are interconnected physically such that their trajectories must satisfy the following constraint:

$$w_2(t) = w_3(t).$$

Combining the above constraint and the two models (1.4), (1.5), the obtained network model can be written as

$$\begin{bmatrix} R_1(\frac{d}{dt}) & R_2(\frac{d}{dt}) & 0 \\ 0 & Q_1(\frac{d}{dt}) & Q_2(\frac{d}{dt}) \end{bmatrix} \begin{bmatrix} w_1(t) \\ w_2(t) \\ w_4(t) \end{bmatrix} = 0,$$

where $w_3(t)$ is eliminated due to the equality constraint. The corresponding graphical representation is shown in Figure 1.10(b).

In the above modeling framework, each subsystem can be modeled separately and then interconnected to form a network. The interconnection among subsystems can be simply done by concatenating the models of subsystems. This procedure of first obtaining local models and then interconnecting them is much more appealing than directly modeling the complete network.

1.2.8 SUMMARY OF NETWORK MODELS

Several model frameworks for modeling dynamic networks have been introduced in this section. The PGMs, SEMs, and VAR models are typically used for data-driven modeling problems, where mappings among the measured signals are of interest and need to be estimated. These models may not have physical interpretation and are commonly used to predict the future trajectories of the considered system. PGMs and SEMs are common model classes in statistics, machine learning, and computer science communities. While they have variants like DBNs to model the dynamic behavior of physical systems, they are typically used to model static phenomena that are not dependent on time. VAR models are popular models for multivariate analysis in statistics and time series analysis, and they can be used for forecasting or analyzing the causal relation among time series [127].

Network models based on state-space models or differential equations are typically motivated by modeling based on physical principles. In addition, it is well known that high-order differential equations can be reformulated into first-order state-space models by introducing extra latent state variables. Therefore, the network topology of state-space networks can express different information from the topology of data-driven models, e.g., the VAR models: While the VAR models represent the interconnection of the measured signals, the state-space networks represent the interconnection between both the measured signals and the extra latent state variables.

Module networks are in a middle ground between the above data-driven models and the models motivated by physics [76]. Transfer functions are used intensively in signal processing, and many techniques for estimating transfer functions originated from time series analysis [57]. From a data-driven perspective, it is also a natural modeling choice to use transfer functions to

encode the causal relationships among the measured signals.

On the other hand, it is well known in the system and control community that there is a close relationship between transfer functions and state-space models. A high-order differential equation can also be reformulated into a transfer function through Laplace transformation. More importantly, many classical control techniques are also based on transfer functions. While these techniques typically consider relatively simple configurations such as the open-loop and the closed-loop settings, transfer function networks go beyond the above settings and incorporate more complex interconnection structures.

In this thesis, we are interested in identifying models that have a physical interpretation. In addition, since the state variables are typically only partially measured, the state-space networks cannot be uniquely identified in this case. Therefore, we will focus on module networks that represent the interconnection among the measured signals. In addition, we will also consider the general situations where there are unmeasured signals in module networks, such that the module networks can cover the state-space networks as special cases. In addition, linear dynamic networks are considered in this thesis, since the understanding of linear networks serves as the basis for the study of more complex nonlinear dynamic networks. From now on, the notion of dynamic networks in this thesis will particularly refer to module networks.

I.3 IDENTIFICATION OF DYNAMIC NETWORKS

Data-driven modeling problems of module networks concern the identification of characteristics of module networks, given the measured node signals, e.g., the measured $r(t)$, $w_1(t)$, $w_2(t)$ and $w_3(t)$ in Figure 1.7. Various data-driven modeling problems of dynamic networks can be formulated. We discuss these problems and the related literature in this section. The literature related to the identification of state-space networks will also be briefly discussed, due to the important role of state-space models in the system and control community.

I.3.1 TOPOLOGY IDENTIFICATION

The topology identification problem aims to estimate the graph topology of dynamic networks, e.g. the interconnection structure of Figure 1.7. This is an important problem in various applications, e.g. systems biology [68, 92] and social science [181], where the topology is an important feature to understand the collective behavior of a dynamic network.

The topology identification problem can be formulated as a parameter estimation problem. To reveal the topology, the sparsity of the parameter estimates needs to be enforced such that some of the obtained parameters are zero, which reflects the absence of the corresponding edges in the dynamic network. The literature which approaches the problem from the above perspective includes, e.g., [27, 41, 81, 160, 179].

A different way to identify the topology is to conduct a sequence of correlation, or cross-spectrum, tests [95, 96, 137]. The correlation structure among the signals can also reveal the underlying network topology. However, this approach typically cannot recover a unique topology, since there can be a set of equivalent graphs that are not distinguishable by the tests [95, 96].

The topology identification problem also leads to many theoretical challenges for the statistical methods. For example, in topology identification of biological networks, there is typically a limited amount of data compared to the number of unknown parameters, as the data collection is very expensive in these applications, and the network can also be large-scale. The situations like the above one trigger the study of high-dimensional statistics [99, 162], where the finite-sample analysis receives considerable interests to provide error bounds on any data length. This is in contrast to the classical asymptotic analysis considered in the parametric system identification, where the parameter dimension is fixed when the data length approaches infinity [90]. Motivated by the results in the high-dimensional statistics, there are recent works that extend the classical asymptotic results in the system identification community to the finite-sample setting [150].

1.3.2 SINGLE MODULE IDENTIFICATION

Identification of a single module is the problem of estimating a single transfer function in a dynamic network. This is motivated by the situations where a local part of the dynamic network is of interest and needs to be estimated.

One way to approach this identification problem is to identify a multiple-input-single-output (MISO) or a single-input-multiple-output model (SIMO) that contains the target module [59, 121, 152]. More interestingly, the freedom of signal selection can be exploited to identify a single module. While the approach based on the MISO model makes use of all the inputs of the MISO model, it is possible to choose other sets of signals. This extra freedom is important, e.g., when some signals in the network cannot be measured. The approaches that exploit the above freedom include, for example, the ones in [47, 88, 97, 98, 123, 168]. In addition, to reduce the experimental cost for single module identification, the design of the optimal power spectrum of the excitation signals has been considered in [103]. There are also works that consider identifying a single subsystem in a network of state-space models [177, 178].

1.3.3 IDENTIFICATION OF FULL NETWORK DYNAMICS

Identification of the whole dynamic network is a challenging problem as the network can be large-scale. There are some approaches that address this problem by assuming a pre-specified topology [53, 170]. In addition, identification approaches without pre-specified topology have also been developed, e.g. in [27, 41, 67]. In some approaches, network dynamics and its topology are identified jointly, where parameters are estimated to reflect the dynamics, and the parameters

that are equal to zero encode the topology [41]. The identification of a full state-space network has also been addressed in [66, 159].

I.3.4 IDENTIFIABILITY OF DYNAMIC NETWORKS

By contrast to the previous identification methods, the identifiability question is a theoretical problem that concerns whether the stochastic properties, typically the mean and the power spectral density, of the measured signals can be uniquely represented by a network model. If it is not unique, any identification method that relies on these stochastic properties cannot lead to a unique estimate for the dynamic network. This uniqueness is important, e.g., when the network has a physical interpretation. Network identifiability is typically dependent on several structural properties of the module network, such as the network topology, the modeled correlation structure of process noises, the presence and location of external excitation signals, and the availability of measured vertex signals.

Based on the deterministic network reconstruction problems in [3, 62], a novel concept of network identifiability is introduced in an identification setting in [167, 169]. The conditions derived there are rank-based and need to be evaluated for all the models in a model set, which can be hard to be implemented in practice. Then graphical conditions are investigated in [69], and additionally, by exploiting a new concept called generic identifiability, novel path-based conditions are developed in [13, 14, 69] for the identifiability analysis. These conditions are graph-based and can be tested efficiently by inspecting the network topology only. However, the limitation is that the graphical analysis requires a pre-specified network topology, while this topological information may not be available.

Another important issue is where to allocate actuators and sensors such that network modules become identifiable. This experimental design problem has been considered in [13, 59]. The results in [59] concern both identifiability and identification of a single transfer function in a network, and the results in [13] consider the experimental design issue for full networks with special structures, e.g. trees or loops.

I.4 RESEARCH PROBLEM

I.4.1 OPEN QUESTIONS

We have seen many examples of networked systems and different modeling frameworks that can be used to model networked systems. Motivated by the data-driven modeling problems in the system and control community, module networks have been chosen to be the main focus of this thesis. The data-driven modeling problems and the literature related to module networks have also been discussed. However, besides the problems that have been addressed by the literature, there are still many open questions in the data-driven modeling of module networks.

IDENTIFICATION OF PHYSICAL NETWORKS

In most literature related to the identification of dynamic networks, the starting point is the transfer function network, based on which a data-driven modeling problem is formulated. However, if the goal is to identify a physical network, the starting point should be a model structure that is obtained from physical laws and typically consists of differential equations. Then a possible way to identify this physical model is to reformulate it into a module network, and then apply the identification methods to the obtained module networks[76]. However, this reformulation typically leads to module networks with special structures and constraints.

As shown in [76], in the module networks obtained from one particular class of physical models, every pair of node signals has a bidirectional connection that represents two transfer functions. More importantly, these two transfer functions are constrained to have the same numerator. The study of modeling such networks, including devising an efficient algorithm to estimate modules subject to the above physical constraint, is still in a relatively rudimentary stage. Moreover, it is also not completely clear how the module network framework is connected with other types of physical networks, e.g. the one in Figure 1.10, and how the undirected connection nature of physical networks can be incorporated into the module network framework with a directed topology in e.g. Figure 1.7.

Another important issue is to identify physical networks with nonlinear dynamics. Almost all of the available results in the literature are based on the assumption that the modules in a network are linear operators. While a preliminary effort has been made in [133] to identify the location of the nonlinear subsystem in a module network, the identification of a single module or a full physical network with nonlinearity is still an open question.

IDENTIFICATION WITH UNMEASURED SIGNALS

The single module identification problem with unmeasured node signals, e.g., unmeasured $w_1(t)$ in Figure 1.7, has been addressed in various literature [47, 88, 97, 98, 123, 168]. The solutions typically rely on exploiting the freedom of signal selection such that only measured signals are used for the identification procedure, or to provide an indication on which signal to measure.

However, the full network identification and the topology identification problems with unmeasured signals have not received much attention. An algorithm has been developed in [185] to obtain a sparse approximation of a network with unmeasured signals. However, many fundamental questions remain open. For example, when there are unmeasured signals, under what conditions can the dynamics or the topology of a full network be identified?

IDENTIFICATION WITH MULTIPLE EXPERIMENTS

In some practical situations, there can be data sets collected from different experiments on the same physical network [65]. It can be beneficial to take advantage of all the available data for

identifying the network topology or dynamics. This identification problem with multiple data sets is considered in [180], however, in a simple setting where the network topology stays invariant over different experiments. Many important issues require further investigation. For instance, a physical network under different experiments may need to be represented by module networks with different network topologies. How to combine the different module networks to obtain an estimate of the underlying physical network is still waiting for a satisfactory solution.

ADVANCED TOPOLOGY IDENTIFICATION

Despite the existing approaches for topology identification, there are many advanced aspects of the topology identification problem that have not been addressed in the literature. The methods in the topology identification literature typically require certain tuning parameters to decide the sparsity pattern of the topology estimate, e.g., the threshold value or the regularization parameter [95, 96, 137, 137, 160]. These tuning parameters are critical for the approaches to achieve a good performance. However, in many cases it is not clear how to choose these parameters in an optimal way, and thus they are commonly chosen in an ad hoc manner. In addition, the above-mentioned methods do not take into account available prior knowledge of dynamic networks, e.g., the stability of the modules as exploited in the kernel-based system identification methods [117]. While there is one Bayesian approach that can incorporate this prior knowledge [41], the resulting approach is rather complex and consists of multiple stages as it aims for joint estimation of both the dynamics and the network topology. Therefore, it is attractive to develop topology identification approaches that do not require any tuning effort from the user as well as incorporate the available prior knowledge.

TOPOLOGICAL ANALYSIS AND SYNTHESIS FOR IDENTIFIABILITY

The existing identifiability literature has addressed the analysis question for identifiability, i.e. under what conditions is a transfer function network identifiable [13, 14, 69, 83, 157, 169, 171]? With a concept of generic identifiability, attractive path-based conditions are developed in [14, 69] such that identifiability can be verified by only inspecting the network topology. These conditions show that generic identifiability can be achieved if there are sufficient measured node signals and measured external excitation signals. However, the original notion of generic identifiability in [14, 69] does not consider noise information nor the possible appearance of prior known local components in the network, while the above information may make the identifiability conditions significantly less conservative. In addition, the classical identifiability concept [90] is typically formulated as a property of a model set such that the models in the model set, which is later used for an identification procedure, can be distinguished. However, the above consideration of model sets is not incorporated into the notion of generic identifiability introduced in [14, 69], since this notion is formulated on the basis of a single network model and its

network topology. Preliminary efforts to address the above limitations are made in [171] to formulate a generic identifiability concept on the basis of model sets; however, the other issues have not been addressed. Therefore, there is a need for further investigation in the graphical analysis for identifiability.

Moreover, while the results in the above literature focus on the verification of identifiability, there is no comprehensive approach for the synthesis problem, i.e. what actions can the user take to achieve identifiability when a network model is not identifiable? Some preliminary aspects of the above synthesis problem have been addressed in [13, 59], which show that identifiability can be achieved by allocating additional actuators and sensors. However, the experimental setup in [59] for identifying a single module is relatively simple, where all the inputs of the module's output need to be measured and excited. On the other hand, the synthesis problem for identifiability of a full network is addressed in [13], and it is shown that the required graphical tools for this problem are very different from the tools in [59] for identifiability synthesis of a single module. However, the results in [13] are limited to networks with special network topology, e.g. trees. Therefore, the synthesis problems for both local modules and a full network in more general situations need to be investigated. In addition, besides allocating sensors and actuators, other actions may also be taken to achieve identifiability, e.g. modifying the network topology by removing and adding edges, or combining data from multiple experiments.

1.4.2 PROBLEM FORMULATION

As discussed in the previous subsection, there are various open problems in the data-driven modeling of transfer function networks. It is intractable to address all these problems in this thesis, and thus essential problems are selected to formulate the main question of this thesis.

Identifiability is one fundamental problem and serves as a pre-requirement for the identification methods. Before applying an identification method, it is important to first analyze identifiability to ensure that different network models are distinguishable by the identification method. Due to its fundamental importance, the topological analysis and synthesis for identifiability are chosen to be two of the core research topics in this thesis.

Furthermore, topology identification is an important problem in various applications. It also has a close relation with the identifiability study, as the graphical results of identifiability are based on pre-specified network topology. This topological information may not be available for the user, and thus one way to obtain it is to identify the topology from data. Therefore, this thesis will also address some advanced aspects of the topology identification problem.

The above choices of problems lead to the main research question of this thesis.

How to exploit the topological information of dynamic networks for achieving identifiability and how to identify this topological information from data?

The above topology identification problem and identifiability problem are interdependent. In topology identification, a model set associated with a complete graph, where every pair of signals is interconnected, should be used for the estimation, as there is no prior information about the topology. This complete graph leads to a large number of to-be-estimated parameters, which may make the network topology not identifiable. On the other hand, the graphical analysis of identifiability requires the specification of the topology. Therefore, when there are no other means to specify the topology for the identifiability study, an iterative procedure of topology identification and topological identifiability analysis may be required in practice.

1.5 FORMULATION OF SUB-PROBLEMS

The main research question can be further analyzed and decomposed into a set of sub-questions, as shown in the following subsections.

1.5.1 SUB-QUESTION 1

There are two important aspects of the identifiability study, i.e. the topological analysis and the synthesis for identifiability. The topological analysis aspect concerns the development of graphical conditions on the network topology to verify identifiability for a given module network. If the module network is not identifiable, the synthesis aspect concerns the development of tools that can achieve network identifiability, e.g., by allocating additional actuators and sensors. In addition, graphical tools for the identifiability analysis are instrumental for the development of synthesis tools.

Therefore, the first sub-question concerns the topological analysis for network identifiability.

Under what conditions on the network topology are modules in a linear dynamic network identifiable?

In this sub-question, the network topology depends on the interconnection of the internal (node) signals and also on the location and the appearance of actuators and sensors. Following the preliminary efforts in [171], the particular focus of this sub-question is to extend the existing concept of generic identifiability and the related graphical conditions for identifiability in [14, 69] to incorporate the concepts of model sets, the prior known local components, and the noise information.

In large-scale networks, there can be prior knowledge about the local components of the module network, and thus it is important to take advantage of this knowledge in the identifiability analysis. Furthermore, noise information is also important in many applications, e.g., biological networks [54, 92], where there may be only observational data collected without the user-provided excitation signals. Since external excitation signals are required to achieve identifiabil-

ity, it is necessary in this case to exploit the noises as the excitation sources for the identifiability analysis.

1.5.2 SUB-QUESTION 2

With the fundamental graphical results from the solution to sub-question 1, synthesis approaches for identifiability will be further developed. Various actions may be taken to achieve identifiability. For example, the existing analysis results indicate that identifiability requires sufficient excitation signals and measured signals [169]. Therefore, additional actuators and sensors can be allocated to achieve identifiability. Another possibility is to modify the network topology, as the existing results show that identifiability can be guaranteed if the network topology satisfies certain conditions [13, 14, 69, 157]. However, it is not clear what the physical interpretation is when the topology of a module network is modified.

Therefore, this thesis will focus on synthesis procedures that achieve identifiability by allocating additional sensors and actuators. This leads to the second sub-question of this thesis.

Where to allocate actuators and sensors such that modules in a network are identifiable?

1.5.3 SUB-QUESTION 3

The previous sub-questions exploit the topological information to develop synthesis approaches for identifiability. In this sub-question, the topology identification problem will be addressed to identify the topological information from data.

In the existing topology identification methods, the methods based on correlation or cross-spectrum tests typically rely on an enormous amount of data to achieve accurate results [95, 96, 137]. However, when the network is large-scale, the data for topology identification is typically limited relative to the size of the network. On the other hand, other methods, which do not rely on those tests, do not address the advanced aspects in the topology identification problem, including how to choose the tuning parameters and the incorporation of available prior knowledge. Therefore, novel topology identification methods will be investigated to address the above issues.

How to identify the network topology without the need for tuning efforts while including the available prior knowledge?

In particular, we will focus on the topology identification problem from a Bayesian point of view in this thesis, due to the capability of the Bayesian framework to incorporate prior knowledge. The developed method will also be exploited to address a practical problem, where the goal is to infer the topological changes in brain networks caused by Mozart's music. This problem is

important for understanding the effect of music on human brains, a topic that is of interest in the neuroscience community, and the result also demonstrates the effectiveness of the developed topology identification method.

I.6 STRUCTURE OF THESIS

This thesis is organized as follows.

Chapter 2 - Preliminaries. In this chapter the dynamic network model and other important concepts, such as identifiability, are introduced formally.

Chapter 3 - Identifiability with full measurement: Analysis. The sub-question 1 is addressed in a special setting where all node signals in the network are measured. Based on the notions of generic identifiability [14, 69] and global identifiability [169], a new version of generic identifiability concept is formulated by incorporating the concept of model sets and a different notation of genericity based on the open and dense sets in a topological space. Then the existing path-based conditions in [14, 69] for generic identifiability are extended for the new generic identifiability concept. More importantly, the obtained path-based conditions incorporate additionally the prior known local modules and the noise information, compared to the original results in [14, 69].

The material of this chapter is based on the following papers:

- S.Shi, X. Cheng and P. M. J. Van den Hof. “Generic identifiability of subnetworks in a linear dynamic network: the full measurement case.” Submitted to *Automatica*, 2020.
- S.Shi, X. Cheng and P. M. J. Van den Hof. “On the genericity concept in identifiability of linear dynamic networks.” report, 2021.

Chapter 4 - Identifiability with full measurement: Synthesis. Sub-question 2 is considered in the setting where all node signals in networks are measured. Novel synthesis procedures to allocate excitation signals are developed to achieve generic identifiability of local modules, by exploiting the graphical conditions in Chapter 3 and the concept of disconnecting sets. Furthermore, the synthesis problem for a full network is also addressed by exploiting a novel graphical concept called pseudotrees, which leads to a novel synthesis approach to achieve the generic identifiability of a full network.

The material of this chapter is based on the following papers:

- S.Shi, X. Cheng and P. M. J. Van den Hof. “Excitation allocation for generic identifiability of a single module in dynamic networks: A graphic approach.” *The 21st IFAC World Congress*, 2020.

- X. Cheng, S. Shi and P. M. J. Van den Hof. “Allocation of Excitation Signals for Generic Identifiability of Dynamic Networks.” In *Proc. 58th IEEE Conf. Decis Control (CDC)*, 2019.
- X. Cheng, S. Shi and P. M. J. Van den Hof. “Allocation of Excitation Signals for Generic Identifiability of Linear Dynamic Networks.” *IEEE Trans. Autom. Control*, 67(2), 2022.

The author’s contribution: In the above list, the last two works were led by their first author. The author of this thesis assisted the first author and contributed to the development of both the theoretical and the algorithmic parts of the works. In addition, the author of this thesis led the development of an important algorithmic step, i.e. Lemma 5 of the last publication.

Chapter 5 - Identifiability with partial measurement and excitation. This chapter addresses Sub-questions 1 and 2 in a more general setting, where not all node signals are measured nor excited. Both the path-based conditions in Chapter 3 and the synthesis procedures for local modules in Chapter 4 are extended to the partial measurement and excitation setting. It is shown that disconnecting sets provide important information regarding which signals to be measured or excited such that modules in a network are identifiable. This information also leads to novel indirect identification methods for the consistent identification of local modules.

The material of this chapter is based on

- S. Shi, X. Cheng and P. M. J. Van den Hof. “Single module identifiability in linear dynamic networks with partial excitation and measurement.” Provisionally accepted by *IEEE Trans. Autom. Control*, 2020.
- S. Shi, X. Cheng and P. M. J. Van den Hof. “Exploiting unmeasured disturbance signals in identifiability of linear dynamic networks with partial measurement and partial excitation.” Accepted abstract in *19th IFAC Symposium on System Identification*, 2021.

Chapter 6- Bayesian topology identification. The topology identification problem, i.e. sub-question 3, is considered in this chapter. As a preliminary step to achieve topology identification with uncertainty quantification, a novel Bayesian model selection approach is developed to obtain a point estimate of the network topology, by modeling the modules in a network as Gaussian processes. The effectiveness of the developed approach is demonstrated in the numerical analysis.

The material of this chapter is based on the following paper:

- S. Shi, G. Bottegal and P. M. J. Van den Hof. “Bayesian topology identification of linear dynamic networks” In *Proc. 18th European Control Conference (ECC)*, p. 2814-2819, 2019.

Chapter 7- Topology identification of brain networks for the Mozart effect. While the algorithm in Chapter 6 provides a topology estimate of a single data set, it is further extended

in this chapter to infer topological changes from a group of data sets. More importantly, the developed approach is applied to a brain network study, in order to reveal the topological changes in brain networks caused by listening to the Mozart's music. Potential changes related to the cognitive processing in the brain networks are observed in the study.

This chapter is based on

- R. J.C. van Esch, S, Shi*, A. Bernas, S. Zinger, A. P. Aldenkamp and P. M. J. Van den Hof. "A Bayesian method for inference of effective connectivity in brain networks for detecting the Mozart effect." *Comput. Biol. Med.*, p. 104055, 2020. *Corresponding author.

The author's contribution: The material of this chapter is joint work with other coauthors and is extended from the MSc project of the first author. The author of this thesis contributed to the development of the Bayesian approach, the supervision of the student, the validation of the results, and reviewing and revising the paper.

Chapter 8- Conclusions and future work. In this chapter conclusions are drawn, and several open problems are discussed.

醉漾轻舟，信流引到花深处。尘缘相误，无计花间住。

秦观（宋）

Drunk, at random I float. Along the stream my little boat. By misfortune, among. The flowers I cannot stay long.

Guan Qin (Song dynasty); Translated by Yuanchong Xu

2

Preliminaries

The linear dynamic network model is introduced in this chapter. Then network identifiability is defined, which is one of the core concepts in this thesis. This is followed by the graphical representation of dynamic networks, which serves as the basis for the graphical analysis in the following chapters. Finally, the connections between the linear dynamic network and the network models introduced in Chapter 1 are also investigated.

2.1 DYNAMIC NETWORK MODEL

The dynamic network describes the causal relationship among an L -dimensional *internal signal* vector $w(t)$, a K -dimensional deterministic excitation signal vector $r(t)$, and an L -dimensional signal vector $v(t)$ of zero-mean stationary stochastic processes [152]. The model is formulated as

$$w(t) = G(q)w(t) + R(q)r(t) + v(t), \quad (2.1a)$$

$$w_C(t) = Cw(t), \quad (2.1b)$$

where q^{-1} is the delay operator, i.e. $q^{-1}w_i(t) = w_i(t-1)$, and

- $G(q)$ is an $L \times L$ matrix of rational transfer operators, whose entries are referred to as

modules;

- $R(q)$ is an $L \times K$ matrix of rational transfer operators;
- $C \in \mathbb{R}^{m \times L}$ is a binary selection matrix which extracts a subvector $w_C(t)$ from $w(t)$, i.e. C consists of a subset of rows from an $L \times L$ identity matrix;
- Internal signal $w_C(t)$ and excitation signal $r(t)$ are measured;
- Disturbance signal $v(t)$ is not measured.

As a special case, when $C = I$, i.e. all the internal signals in $w(t)$ are measured, the measurement equation (2.1b) can be omitted. In addition, let $G(z)$ denote the transfer function corresponding to $G(q)$, and

$$G(e^{j\omega}), \quad \omega \in [-\pi, \pi],$$

is the frequency function of $G(z)$. $G(q)^*$ and $G(z)^*$ denote $G^\top(q^{-1})$ and $G^\top(z^{-1})$, respectively.

A noise model for $v(t)$ can be further introduced as follows. Let $\Phi_v(z)$ with dimension $L \times L$ be the (power) spectrum of $v(t)$, defined as

$$\Phi_v(z) \triangleq \sum_{\tau=-\infty}^{\infty} \Xi_v(\tau) z^{-\tau},$$

where $\Xi_v(\tau)$ is the auto-covariance function of $v(t)$, i.e.

$$\Xi_v(\tau) \triangleq E[v(t)v(t-\tau)^\top].$$

In addition, consider that $\Phi_v(z)$ has rank $p \leq L$, and $v(t)$ is called a singular disturbance process if $p < L$ holds. Based on the spectral factorization theory, $\Phi_v(z)$ admits a decomposition as

$$\Phi_v(z) = H(z)\Lambda H(z)^*, \quad (2.2)$$

where

- Λ is a real and positive semi-definite matrix with either dimension $L \times L$ or $p \times p$, depending on the chosen spectral factorization method [60, 169];
- $H(z)$ is proper, stable, and has a stable left inverse [169] with a suitable dimension according to Λ .

Motivated by (2.2), $v(t)$ can be modeled as

$$v(t) = H(q)e(t), \quad (2.3)$$

where $e(t)$ is a white noise process with covariance matrix Λ , because $H(q)e(t)$ admits the same spectral density matrix as $v(t)$. The specific spectral factorization in (2.2) and thus the corresponding dimensions of Λ and $H(q)$ will be specified in Chapters 3 and 5.

Combining (2.1) with the noise model in (2.3) leads to a complete network model specified by a quintuple

$$M \triangleq (G(q), R(q), H(q), C, \Lambda), \quad (2.4)$$

on which the following assumptions are made:

Assumption 2.1. (a) $G(q)$ is stable*, proper, and hollow;

(b) The network is well-posed in the sense that all principal minors of $\lim_{z \rightarrow \infty} [I - G(z)]$ are non-zero [46];

(c) $[I - G(q)]^{-1}$ is stable;

(d) $H(z)$ is proper, stable, and has a stable left inverse;

(e) $R(q)$ is stable and proper;

(f) Λ is real and positive semi-definite.

In Assumption 2.1, $G(q)$ is hollow such that there is no self-loop in the network, i.e. an internal signal does not directly influence itself in (2.1). Furthermore, Assumption 2.1(b) ensures that every principal submatrix of $[I - G(q)]$ has a proper inverse, i.e. every closed-loop transfer function in the dynamic network is proper [46, 131].

The following sets are also defined based on the network model (2.4):

- $\mathcal{W} \triangleq \{w_1, \dots, w_L\}$ is the set of all the internal signals, where the dependency of signal $w_i(t)$ on the time index t is omitted for simplicity;
- Set \mathcal{C} contains all the measured internal signals, i.e. the entries in $w_{\mathcal{C}}(t)$;
- $\mathcal{Z} = \mathcal{W} \setminus \mathcal{C}$ contains all the unmeasured internal signals;
- $\mathcal{R} \triangleq \{r_1, \dots, r_K\}$ is the set of all the excitation signals;
- The signals in vectors $r(t)$ and $e(t)$ are called *external signals* and are collected into set \mathcal{X} .

2.2 MODEL SET

Instead of a single network model (2.4), a set of models is typically considered in identification methods that search for an optimal model within the set.

*Stability is assumed to ensure that $T(z)H(z)$ in (2.9) is inversely stable and thus an appropriate spectral factor of $\Phi(z)$ [169].

Definition 2.1. A network model set \mathcal{M} is a set of network models in the form of (2.4) which satisfy Assumption 2.1 and have the same C matrix, i.e. the same measurement scheme.

In many practical situations, a special type of network model set is obtained by a rational parameterization of the entries in $(G(q), R(q), H(q))$. Consider the following two polynomials:

$$\begin{aligned} A(q) &= 1 + a_1 q^{-1} + \cdots + a_{n_a} q^{-n_a}, \\ B(q) &= q^{-n_k} (b_0 + b_1 q^{-1} + \cdots + b_{n_b} q^{-n_b}). \end{aligned}$$

Then each transfer operator, e.g. $G_{ji}(q)$, can be parameterized as

$$G_{ji}(q, \theta) = \frac{B(q, \theta)}{A(q, \theta)}, \quad (2.5)$$

where the parameter vector θ contains all the coefficients in the polynomials [90]. We say that two transfer operators are parameterized independently if they contain distinct parameters. In addition, entries in the covariance matrix Λ can also be parameterized.

Definition 2.2. A parametric model set \mathcal{M}_Θ is defined as

$$\mathcal{M}_\Theta = \{M(\theta) | M(\theta) = (G(q, \theta), R(q, \theta), H(q, \theta), C, \Lambda(\theta)), \theta \in \Theta\},$$

where the transfer operators are parameterized in the form of (2.5), $M(\theta)$ satisfies Assumption 2.1 for all $\theta \in \Theta$, and Θ is an open and connected subset of \mathbb{R}^n .

In the above definition, the openness and the connectedness of the parameter space are required such that the parametric model set is well-behaved, i.e. the derivative of the model structure over the parameters is well defined. See [90, Definition 4.3] for more details. Furthermore, we assume that each parameterized transfer function has distinct parameters.

Assumption 2.2. The transfer functions in a parametric network model set are parameterized independently.

Remark 2.1. A parametric model set \mathcal{M}_Θ is a particular type of model set, and thus the notation \mathcal{M} may refer to a parametric model set or a model set that does not depend on a finite-dimensional parameter. A model set \mathcal{M} that does not depend on a finite-dimensional parameter is referred to as a **non-parametric model set**.

2.3 NETWORK IDENTIFIABILITY

Motivated by identification procedures where different models in a model set are compared and then an optimal one is selected, the classical identifiability concept concerns the ability to distinguish different models in the model set [90] such that the identification procedures can obtain a

unique model. Following the above classical identifiability concept, global network identifiability for dynamic networks is introduced in an identification setting in [167, 169], as a property that reflects the ability to distinguish between network models in a network model set. There is also another version of network identifiability called generic identifiability which is based on a single network and its network topology [14, 69]. This concept will be discussed in Section 3.2.

Firstly, to compare different models, we define the equality of transfer matrices by following [90]: two transfer matrices $G_1(q)$ and $G_2(q)$ are said to be equal if

$$G_1(e^{j\omega}) = G_2(e^{j\omega}), \text{ for almost all } \omega.$$

Then identifiability is defined based on the external-to-internal mapping (MIMO system) of a network model (2.1):

$$w_C(t) = CT(q)R(q)r(t) + CT(q)H(q)e(t), \quad (2.6)$$

where

$$T(q) \triangleq [I - G(q)]^{-1}. \quad (2.7)$$

Based on the above model, $w_C(t)$ is a quasi-stationary signal with its mean as

$$E[w_C(t)] = CT(q)R(q)r(t), \quad (2.8)$$

and its covariance function as

$$\Xi_{\bar{v}}(\tau) = E[\bar{v}(t)\bar{v}(t - \tau)^\top], \text{ where } \bar{v}(t) \triangleq CT(q)H(q)e(t),$$

and the expectation operator E is with respect to the white noise $e(t)$. Then the z-transform of the covariance function $\Xi_{\bar{v}}(\tau)$ leads to the spectrum $C\Phi(z)C^\top$ of $\bar{v}(t)$, where

$$\Phi(z) \triangleq T(z)H(z)\Lambda H(z)^*T(z)^*. \quad (2.9)$$

The mean (2.8) and the spectrum $C\Phi(z)C^\top$ contain the statistical second-order properties of the measured internal signals. These properties are uniquely specified by the measured $w_C(t)$ and $r(t)$. Furthermore, under certain conditions on $r(t)$, the mean (2.8) also determines a unique mapping $CT(q)R(q)$.

Proposition 2.1. *If the power spectrum $\Phi_r(e^{j\omega})$ of $r(t)$ satisfies*

$$\Phi_r(e^{j\omega}) > 0, \text{ for almost all } \omega \in [-\pi, \pi], \quad (2.10)$$

then the mean (2.8) determines a unique mapping $CT(q)R(q)$.

Proof. Let $F(q) = CT(q)R(q)$, and consider the same mean under two mappings $F_1(q)$ and $F_2(q)$, i.e.

$$F_1(q)r(t) = F_2(q)r(t).$$

This means the spectrum of $\bar{F}(q)r(t)$ is zero for almost all ω , where $\bar{F}(q) = F_1(q) - F_2(q)$. Thus, it holds that

$$\int_{-\pi}^{\pi} \bar{F}(e^{j\omega})\Phi_r(e^{j\omega})\bar{F}(e^{j\omega})^* d\omega = 0.$$

Combining the above equation and (2.10) shows that $\bar{F}(e^{j\omega})$ is zero for almost all ω , and thus $F_1(q) = F_2(q)$. \square

$r(t)$ is said to be persistently exciting if (2.10) is satisfied. Under this condition, measured signals $w_C(t)$ and $r(t)$ lead to unique objects $CT(q)R(q)$ and $C\Phi(z)C^\top$. Therefore, the identifiability concept introduced in [169] concerns whether the above objects further lead to a unique network model.

Definition 2.3. *Given a parametric network model set \mathcal{M}_Θ , consider $M(\theta_0) \in \mathcal{M}_\Theta$ and the following implication:*

$$\left. \begin{aligned} CT(q, \theta_0)R(q, \theta_0) &= CT(q, \theta_1)R(q, \theta_1) \\ C\Phi(z, \theta_0)C^\top &= C\Phi(z, \theta_1)C^\top \end{aligned} \right\} \Rightarrow G_{ji}(q, \theta_0) = G_{ji}(q, \theta_1), \quad (2.11)$$

for all $M(\theta_1) \in \mathcal{M}_\Theta$. Then module G_{ji} is globally identifiable in \mathcal{M} from (w_C, r) if the implication (2.11) holds for all $M(\theta_0) \in \mathcal{M}_\Theta$.

The above definition concerns the statistical second-order properties of the measured signals, while higher-order properties or the full distribution are not considered, since the mean and the spectrum are the typical objects of interest in system identification methods. The above definition also extends trivially to multiple modules by replacing G_{ji} in (2.11) with the objects of interest. If all the modules in $G(q)$ are globally identifiable, it is said that the model set \mathcal{M} or the full network is globally identifiable.

When a model set is globally identifiable and if $r(t)$ is persistently exciting, a unique model can be found by an identification method that relies on the second-order properties of the measured signals. This uniqueness is important, for example, when the network model has a physical interpretation. However, some models, e.g. models with latent variables such as a state-space model [132], are inherently not identifiable. In this case, one may choose to accept that a model set is not identifiable and thus accept the non-uniqueness.

Remark 2.2. *The concept in Definition 2.3 considers the identifiability of a module (transfer function) instead of the identifiability of its parameters. Given the unique rational transfer function, the identifiability of its parameters is a classical topic and can be achieved by appropriate parameterization of this transfer function as shown in [90, Section 4.6].*

2.4 GRAPHICAL REPRESENTATION

2.4.1 BASIC GRAPHICAL CONCEPTS

A graphical representation can be used to encode the topological information of a network model set or a network model. Relevant graphical concepts are first introduced in this subsection.

A directed graph \mathcal{G} is defined as $\mathcal{G} \triangleq (\mathcal{V}, \mathcal{E})$, where $\mathcal{V} \triangleq \mathcal{W} \cup \mathcal{X}$ is a set of vertices representing both the internal signals and the external signals, and $\mathcal{E} \subseteq \mathcal{V} \times \mathcal{V}$ denotes a set of directed edges between the vertices. Note that $w_i(t)$ denotes both a signal and a vertex in \mathcal{G} , and it is often written as w_i for the simplicity of notation. In addition, this thesis mainly considers simple graphs, i.e. \mathcal{E} does not contain any edge of the form (w_i, w_i) , and there exists maximally one directed edge from one vertex to another vertex.

In \mathcal{G} a directed edge from w_i to w_j , denoted by (w_i, w_j) , is called an *in-coming* edge of w_j and an *out-going* edge of w_i . In this case, w_i is also called an *in-neighbor* of w_j , and w_j is an *out-neighbor* of w_i . The out-degree of w_i is the total number of out-neighbors of w_i . A *source* is a vertex without any in-neighbors, and likewise, a *sink* is a vertex without any out-neighbors. A (directed) *path* from w_i to w_j is a sequence of vertices and out-going edges starting from w_i to w_j without repeating any vertex. If a path from w_i to w_j exists, w_j is also said to be *reachable* by w_i . The length of a path is the number of edges in the path. Note that a single vertex is also regarded as a directed path with length zero. In a path, *internal vertices* are the vertices excluding the starting and the ending vertices. A (directed) cycle or loop around w_i is a sequence of vertices and out-going edges from w_i to w_i , in which only the starting and the ending vertices are repeated. A directed simple graph \mathcal{G} is *connected* if the underlying undirected graph, obtained by replacing all the directed edges of \mathcal{G} with undirected edges, is connected, i.e., in the undirected graph, there is an undirected path between any pair of vertices.

Two directed paths are called *vertex disjoint* if they do not share any vertex, including the starting and ending vertices, otherwise, they *intersect*. They are *internally vertex disjoint* if they do not share any internal vertex. Similarly, two sets of paths \mathcal{P}_1 and \mathcal{P}_2 are said to be vertex disjoint if every path in \mathcal{P}_1 is vertex disjoint with the paths in \mathcal{P}_2 . Given two subsets of vertices \mathcal{V}_1 and \mathcal{V}_2 , $b_{\mathcal{V}_1 \rightarrow \mathcal{V}_2}$ denotes the maximum number of vertex disjoint paths from \mathcal{V}_1 to \mathcal{V}_2 . A vertex set \mathcal{D} is called a $\mathcal{V}_1 - \mathcal{V}_2$ *disconnecting set*, or equivalently a disconnecting set from \mathcal{V}_1 to \mathcal{V}_2 , if it intersects with all the paths from \mathcal{V}_1 to \mathcal{V}_2 . Note that \mathcal{D} may also include vertices in $\mathcal{V}_1 \cup \mathcal{V}_2$. It is a minimum disconnecting set if it has the minimum cardinality among all $\mathcal{V}_1 - \mathcal{V}_2$ disconnecting sets [135].

The duality between vertex disjoint paths and disconnecting sets is explained in the following result.

Theorem 2.1 (Menger's theorem [135]). *Let $\mathcal{V}_1, \mathcal{V}_2$ be two subsets of vertices in a directed graph.*

The maximum number of vertex disjoint paths from \mathcal{V}_1 to \mathcal{V}_2 equals the cardinality of a minimum disconnecting set from \mathcal{V}_1 to \mathcal{V}_2 .

The concepts of disconnecting sets and vertex disjoint paths are further illustrated in the following example.

Example 2.1. Consider the directed graph in Figure 2.1, where two vertex sets $\mathcal{V}_1 = \{w_1, w_2, w_3\}$ and $\mathcal{V}_2 = \{w_7, w_8, w_9\}$ are indicated by blue circles. The goal is to find a set of maximum number of vertex disjoint paths \mathcal{P} and a minimum disconnecting set \mathcal{D} from \mathcal{V}_1 to \mathcal{V}_2 .

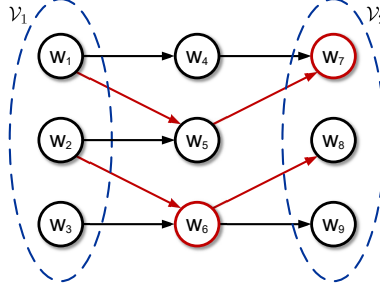


Figure 2.1: In this directed graph, the two red paths form a set of maximum number of vertex disjoint paths from \mathcal{V}_1 to \mathcal{V}_2 . Set $\{w_6, w_7\}$, i.e. the two red vertices, is a minimum $\mathcal{V}_1 - \mathcal{V}_2$ disconnecting set.

Consider the paths from $w_1 \in \mathcal{V}_1$ to the vertices in \mathcal{V}_2 . It can be found that w_1 only has two paths to w_7 which pass through either w_4 or w_5 . These two paths are not vertex disjoint because they share the starting vertex w_1 and the ending vertex w_7 . This shows that the paths from w_1 and w_7 only contribute one vertex disjoint path to \mathcal{P} , i.e. the upper red path in Figure 2.1. Similarly, even if there are multiple paths from $\{w_2, w_3\}$ to $\{w_8, w_9\}$, all of them share the common vertex w_6 . Thus, these paths also contribute only one vertex disjoint path to \mathcal{P} , i.e. the lower red path in Figure 2.1. Based on the above observations, there are maximally two vertex disjoint paths from \mathcal{V}_1 to \mathcal{V}_2 , i.e. $b_{\mathcal{V}_1 \rightarrow \mathcal{V}_2} = 2$. One choice of \mathcal{P} is to collect path $w_1 \rightarrow w_5 \rightarrow w_7$ and path $w_2 \rightarrow w_6 \rightarrow w_8$, i.e. the two red paths in Figure 2.1; however, this choice is not unique.

For the minimum disconnecting set \mathcal{D} , one choice is $\mathcal{D} = \{w_6, w_7\}$, i.e. the two red vertices in Figure 2.1. It can be found that if $\{w_6, w_7\}$ is removed, there is no directed path from \mathcal{V}_1 to \mathcal{V}_2 . Therefore, $\{w_6, w_7\}$ is a disconnecting set from \mathcal{V}_1 to \mathcal{V}_2 . In addition, the set is minimum according to the Menger's theorem, since its cardinality equals $b_{\mathcal{V}_1 \rightarrow \mathcal{V}_2}$. Note that the choice for a minimum disconnecting set may not be unique, and a different choice in this example can be $\{w_1, w_6\}$.

The following important property of disconnecting sets will also be used [69].

Lemma 2.1. For a directed graph and given a $\mathcal{V}_1 - \mathcal{V}_2$ disconnecting set \mathcal{D} , consider the division of all the vertices \mathcal{V} into three disjoint sets $\mathcal{S} \cup \mathcal{D} \cup \mathcal{P}$ as follows: set \mathcal{S} contains all the vertices reachable by \mathcal{V}_1 without intersecting with \mathcal{D} , and $\mathcal{P} = \mathcal{V} \setminus (\mathcal{D} \cup \mathcal{S})$. Then It holds that no directed edge exists from \mathcal{S} to \mathcal{P} .

The above result has an important algebraic consequence. Consider a square matrix A that encodes the topology of a directed graph, i.e., A_{ji} is zero if and only if the directed edge (i, j) does not exist. Then given a disconnecting set \mathcal{D} from a vertex set \mathcal{V}_1 to another vertex set \mathcal{V}_2 in the above directed graph, A can be permuted as

$$\begin{bmatrix} A_{\mathcal{P}\mathcal{P}} & A_{\mathcal{P}\mathcal{D}} & 0 \\ A_{\mathcal{D}\mathcal{P}} & A_{\mathcal{D}\mathcal{D}} & A_{\mathcal{D}\mathcal{S}} \\ A_{\mathcal{S}\mathcal{P}} & A_{\mathcal{S}\mathcal{D}} & A_{\mathcal{S}\mathcal{S}} \end{bmatrix}, \quad (2.12)$$

where sets \mathcal{P}, \mathcal{S} are formulated as in Lemma 2.1, and the submatrix $A_{\mathcal{D}\mathcal{P}}$ collects all the entries in A that represent the directed edges from \mathcal{P} to \mathcal{D} . More importantly, there is a block zero in (2.12) which denotes the submatrix $A_{\mathcal{P}\mathcal{S}}$, since there is no directed edge from \mathcal{S} to \mathcal{P} according to Lemma 2.1. The sparsity pattern of the permuted A in (2.12) induced by a disconnecting set can facilitate the graphical analysis for identifiability and will be exploited in Section 4.2.2.

2.4.2 GRAPHS OF MODEL SETS AND DYNAMIC NETWORKS

Recall that in graph \mathcal{G} , its vertices represent both the internal signals and the external signals in a dynamic network. The directed graph \mathcal{G} can thus be used to encode the following structural information of a model set \mathcal{M} . Certain entries in $G(q)$, $R(q)$, and $H(q)$ may have fixed values for all models in \mathcal{M} , based on the prior knowledge or simply on the user's modeling assumptions. For example, the absence of an interconnection between internal signals is represented by a fixed 0 in $G(q)$ for all models in \mathcal{M} ; some entries in $G(q)$ may be particularly designed controllers that are fixed and known.

- The fixed entries in the transfer matrices are also called *known* entries;
- The entries that are not fixed are called *unknown* entries.

Note that the known entries include the fixed zeros and the known non-zero entries in the matrices of the models. In addition, all the network models in a network model set have the same fixed entries.

Based on the fixed entries, a directed graph $\mathcal{G} = (\mathcal{V}, \mathcal{E})$ associated with the model set \mathcal{M} satisfies that an edge exists in \mathcal{G} if and only if the corresponding entry in $G(q)$, $R(q)$ and $H(q)$ is not fixed to be zero. For example, the directed edge from w_i to w_j exists if and only if $G_{ji}(q)$ is not fixed to be zero in \mathcal{M} , and similarly, a directed edge from e_i to w_j exists if and only if $H_{ji}(q)$ is not fixed to be zero in \mathcal{M} . In addition, the set of edges \mathcal{E} can be decomposed into two disjoint subsets as $\mathcal{E} = \mathcal{E}_1 \cup \mathcal{E}_2$, where \mathcal{E}_1 contains the edges representing the unknown entries of the transfer matrices in \mathcal{M} , and \mathcal{E}_2 consists of the edges representing the known non-zero entries.

Example 2.2. Consider a graph of a network model set \mathcal{M} in Figure 2.2, where there are three

internal signals, one excitation signal $r_1(t)$, and one noise signal $e_2(t)$. Therefore, \mathcal{M} contains network models with 3×3 matrix $G(q)$, 3×1 matrix $R(q)$ and 3×1 matrix $H(q)$.

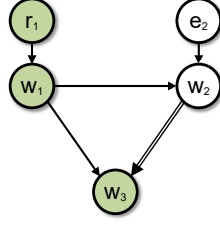


Figure 2.2: A graph of a network model set \mathcal{M} , where the signals represented by green vertices, i.e. $w_1(t)$, $w_3(t)$ and $r_1(t)$, are measured. The double-lined edge (w_2, w_3) represents the known non-zero entry G_{32}^0 in \mathcal{M} , while the other edges denote the unknown entries.

Since the edge from w_2 to w_1 does not exist in the graph, module $G_{12}(q)$ in $G(q)$ is fixed to be zero for all the models in \mathcal{M} . In addition, the module $G_{32}(q)$, represented by the double-lined edge, has a fixed non-zero value for all the models in \mathcal{M} . Since the internal signals $w_1(t)$ and $w_3(t)$ are measured, the C matrix in (2.1b) can also be determined as

$$C = \begin{bmatrix} 1 & 0 & 0 \\ 0 & 0 & 1 \end{bmatrix}.$$

Similarly, the information regarding the other entries of the matrices in \mathcal{M} can be read from the graph. It can be found that the graph denotes a model set that contains models with the following structure:

$$\begin{bmatrix} w_1(t) \\ w_2(t) \\ w_3(t) \end{bmatrix} = \begin{bmatrix} 0 & 0 & 0 \\ G_{21}(q) & 0 & 0 \\ G_{31}(q) & G_{32}^0(q) & 0 \end{bmatrix} \begin{bmatrix} w_1(t) \\ w_2(t) \\ w_3(t) \end{bmatrix} + \begin{bmatrix} R_1(q) \\ 0 \\ 0 \end{bmatrix} r_1(t) + \begin{bmatrix} 0 \\ H_2(q) \\ 0 \end{bmatrix} e_2(t),$$

$$\begin{bmatrix} w_1(t) \\ w_3(t) \end{bmatrix} = \begin{bmatrix} 1 & 0 & 0 \\ 0 & 0 & 1 \end{bmatrix} \begin{bmatrix} w_1(t) \\ w_2(t) \\ w_3(t) \end{bmatrix},$$

where $G_{32}^0(q)$'s superscript denotes that this entry takes a fixed value over different models in \mathcal{M} .

Note that in the graph \mathcal{G} of a model set \mathcal{M} , the absence of one edge leads to a stronger restriction on \mathcal{M} than the existence of one edge. For example, in Figure 2.2, while the absence of edge (w_2, w_1) enforces $G_{12}(q)$ to be zero for all the models in \mathcal{M} , the existing edge (w_1, w_2) allows models in \mathcal{M} to have different values for module $G_{21}(q)$, possibly including $G_{21}(q) = 0$.

A parametric model set \mathcal{M}_Θ is a model set obtained from parameterization, and thus the graphical representation also applies to \mathcal{M}_Θ . In \mathcal{M}_Θ , its unknown entries are parameterized

as functions of the parameters, while the known (fixed) entries, either zero or non-zero, do not depend on the parameters because they have fixed values.

2.5 NOTATIONS AND DEFINITIONS

Some basic notations and definitions are first collected here, and these notations will be used intensively in the identifiability study in Chapters 3, 4 and 5.

Recall the defined sets in Section 2.1. In addition, we define the following sets for a model set \mathcal{M} and its associated graph based on the known and unknown entries:

- Set \mathcal{W}_j^- contains all the internal signals that have *unknown* directed edges (modules) to w_j ;
- \mathcal{W}_i^+ contains all the internal signals to which w_i has *unknown* directed edges;
- Let \mathcal{X}_j include all the external signals that do not have any unknown edge to w_j ;
- For a set of vertices $\bar{\mathcal{V}}$ in \mathcal{G} , let the set $\bar{\mathcal{N}}_{\bar{\mathcal{V}}}^+$ contain all the out-neighbors of the vertices in $\bar{\mathcal{V}}$.

For two sets \mathcal{V}_1 and \mathcal{V}_2 , $\mathcal{V}_1 \setminus \mathcal{V}_2$ denotes the set subtraction, i.e.

$$\mathcal{V}_1 \setminus \mathcal{V}_2 \triangleq \{x \in \mathcal{V}_1 | x \notin \mathcal{V}_2\}.$$

In our notation, the dependency of signals on t is often omitted. In the proofs, the dependency of transfer operators on q and θ is often omitted for the simplicity of notation.

Recall from Section 2.1 that \mathcal{X} is the set of all the external signals. A vertex w_i is said to be *directly excited* by a vertex $x_i \in \mathcal{X}$ if there is a directed edge from x_i to w_i , and w_i is (*indirectly*) *excited* by x_i if there exists a path from x_i to w_i . Similarly, w_i is said to be indirectly measured if it has a path to a measured internal signal.

In addition, recall (2.6) and define

$$T_{\mathcal{WR}}(q) \triangleq T(q)R(q), \quad X(q) \triangleq \begin{bmatrix} R(q) & H(q) \end{bmatrix}, \quad \text{and } T_{\mathcal{WX}}(q) \triangleq T(q)X(q). \quad (2.13)$$

Therefore, $T_{\mathcal{WX}}(q)$ denotes the mapping in (2.6) from all the external signals in \mathcal{X} to all the internal signals in \mathcal{W} . Given two subsets $\bar{\mathcal{W}} \subseteq \mathcal{W}$ and $\bar{\mathcal{X}} \subseteq \mathcal{X}$, we use $T_{\bar{\mathcal{W}}\bar{\mathcal{X}}}(q)$ to represent the mapping from the external signals in $\bar{\mathcal{X}}$ to the internal signals in $\bar{\mathcal{W}}$, i.e. the submatrix of $T_{\mathcal{WX}}(q)$ whose rows and columns correspond to the elements in $\bar{\mathcal{W}}$ and $\bar{\mathcal{X}}$, respectively. When the set contains a single element, e.g. $\bar{\mathcal{W}} = \{w_j\}$, $T_{\bar{\mathcal{W}}\bar{\mathcal{X}}}(q)$ is simply written as $T_{j\bar{\mathcal{X}}}(q)$.

The above notion for submatrices applies to other matrices and vectors similarly. For example, given subsets $\bar{\mathcal{W}}_1$ and $\bar{\mathcal{W}}_2$ of \mathcal{W} , $G_{\bar{\mathcal{W}}_1\bar{\mathcal{W}}_2}(q)$ and $T_{\bar{\mathcal{W}}_1\bar{\mathcal{W}}_2}(q)$ denote the submatrices of $G(q)$

and $T(q)$ whose rows and columns correspond to the subsets. Similarly, $w_{\mathcal{C}}(t)$ denotes a sub-vector of $w(t)$ whose components correspond to the elements in \mathcal{C} , i.e. the measured internal signals.

Furthermore, given any transfer matrix or spectrum $A(z)$, the notation A^∞ is defined as

$$A^\infty \triangleq \lim_{z \rightarrow \infty} A(z).$$

A square transfer matrix $A(z)$ is said to be *monic* if A^∞ is an identity matrix. It is said to be *minimum-phase* if both this transfer matrix and its inverse are proper and stable.

The concept of the absence of *algebraic loops* is often used.

Definition 2.4. *Given a network model set \mathcal{M} , it is said to have no algebraic loop if there exists a permutation matrix P such that for all models in \mathcal{M} , $PG^\infty P^\top$ is lower triangular.*

The above definition requires a single P matrix to work for all the elements in \mathcal{M} . Similarly, we can also consider the absence of algebraic loops for a single network model.

2.6 CONNECTIONS TO OTHER NETWORK MODELS

2.6.1 INTRODUCTION

Several different network models have been discussed in Section 1.2; however, their connections have not been formulated. After having the relevant background for dynamic networks in the previous sections, we establish the connections between the dynamic network model and other network models in Section 1.2. In particular, the VAR model, the SEM model and the Bayesian network will be considered. Building these connections can be helpful for understanding the relevant literature and extending techniques from other domains to the identification of dynamic networks.

For simplicity, a special network model $(G(q), R(q), H(q), I, \Lambda)$ is considered in this subsection, where $C = I$, $\Lambda \in \mathbb{R}^{L \times L}$ is non-singular, $H(q)$ is diagonal and monic, and there is no external excitation, i.e. $R(q) = 0$. In addition, instead of the direct connection between the network model and the models in Section 1.2, the connection between the *predictor model* of the network model and the models in Section 1.2 is established. Thus, the predictor model of the dynamic network is first introduced [90].

Consider the j -th row of the network model

$$w_j(t) = \sum_{i \in \mathcal{I} \setminus \{j\}} G_{ji}(q) w_i(t) + H_j(q) e_j(t), \quad (2.14)$$

where $\mathcal{I} = \{1, \dots, L\}$ and $H_j(q)$ is the j -th entry on the main diagonal of $H(q)$. Then it can

be reformulated as

$$w_j(t) = \hat{w}_j(t) + e_j(t) \quad (2.15)$$

where

$$\hat{w}_j(t) = [1 - H_j(q)^{-1}]w_j(t) + \sum_{i \in \mathcal{I} \setminus \{j\}} H_j(q)^{-1} G_{ji}(q) w_i(t).$$

Since $H(q)$ is monic, $1 - H_j(q)^{-1}$ is strictly proper and thus the power series expansion of $\hat{w}(t)$ is

$$\hat{w}_j(t) = \sum_{k=1}^{\infty} h_j^{(k)} w_j(t-k) + \sum_{i \in \mathcal{I} \setminus \{j\}} \sum_{k=0}^{\infty} g_{ji}^{(k)} w_i(t-k), \quad (2.16)$$

where $g_{ji}^{(k)}$ is the k -th impulse response coefficient of $H_j(q)^{-1} G_{ji}(q)$, and $h_j^{(k)}$ is the k -th impulse response coefficient of $[1 - H_j(q)^{-1}]$. $\hat{w}_j(t)$ is the so-called one-step-ahead predictor [90], since it can predict $w_j(t)$ given the past and the present values of $w_i(t)$, and the past values of $w_j(t)$, as shown in (2.16). Model (2.15) is referred to as a *predictor network* associated with the network model (2.14).

The predictor model is used extensively in the so-called prediction-error methods (PEMs) for identifying dynamic systems [90]. By exploiting the predictor model obtained from (2.14), the goal of PEMs is to find the optimal parameters such that the error between $w_j(t)$ and its prediction $\hat{w}_j(t)$ is minimized. Therefore, what matters in the end is the predictor $\hat{w}_j(t)$ and thus (2.15) of the network, while the original network model (2.14) only serves as a vehicle to arrive at the expression for (2.15) [89]. In this section, the connections between the predictor (2.15) and the different network models in Section 1.2 will be studied.

2.6.2 VAR MODEL

When the modules in $G(q)$ are strictly proper, it holds that $g_{ji}^{(0)} = 0$ in (2.16). Then combining (2.15) with (2.16), for all j , into a matrix form leads to

$$w(t) = \sum_{k=1}^{\infty} A^{(k)} w(t-k) + e(t), \quad (2.17)$$

where $A^{(k)}$ contains all the k -th impulse response coefficients in (2.16) for $j \in \mathcal{I}$. Based on the above model and (1.2), it can be found that (2.15) is an infinite-order VAR model.

Therefore, if the impulse responses in (2.17) are truncated to a finite order n , all techniques for estimating a VAR model can be applied to the estimation of (2.15). Conversely, the techniques developed for estimating (2.15) with the power series expansion can also be used for a VAR model.

2.6.3 SEM

Recall the structural equation models (SEMs) in Section 1.2.3. In general, an SEM model consists of a set of equations

$$x_j = f_j(\mathcal{P}_j, v_j), j \in \{1, \dots, L\}, \quad (2.18)$$

where \mathcal{P}_j is a subset of $\{x_1, \dots, x_L\}$ whose elements determine the value of x_j , and v_j is a disturbance term [113]. In addition, a directed graph \mathcal{G}_S associated with an SEM model can be obtained by using vertices to denote the variables in $\{x_1, \dots, x_L\}$ and drawing one edge from x_i to x_j if $x_i \in \mathcal{P}_j$.

Model (2.15) can be reformulated into the following SEM model:

$$w_j(t) = f_{j,t}(\mathcal{P}_{j,t}, e_j(t)), j \in \mathcal{I} \text{ and } t \in \{1, \dots, N\}, \quad (2.19)$$

where set $\mathcal{P}_{j,t}$ contains the present and the past values of $w_i(t)$ and the past values of $w_j(t)$; N denotes the time index of the final measurement of $w(t)$, and it is assumed that $w(t) = 0$ for all $t \leq 0$. Furthermore, the graph \mathcal{G}_S associated with the above model can be obtained, where, for example, $w_i(t-1)$ and $w_i(t)$ are represented by two vertices, and the edge from $w_i(t-1)$ to $w_j(t)$ exists if $w_i(t-1)$ is in $\mathcal{P}_{j,t}$. The important difference between the graph \mathcal{G}_S and the graph \mathcal{G} in Section 2.4 is that a vertex in \mathcal{G} represents a complete signal, while a vertex in \mathcal{G}_S denotes a time instance of the signal.

2.6.4 BAYESIAN NETWORKS

An equivalence between (2.15) and the Bayesian network can also be obtained. In the graph \mathcal{G}_S , let Pa_j or $Pa(x_j)$ denote the set of parents of x_j , i.e. the vertices that have directed edges to x_j . Then the Bayesian network is defined as follows.

Definition 2.5. Let \mathcal{G}_S be a directed acyclic graph where each vertex denotes a random variable x_j , $j \in \{1, \dots, L\}$. Let P denote a joint distribution over all the above random variables. A Bayesian network is a pair (P, \mathcal{G}_S) such that the joint distribution P can be expressed as

$$P(x_1, \dots, x_L) = \prod_{j=1}^L P(x_j | Pa_j).$$

Then the equivalence between the SEM model and the Bayesian network can be first exploited as follows.

Lemma 2.2. If model (2.18) satisfies the following assumptions:

- the corresponding graph \mathcal{G}_S is acyclic,
- v_j are jointly independent with probability distribution $P(v_j)$,

then (2.18) induces a joint distribution $P(x_1, \dots, x_L)$ that satisfies

$$P(x_1, \dots, x_L) = \prod_{j=1}^L P(x_j | Pa_j).$$

Proof. This result follows from [113, Definition 1.2.2] and [113, Theorems 1.2.7, 1.4.1]. \square

The above theorem states that an SEM and its associated graph leads to a Bayesian network if the graph is acyclic and the disturbances are independent. Since (2.15) also leads to an SEM model (2.19), an equivalence between (2.15) and the Bayesian network can be obtained.

Theorem 2.2. *Consider (2.15) for $t \in \{1, \dots, N\}$ with $w(t) = 0$ for $t < 1$. If (2.15) also satisfies the following conditions:*

- *the network model does not have any algebraic loop;*
- *The random variables in $\{e_j(t) | j \in \mathcal{I} \text{ and } t \in \{1, \dots, N\}\}$ are mutually independent with probability distribution $P(e_j(t))$,*

then (2.15) induces a joint distribution $P(\{w_i(t), \dots, w_L(t)\}_{t=1}^N)$ which satisfies

$$P(\{w_i(t), \dots, w_L(t)\}_{t=1}^N) = \prod_{t=1}^N \prod_{j=1}^L P(w_j(t) | Pa(w_j(t))),$$

where $Pa(w_j(t))$ contains the parents of $w_j(t)$ in the graph \mathcal{G}_S associated with (2.19).

Proof. We only need to prove that (2.19) satisfies the conditions in Lemma 2.2.

To prove that \mathcal{G}_S is acyclic, we consider each subgraph \mathcal{G}_t of \mathcal{G}_S independently, where \mathcal{G}_t contains only the vertices of \mathcal{G}_S with time instance t and their corresponding edges. Since directed edges can only point from the past to the present, no cycle in \mathcal{G} can contain both vertices in \mathcal{G}_{t-1} and vertices in \mathcal{G}_t , and thus cycles can only exist within the subgraph \mathcal{G}_t , for some t . In addition, the graphical structure of \mathcal{G}_t is determined by the sparsity pattern of G^∞ , based on (2.16). Since G^∞ can be permuted to be lower triangular, \mathcal{G}_t must be acyclic for all t , which means \mathcal{G}_S is also acyclic. Finally, as $e_j(t)$ is independent over j and t , all the conditions in Lemma 2.2 are satisfied, which concludes the proof. \square

The above theorem shows that the predictor network (2.15) induces a Bayesian network under certain conditions. In addition, the absence of algebraic loops in a network model also means that the associated graph \mathcal{G}_S is acyclic, where each vertex denotes one time instance of a signal instead of a complete signal as in the graph \mathcal{G} introduced in Section 2.4. When the graph \mathcal{G}_S is “folded” such that each vertex represents a complete signal instead, the obtained graph can still contain cycles.

If (2.15) is parameterized with a parameter vector θ , Theorem 2.2 has an important application when the maximum likelihood estimator of (2.15) is considered. In this case, Theorem 2.2 shows that the log-likelihood function

$$\log P(\{w_i(t), \dots, w_L(t)\}_{t=1}^N | \theta)$$

can be further decomposed into independent terms, which simplifies the maximum likelihood estimation problem significantly.

2.7 CONCLUSIONS

The basic background for linear dynamic networks has been introduced in this chapter. Compared to the classical MIMO model which considers the mapping from the input to the output, the network model further captures the causal relationship between the output signals. When a set of network models is considered for identification, network identifiability is an important property ensuring that different network models in the set can be distinguished given the stochastic properties of the measured signals. Based on the identifiability concept and the topological information of a model set, graphical conditions will be investigated in the coming chapters to verify the identifiability of a model set.

Finally, connections between the predictor model of a dynamic network and network models from other domains have been studied. It is shown that under some conditions, the predictor model induces a VAR model, an SEM model, or a Bayesian network. This relation allows for the possible extensions of the estimation techniques for other network models to the identification problems in dynamic networks.

旁观拍手笑疏狂，疏又何妨，狂又何妨！

刘克庄（宋）

*People clap hands so glad, laughing to say we're mad. What if we're free.
Or in high glee?*

Kezhuang Liu (Song dynasty); Translated by Yuanchong Xu

3

Identifiability with full measurement: Analysis

3.1 INTRODUCTION

In this chapter, graph-based conditions for the analysis of network identifiability are investigated in the situation where all the internal signals are measured. In the literature, there are three notions of network identifiability, namely, *global identifiability* in Definition 2.3 that requires all the models to be distinguishable from the other models in a model set [157, 167, 169]*; *generic identifiability* [14, 69], which means that *almost all* models can be distinguished from the other models; and *generic local identifiability* that requires models to be distinguishable from other models in a neighborhood [83]. It has been shown in [14, 69] that by considering generic identifiability, the algebraic conditions for identifiability can be reformulated into path-based conditions on the graph of the network models, which largely simplifies the analysis. Note that generic local identifiability is a weaker notion than generic identifiability, and its graph-theoretical characterization remains an open question. In this thesis, we focus on global identifiability and generic identifiability of dynamic networks.

The material of this chapter is partly based on the results in [140, 141].

*There are actually two versions of global identifiability, reflecting whether either one particular model in the set can be distinguished or all models in the set [169].

Network identifiability is typically dependent on several structural properties of the model set, such as the network topology, the modeled correlation structure of process noises, the presence and location of external excitation signals, and the availability of measured internal signals. Conditions for network identifiability have been analyzed for different problem settings. In [14, 69, 157], all internal signals are excited by external excitation signals, while only a subset of internal signals is measured. In contrast, the analysis in [169, 171] assumes that all internal signals are measured, while a subset of them is excited. Recent contributions [13, 83] also address the combined situation.

In this chapter our objective is to derive path-based conditions for generic identifiability of a subset of modules (a subnetwork) in the network, while we assume all the internal signals in the network to be available for measurement, i.e. $C = I$ in (2.1) and thus (2.1b) is omitted. The results are presented in [140] and will serve as a foundation for the graphical identifiability analysis and synthesis in Chapters 4 and 5.

To analyze this problem, we start with the concept of generic identifiability as presented in [14, 69], since this allows for attractive graphical conditions. However, this concept in [14, 69] is defined as a property of a network model, while in the conventional system identification theory, identifiability is defined as a property of a model set, and then identification methods are implemented to compare models in the set and then select the optimal one. In line with the global identifiability concept in Definition 2.3 from [169], a different generic identifiability concept was presented in [171] based on a parametric model set, in which models can be distinguished from other models with the parameter value in a prescribed parameter space excluding a subset with measure zero. However, the notion of measure zero is defined on a finite-dimensional space [112], and thus the generic identifiability concept in [14, 69] is essentially limited to finite-dimensional parameters. This limitation becomes an issue as infinite-dimensional parameters are required for formulating the necessary conditions for the model-set-based generic identifiability.

This issue is addressed in this chapter by reconsidering the notion of generic identifiability defined in a topological space, where the genericity is defined on the basis of an open and dense subset in the topological space. This new approach allows us to consider models with infinite-dimensional parameters so that sufficient and necessary graphical conditions for the model-set-based generic identifiability can be derived. Furthermore, compared to the original concept of generic identifiability from [14], the following attractive features are incorporated into the model-set-based generic identifiability: (a) the effect of unmeasured disturbance signals in the network is considered; (b) modules in the network that are a priori known to the user and thus do not need to be identified are incorporated.

The chapter proceeds as follows. After introducing basic notations and definitions in Section 2.5, the existing concepts of generic identifiability and their limitations are discussed in Section 3.2, which motivates a different notion of generic identifiability in Section 3.3. Then algebraic conditions and path-based conditions are developed in Section 3.4 and Section 3.5,

respectively. This chapter is concluded in Section 3.6, and *some of the proofs are collected in Section 3.7.*

3.2 EXISTING CONCEPTS OF GENERIC IDENTIFIABILITY AND THEIR LIMITATIONS

The concept of generic identifiability has been exploited in [7] for multivariate autoregressive models and was first introduced in [14, 69] for dynamic networks in the setting where all the internal signals are excited. Here, for consistency of the presentation, we reinterpret the concept from [14, 69] in a dual setting where all the internal signals are measured. Given a directed graph with \mathcal{W} as the vertex set, a network matrix $G(q)$ is said to be consistent with this graph if the absence of the directed edge from w_i to w_j implies $G_{ji}(q) = 0$. Conversely, a graph is associated with $G(q)$ if $G_{ji}(q) \neq 0$ implies that an edge from w_i and w_j exists. Let $G^0(q)$ denote a particular network matrix. Then the following definition of generic identifiability is directly obtained from [69, Definition 1].

Definition 3.1. *A network matrix $G^0(q)$ is generically identifiable from the set of excitation signals \mathcal{R} if for any rational transfer matrix parameterization $G(q, \theta)$ consistent with the directed graph associated with $G^0(q)$, it holds that*

$$[I - G(q, \theta)]^{-1}R(q) = [I - \bar{G}(q)]^{-1}R(q) \Rightarrow G(q, \theta) = \bar{G}(q), \quad (3.1)$$

for almost all θ in \mathbb{R}^n , where $\bar{G}(q)$ is any network matrix consistent with the graph.

The above concept is to distinguish $\bar{G}(q)$ from almost all $G(q, \theta)$ consistent with the underlying graph, and it extends trivially to the single module case, where $G_{ji}(q, \theta)$ and $\bar{G}_{ji}(q)$ are considered instead in the right-hand side (RHS) of (3.1). The notion of almost all θ in Definition 3.1 refers to all θ except a set of measure zero in \mathbb{R}^n . Recall the mapping $T_{\mathcal{W}\mathcal{X}}(q)$ defined in (2.13) and its submatrices. Then for the concept in Definition 3.1, a sufficient and necessary condition for generic identifiability can be obtained, based on the proof of [69, Theorem V.1].

Corollary 3.1. *Consider any subset $\bar{\mathcal{W}}_j \subseteq \mathcal{W}_j^-$, $G_{\bar{\mathcal{W}}_j}^0(q)$ is generically identifiable if and only if the following two conditions hold:*

$$\begin{aligned} \text{rank}[T_{\bar{\mathcal{W}}_j\mathcal{R}}(q, \theta)] &= |\bar{\mathcal{W}}_j|, \text{ and} \\ \text{rank}[T_{\mathcal{W}_j^-\mathcal{R}}(q, \theta)] &= \text{rank}[T_{\bar{\mathcal{W}}_j\mathcal{R}}(q, \theta)] + \text{rank}[T_{(\mathcal{W}_j^-\setminus\bar{\mathcal{W}}_j)\mathcal{R}}(q, \theta)], \end{aligned}$$

for almost all θ in \mathbb{R}^n .

The concept of generic identifiability in Definition 3.1 is essentially based on the graph induced by the matrix $G^0(q)$. This concept is not defined on a particular parametric model set

like Definition 2.3, and instead, it concerns all possible parametric model sets with the same topology. In addition, if we consider a particular parameterization $G(q, \theta)$ instead of any parameterization as stated in Definition 3.1, then (3.1) will have an asymmetry when comparing $G(q, \theta)$ and $\bar{G}(q)$, because $\bar{G}(q)$ does not depend on θ and thus may not belong to the considered parametric model set as $G(q, \theta)$. This asymmetry in the definition is in contrast to the typical application of the identifiability concept in the identification procedure, where models from the same parametric model set are compared.

Furthermore, Definition 3.1 concerns only the mapping $[I - G(q)]^{-1}R(q)$ from $r(t)$ to $w(t)$, while the information regarding the noise signals, i.e. the power spectrum of the noises as considered in Definition 2.3, is not incorporated. The noise information is important in many practical situations, e.g., in [95, 156] where the data is collected without the user's intervention and thus does not contain any r signal.

Due to the above limitations, we consider an alternative concept of generic identifiability from [171] which is obtained by combining Definition 2.3 and the genericity concept from [14, 69]. In addition, the concept in [171] is slightly reformulated here to incorporate more explicitly the genericity notion from [14, 69].

Definition 3.2. *Given a parametric network model set \mathcal{M}_Θ , consider $M(\theta_0) \in \mathcal{M}_\Theta$ and the following implication:*

$$\left. \begin{aligned} T(q, \theta_0)R(q) &= T(q, \theta_1)R(q) \\ \Phi(z, \theta_0) &= \Phi(z, \theta_1) \end{aligned} \right\} \Rightarrow G_{ji}(q, \theta_0) = G_{ji}(q, \theta_1), \quad (3.3)$$

for all $\theta_1 \in \Theta$. Then $G_{ji}(q, \theta)$ is generically identifiable from (w, r) if the implication (3.3) holds for almost all $\theta_0 \in \Theta$.

Compared to Definition 3.1, Definition 3.2 defines model-set-based generic identifiability as a property of a parametric model set \mathcal{M}_Θ . Moreover, the noise spectrum $\Phi(z)$ in (2.9) that encodes the second moment of the measured signal $w(t)$ is included in Definition 3.2 as a basis for the identifiability analysis. Note that the original formulation of Definition 3.2 in [171] concerns genericity in the model space, i.e. for almost all $M(\theta_0) \in \mathcal{M}_\Theta$ instead of for almost all θ_0 in the parameter space as stated in Definition 3.2. The genericity notion in the model space requires a different definition from the measure zero in the parameter space, since the concept of measure zero is not defined for the infinite-dimensional model space [112]. However, this genericity notion in model space is not specified in [171]. In addition, the genericity notion, that is actually used in the results of [171], is in the parameter space, as shown in [171, Corollary 2]. Therefore, we have reformulated the original definition in [171] into Definition 3.2 where the genericity notion in the parameter space is considered.

To exploit spectrum $\Phi(z)$ for the identifiability analysis, we need to specify the noise model $(H(z), \Lambda)$ and thus the particular spectral factorization method for $\Phi_v(z)$ in (2.2). Recall that

$\Phi_v(z)$ has rank $p \leq L$, and the following noise model is considered in [169]:

Assumption 3.1. *The noise model of all elements in \mathcal{M} satisfies that*

- $H(q) \in \mathbb{R}(q)^{L \times p}$ is proper, stable, full rank, and is structured such that its upper $p \times p$ block matrix is minimum-phase and monic;
- $\Lambda \in \mathbb{R}^{p \times p}$ is real and positive definite.

The above choice of noise model is rather general, since any $\Phi_v(z)$ admits a spectral factorization (2.2) with $H(q)$ and Λ satisfying the properties in Assumption 3.1 [169, Lemma 1]. Then with the following mild assumption, $\Phi(z)$ in Definition 3.2 can be exploited such that (3.3) is simplified.

Assumption 3.2. *Model set \mathcal{M} satisfies at least one of the following two conditions:*

- (a) $G(q)$ matrices of the models in \mathcal{M} are strictly proper;
- (b) \mathcal{M} has no algebraic loop, and Φ_v^∞ is diagonal for all models in \mathcal{M} .

Then with Assumption 3.2, the following result can be obtained.

Proposition 3.1 ([169]). *Given a network model set \mathcal{M}_Θ that satisfies Assumptions 3.1 and 3.2, implication (3.3) is equivalently formulated as*

$$T_{\mathcal{W}\mathcal{X}}(q, \theta_0) = T_{\mathcal{W}\mathcal{X}}(q, \theta_1) \Rightarrow G_{ji}(q, \theta_0) = G_{ji}(q, \theta_1),$$

for all $\theta_1 \in \Theta$.

The attractive feature of the above result is that $T_{\mathcal{W}\mathcal{X}}(q, \theta)$ can now be taken as a starting point for analyzing identifiability. Recall the set \mathcal{X}_j defined in Section 2.5, and then an identifiability result similar to Corollary 3.1 can be obtained, whose proof is analogous to the proof of [69, Theorem V.1] and thus omitted.

Lemma 3.1. *Consider the notion of generic identifiability in Definition 3.2 and any subset $\bar{\mathcal{W}}_j \subseteq \mathcal{W}_j^-$. Let \mathcal{M}_Θ be a parametric model set satisfying Assumptions 3.1 and 3.2. Then $G_{j\bar{\mathcal{W}}_j}(q)$ is generically identifiable in \mathcal{M}_Θ from (w, r) if*

$$\text{rank}[T_{\bar{\mathcal{W}}_j\mathcal{X}_j}(q, \theta)] = |\bar{\mathcal{W}}_j|, \text{ and} \tag{3.4a}$$

$$\text{rank}[T_{\mathcal{W}_j^-\mathcal{X}_j}(q, \theta)] = \text{rank}[T_{\bar{\mathcal{W}}_j\mathcal{X}_j}(q, \theta)] + \text{rank}[T_{(\mathcal{W}_j^-\setminus\bar{\mathcal{W}}_j)\mathcal{X}_j}(q, \theta)] \tag{3.4b}$$

hold for almost all $\theta_0 \in \Theta$.

Note that the mappings from both r and e , i.e. the vertices in \mathcal{X}_j , to $\bar{\mathcal{W}}_j$ are considered in Lemma 3.1, which provides a more relaxed condition for generic identifiability than Corollary 3.1. This is achieved by exploiting the spectrum $\Phi(z)$ in Definition 3.2 under Assumptions 3.1 and 3.2. The incorporation of the noise information is also of practical importance, since in many cases no measured r signal is available, e.g., when the data is observational and collected without the user's intervention as considered in [96, 138, 156]. However, Lemma 3.1 only provides a sufficient condition, in contrast to the necessary and sufficient condition in Corollary 3.1. The generic identifiability concept in Definition 3.2 leads to an issue when the necessity is considered in Lemma 3.1, as discussed as follows.

To verify the necessity of (3.4) in Lemma 3.1, we need to show that there exists a different network model M_2 which belongs to \mathcal{M}_Θ and is not distinguishable from $M(\theta_1)$, when (3.4) are not satisfied for θ_1 . An additional assumption is then required such that M_2 is an element of \mathcal{M}_Θ . This extra assumption considered in [169, Theorem 2] is to make set \mathcal{M}_Θ sufficiently large, i.e., every parameterized transfer function in \mathcal{M}_Θ covers all possible transfer functions. However, to satisfy this assumption, the dimension of θ should approach infinity, which contradicts the concept of genericity from [69] in both Definitions 3.1 and 3.2, where the definition of measure zero is restricted to finite-dimensional parameters [112]. Therefore, the necessity in Lemma 3.1 cannot be achieved by the notion of genericity in [69] and parametric model sets \mathcal{M}_Θ .

Since the necessity of the identifiability conditions requires an infinite dimensional parameter, we need to analyze identifiability in parametric model sets and in non-parametric model sets separately. For the non-parametric model sets, in contrast to Definitions 3.1 and 3.2, we introduce a different notion of genericity in this chapter such that the notion is not limited to finite-dimensional parameters. More importantly, with the above notion, we will show that a sufficient and necessary condition for the model-set-based identifiability can be obtained for non-parametric model sets. On the other hand, since parametric model sets depend on finite-dimensional parameters, we will show that only sufficient conditions for the model-set-based identifiability can be obtained for parametric model sets. We will also summarize the above results to obtain conditions that are valid for generic identifiability in both parametric model sets and non-parametric model sets.

3.3 GENERIC IDENTIFIABILITY: REVISIT

The limitation of the generic identifiability concept in Definition 3.2 is mainly due to the finite-dimensional parameter space, such that the necessity in Lemma 3.1 cannot be achieved. Therefore, we consider a different genericity notion in a topological space for non-parametric model sets [148].

This genericity notion is defined based on the concept of *open and dense sets* [7, 130]. Consider a metric space (\mathcal{A}, d) , where \mathcal{A} is a set and d is a metric function. An *open ball* of center

$x_0 \in \mathcal{A}$ and radius $r > 0$, where r is a real number, is defined as

$$\mathcal{B}(x_0, r) \triangleq \{x \in \mathcal{A} \mid d(x, x_0) < r\}.$$

Then a subset $\mathcal{A}_1 \subseteq \mathcal{A}$ is said to be *open*, if for any $x_0 \in \mathcal{A}_1$, there exists a $r > 0$ such that $\mathcal{B}(x_0, r) \subseteq \mathcal{A}_1$. Therefore, the openness reflects the robustness of the subset, such that a small perturbation of its element still leads to an element in the set. Furthermore, \mathcal{A}_1 is said to be *dense* in the metric space \mathcal{A} if every open ball of \mathcal{A} contains an element in \mathcal{A}_1 . The denseness shows that \mathcal{A}_1 is universal, i.e., an element in \mathcal{A} either belongs to \mathcal{A}_1 , or an arbitrarily small perturbation of the element can lead to an element in \mathcal{A}_1 .

Then the following notion of genericity and “almost all” is considered for non-parametric model sets.

Definition 3.3. *Given a metric space (\mathcal{A}, d) , a property is said to hold generically in \mathcal{A} , or hold for almost all points in \mathcal{A} , if there exists an open and dense subset $\bar{\mathcal{A}}$ in the metric space such that all points in $\bar{\mathcal{A}}$ have the property.*

To define generic identifiability based on the above genericity notion, we consider a metric space (\mathcal{M}, d) with a network model set \mathcal{M} and its metric function $d(M_1, M_2)$, where for any two models M_1 and M_2 in \mathcal{M} , the metric $d(M_1, M_2)$ is defined to be equal

$$\|(\|G_1(z) - G_2(z)\|_\infty, \|R_1(z) - R_2(z)\|_\infty, \|H_1(z) - H_2(z)\|_\infty, \|\Lambda_1 - \Lambda_2\|_\infty)\|_1,$$

where $\|\cdot\|_1$ and $\|\cdot\|_\infty$ denote l_1 -norm of a vector and the H_∞ norm of a transfer matrix, respectively. Note that the C matrix does not appear in the definition of the metric as all the models in \mathcal{M} have the same C matrix, as defined in Definition 2.1. For simplicity, we use \mathcal{M} without the metric d to represent the metric space throughout this thesis. Then we introduce the following definition of generic identifiability by considering the metric space \mathcal{M} , rather than the parameter space of \mathcal{M}_Θ .

Definition 3.4. *Given a non-parametric network model set \mathcal{M} , consider $M_0 \in \mathcal{M}$ and the following implication: For all $M_1 \in \mathcal{M}$,*

$$\left. \begin{aligned} CT_0(q)R(q) &= CT_1(q)R_1(q) \\ C\Phi_0(z)C^\top &= C\Phi_1(z)C^\top \end{aligned} \right\} \Rightarrow G_{ji,0}(q) = G_{ji,1}(q), \quad (3.5)$$

where $G_{ji,0}(q)$ and $G_{ji,1}(q)$ denote the module $G_{ji}(q)$ in M_0 and M_1 , respectively. Then $G_{ji}(q)$ is generically identifiable from (w_C, r) if the implication (3.5) holds for almost all $M_0 \in \mathcal{M}$, or equivalently, for all M_0 in an open and dense subset of \mathcal{M} .

The above definition considers the non-parametric model sets that are not limited to finite-dimensional parameters. Even if we consider the case where $C = I$ in this chapter, Definition 3.4

is formulated in a general form by incorporating the C matrix. With the new concepts, sufficient and necessary conditions for generic identifiability will be developed.

Remark 3.1. *The concept of generic identifiability in Definition 3.4 also extends trivially to a parametric model set \mathcal{M}_Θ . In this case, $G_{ji}(q, \theta)$ is generically identifiable if the implication (3.3) holds for almost all $\theta_0 \in \Theta$. For the notion of almost all in the parameter space, we can consider either all $\theta_0 \in \Theta$ except a set of Lebesgue measure zero or all θ_0 in an open and dense subset of Θ .*

Remark 3.2. *Definition 3.4 also extends trivially to global identifiability: $G_{ji}(q)$ is globally identifiable from (w_C, r) if the implication (3.5) holds for all $M_0 \in \mathcal{M}$.*

When $C = I$, the noise spectrum $\Phi(z)$ in Definition 3.4 can be exploited analogously as in Proposition 3.1 under Assumptions 3.1 and 3.2. Therefore, instead of $T(q)R(q)$ and $\Phi(z)$ in Definition 3.4, the mapping $T_{\mathcal{W}\mathcal{X}}(q)$ can be taken as a starting point for analyzing generic identifiability in the sense of Definition 3.4.

Corollary 3.2. *Consider a network model set \mathcal{M} that satisfies Assumptions 3.1, 3.2, and $C = I$. Then implication (3.5) is equivalently formulated as for all $M_1 \in \mathcal{M}$,*

$$T_{\mathcal{W}\mathcal{X},0}(q) = T_{\mathcal{W}\mathcal{X},1}(q) \Rightarrow G_{ji,0}(q) = G_{ji,1}(q).$$

3.4 ALGEBRAIC CONDITIONS

Sufficient conditions for the generic identifiability of modules in a parametric model set, in the sense of Remark 3.1, have been presented in Lemma 3.1. When the genericity notion based on open and dense subsets is concerned, we only need to interpret the notion of almost all in Lemma 3.1 based on open and dense sets. However, as discussed in Section 3.2, the necessity of (3.4) in Lemma 3.1 requires an additional assumption, i.e. every entry in the model set covers all possible transfer functions. This assumption requires an infinite-dimensional parameter, and thus we need to analyze the necessity for non-parametric model sets. In addition, the above assumption makes the model set unnecessarily large, and thus we will also develop a less conservative condition as follows.

To introduce this condition, we first define a new model set associated with \mathcal{M} .

Definition 3.5. *Given a non-parametric model set \mathcal{M} , \mathcal{M}_0 associated with \mathcal{M} is a set that contains all the network models such that:*

- \mathcal{M}_0 has the same fixed entries as in \mathcal{M} ;
- \mathcal{M}_0 satisfies Assumption 3.1 if \mathcal{M} satisfies Assumption 3.1;

- \mathcal{M}_0 has the same feedthrough structure as \mathcal{M} if \mathcal{M} satisfies Assumption 3.2, i.e., (i) $G(q)$ of all the models in \mathcal{M}_0 is strictly proper if \mathcal{M} satisfies Assumption 3.2(a), and (ii) if \mathcal{M} satisfies Assumption 3.2(b), \mathcal{M}_0 and \mathcal{M} satisfy Assumption 3.2(b) under the same permutation matrix as described in Definition 2.4.

The above construction of \mathcal{M}_0 means that \mathcal{M}_0 is the largest model set that shares the same properties, i.e. the same fixed entries and feedthrough structure, with \mathcal{M} . With the set \mathcal{M}_0 , we introduce the following topological condition on \mathcal{M} .

Assumption 3.3. Consider a non-parametric model set \mathcal{M} and its associated \mathcal{M}_0 , \mathcal{M} is a non-empty open subset of \mathcal{M}_0 .

Note that the rank condition in Lemma 3.1 can only be shown as a sufficient condition for parametric model sets and generic identifiability in the sense of Remark 3.1. This sufficient condition also extends trivially to non-parametric model sets and the generic identifiability concept in Definition 3.4. More importantly, we can show that the rank condition is necessary by considering non-parametric model sets under Assumption 3.3 and the generic identifiability concept in Definition 3.4.

Theorem 3.1. Let \mathcal{M} be a non-parametric model set satisfying Assumptions 3.1 and 3.2, and consider any subset $\bar{\mathcal{W}}_j \subseteq \mathcal{W}_j^-$. Then $G_{j\bar{\mathcal{W}}_j}(q)$ is generically identifiable in \mathcal{M} from (w, r) if

$$\text{rank}[T_{\bar{\mathcal{W}}_j, \mathcal{X}_j}(q)] = |\bar{\mathcal{W}}_j|, \text{ and} \quad (3.6a)$$

$$\text{rank}[T_{\mathcal{W}_j^-, \mathcal{X}_j}(q)] = \text{rank}[T_{\bar{\mathcal{W}}_j, \mathcal{X}_j}(q)] + \text{rank}[T_{(\mathcal{W}_j^- \setminus \bar{\mathcal{W}}_j), \mathcal{X}_j}(q)] \quad (3.6b)$$

hold for almost all $M \in \mathcal{M}$. If \mathcal{M} additionally satisfies Assumption 3.3, the above rank conditions are also necessary for the generic identifiability of $G_{j\bar{\mathcal{W}}_j}(q)$.

The proof of the above theorem is presented in Section 3.7.

We have obtained rank conditions for generic identifiability in parametric model sets as shown in Lemma 3.1 and in non-parametric model sets as shown in Theorem 3.1. While the rank tests in the above results require computing the inverse of $I - G(q)$, these tests can be further simplified without the need to invert $I - G(q)$.

Lemma 3.2. Consider a dynamic network and any subsets $\bar{\mathcal{W}} \subseteq \mathcal{W}$ and $\bar{\mathcal{X}} \subseteq \mathcal{X}$. Define the matrix $F(\bar{\mathcal{W}}, \bar{\mathcal{X}})$ as

$$F(\bar{\mathcal{W}}, \bar{\mathcal{X}}) \triangleq \begin{bmatrix} (G(q) - I)_{\mathcal{W}(\mathcal{W} \setminus \bar{\mathcal{W}})} & X_{\mathcal{W}\bar{\mathcal{X}}}(q) \end{bmatrix}. \quad (3.7)$$

Then it holds that

$$\text{rank}[T_{\bar{\mathcal{W}}, \bar{\mathcal{X}}}(q)] = \text{rank}[F(\bar{\mathcal{W}}, \bar{\mathcal{X}})] + |\bar{\mathcal{W}}| - L, \quad (3.8)$$

where L is the total number of internal signals.

Proof. Recall that $T_{\bar{\mathcal{W}}\bar{\mathcal{X}}} = C(I - G)^{-1}\bar{\mathcal{X}}$, where $\bar{\mathcal{X}} = X_{\mathcal{W}\bar{\mathcal{X}}}$ and C is a selection matrix that extracts the rows of $(I - G)^{-1}$ corresponding to $\bar{\mathcal{W}}$. Define

$$\bar{F} = \begin{bmatrix} G - I & \bar{\mathcal{X}} \\ C & 0 \end{bmatrix}, \quad (3.9)$$

then according to [154], we have

$$\bar{F} = \begin{bmatrix} I & 0 \\ C(G - I)^{-1} & I \end{bmatrix} \begin{bmatrix} G - I & 0 \\ 0 & C(I - G)^{-1}\bar{\mathcal{X}} \end{bmatrix} \begin{bmatrix} I & (G - I)^{-1}\bar{\mathcal{X}} \\ 0 & I \end{bmatrix}.$$

According to the above equation, $\text{rank}(\bar{F}) = \text{rank}(T_{\bar{\mathcal{W}}\bar{\mathcal{X}}}) + L$. Based on (3.7) and (3.9), F is obtained from \bar{F} by removing the columns in \bar{F} that correspond to the nonzero entries of C , and these columns are linearly independent in F due to the structure of C . Then it follows that $\text{rank}(F) = \text{rank}(\bar{F}) - |\bar{\mathcal{W}}|$, which proves the result. \square

Based on (3.8), the rank conditions in Theorem 3.1 can be reformulated straightforwardly as follows.

Proposition 3.2. *Consider a non-parametric network model set and the matrix F defined in (3.7). The conditions (3.6) in Theorem 3.1 are equivalently reformulated as $F(\bar{\mathcal{W}}_j, \mathcal{X}_j)$ is full row rank and*

$$\text{rank}[F(\mathcal{W}_j^-, \mathcal{X}_j)] = \text{rank}[F(\bar{\mathcal{W}}_j, \mathcal{X}_j)] + \text{rank}[F(\mathcal{W}_j^- \setminus \bar{\mathcal{W}}_j, \mathcal{X}_j)] - L,$$

for almost all $M \in \mathcal{M}$.

A similar result to the above one can be obtained for parametric model sets, by combining (3.4) and (3.8). Thus, efficient rank tests for identifiability can be conducted without the need to invert $I - G(q)$.

3.5 PATH-BASED CONDITIONS

3.5.1 PATH-BASED CONDITIONS FOR NON-PARAMETRIC MODEL SETS

It is attractive to derive graph-based conditions for identifiability when considering complex networks, since these conditions can be tested efficiently by inspecting the network topology rather than analyzing the dynamics of the network. Here, we first derive path-based conditions for non-parametric model sets and the concept of generic identifiability in Definition 3.4. In this setting, we are able to derive necessary and sufficient path-based conditions.

As shown in [14, 69], when a parametric model set is considered as in Definition 3.2, path-based conditions can be obtained from Lemma 3.1 by using the following path-rank relationship [14, 69]: for all θ except a set of measure zero, it holds that

$$b_{\bar{\mathcal{X}} \rightarrow \bar{\mathcal{W}}} = \text{rank}[T_{\bar{\mathcal{W}}\bar{\mathcal{X}}}(q, \theta)], \quad (3.10)$$

where $b_{\bar{\mathcal{X}} \rightarrow \bar{\mathcal{W}}}$ denotes the maximum number of vertex disjoint paths from $\bar{\mathcal{X}}$ to $\bar{\mathcal{W}}$ in the graph associated with the parametric model set. Equation (3.10) is an attractive result since it shows opportunities to conduct the rank tests in the identifiability conditions, e.g. the ones in Theorem 3.1, in a graphical way.

However, (3.10) only holds when finite-dimensional models are considered since this result is based on the property of analytic functions defined on finite-dimensional spaces, as shown in the proof of [69, Lemma V.2] and [102]. In addition, (3.10) has been derived for the particular situation where $X(q) = I$, and there is no non-zero fixed/known modules in the model set.

The issues caused by known transfer functions and non-parametric models are explained in the following example.

Example 3.1. Firstly, we recall the path-rank relation (3.10) from [14, 69] for parametric model sets. Consider two parametric network model sets whose graphs are indicated in Fig. 3.1, where the model set in (b) contains known non-zero modules, indicated by the double-lined arrows. In addition, assume $R_{11}(q) = R_{22}(q) = 1$ to match the setting in [14, 69] such that (3.10) is applicable.

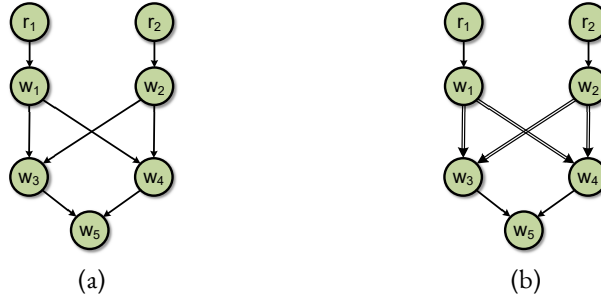


Figure 3.1: Two network model sets where (b) contains known modules (double-lined edges) while (a) has only unknown modules.

Then for the model set in Fig. 3.1(a), it holds $b_{\{r_1, r_2\} \rightarrow \{w_3, w_4\}} = 2$, i.e. there exist maximally two paths, e.g., $r_1 \rightarrow w_1 \rightarrow w_3$ and $r_2 \rightarrow w_2 \rightarrow w_4$, that are vertex disjoint. According to (3.10), this implies that

$$\text{rank}[T_{\{w_3, w_4\}\{r_1, r_2\}}(q, \theta)] = 2,$$

for all θ except a set of measure zero. This can also be seen from

$$\det[T_{\{w_3, w_4\}\{r_1, r_2\}}(q, \theta)] = G_{31}(q, \theta)G_{42}(q, \theta) - G_{41}(q, \theta)G_{32}(q, \theta). \quad (3.11)$$

As each module is an analytic function of independent parameters, the determinant is a non-constant analytic function of θ and thus only vanishes on a set of measure zero. This matches with (3.10) that $b_{\{r_1, r_2\} \rightarrow \{w_3, w_4\}} = \text{rank}[T_{\{w_3, w_4\}\{r_1, r_2\}}(q, \theta)] = 2$ for almost all θ .

However, $T_{\{w_3, w_4\}\{r_1, r_2\}}(q, \theta)$ may not be full rank in the situation of Fig. 3.1(b) if the known modules $G_{31}^0(q)$, $G_{42}^0(q)$, $G_{41}^0(q)$, $G_{32}^0(q)$ take values such that

$$G_{31}^0(q)G_{42}^0(q) - G_{41}^0(q)G_{32}^0(q) = 0. \quad (3.12)$$

Then $\det[T_{\{w_3, w_4\}\{r_1, r_2\}}(q, \theta)] = 0$ for all parameter values, and thus the path-rank relation in (3.10) fails.

In addition, if Fig. 3.1(a) denotes a non-parametric model set instead, (3.11) is not a function of a finite-dimensional parameter, and thus the reasoning in (3.11) based on parametric model sets with a finite-dimensional parameter does not apply.

As shown in Example 3.1, the presence of known transfer functions may cause equality in (3.10) to fail. To circumvent this, an additional condition is introduced based on the concept of structural rank.

Definition 3.6 ([145]). *The structural rank of a matrix is the maximum rank of all matrices with the same nonzero pattern. A matrix has full structural rank if it can be permuted so that the diagonal has no zero entries.*

The property of structural full rank depends solely on the sparsity pattern of the matrix and does not depend on the numerical values of the entries. In order to characterize and exclude the situations caused by fixed modules as presented in Example 3.1, we introduce the following regularity condition on the known entries.

Assumption 3.4. *In model set \mathcal{M} , the rank of any submatrix of $[G(q) - IX(q)]$, that contains only known entries, is equal to its structural rank.*

The above assumption prevents the fixed/known modules in the model set from inducing a loss of generic rank. For example, recall (3.12) where the mapping

$$T_{\{w_3, w_4\}\{r_1, r_2\}}(q) = \begin{bmatrix} G_{31}^0(q) & G_{32}^0(q) \\ G_{41}^0(q) & G_{42}^0(q) \end{bmatrix}$$

is singular even if it has a full structural rank, and this singular mapping causes the path-rank relationship in (3.10) to fail as discussed in Example 3.1. However, since $T_{\{w_3, w_4\}\{r_1, r_2\}}(q)$ is a submatrix of $[G(q) - IX(q)]$, Assumption 3.4 prevents the situation in (3.12) and thus the mapping $T_{\{w_3, w_4\}\{r_1, r_2\}}(q)$ will always be full rank under this assumption.

With Assumption 3.4 and then as a first step to obtain the path-rank relation for non-parametric model sets with fixed entries, the following result can be formulated.

Lemma 3.3. *Consider a non-parametric model set \mathcal{M} that satisfies Assumption 3.3 and 3.4. Then for any subsets $\bar{\mathcal{W}} \subseteq \mathcal{W}$ and $\bar{\mathcal{X}} \subseteq \mathcal{X}$, $T_{\bar{\mathcal{W}}\bar{\mathcal{X}}}(q)$ is full rank for almost all $M \in \mathcal{M}$ if and only if $F(\bar{\mathcal{W}}, \bar{\mathcal{X}})$, as defined in (3.7), has full structural rank.*

The proof of Lemma 3.3 is presented in Section 3.7, where the instrumental Lemma 3.7 plays an important role. This result suggests that testing the generic rank of $T_{\bar{\mathcal{W}}\bar{\mathcal{X}}}(q)$ does not require to check the numerical values of the network matrices, while only the sparsity pattern of $F(\bar{\mathcal{W}}, \bar{\mathcal{X}})$ needs to be investigated. Then due to the connection between the graph of a model set and F 's sparsity pattern, this result allows us to formulate the equivalence between generic rank and vertex disjoint paths that also applies to non-parametric model sets with known modules.

Theorem 3.2. *Consider a non-parametric model set \mathcal{M} that satisfies Assumptions 3.3 and 3.4. Then for any subsets $\bar{\mathcal{W}} \subseteq \mathcal{W}$ and $\bar{\mathcal{X}} \subseteq \mathcal{X}$, the transfer matrix $T_{\bar{\mathcal{W}}\bar{\mathcal{X}}}(q)$ satisfies*

$$b_{\bar{\mathcal{X}} \rightarrow \bar{\mathcal{W}}} = \text{rank}[T_{\bar{\mathcal{W}}\bar{\mathcal{X}}}(q)] \text{ for almost all } M \in \mathcal{M}.$$

Proof. With Lemma 3.3, the proof of this theorem is then analogous to the proof of Proposition V.1 in [69]: For $\text{rank}(T_{\bar{\mathcal{W}}\bar{\mathcal{X}}}) \geq b_{\bar{\mathcal{X}} \rightarrow \bar{\mathcal{W}}}$ generically, consider a subgraph of the network containing all the vertices but only the edges of the paths from a set of maximum number vertex disjoint paths from $\bar{\mathcal{X}}$ to $\bar{\mathcal{W}}$. Let $\bar{\mathcal{X}}_1 \subseteq \bar{\mathcal{X}}$ and $\bar{\mathcal{W}}_1 \subseteq \bar{\mathcal{W}}$ denote the starting and ending vertices of the vertex disjoint paths, respectively. The obtained subgraph's structure can then be encoded by matrices A and B with only zeros and ones, where $A_{ji} = 1$ and $B_{kn} = 1$ if and only if G_{ji} and X_{kn} denote the edges in the subgraph, respectively. Then following the same analysis of Proposition V.1 in [69], we can show that $C(I - A)^{-1}B_{\mathcal{W}\bar{\mathcal{X}}_1}$ is a permutation matrix and thus has full rank that equals $b_{\bar{\mathcal{X}} \rightarrow \bar{\mathcal{W}}}$, where C is a binary matrix that extracts rows of $(I - A)^{-1}$ corresponding to $\bar{\mathcal{X}}_1$. Then following Lemma 3.2 similarly, it holds that

$$\begin{bmatrix} (A - I)_{\mathcal{W}(\mathcal{W} \setminus \bar{\mathcal{W}}_1)} & B_{\mathcal{W}\bar{\mathcal{X}}_1} \end{bmatrix}$$

is full rank, and thus $F(\bar{\mathcal{W}}_1, \bar{\mathcal{X}}_1)$ defined in (3.7) is structural full rank. Then based on Lemma 3.3, $T_{\bar{\mathcal{W}}_1\bar{\mathcal{X}}_1}$ is generically full rank that equals $b_{\bar{\mathcal{X}} \rightarrow \bar{\mathcal{W}}}$, and thus $\text{rank}(T_{\bar{\mathcal{W}}\bar{\mathcal{X}}}) \geq b_{\bar{\mathcal{X}} \rightarrow \bar{\mathcal{W}}}$ generically.

For $\text{rank}(T_{\bar{\mathcal{W}}\bar{\mathcal{X}}}) \leq b_{\bar{\mathcal{X}} \rightarrow \bar{\mathcal{W}}}$ generically, a minimum $\bar{\mathcal{X}} - \bar{\mathcal{W}}$ disconnecting set can be considered as in [69], which leads to permuted network matrices with block zeros (as also explored later in (4.10)). Then the proof can be achieved similarly as in [69]. Note that [69] requires its Lemma V.2 to ensure the invertibility of certain submatrix $I - G_{\bar{\mathcal{W}}_1\bar{\mathcal{W}}_1}$, which is guaranteed by Assumption 2.1(b) in this work and thus the lemma is not needed. \square

By combining Theorem 3.1 and Theorem 3.2, we can now formulate the path-based condition for generic identifiability, that follows immediately from the previous results.

Theorem 3.3. *Consider a non-parametric model set \mathcal{M} that satisfies Assumptions 3.1, 3.2, 3.3 and 3.4, and let $\bar{\mathcal{W}}_j$ be any subset of \mathcal{W}_j^- . Then the modules in $G_{j\bar{\mathcal{W}}_j}(q)$ are generically identifiable in \mathcal{M} from (w, r) if and only if the following conditions hold for the graph associated with \mathcal{M} :*

$$b_{\mathcal{X}_j \rightarrow \bar{\mathcal{W}}_j} = |\bar{\mathcal{W}}_j|, \text{ and} \quad (3.13a)$$

$$b_{\mathcal{X}_j \rightarrow \mathcal{W}_j^-} = b_{\mathcal{X}_j \rightarrow \bar{\mathcal{W}}_j} + b_{\mathcal{X}_j \rightarrow \mathcal{W}_j^- \setminus \bar{\mathcal{W}}_j}. \quad (3.13b)$$

In the above theorem, condition (3.13a) requires that all the inputs of the target modules are excited by external signals through vertex disjoint paths. In addition, (3.13b) ensures that the excitation signals for the inputs of interest $\bar{\mathcal{W}}_j$ and the other inputs $\mathcal{W}_j^- \setminus \bar{\mathcal{W}}_j$ of w_j are independent.

Similar to [69], generic identifiability can be analyzed by inspecting path-based properties of \mathcal{G} only. Given \mathcal{G} , standard graphical algorithms are available for computing the maximum number of vertex disjoint paths [135]. Note that the conditions (3.13) are similar to the ones in [69], but now applied to a different situation. Besides the handling of fixed (known) modules in the model set, the result is obtained for the notion of generic identifiability in Definition 3.4 and more importantly, the non-parametric model sets that are not limited to a finite-dimensional parameter space. In addition, the set \mathcal{X}_j contains both measured excitation signals and unmeasured noise signals, which is in contrast to [69] where only measured excitation signals are considered. Thus, to satisfy the graphical conditions in Theorem 3.3, the noises can compensate for a possible lack of excitation signals, which significantly relaxes the requirement on the number of measured excitation signals for generic identifiability.

3.5.2 PATH-BASED CONDITIONS FOR PARAMETRIC MODEL SETS

As shown in [69], the path-rank relation (3.10) can also lead to a path-based condition similar to Theorem 3.3 for a parametric model set with the corresponding identifiability concept in Remark 3.1. This result in [69] concerns the genericity notion based on the concept of measure zero and does not take into account the prior known modules in the network, as illustrated in Example 3.1. Therefore, we extend (3.10) from [69] to incorporate the genericity concept based on open dense sets and the prior known modules in the parametric model set by making use of Assumption 3.4.

Proposition 3.3. *Consider a parametric model set \mathcal{M}_Θ that satisfies Assumptions 2.2 and 3.4, any subsets $\bar{\mathcal{W}} \subseteq \mathcal{W}$ and $\bar{\mathcal{X}} \subseteq \mathcal{X}$. The transfer matrix $T_{\bar{\mathcal{W}}\bar{\mathcal{X}}}(q, \theta)$ satisfies*

$$b_{\bar{\mathcal{X}} \rightarrow \bar{\mathcal{W}}} = \text{rank}[T_{\bar{\mathcal{W}}\bar{\mathcal{X}}}(q, \theta)] \text{ for all } \theta \in \tilde{\Theta} \subseteq \Theta, \quad (3.14)$$

where set $\tilde{\Theta}$ satisfies the following properties:

1. $\tilde{\Theta}$ is an open and dense subset of Θ and

2. $\Theta \setminus \tilde{\Theta}$ has Lebesgue measure zero.

Proof. The rank-path relationship with property (2) follows analogously from [69] and the proof of Theorem 3.2 to deal with the prior known entries by exploiting Assumption 3.4. The main tool in [69] is based on the openness and connectedness of Θ , and the property of the zero set of complex analytic functions [64, Corollary 10].

To prove the result with property 1, let $\mathbb{C}_1 \subset \mathbb{C}$ denote the complex region outside of the unit circle, and let $\bar{\Theta}$ denote the set of parameters such that $\det[F(z, \theta)] = 0$ for all $z \in \mathbb{C}_1$. Then we only need to modify Lemma 3.7 by proving that if $\det[F(z, \theta)]$ is not constant zero, it becomes zero (as a function of z) only for a closed and nowhere dense subset of Θ , and then the result follows similarly as the proofs of Lemma 3.3 and Theorem 3.2. The above proof can be achieved by contradiction as follows. Assuming that $\bar{\Theta}$ is not a closed nowhere dense set, then $\bar{\Theta}$ must contain a limit point of $\bar{\Theta}$. As $\det[F(z, \theta)]$ is a complex analytic function in $\mathbb{C}_1 \times \bar{\Theta}$, it holds that $\det[F(z, \theta)] = 0$ for all $(z, \theta) \in \mathbb{C}_1 \times \bar{\Theta}$ by the identity theorem [2] and the openness and connectedness of Θ , which contradict that it is not constant zero. This concludes that $\det[F(z, \theta)]$ is zero (as a function of z) only for a closed and nowhere dense subset of Θ if it is not constant zero, and thus $\tilde{\Theta} = \Theta \setminus \bar{\Theta}$ is open and dense in Θ . \square

It can be found that the path-rank relation in (3.14) holds for both the genericity notion based on Lebesgue measure and the notion based on open and dense sets. In addition, by combining Lemma 3.1 and Proposition 3.3, the path-based condition in Theorem 3.4 can be obtained as a sufficient condition for the concept of generic identifiability in Remark 3.1 for \mathcal{M}_Θ , with either the genericity notion based on the measure zero or the one based on open dense sets.

Corollary 3.3. *Consider a parametric model set \mathcal{M}_Θ that satisfies Assumptions 2.2, 3.1, 3.2 and 3.4, module $G_{ji}(q)$ is generically identifiable in \mathcal{M}_Θ from (w, r) if (3.13) hold for the graph associated with \mathcal{M}_Θ .*

However, the necessity in the above result cannot be achieved since Assumption 3.3 is still required, leading to an infinite-dimensional parameter and thus a non-parametric model set.

3.5.3 PATH-BASED CONDITIONS: SUMMARY

Since the path-based conditions (3.13) are sufficient for the generic identifiability of modules in both non-parametric model sets, as shown in Theorem 3.3, and parametric model sets, as shown in Corollary 3.3, we will merge the above graphical results to obtain a more compact result that is valid for both parametric and non-parametric model sets.

Firstly, we summarize the different assumptions in Theorem 3.3 and Corollary 3.3 on parametric and non-parametric model sets into a single assumption. Recall from Remark 2.1 that a model set \mathcal{M} may refer to either a non-parametric model set or a parametric model set.

Assumption 3.5. *Given a network model set \mathcal{M} ,*

- (a) if \mathcal{M} is a non-parametric model set, it satisfies Assumption 3.3;
- (b) If \mathcal{M} is a parametric model set, it satisfies Assumptions 2.2.

The above different assumptions are required because the identifiability analysis of the parametric model sets lies in the parameter space, while the analysis of the non-parametric model sets depends on the model space. Then Theorem 3.3 for non-parametric model sets and Corollary 3.3 for parametric model sets can be summarized into a more compact result.

Theorem 3.4. *Consider a model set \mathcal{M} that satisfies Assumptions 3.1, 3.2, 3.4 and 3.5, and let $\bar{\mathcal{W}}_j$ be any subset of \mathcal{W}_j^- . Then the modules in $G_{j\bar{\mathcal{W}}_j}(q)$ are generically identifiable in \mathcal{M} from (w, r) if the following conditions hold for the graph associated with \mathcal{M} :*

$$b_{\mathcal{X}_j \rightarrow \bar{\mathcal{W}}_j} = |\bar{\mathcal{W}}_j|, \text{ and} \quad (3.15a)$$

$$b_{\mathcal{X}_j \rightarrow \mathcal{W}_j^-} = b_{\mathcal{X}_j \rightarrow \bar{\mathcal{W}}_j} + b_{\mathcal{X}_j \rightarrow \mathcal{W}_j^- \setminus \bar{\mathcal{W}}_j}. \quad (3.15b)$$

If \mathcal{M} is additionally a non-parametric model set, the above conditions are also necessary for the generic identifiability of $G_{j\bar{\mathcal{W}}_j}(q)$.

The above result applies to both parametric and non-parametric model sets, where the necessity of the path-based conditions can be achieved when a non-parametric model set, that satisfies Assumption 3.3, is concerned. It is important to keep in mind that the generic identifiability of non-parametric model sets is based on the genericity notion in the model space, while the generic identifiability of parametric model sets is based on the genericity notion in the parameter space.

Example 3.2. *Consider a network model set with its graph depicted in Figure 3.2(a). The modules $G_{54}^0(q)$ and $G_{21}^0(q)$ are known, and there are two external signals e_1 and r_4 . The goal is to analyze the generic identifiability of all the modules in Figure 3.2(a) using Theorem 3.4. To this end, we need to check conditions (3.15) with $\mathcal{W}_j^- = \bar{\mathcal{W}}_j$ for all j , and thus in this special case, (3.15) can be reformulated equivalently as*

$$b_{\mathcal{X}_j \rightarrow \mathcal{W}_j^-} = |\mathcal{W}_j^-|. \quad (3.16)$$

The internal signals that have unknown in-coming modules are w_5 and w_3 , while the in-coming module $G_{21}^0(q)$ of w_2 is known, and w_4 does not have any internal signal as an in-neighbor. Therefore, we only need to verify condition (3.16) for $j = 5$ and $j = 3$.

When $j = 5$, we have $\mathcal{W}_5^- = \{w_2, w_3\}$ which contains the internal signals having unknown directed edges to w_5 . In addition, $\mathcal{X}_5 = \{e_1, r_4\}$ since the two external signals do not have unknown edges to w_5 . There are maximally two vertex disjoint paths from \mathcal{X}_5 to \mathcal{W}_5 , i.e. the path from e_1 via w_1 to w_2 and the one from r_4 via w_4 to w_3 , denoted by the red paths in Figure 3.2(a). Since $b_{\mathcal{X}_5 \rightarrow \mathcal{W}_5} = |\mathcal{W}_5| = 2$, the identifiability condition (3.16) holds for $j = 5$.

Similarly, when $j = 3$, we have $\mathcal{X}_3 = \{e_1, r_4\}$ and $\mathcal{W}_3^- = \{w_1, w_4\}$. It then holds that $b_{\mathcal{X}_3 \rightarrow \mathcal{W}_3^-} = |\mathcal{W}_3| = 2$, where the two vertex disjoint paths from \mathcal{X}_3 to \mathcal{W}_3 , i.e. the paths (e_1, w_1)

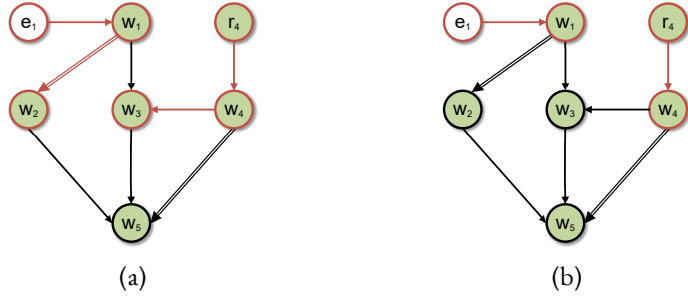


Figure 3.2: The graph of a network model set with G_{54}^0 and G_{21}^0 (double-lined edges) known. All the signals represented by green vertices are measured.

and (r_4, w_4) , are shown in red in Figure 3.2(b). This concludes the generic identifiability of all the unknown modules and thus the full network in Figure 3.2.

It can be found from Example 3.2 that by utilizing Theorem 3.4, generic identifiability can be verified graphically given the modeling assumptions on the topology of the network model set. This verification can be done efficiently since it is fully graphical and does not rely on the dynamics of the network models.

An important special case of Theorem 3.4 concerns identifiability of a single target module $G_{ji}(q)$, i.e. $\bar{\mathcal{W}}_j = \{w_i\}$. The identification of a single module has received considerable attention [48, 52, 59, 152], and the following identifiability condition for a single module is a prerequisite for the single module identification methods.

Corollary 3.4. *Consider a model set \mathcal{M} that satisfies Assumptions 3.1, 3.2, 3.4 and 3.5. Then module $G_{ji}(q)$ is generically identifiable in \mathcal{M} from (w, r) if the following conditions hold for the graph associated with \mathcal{M} :*

$$b_{\mathcal{X}_j \rightarrow \{w_i\}} = 1, \text{ and}$$

$$b_{\mathcal{X}_j \rightarrow \mathcal{W}_j^-} = b_{\mathcal{X}_j \rightarrow \{w_i\}} + b_{\mathcal{X}_j \rightarrow \mathcal{W}_j^- \setminus \{w_i\}}.$$

If \mathcal{M} is additionally a non-parametric model set, the above conditions are also necessary for generic identifiability of $G_{ji}(q)$.

In the above result, the condition $b_{\mathcal{X}_j \rightarrow \{w_i\}} = 1$ is equivalent to the condition that there is a directed path from \mathcal{X}_j to w_i .

3.6 CONCLUSIONS

The identifiability analysis for non-parametric model sets and parametric model sets has been investigated separately in this chapter. For the non-parametric model sets, a different notion of

genericity based on open and dense sets in a topological space has been introduced, and this notion is not limited to finite-dimensional parameters. With this genericity notion, sufficient and necessary algebraic and path-based conditions for generic identifiability are derived. Compared to the existing graphical results, these conditions also address the appearance of prior known modules and take advantage of noises as excitation sources. When a parametric model set with finite-dimensional parameters is considered, the formulated conditions for generic identifiability become only sufficient. Finally, the above identifiability results are combined into path-based conditions that are valid for the generic identifiability in both non-parametric and parametric model sets.

3.7 APPENDIX

3.7.1 PROOF OF THEOREM 3.1

We first prove the following lemma which is instrumental for establishing the necessity in this theorem.

Lemma 3.4. *Consider a model set \mathcal{M} that satisfies Assumptions 3.1 and 3.2 and its associated set \mathcal{M}_0 . If $M_0 \in \mathcal{M}$ does not satisfy (3.6), then for any positive real number r , there exists another model M_1 such that (i) M_1 differs from M_0 only in $G_{j\bar{\mathcal{W}}_j^-}(q)$; (ii) $M_1 \in \mathcal{M}_0$; (iii) $0 < d(M_0, M_1) < r$; (iv) M_1 and M_0 lead to the same mapping $T_{\mathcal{W}\mathcal{X}}(q)$.*

Proof. Recall the set \mathcal{X}_j , (2.7), (2.13) and for the simplicity of notation, we omit the dependency of transfer operators on q . Consider j th row of $(I - G)T_{\mathcal{W}\mathcal{X}} = X$ and its columns corresponding to signals in \mathcal{X}_j , and after permutation, it leads to

$$\begin{bmatrix} -G_{j\bar{\mathcal{W}}_j} & -G_{j(\mathcal{W}_j^- \setminus \bar{\mathcal{W}}_j)} & -G_{j\bar{\mathcal{W}}_j} & 1 & 0 \end{bmatrix} T_{\star\mathcal{X}_j} = X_j,$$

where X_j is a known vector by the definition of \mathcal{X}_j , $G_{j\bar{\mathcal{W}}_j}$ contains all the known non-zero entries in the j th row of $(I - G)$. Thus, the above equation leads to

$$\begin{bmatrix} -G_{j\bar{\mathcal{W}}_j} & -G_{j(\mathcal{W}_j^- \setminus \bar{\mathcal{W}}_j)} \end{bmatrix} \begin{bmatrix} T_{\bar{\mathcal{W}}_j\mathcal{X}_j} \\ T_{(\mathcal{W}_j^- \setminus \bar{\mathcal{W}}_j)\mathcal{X}_j} \end{bmatrix} = P, \quad (3.18)$$

where $P = X_j - T_{j\mathcal{X}_j} + G_{j\bar{\mathcal{W}}_j}T_{\bar{\mathcal{W}}_j\mathcal{X}_j}$ is given. Then based on Corollary 3.2, generic identifiability concerns if a unique vector $G_{j\bar{\mathcal{W}}_j}$ can be obtained given $T_{\mathcal{W}\mathcal{X}}$ and P , for almost all models in \mathcal{M} .

Consider the network matrix G_0 in M_0 and (3.6a). If $T_{\bar{\mathcal{W}}_j\mathcal{X}_j}$ formulated from M_0 is not full rank, then according to (3.6a), there exists a nonzero transfer vector Q such that $QT_{\bar{\mathcal{W}}_j\mathcal{X}_j} = 0$ and thus

$$\begin{bmatrix} -(G_{j\bar{\mathcal{W}}_j} + FQ) & -G_{j(\mathcal{W}_j^- \setminus \bar{\mathcal{W}}_j)} \end{bmatrix} \begin{bmatrix} T_{\bar{\mathcal{W}}_j\mathcal{X}_j} \\ T_{(\mathcal{W}_j^- \setminus \bar{\mathcal{W}}_j)\mathcal{X}_j} \end{bmatrix} = P, \quad (3.19)$$

where F is any non-zero scalar transfer operator. Consider now a new network model M_1 with network matrix G_1 , which is obtained from M_0 by replacing only $G_{j\bar{w}_j}$ in G_0 by $G_{j\bar{w}_j} + FQ$. Our goal is then to show that there exists an F , such that the obtained new network model M_1 satisfies conditions (i), (ii), (iii) and (iv). Note that by construction, M_1 already satisfies (i) and (iv) for any non-zero F .

To show that there exists an F such that condition (ii) holds, we need to find an F such that: G_1 satisfies Assumptions 2.1 (a), (b), (c) and Assumption 3.2; G_1 has the same feedthrough structure as G_0 ; and G_1 has the same fixed entries as G_0 . It can be found that F can be chosen as $F = aF_1$, where a is an arbitrarily small positive real number and F_1 satisfies the following conditions: F_1 is stable and has zeros equal all unstable poles of Q ; it has a delay of sufficiently high order such that F_1Q is strictly proper. Then with $F = aF_1$, it is straightforward that G_1 satisfies Assumption 2.1(a), (b), Assumption 3.2 and the conditions on its feedthrough structure and its fixed entries. Furthermore, G_1 can be shown to satisfy the Assumption 2.1(c) with $F = aF_1$ as follows. As $(I - G_0)^{-1}$ is stable, $1/\det(I - G_0)$ is also stable. Based on the Laplace formula, it holds that

$$\frac{1}{\det(I - G_0)} = \frac{1}{1 + [\sum_{i=1}^L (-1)^{i+j} g_{ji} M_{ji} - 1]}$$

where M_{ji} is the (j, i) minor of $I - G_0$ and g_{ji} is the (j, i) entry of $I - G_0$. Define that $L \triangleq \sum_{i=1}^L (-1)^{i+j} g_{ji} M_{ji} - 1$, and based on the Nyquist stability theorem, the Nyquist plot of $L(j\omega)$ for $\omega \in \mathbb{R}$ in the complex domain does not encircle point $(-1, 0)$, because $I - G_0$ is stable and thus L is stable.

Now consider G_1 , which differs from G_0 only in the j th row. It holds that

$$\det(I - G_1) = \sum_{i=1}^L (-1)^{i+j} (g_{ji} + a[F_1 G_1]_i) M_{ji},$$

where $[F_1 G_1]_i$ denotes the i th entry of vector $F_1 G_1$ and $[F_1 G_1]_i = 0$ for some i . Similarly,

$$\frac{1}{\det(I - G_1)} = \frac{1}{1 + \bar{L}(z)},$$

where $\bar{L} \triangleq L + a \sum_{i=1}^L (-1)^{i+j} [F_1 G_1]_i M_{ji}$. As the Nyquist plot of $L(j\omega)$ does not encircle $(-1, 0)$ and a is arbitrarily small, the real part and the imaginary part of $\bar{L}(j\omega) - L(j\omega)$ is arbitrarily small for all ω , and thus the Nyquist plot of $\bar{L}(j\omega)$ also does not encircle $(-1, 0)$. This means that there exists $F = aF_1$ such that $1/\det(I - G_1)$ and consequently $(I - G_1)^{-1}$ are stable because G_1 is stable. This concludes that with $F = aF_1$, G_1 satisfies Assumptions 2.1(c), and thus M_1 satisfies condition (ii). Finally, for condition (iii), with $F = aF_1$, $d(M_1, M_0) = \|G_1 - G_0\|_\infty = a\|\Delta\|_\infty$, where Δ is a matrix contains the vector $F_1 Q$ and has all the other entries as zeros. As a is arbitrarily small, $\|G_1 - G_0\|_\infty$ can also be made arbitrarily small, which concludes the proof

for the case that $T_{\bar{\mathcal{W}}_j \mathcal{X}_j}$ is not full row rank.

Secondly, consider (3.6b) and assume that the following holds:

$$\text{rank}(T_{\mathcal{W}_j^- \mathcal{X}_j}) < \text{rank}(T_{\bar{\mathcal{W}}_j \mathcal{X}_j}) + \text{rank}(T_{(\mathcal{W}_j^- \setminus \bar{\mathcal{W}}_j) \mathcal{X}_j}).$$

Then there exist a vector in the row space of $T_{\bar{\mathcal{W}}_j \mathcal{X}_j}$ which is linearly dependent on the row space of $T_{(\mathcal{W}_j^- \setminus \bar{\mathcal{W}}_j) \mathcal{X}_j}$. Equivalently, this means that there exist two non-zero vectors Q_1 and Q_2 such that $Q_1 T_{\bar{\mathcal{W}}_j \mathcal{X}_j} + Q_2 T_{(\mathcal{W}_j^- \setminus \bar{\mathcal{W}}_j) \mathcal{X}_j} = 0$, and thus it holds that

$$\begin{bmatrix} -(G_j \bar{\mathcal{W}}_j + F Q_1) & -(G_j(\mathcal{W}_j^- \setminus \bar{\mathcal{W}}_j) + F Q_2) \end{bmatrix} \begin{bmatrix} T_{\bar{\mathcal{W}}_j \mathcal{X}_j} \\ T_{(\mathcal{W}_j^- \setminus \bar{\mathcal{W}}_j) \mathcal{X}_j} \end{bmatrix} = P,$$

where F is any non-zero scalar transfer operator. Now, let M_1 be a new model obtained from M_0 by replacing $G_j \bar{\mathcal{W}}_j$ and $G_j(\mathcal{W}_j^- \setminus \bar{\mathcal{W}}_j)$ in G_0 with $G_j \bar{\mathcal{W}}_j + F Q_1$ and $G_j(\mathcal{W}_j^- \setminus \bar{\mathcal{W}}_j) + F Q_2$, respectively. Then similarly, there always exists a F such that $M_1 \in \mathcal{M}_0$, and $d(M_1, M_0)$ is positive and arbitrary small. \square

With the above lemma, we prove the necessity in this theorem under Assumption 3.3. As \mathcal{M} is an open set of \mathcal{M}_0 , for any $M \in \mathcal{M}$, there exists an open ball $B(M, r_0)$ in \mathcal{M}_0 that is a subset of \mathcal{M} . Let $\bar{\mathcal{M}}$ be any open and dense subset of \mathcal{M} . If the rank conditions are not satisfied for $M \in \bar{\mathcal{M}}$, there exists another model $M_1 \in \mathcal{M}_0$ that satisfies $0 < d(M_1, M) < r_0$ and is not distinguishable from M , i.e. M_1 and M lead to the same mapping $T_{\mathcal{W} \mathcal{X}}(q)$. Thus, $M_1 \in \mathcal{B}(M, r_0) \subseteq \mathcal{M}$, which contradicts generic identifiability.

3.7.2 PROOF OF LEMMA 3.3

Before proceeding to the proof of Lemma 3.3, some preliminary results on structural rank are presented. Consider a block matrix whose entries are either zeros or distinct indeterminates

$$K = \begin{bmatrix} A - I & B \\ C & D \end{bmatrix}, \quad (3.20)$$

where A is hollow, A and D are of dimensions $L \times L$ and $m \times m$, respectively. Here L or m is allowed to be zero.

Lemma 3.5. *If K in (3.20) is **not** structural full rank, then K can be permuted as*

$$\begin{bmatrix} \bar{A} & 0 \\ \bar{C} & \bar{D} \end{bmatrix}, \quad (3.21)$$

where \bar{A} has dimension $k_1 \times (k_1 - 1)$ for some $k_1 \geq 1$.

Proof. The non-zero structure of K can be characterized by a graph $\bar{\mathcal{G}} := (\bar{\mathcal{V}}, \bar{\mathcal{E}})$ with $\bar{\mathcal{V}} := \bar{\mathcal{W}} \cup \bar{\mathcal{X}} \cup \bar{\mathcal{Y}}$, where $\bar{\mathcal{W}} = \{w_1, \dots, w_L\}$, $\bar{\mathcal{X}} = \{x_1, \dots, x_m\}$, and $\bar{\mathcal{Y}} = \{y_1, \dots, y_m\}$ correspond to the rows/columns of A , the columns of B and the rows of C , respectively. Besides, a directed edge $(j, i) \in \bar{\mathcal{E}} := \bar{\mathcal{V}} \times \bar{\mathcal{V}}$ if and only if K_{ij} is non-zero. When K is not structural full rank, it follows from [154] that $b_{\bar{\mathcal{X}} \rightarrow \bar{\mathcal{W}}} < |\bar{\mathcal{X}}| = m$ in $\bar{\mathcal{G}}$. Then, from Theorem 2.1, there exists a $\bar{\mathcal{X}} - \bar{\mathcal{W}}$ disconnecting set \mathcal{D} with $|\mathcal{D}| = m - 1$ in $\bar{\mathcal{G}}$. Note that with \mathcal{D} and based on Lemma 2.1, we can divide $\bar{\mathcal{V}}$ into three disjoint sets \mathcal{D}, \mathcal{S} and \mathcal{P} with $|\mathcal{S}| + |\mathcal{P}| = L + m + 1$. Moreover, there is no edge from \mathcal{S} to \mathcal{P} , where $\mathcal{S} \subseteq \bar{\mathcal{W}} \cup \bar{\mathcal{X}}, \mathcal{P} \subseteq \bar{\mathcal{W}} \cup \bar{\mathcal{Y}}$. Thus, from the definition of $\bar{\mathcal{E}}$, we can find a permutation of K in the form of (3.21) with a zero block, whose rows and columns correspond to \mathcal{P} and \mathcal{S} , respectively. Furthermore, the column dimension of \bar{A} is computed as $L + m - |\mathcal{S}| = |\mathcal{P}| - 1$, which completes the proof. \square

Lemma 3.6. *Let the non-zero entries of K in (3.20) be divided into two disjoint sets \mathcal{P}_1 and \mathcal{P}_2 . If $\det(K)$ does not depend on the entries in \mathcal{P}_1 , then*

$$\det(K) = (-1)^j \prod_{i=1}^l \det(A_i), \text{ for some } l \geq 1, j \in \{0, 1\},$$

where A_i is a square submatrix of K that contains only non-zero entries in \mathcal{P}_2 .

Proof. When $\mathcal{P}_1 = \emptyset$, the proof is trivial. Now suppose $\mathcal{P}_1 \neq \emptyset$, and consider the cofactor expansion formula of $\det(K)$, which contains a term $b \det(\bar{B})$ with $\det(\bar{B})$ the cofactor of the nonzero entry $b \in \mathcal{P}_1$. Since $\det(K)$ does not depend on b , we obtain $\det(\bar{B}) = 0$, i.e., \bar{B} is not structural full rank. Then it follows from Lemma 3.5 that K can be permuted as

$$\begin{bmatrix} \star & \begin{bmatrix} \bar{B}_{11} & 0 \\ \bar{B}_{21} & \bar{B}_{22} \end{bmatrix} \\ b & \star \end{bmatrix} := \begin{bmatrix} \tilde{A} & 0 \\ \tilde{C} & \tilde{D} \end{bmatrix},$$

with square matrices \tilde{A} and \tilde{D} , and \tilde{C} containing b . Then, we have

$$\det(K) = \pm \det(\tilde{A}) \det(\tilde{D}),$$

which does not depend on b . Here, the sign \pm depends on the permutation. If \tilde{A} or \tilde{D} contains other entries in \mathcal{P}_1 , the above analysis can be applied recursively, which proves the lemma. \square

With the above results based on the structural rank, we need one additional lemma which is instrumental for the proof of Lemma 3.3.

Lemma 3.7. *Given a model set \mathcal{M} that satisfies Assumption 3.3, and consider any $\bar{\mathcal{W}} \subseteq \mathcal{W}$ and any $\bar{\mathcal{X}} \subseteq \mathcal{X}$ with $|\bar{\mathcal{W}}| = |\bar{\mathcal{X}}|$. If $\det[F(\bar{\mathcal{W}}, \bar{\mathcal{X}})]$ is not constant zero (as a function of the unknown entries), $F(\bar{\mathcal{W}}, \bar{\mathcal{X}})$ is full rank for almost all M in \mathcal{M} .*

Proof. Consider the set \mathcal{M}_0 corresponding to \mathcal{M} in Assumption 3.3. Since $C = I$, and Λ i.e. the fifth coordinate of M in (2.4), does not influence the rank of F , we only need to consider the first three coordinates, i.e. $\bar{M} \triangleq (G, R, H)$. Let $\bar{\mathcal{M}}_0$ denote the projection of \mathcal{M}_0 on its first three coordinates. Let \mathcal{F} denote the set of elements in $\bar{\mathcal{M}}_0$ with full rank F . We aim to prove if $\det[F(\bar{\mathcal{W}}, \bar{\mathcal{X}})]$ is not constant zero, \mathcal{F} is an open dense subset of $\bar{\mathcal{M}}_0$. Then this gives F full rank for almost all elements in \mathcal{M}_0 and thus in \mathcal{M} , since the intersection of the open set \mathcal{M} and any open dense subset of \mathcal{M}_0 is also open and dense in \mathcal{M} .

If $\det(F)$ is a non-zero constant as a function of $\bar{M} \in \bar{\mathcal{M}}_0$, F is full rank for all \bar{M} in $\bar{\mathcal{M}}_0$ and thus the lemma holds. Then we focus on the case where $\det(F)$ is not a constant and show that \mathcal{F} is open and dense in $\bar{\mathcal{M}}_0$.

For denseness, consider any network $\bar{M} \in \bar{\mathcal{M}}_0$ whose F is not full rank, i.e. $\det(F) = 0$. Then consider an open ball in $\bar{\mathcal{M}}_0$ denoted as $\mathcal{B}(\bar{M}, \varepsilon)$ with any radius $\varepsilon > 0$, and we aim to prove the existence of a different model \bar{M}_1 in $\mathcal{B}(\bar{M}, \varepsilon)$ such that $\det(F_1)$, which is formulated on \bar{M}_1 , is non-zero. Firstly consider a model $\bar{M}_2 \in \bar{\mathcal{M}}_0$ whose corresponding F matrix is full rank, and we define $\Delta \triangleq \bar{M}_2 - \bar{M}$ with $d(\Delta, \mathbf{0}) = \delta$, where δ is some positive real number, and $\mathbf{0}$ denotes a model with all entries being zeros. Then we formulate a new model as $\bar{M}_1(\gamma) = \gamma\Delta + \bar{M}$, which depends on a real number γ . It is clear that $\bar{M}_1(1) = \bar{M}_2$, and thus the $\det(F)$ of $\bar{M}_1(1)$ is non-zero. Similarly, $\det(F)$ of $\bar{M}_1(0)$ is zero. This shows that the analytic function $h(z, \gamma)$, obtained from $\det(F)$ formulated on $\bar{M}_1(\gamma)$, is not constant on $\mathbb{C} \times \mathbb{R}$. Then by the property of non-constant analytic functions, there exists $\gamma_0 \in (0, \varepsilon/\delta)$, such that $h(z, \gamma_0)$ and thus $\det(F)$ of $\bar{M}_1(\gamma_0)$ is non-zero. In addition, it holds that $d(\bar{M}_1(\gamma_0), \bar{M}) = d(\gamma_0\Delta, \mathbf{0}) = \gamma_0\delta < \varepsilon$, where the second equality holds as the definition of the metric function after Definition 3.3 is based on norms. This shows that $\bar{M}_1(\gamma_0) \in \mathcal{B}(\bar{M}, \varepsilon)$, and recall that the F matrix formulated on $\bar{M}_1(\gamma_0)$ is full rank. This concludes the proof for denseness.

For openness, given any $\bar{\mathcal{W}}$ and $\bar{\mathcal{X}}$, denote the corresponding $\|\det(F(M))\|_\infty$ as a function f from $\bar{\mathcal{M}}_0$ to \mathbb{R} . As f is a composition of continuous functions, i.e. the determinant function and the norm, f is also continuous. It also holds that the set \mathcal{F} equals $f^{-1}((0, +\infty))$. Moreover, by the property of a continuous function, i.e. the preimage of an open interval is open, $f^{-1}((0, +\infty))$ is an open subset of $\bar{\mathcal{M}}_0$. This concludes both openness and denseness. \square

Finally, with all the above preliminary lemmas, Lemma 3.3 can be proved as follows.

Proof. Without loss of generality, consider that $|\bar{\mathcal{W}}| \leq |\bar{\mathcal{X}}|$, and thus $T_{\bar{\mathcal{W}}\bar{\mathcal{X}}}$ being full generic rank implies that its square submatrix $T_{\bar{\mathcal{W}}\bar{\mathcal{X}}_1}$ is full rank generically for some \mathcal{X}_1 . Denote $|\bar{\mathcal{X}}_1| = m$, and use \bar{F} to represent $F(\bar{\mathcal{W}}, \bar{\mathcal{X}}_1)$. It holds that \bar{F} is generically full rank if and only if $T_{\bar{\mathcal{W}}\bar{\mathcal{X}}_1}$ is generically full rank based on (3.8), and \bar{F} is structural full rank if and only if F is structural full rank. Therefore, the proof aims to prove that \bar{F} is structural full rank if and only if it is generically full rank. Let a_{ij} denote the (i, j) entry of \bar{F} . The “if” part is clear as being structural full rank is a necessary condition for being full rank generically. For the “only if” part, consider

now all the summands in the Leibnitz formula for $\det(\bar{F})$. If \bar{F} is structural full rank, without loss of generality, $\det(\bar{F})$ contains a term according to a permutations $\bar{\sigma}$ of $[1, \dots, L+m]$ as

$$a \prod_{i=p+1}^{L+m} a_{\bar{\sigma}(i)i} \neq 0, \quad (3.22)$$

for some $p \geq 0$, where $\sigma(i)$ denotes the i -th index in the permutation, and a is the product of all unknown entries in the term and also contains the maximum number of unknown entries among the other permutations of $[1, \dots, L+m]$. In addition, the summation of all terms with the common factor a in $\det(\bar{F})$ equals

$$a \det(\bar{F}_{\{\bar{\sigma}(p+1), \dots, \bar{\sigma}(L+m)\} \{p+1, \dots, L+m\}}). \quad (3.23)$$

Denote the above submatrix of \bar{F} as F_1 . Then the determinant of \bar{F} is proved to be non-zero (as a function of unknown entries) by showing that the term (3.23) is non-zero as follows. As (3.22) contains the maximum number of unknown entries compared to the other permutations, $\det(F_1)$ does not depend on the unknown entries when considered as a polynomial of F_1 's all non-zero entries. Based on Lemma 3.6, (3.23) can be reformulated as

$$(-1)^j a \prod_{i=1}^l \det(A_i), \quad (3.24)$$

for some $l \geq 1$ and $j \in \{0, 1\}$, where A_i contains only known transfer functions and is square submatrix of F_1 and thus of \bar{F} . As (3.24) contains the non-zero term (3.22) after expansion, A_i is structural full rank and thus full rank by Assumption 5, for all i . This means that $\det(F_1)$ is non-zero, and thus $\det(\bar{F})$ contains the non-zero term (3.23) and is not constant zero. Then based on Lemma 3.7, \bar{F} is full rank for almost all $M \in \mathcal{M}$, which concludes the proof. \square

人生如逆旅，我亦是行人。

苏轼（宋）

Life is like a journey. I too am on my way.

Shi Su (Song dynasty); Translated by Yuanchong Xu

4

Identifiability with full measurement: Synthesis

4.1 INTRODUCTION

The results in Chapter 3 and the related graphical results in [14, 69, 157] for identifiability focus on the analysis question, i.e. under what conditions modules in a network are (generically) identifiable? However, none of these conditions has referred to the synthesis problem, that is: where to allocate excitation or measurement signals to achieve network identifiability? Preliminary results to achieve identifiability of a full network in [13] are limited to special network structures, e.g. trees. While the allocation of excitation signals has been considered in the identification literature for identifying local modules, e.g., in [48, 59, 122, 152, 168], these results do not consider the identifiability aspect and typically depend on the particular identification method under consideration.

To the best of our knowledge, the synthesis problem for a general dynamic network has not been addressed in the literature so far. Actually, such a synthesis problem has more realistic significance in the identification of dynamic networks, since it determines the cost of identification experiments in networks. This becomes the motivation of this chapter.

The material of this chapter is based on the results in [36, 38, 139].

In this chapter, we address the synthesis problem for the situation where all the internal signals are measured, and our goal is to develop synthesis approaches to allocate excitation signals (actuators) such that a subset of modules or a full network becomes generically identifiable. The synthesis procedures for identifiability of a subnetwork, i.e. a subset of modules, and identifiability of a full network are discussed separately since they require different graphical tools.

For the synthesis problem for a subnetwork, a novel graphical condition for generic identifiability of a subnetwork is developed, by exploiting the concepts of disconnecting sets. Compared to the existing path-based condition, the new result makes explicit suggestions regarding which internal signals should be excited for generic identifiability. Based on that information, a novel synthesis approach is developed to allocate excitation signals, such that generic identifiability of a subnetwork can be achieved.

When the synthesis problem for a full network is concerned, a more compact synthesis approach can be developed based on a novel graphical concept, called pseudotrees. A new analysis result for generic identifiability of a full network is obtained, which shows that identifiability can be achieved if the full network is covered by pseudotrees, and a root of each pseudotree is excited. This leads to a novel synthesis procedure to achieve generic identifiability of a full network, by first decomposing a network into a set of pseudotrees and then allocating signals to excite these pseudotrees.

This chapter is organized as follows. The novel analysis result for a subnetwork is presented in Section 4.2, and the synthesis procedure for a subnetwork is developed in Section 4.3. Then the concept of pseudotrees is introduced in Section 4.4, which leads to a synthesis approach for identifiability of a full network in Section 4.5. Some of the proofs are collected in Section 4.7.

4.2 DISCONNECTING-SET-BASED CONDITIONS FOR SUBNETWORK IDENTIFIABILITY

4.2.1 GENERIC IDENTIFIABILITY BASED ON DISCONNECTING SETS

The graphical condition in Theorem 3.4 can be applied to analyzing generic identifiability in a given model set. However, it does not explicitly indicate where to allocate external signals such that a particular set of modules becomes generically identifiable. To solve this synthesis question, a new analytic result is developed in this section by exploring the duality between vertex disjoint paths and disconnecting sets, as also indicated in [69]. In this section, we will exploit this relationship in a novel way for subnetwork generic identifiability, while providing a solution to the synthesis question as well. This synthesis question will be addressed in more detail in Section 4.3.

Recall the Menger's theorem in Theorem 2.1, from which the generic identifiability condition in Theorem 3.4 can be reformulated using the concept of disconnecting sets.

Corollary 4.1. Consider a model set \mathcal{M} that satisfies Assumptions 3.1, 3.2, 3.4 and 3.5, and let $\bar{\mathcal{W}}_j$ be any subset of \mathcal{W}_j^- . The conditions (3.15) hold if and only if

$$\begin{aligned} |\mathcal{D}_2| &= |\bar{\mathcal{W}}_j|, \text{ and} \\ |\mathcal{D}_1| &= |\mathcal{D}_2| + |\mathcal{D}_3|, \end{aligned} \quad (4.1)$$

where \mathcal{D}_1 , \mathcal{D}_2 and \mathcal{D}_3 are minimum $\mathcal{X}_j - \mathcal{W}_j^-$, $\mathcal{X}_j - \bar{\mathcal{W}}_j$ and $\mathcal{X}_j - \mathcal{W}_j^- \setminus \bar{\mathcal{W}}_j$ disconnecting sets, respectively.

The relevance of disconnecting sets and generic identifiability is further illustrated in the following example.

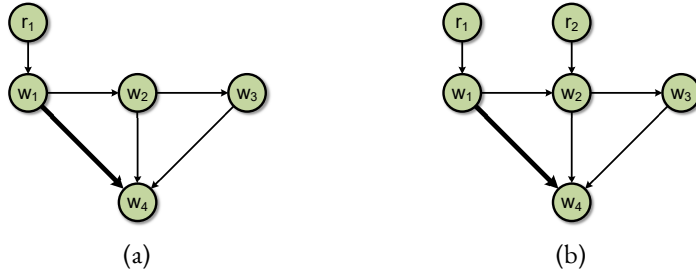


Figure 4.1: Generic identifiability of G_{41} is considered (thick line). G_{41} is not generically identifiable in (a) but becomes generically identifiable in (b) if an extra signal r_2 is allocated at w_2 .

Example 4.1. Given the network model in Figure 4.1(a), where G_{41} is the target module. In this setting, $\mathcal{X}_4 = \{r_1\}$, $\mathcal{W}_4^- = \{w_1, w_2, w_3\}$ and $\bar{\mathcal{W}}_4 = \{w_1\}$. Minimum disconnecting sets in Corollary 4.1 are then $\mathcal{D}_1 = \mathcal{D}_2 = \{w_1\}$, $\mathcal{D}_3 = \{w_2\}$, where \mathcal{D}_3 is a disconnecting set from $\{w_1\}$ to the other in-neighbors of w_4 , i.e., $\{w_2, w_3\}$. The module G_{41} is not generically identifiable in Figure 4.1(a) since (4.1) is not satisfied. To achieve generic identifiability of G_{41} , an extra excitation signal r_2 can be allocated at w_2 , which changes \mathcal{D}_1 to $\{w_1, w_2\}$ and thus (4.1) are satisfied. This is shown in Figure 4.1(b). It can also be verified that $b_{\mathcal{X}_4 \rightarrow \mathcal{W}_4} = b_{\mathcal{X}_4 \rightarrow \mathcal{W}_4 \setminus \{w_1\}} + 1$, which implies that G_{41} is generically identifiable according to Theorem 3.4.

It is observed from this example that generic identifiability of G_{ji} is achieved when the vertices in a disconnecting set from $\{w_i\}$ to the other in-neighbors of w_j are excited. This observation is generalized to obtain a new graphical condition based on disconnecting sets.

Theorem 4.1. Consider a model set \mathcal{M} that satisfies Assumptions 3.1, 3.2, 3.4 and 3.5, and let $\bar{\mathcal{W}}_j$ be any subset of \mathcal{W}_j^- . The conditions (3.15) hold if and only if the following two equivalent conditions hold:

1. There exists a $\mathcal{X}_j - \mathcal{W}_j^- \setminus \bar{\mathcal{W}}_j$ disconnecting set \mathcal{D} such that

$$b_{\mathcal{X}_j \rightarrow \bar{\mathcal{W}}_j \cup \mathcal{D}} = |\mathcal{D}| + |\bar{\mathcal{W}}_j|.$$

2. There exist a set of external signals $\bar{\mathcal{X}}_j \subseteq \mathcal{X}_j$ and a $\bar{\mathcal{X}}_j - \mathcal{W}_j^- \setminus \bar{\mathcal{W}}_j$ disconnecting set \mathcal{D} such that

$$b_{\bar{\mathcal{X}}_j \rightarrow \bar{\mathcal{W}}_j \cup \mathcal{D}} = |\mathcal{D}| + |\bar{\mathcal{W}}_j|. \quad (4.2)$$

The proof of the above theorem is presented in Section 4.7. In the above result, condition 1 is more similar to Theorem 3.4 than condition 2 as all signals in \mathcal{X}_j are considered in condition 1; on the other hand, condition 2 shows that there is extra freedom in considering a subset of signals in \mathcal{X}_j . In addition, compared to Theorem 3.4, Theorem 4.1 explicitly states that the signals in $\bar{\mathcal{W}}_j \cup \mathcal{D}$ should be indirectly excited, i.e. there are vertex disjoint paths from external signals $\bar{\mathcal{X}}_j$ to $\bar{\mathcal{W}}_j \cup \mathcal{D}$. The above information will be helpful for the design of synthesis approaches to allocate excitation signals.

Condition 2 of Theorem 4.1 is visualized in Figure 4.2, and this condition implies that \mathcal{D} is also a disconnecting set from the inputs of the target modules $\bar{\mathcal{W}}_j$ to the other inputs $\mathcal{W}_j^- \setminus \bar{\mathcal{W}}_j$ of w_j . In addition, to guarantee generic identifiability of the target modules, condition 2 shows that $\bar{\mathcal{W}}_j$ and $\mathcal{W}_j^- \setminus \bar{\mathcal{W}}_j$ should receive independent excitation provided by the external signals, which have paths via \mathcal{D} to $\mathcal{W}_j^- \setminus \bar{\mathcal{W}}_j$. Moreover, each input of the target modules should be excited by a distinct excitation signal.

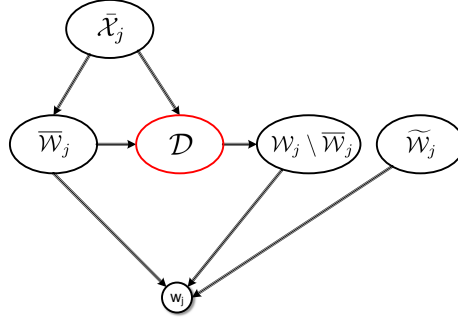


Figure 4.2: Visualization of condition 2 in Theorem 4.1, where $\bar{\mathcal{W}}_j$ collects all inputs of w_j through known modules.

4.2.2 ALGEBRAIC INTERPRETATION OF DISCONNECTING SETS

From Lemma 2.1, a disconnecting set in a graph separates its vertex set into several disjoint subsets. This graph separation also leads to a factorization of the external-to-internal mappings for the associated dynamic network.

Theorem 4.2. Consider a network model M with the induced graph \mathcal{G} and a disconnecting set $\mathcal{D} \subseteq \mathcal{V}$ from $\bar{\mathcal{X}} \subseteq \mathcal{X}$ to $\bar{\mathcal{W}} \subseteq \mathcal{W}$. Then there exists a proper transfer matrix $K(q)$ such that

$$T_{\bar{\mathcal{W}}\bar{\mathcal{X}}}(q) = K(q)T_{\mathcal{D}\bar{\mathcal{X}}}(q). \quad (4.3)$$

The transfer matrix $K(q)$ can be explicitly expressed as follows:

The $\bar{\mathcal{X}} - \bar{\mathcal{W}}$ disconnecting set \mathcal{D} divides all vertices in three disjoint sets, i.e. $\mathcal{V} = \mathcal{S} \cup \mathcal{D} \cup \mathcal{P}$, according to Lemma 2.1, on the basis of which the following sets are defined: $\bar{\mathcal{W}}_{\mathcal{D}} = \bar{\mathcal{W}} \cap \mathcal{D}$, $\bar{\mathcal{W}}_{\mathcal{P}} = \bar{\mathcal{W}} \cap \mathcal{P}$, $\bar{\mathcal{X}}_{\mathcal{D}} = \bar{\mathcal{X}} \cap \mathcal{D}$, $\mathcal{D}_w = \mathcal{W} \cap \mathcal{D}$, $\mathcal{D}_x = \mathcal{X} \cap \mathcal{D}$, $\mathcal{P}_w = \mathcal{W} \cap \mathcal{P}$. Consider $T_{\mathcal{D}\bar{\mathcal{X}}}$ to be ordered in three block rows, according to the decomposition of $\mathcal{D} = \mathcal{D}_w \cup \bar{\mathcal{X}}_{\mathcal{D}} \cup (\mathcal{D}_x \setminus \bar{\mathcal{X}}_{\mathcal{D}})$. Then

$$K = \begin{bmatrix} [(I - G_{\mathcal{P}_w \mathcal{P}_w})^{-1}]_{\bar{\mathcal{W}}_{\mathcal{P}} \star} & 0 \\ 0 & C \end{bmatrix} \begin{bmatrix} G_{\mathcal{P}_w \mathcal{D}_w} & X_{\mathcal{P}_w \bar{\mathcal{X}}_{\mathcal{D}}} & 0 \\ I & 0 & 0 \end{bmatrix} \quad (4.4)$$

where C is a selection matrix that extracts the rows of $T_{\mathcal{D}_w \bar{\mathcal{X}}}$ corresponding to $\bar{\mathcal{W}}_{\mathcal{D}}$.

The proof of the above theorem is presented in Section 4.7. The decomposition in (4.3) means that if all paths from $\bar{\mathcal{X}}$ to $\bar{\mathcal{W}}$ intersect with \mathcal{D} , then the signals in \mathcal{D} act as auxiliary signals that contain all information, that is relevant for $\bar{\mathcal{W}}$, from $\bar{\mathcal{X}}$. It is easier to interpret $K(q)$ matrix in a special case where $\bar{\mathcal{W}}_{\mathcal{D}} = \mathcal{D}_x \setminus \bar{\mathcal{X}}_{\mathcal{D}} = \emptyset$, which leads to

$$K(q) = [(I - G_{\mathcal{P}_w \mathcal{P}_w})^{-1}]_{\bar{\mathcal{W}}_{\mathcal{P}} \star} \begin{bmatrix} G_{\mathcal{P}_w \mathcal{D}_w} & X_{\mathcal{P}_w \bar{\mathcal{X}}_{\mathcal{D}}} \end{bmatrix}.$$

In this special case, it holds that $\mathcal{D} = \mathcal{D}_w \cup \bar{\mathcal{X}}_{\mathcal{D}}$ and $\bar{\mathcal{W}}_{\mathcal{P}} = \bar{\mathcal{W}}$. Then similar to the mapping $T_{\mathcal{W}\mathcal{X}}(q) = [I - G(q)]^{-1}X(q)$ in a network model with graph \mathcal{G} , the above $K(q)$ matrix can thus be interpreted as an external-to-internal mapping from \mathcal{D} to $\bar{\mathcal{W}}$ in a subgraph of \mathcal{G} , where \mathcal{P}_w contains all the internal signals and \mathcal{D} contains the external signals of the subgraph.

Using the factorization result of Theorem 4.2, if condition 1 of Theorem 4.1 holds, then the $\mathcal{X}_j - \mathcal{W}_j^- \setminus \bar{\mathcal{W}}_j$ disconnecting set \mathcal{D} ensures a factorization as

$$T_{(\mathcal{W}_j^- \setminus \bar{\mathcal{W}}_j)\mathcal{X}_j}(q) = K(q)T_{\mathcal{D}\mathcal{X}_j}(q).$$

Then it can be relatively simple to show how the conditions in Theorem 4.1 directly relate to the original rank conditions in Theorem 3.1, based on the path-rank relation in Theorem 3.2.

In addition, we also show that the factorization result (4.3) is a very attractive result that leads to a generalized indirect identification method for identifying $G_{j\bar{\mathcal{W}}_j}$. Let us first consider the following corollary of Theorem 4.2.

Corollary 4.2. Consider a network model with all fixed modules being zero and any subset $\bar{\mathcal{W}}_j \subseteq \mathcal{W}_j^-$. Let \mathcal{D} be a $\bar{\mathcal{W}}_j - \mathcal{W}_j^- \setminus \bar{\mathcal{W}}_j$ disconnecting set such that $\mathcal{D} \cap \bar{\mathcal{W}}_j = \emptyset$. Let \mathcal{X}_1 denote the set of all external signals that do not have directed edge to w_j . If there exists a set $\bar{\mathcal{X}} \subseteq \mathcal{X}_1$ such that $\begin{bmatrix} T_{\bar{\mathcal{W}}_j \bar{\mathcal{X}}}(q) \\ T_{\mathcal{D} \bar{\mathcal{X}}}(q) \end{bmatrix}$ has full row rank and \mathcal{D} is also a $\bar{\mathcal{X}} - \mathcal{W}_j^- \setminus \bar{\mathcal{W}}_j$ disconnecting set, then

$$G_{j\bar{\mathcal{W}}_j}(q) = T_{j\bar{\mathcal{X}}}(q) \begin{bmatrix} T_{\bar{\mathcal{W}}_j \bar{\mathcal{X}}}(q) \\ T_{\mathcal{D} \bar{\mathcal{X}}}(q) \end{bmatrix}^\dagger \begin{bmatrix} I_{|\bar{\mathcal{W}}_j|} \\ 0 \end{bmatrix}, \quad (4.5)$$

where $(\cdot)^\dagger$ denotes the matrix's right inverse, and $I_{|\bar{\mathcal{W}}_j|}$ is an identity matrix with dimension $|\bar{\mathcal{W}}_j|$.

Proof. From Theorem 4.2, there exists K such that $KT_{\mathcal{D}\bar{\mathcal{X}}} = T_{(\mathcal{W}_j^- \setminus \bar{\mathcal{W}}_j)\bar{\mathcal{X}}}$. In addition, $w_j \notin \mathcal{D}$ and $\mathcal{D} \cap \bar{\mathcal{W}}_j = \emptyset$ hold, as the later is necessary for the matrix being full row rank. Then recall the j th row of $(I - G)T_{\mathcal{W}\mathcal{X}} = X$, and after permutation we have

$$\begin{bmatrix} -G_{j\bar{\mathcal{W}}_j} & -G_{j(\mathcal{W}_j^- \setminus \bar{\mathcal{W}}_j)}K & 1 & 0 \end{bmatrix} \begin{bmatrix} T_{\bar{\mathcal{W}}_j\bar{\mathcal{X}}} \\ T_{\mathcal{D}\bar{\mathcal{X}}} \\ T_{j\bar{\mathcal{X}}} \\ \star \end{bmatrix} = X_{j\bar{\mathcal{X}}},$$

where $X_{j\bar{\mathcal{X}}} = 0$ as $\bar{\mathcal{X}}$ has no directed edge to w_j . Thus the above equation leads to (4.5). \square

The expression (4.5) shows an immediate opportunity to estimate $G_{j\bar{\mathcal{W}}_j}(q)$ on the basis of a selected set of measured internal signals. In the situation that all the signals in $\bar{\mathcal{X}}$ are measured excitation signals r , the transfer functions on the right hand side of (4.5) can all be estimated through so-called open-loop identification methods, on the basis of measured signals in $\bar{\mathcal{X}} \cup \bar{\mathcal{W}}_j \cup \mathcal{D} \cup \{w_j\}$. This method is a generalization of the ‘‘classical’’ indirect method of identification, see e.g. [59], where all inputs of w_j are measured and directly excited to estimate a single module, i.e. $\bar{\mathcal{W}}_j = \{w_i\}$. That situation can be characterized by the choice $\mathcal{D} \cup \bar{\mathcal{W}}_j = \mathcal{W}_j^-$, i.e. all in-neighbors of w_j except w_i are selected into the disconnecting set. The generalization of this indirect method now allows for a more flexible choice of signals as well as more flexibility in providing excitation signals r for estimating $G_{j\bar{\mathcal{W}}_j}$.

The rank condition that is formulated in Corollary 4.2 can be verified in a generic sense by requiring that

$$b_{\bar{\mathcal{X}} \rightarrow \bar{\mathcal{W}}_j \cup \mathcal{D}} = |\bar{\mathcal{W}}_j| + |\mathcal{D}|. \quad (4.6)$$

In other words: there should be sufficient vertex disjoint paths from the measured external excitation signals in $\bar{\mathcal{X}}$ to the internal signals in $\bar{\mathcal{W}}_j$ and \mathcal{D} .

4.2.3 RELATION WITH THE PARALLEL PATH AND LOOP CONDITION

In dynamic network analysis and identification, there is a recurring condition that plays an important role in the selection of a set of measured internal signals that is sufficient for identifying a single target module $G_{ji}(q)$ in the network. The condition was first formulated in [48], as the *parallel path and loop condition* which selects a set of internal signals as follows:

Determine a set of internal signals \mathcal{D} according to:

- Every parallel path from w_i to w_j , i.e. a path that is not the edge $G_{ji}(q)$, passes through an internal vertex in \mathcal{D} , and
- Every loop around w_j passes through a vertex in \mathcal{D} .

If in a network where all signals w_i , w_j and \mathcal{D} are retained, and all other internal signals are eliminated (immersed), e.g., because they can not be measured, then in the obtained immersed network that leaves the signals w_i , w_j and \mathcal{D} invariant, the target module $G_{ji}(q)$ remains invariant too. As a result, the parallel path and loop condition has become an important tool for selecting internal signals to be measured for identification of a single module, see e.g. also [122, 168], where the network abstraction is introduced in the latter reference as a generalization of network immersion.

It can be shown that the parallel path and loop condition has a very strong link to the disconnecting set-based results on generic identifiability in Theorem 4.1 and its later implication in Corollary 4.3, when a single module is concerned, i.e. $\bar{\mathcal{W}}_j = \{w_i\}$.

Proposition 4.1. *Consider a model set with graph \mathcal{G} in which all non-zero modules in $G(\theta)$ are unknown. Consider the module $G_{ji}(q)$ and a set of internal signals \mathcal{D} with $\{w_i\} \notin \mathcal{D}$. Then \mathcal{D} is an $\{w_i\} - \mathcal{W}_j^- \setminus \{w_i\}$ disconnecting set if and only if \mathcal{D} contains an internal vertex in every parallel path from w_i to w_j and a vertex in every loop around w_j .*

The proof of the above result is presented in Section 4.7. The above connection between disconnecting sets and the parallel path and loop condition is preliminarily investigated in [48, Proposition 9], where disconnecting sets are also referred to as separating sets; however, the connection established in [48] requires a modification of the graph \mathcal{G} by splitting the vertices. In addition, the parallel path and loop condition is equivalently formulated into the search of two disconnecting sets in [48], which is less compact than Proposition 4.1 where only a single disconnecting set is needed.

While the parallel path and loop condition has served as a means for selecting internal signals to be measured for identifying $G_{ji}(q)$, it can also be used to select internal signals to be externally excited for single module identifiability, according to the results of Theorem 4.1. Moreover, in the situation of considering the identification of a set of modules, i.e. $|\bar{\mathcal{W}}_j^-| > 1$, the verification whether multiple parallel paths are covered by a selection of internal signals can now be very effectively executed by an algorithm that constructs a (minimum) disconnecting set between the appropriate vertices.

4.3 SIGNAL ALLOCATION FOR SUBNETWORK IDENTIFIABILITY

If $G_{j\bar{\mathcal{W}}_j}(q)$ is not generically identifiable in a given network model set, extra excitation signals can be allocated by users to achieve generic identifiability of $G_{j\bar{\mathcal{W}}_j}(q)$. This section aims to tackle this synthesis problem by means of exploiting condition 2 in Theorem 4.1.

Consider a network model set with a set of initial external signals \mathcal{X}_j^0 that do not have unknown directed edges to w_j . The synthesis problem aims to allocate a minimum number of additional excitation signals \mathcal{X}_j^a such that the generic identifiability of $G_{j\bar{\mathcal{W}}_j}(q)$ is guaranteed.

In this synthesis problem, it is assumed that if r_k is allocated directly at the output of interest w_j , its corresponding transfer function R_{jk} is known.

This main idea for designing synthesis approaches follows from condition 2 of Theorem 4.1, however, in a reversed order. While the condition considers the existence of a $\bar{\mathcal{X}}_j - \mathcal{W}_j^- \setminus \bar{\mathcal{W}}_j$ disconnecting set \mathcal{D} given $\bar{\mathcal{X}}_j$, the synthesis approaches find a set \mathcal{D} first and then construct $\bar{\mathcal{X}}_j$ by allocating signals, such that \mathcal{D} becomes a $\bar{\mathcal{X}}_j - \mathcal{W}_j^- \setminus \bar{\mathcal{W}}_j$ disconnecting set and (4.2) is satisfied. An initial choice for a set \mathcal{D} can be motivated on the basis of the following corollary.

Corollary 4.3. *Assume that one of the conditions in Theorem 4.1 is satisfied, it holds that \mathcal{D} is a $\bar{\mathcal{X}}_j - \mathcal{W}_j^- \setminus \bar{\mathcal{W}}_j$ disconnecting set if and only if it is a $\bar{\mathcal{W}}_j \cup \bar{\mathcal{X}}_j - \mathcal{W}_j^- \setminus \bar{\mathcal{W}}_j$ disconnecting set subject to $\mathcal{D} \cap \bar{\mathcal{W}}_j = \emptyset$.*

Proof. The "if" part is trivial. The "only if" part is proved by contradiction. If \mathcal{D} is not a $\bar{\mathcal{W}}_j - \mathcal{W}_j^- \setminus \bar{\mathcal{W}}_j$ disconnecting set, i.e. there exists a path from $\bar{\mathcal{W}}_j$ to $\mathcal{W}_j^- \setminus \bar{\mathcal{W}}_j$ which does not intersect with \mathcal{D} , then there is also a path from $\bar{\mathcal{X}}_j$ (or $\bar{\mathcal{X}}_j$) via $\bar{\mathcal{W}}_j$ to $\mathcal{W}_j^- \setminus \bar{\mathcal{W}}_j$ and the path does not intersect with \mathcal{D} , which contradicts that \mathcal{D} is a disconnecting set. $\mathcal{D} \cap \bar{\mathcal{W}}_j = \emptyset$ is trivial. \square

As shown in Figure 4.2, the above result indicates that a $\bar{\mathcal{W}}_j - \mathcal{W}_j^- \setminus \bar{\mathcal{W}}_j$ disconnecting set \mathcal{D} subject to $\mathcal{D} \cap \bar{\mathcal{W}}_j = \emptyset$ can be computed first, which is independent of the external signals. Then according to (4.2), extra excitation signals can be allocated such that the signals in $\mathcal{D} \cup \bar{\mathcal{W}}_j$ are excited, and \mathcal{D} becomes a disconnecting set from the allocated signals to $\mathcal{W}_j^- \setminus \bar{\mathcal{W}}_j$.

As the number of required excitation signals depends on the cardinality of the disconnecting set, a minimum disconnecting set is desired. Additionally, based on Corollary 4.3, a minimum disconnecting set \mathcal{D} subject to $\bar{\mathcal{W}}_j \cap \mathcal{D} = \emptyset$ needs to be found. As standard graphical algorithms for computing minimum disconnecting sets do not take into account any constraint, we redefine the disconnecting set so as to make standard algorithms applicable. Recall the notation in Section 2.5 that $\bar{\mathcal{N}}_{\bar{\mathcal{V}}}^+$ denotes the set of all the out-neighbors of the vertices in a set $\bar{\mathcal{V}}$.

Proposition 4.2. *Consider a model set \mathcal{M} with its associated graph \mathcal{G} . For any subset $\bar{\mathcal{X}}_j \subseteq \mathcal{X}_j$, a minimum disconnecting set \mathcal{D} from $\bar{\mathcal{W}}_j \cup \bar{\mathcal{X}}_j$ to $\mathcal{W}_j^- \setminus \bar{\mathcal{W}}_j$ subject to $\bar{\mathcal{W}}_j \cap \mathcal{D} = \emptyset$ is a minimum disconnecting set from $\bar{\mathcal{N}}_{\bar{\mathcal{W}}_j}^+ \cup \bar{\mathcal{X}}_j$ to $\mathcal{W}_j^- \setminus \bar{\mathcal{W}}_j$.*

Proof. We will first show that for any vertex set \mathcal{D} subject to $\bar{\mathcal{W}}_j \cap \mathcal{D} = \emptyset$, \mathcal{D} is a disconnecting set from $\bar{\mathcal{N}}_{\bar{\mathcal{W}}_j}^+ \cup \bar{\mathcal{X}}_j$ to $\mathcal{W}_j^- \setminus \bar{\mathcal{W}}_j$ if and only if it is also a disconnecting set from $\bar{\mathcal{W}}_j \cup \bar{\mathcal{X}}_j$ to $\mathcal{W}_j^- \setminus \bar{\mathcal{W}}_j$. The "only if" part holds because if \mathcal{D} intersects with all the paths from $\bar{\mathcal{N}}_{\bar{\mathcal{W}}_j}^+ \cup \bar{\mathcal{X}}_j$ to $\mathcal{W}_j^- \setminus \bar{\mathcal{W}}_j$, then it also intersects with the paths from $\bar{\mathcal{W}}_j \cup \bar{\mathcal{X}}_j$ to $\mathcal{W}_j^- \setminus \bar{\mathcal{W}}_j$. For the "if" part, since $\bar{\mathcal{W}}_j \cap \mathcal{D} = \emptyset$ and \mathcal{D} intersects with all the paths from $\bar{\mathcal{W}}_j \cup \bar{\mathcal{X}}_j$ to $\mathcal{W}_j^- \setminus \bar{\mathcal{W}}_j$, those paths from $\bar{\mathcal{W}}_j$ to $\mathcal{W}_j^- \setminus \bar{\mathcal{W}}_j$ must intersect with \mathcal{D} at their internal vertices or ending vertices. Since the first internal vertices of the paths belong to set $\bar{\mathcal{N}}_{\bar{\mathcal{W}}_j}^+$, then \mathcal{D} is also a disconnecting set from $\bar{\mathcal{N}}_{\bar{\mathcal{W}}_j}^+ \cup \bar{\mathcal{X}}_j$ to $\mathcal{W}_j^- \setminus \bar{\mathcal{W}}_j$.

Having the above result, the proposition is proved by showing that a minimum disconnecting set \mathcal{D} from $\bar{\mathcal{N}}_{\bar{\mathcal{W}}_j}^+ \cup \bar{\mathcal{X}}_j$ to $\mathcal{W}_j^- \setminus \{w_i\}$ does not contain $\bar{\mathcal{W}}_j$, because if it does, it remains a disconnecting set after $\bar{\mathcal{W}}_j$ is excluded, which contradicts the minimality of \mathcal{D} . \square

Based on the above proposition, a minimum disconnecting set \mathcal{D} from $\bar{\mathcal{N}}_{\bar{\mathcal{W}}_j}^+$ to $\mathcal{W}_j^- \setminus \bar{\mathcal{W}}_j$ can be computed for the synthesis problem, which now is an unconstrained problem and thus can be solved by standard graphic algorithms, e.g. the Ford-Fulkerson algorithm [135]. Then the following synthesis result can be derived from Theorem 4.1(2) and Corollary 4.3.

Corollary 4.4. *Consider a network model set \mathcal{M} that satisfies Assumptions 3.1, 3.2, 3.4 and 3.5. Given any minimum disconnecting set \mathcal{D} from $\bar{\mathcal{N}}_{\bar{\mathcal{W}}_j}^+$ to $\mathcal{W}_j^- \setminus \bar{\mathcal{W}}_j$, assigning distinct excitation signals to every vertex in $\mathcal{D} \cup \bar{\mathcal{W}}_j$ leads to the generic identifiability of $G_{j\bar{\mathcal{W}}_j}(q)$ in \mathcal{M} from (w, r) .*

Proof. Let \mathcal{X}_j^a denote the set of allocated signals, and it holds that $\mathcal{X}_j^a \subseteq \mathcal{X}_j$ in the obtained model set after allocation, i.e. \mathcal{X}_j^a has no unknown direct edge to w_j . As these signals are allocated directly at $\mathcal{D} \cup \bar{\mathcal{W}}_j$, \mathcal{D} is a $\bar{\mathcal{N}}_{\bar{\mathcal{W}}_j}^+ \cup \mathcal{X}_j^a - \mathcal{W}_j^- \setminus \{w_i\}$ and thus a $\bar{\mathcal{W}}_j \cup \mathcal{X}_j^a - \mathcal{W}_j^- \setminus \{w_i\}$ disconnecting set, based on Proposition 4.2. In addition, equation (4.2) clearly holds under $\bar{\mathcal{X}}_j = \mathcal{X}_j^a$. Thus, Theorem 4.1(2) is satisfied under $\bar{\mathcal{X}}_j = \mathcal{X}_j^a$ and the given \mathcal{D} . \square

The above result leads to an approach with a simple implementation. However, it does not consider the initially existing signals \mathcal{X}_j^0 , which can potentially reduce the number of additional excitation signals. Moreover, the signals are directly allocated at the vertices in $\mathcal{D} \cup \bar{\mathcal{W}}_j$. To make use of \mathcal{X}_j^0 and to explore the freedom to allocate the signals, a more comprehensive method is introduced in Algorithm 1. Also, note that \mathcal{X}_j^0 may contain both measured excitation signals and unmeasured noise signals.

Given a network model set with the target modules in $G_{j\bar{\mathcal{W}}_j}(q)$ and the pre-existing external signals \mathcal{X}_j^0 , Algorithm 1 computes a minimum disconnecting set \mathcal{D} from $\bar{\mathcal{N}}_{\bar{\mathcal{W}}_j}^+ \cup \mathcal{X}_j^0$ to $\mathcal{W}_j^- \setminus \bar{\mathcal{W}}_j$ first and then removes the vertices in $\mathcal{D} \cup \bar{\mathcal{W}}_j$ that are already excited by \mathcal{X}_j^0 via vertex disjoint paths. Then the algorithm allocates additional excitation signals to excite the remaining vertices in $\mathcal{D} \cup \bar{\mathcal{W}}_j$ through vertex disjoint paths. The validity of Algorithm 1 is shown in the following result.

Theorem 4.3. *Given a network model set \mathcal{M} that satisfies Assumptions 3.1, 3.2, 3.4 and 3.5. In the returned model set of Algorithm 1 with the allocated excitation signals, $G_{j\bar{\mathcal{W}}_j}(q)$ is generically identifiable from (w, r) .*

Proof. From step 1 to 2 in Algorithm 1, by construction, if $|\mathcal{P}| = |\mathcal{D} \cup \bar{\mathcal{W}}_j|$, equation (4.2) holds with $\bar{\mathcal{X}}_j = \mathcal{X}_j^0$, and thus the modules are generically identifiable in the original model set \mathcal{M} .

When $|\mathcal{P}| < |\mathcal{D} \cup \bar{\mathcal{W}}_j|$, based on Theorem 4.1, we need to allocate extra $|\mathcal{D} \cup \bar{\mathcal{W}}_j| - |\mathcal{P}|$ signals, such that: (i) there are $|\mathcal{D} \cup \bar{\mathcal{W}}_j| - |\mathcal{P}|$ vertex disjoint paths from these signals to $(\mathcal{D} \cup \bar{\mathcal{W}}_j) \setminus \bar{\mathcal{D}}$,

Algorithm 1 Signal allocation for a single module

INPUT: A model set \mathcal{M} with graph \mathcal{G} , the target modules $G_{j\bar{\mathcal{W}}_j}$, and a set of initial external signals \mathcal{X}_j^0 ;

OUTPUT: A new model set \mathcal{M}_{out} with its graph \mathcal{G}_{out} and the allocated signals.

- 1: Compute a minimum disconnecting set \mathcal{D} from $\bar{\mathcal{N}}_{\bar{\mathcal{W}}_j}^+ \cup \mathcal{X}_j^0$ to $\mathcal{W}_j^- \setminus \bar{\mathcal{W}}_j$;
 - 2: Based on Lemma 4.3, compute a set of paths \mathcal{P} that contains the maximum number of vertex disjoint paths from \mathcal{X}_j^0 to $\mathcal{D} \cup \bar{\mathcal{W}}_j$, while the paths are internally vertex disjoint with $\mathcal{D} \cup \bar{\mathcal{W}}_j$;
 - 3: Let $\bar{\mathcal{D}} \subseteq \mathcal{D} \cup \bar{\mathcal{W}}_j$ denote all the ending vertices of the paths in \mathcal{P} ;
 - 4: **if** $|\mathcal{P}| < |\mathcal{D} \cup \bar{\mathcal{W}}_j|$ **then**
 - 5: Find the largest set $\bar{\mathcal{W}} \subseteq \mathcal{W}$ such that \mathcal{D} is a disconnecting set from $\bar{\mathcal{W}}$ to $\mathcal{W}_j^- \setminus \bar{\mathcal{W}}_j$;
 - 6: Build a subgraph $\bar{\mathcal{G}} \subseteq \mathcal{G}$ by removing all the vertices and edges of the paths in \mathcal{P} ;
 - 7: Find a set $\mathcal{W}_{exp} \subseteq \bar{\mathcal{W}}$ such that in $\bar{\mathcal{G}}$, there are $|\mathcal{D} \cup \bar{\mathcal{W}}_j| - |\mathcal{P}|$ vertex disjoint paths from \mathcal{W}_{exp} to $(\mathcal{D} \cup \bar{\mathcal{W}}_j) \setminus \bar{\mathcal{D}}$;
 - 8: In $\bar{\mathcal{G}}$, assign distinct excitation signals to every vertex in \mathcal{W}_{exp} , which leads to a new model set \mathcal{M}_{out} with a new graph \mathcal{G}_{out} ;
 - 9: Return \mathcal{M}_{out} with the graph \mathcal{G}_{out} ;
 - 10: **else**
 - 11: $\mathcal{M}_{out} \leftarrow \mathcal{M}$ and $\mathcal{G}_{out} \leftarrow \mathcal{G}$;
 - 12: Return \mathcal{M}_{out} with the graph \mathcal{G}_{out} .
 - 13: **end if**
-

and these paths are also vertex disjoint with \mathcal{P} ; (ii) \mathcal{D} remains a disconnecting set from the added signals to $\mathcal{W}_j^- \setminus \bar{\mathcal{W}}_j$. Then we can find in the algorithm, step 5 guarantees (ii), and steps 3, 6, 7 and 8 guarantee (i). This concludes the proof. \square

Remark 4.1. In Algorithm 1, the excitation signals do not need to be allocated directly at the vertices in $\mathcal{D} \cup \bar{\mathcal{W}}_j$. It suffices when they reach these vertices through vertex disjoint paths from excitation locations elsewhere in the network. In addition, the obtained experimental setup in Algorithm 1 may not be unique.

Algorithm 1 and the synthesis approach in Corollary 4.4 guarantee the minimum number of allocated signals when $\mathcal{X}_j^0 = \emptyset$, as a minimum disconnecting set is used. When $\mathcal{X}_j^0 \neq \emptyset$, the following bound on the number of additionally required signals can be derived based on Algorithm 1.

Corollary 4.5. Given a network model set \mathcal{M} that satisfies Assumptions 3.1, 3.2, 3.4 and 3.5. Let \mathcal{X}_j^0 denote the set of initial external signals that have no unknown directed edge to w_j . Let \mathcal{D} be a minimum disconnecting set from $\bar{\mathcal{N}}_{\bar{\mathcal{W}}_j}^+ \cup \mathcal{X}_j^0$ to $\mathcal{W}_j^- \setminus \bar{\mathcal{W}}_j$, and let c denote the number of additional excitation signals available for allocation. The number of additional excitation signals

c is sufficient to make $G_{j\bar{\mathcal{W}}_j}(q)$ generically identifiable if

$$c \geq |\mathcal{D} \cup \bar{\mathcal{W}}_j| - b_{\mathcal{X}_j^0 \rightarrow \mathcal{D} \cup \bar{\mathcal{W}}_j}.$$

The procedure of Algorithm 1 is illustrated in the following example for the case where $\bar{\mathcal{W}}_j$ only contains a single vertex.

Example 4.2. For the network model set in Figure 4.3(a), the problem is to allocate excitation signals such that $G_{73}(q)$ becomes generically identifiable. All the internal signals are measured in this model set, and module $G_{75}(q)$ is known. In addition, it holds that $\mathcal{W}_7^- = \{w_3, w_4, w_6, w_8\}$ which contains all the inputs of w_7 through unknown modules.

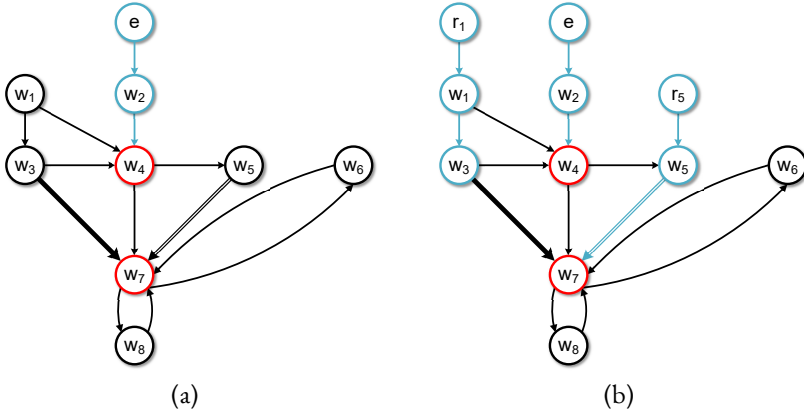


Figure 4.3: An example of allocating signals for generic identifiability of G_{73} (thick line) using Algorithm 1 with a known module G_{75} (double-lined edge). Starting from the network model set, a disconnecting set $\{w_4, w_7\}$ (red vertices) from $\{w_3, e\}$ to $\{w_4, w_6, w_8\}$ is computed in (a). Since there already exists an external signal e which has a path to w_4 , a vertex in the disconnecting set, we only need to add r_1 and r_5 as in (b), which achieves generic identifiability of G_{73} .

$\mathcal{X}_7^0 = \{e\}$ is the only external signal that is initially present. Firstly, a disconnecting set from $\mathcal{X}_7^0 \cup \{w_3\} = \{w_3, e\}$ to $\mathcal{W}_7^- \setminus \{w_3\} = \{w_4, w_6, w_8\}$ is constructed as $\mathcal{D} = \{w_4, w_7\}$, indicated by the red vertices in Figure 4.3(a). Based on Theorem 4.1, the generic identifiability of $G_{73}(q)$ requires three vertex disjoint paths from external signals to $\mathcal{D} \cup \{w_3\} = \{w_3, w_4, w_7\}$, while \mathcal{D} remains a disconnecting set from the external signals to $\mathcal{W}_7 \setminus \{w_3\}$. Following step 2 in Algorithm 1, we find a path $e \rightarrow w_4$ from \mathcal{X}_7^0 to $\mathcal{D} \cup \{w_3\}$ (colored blue in Figure 4.3(a)). Thus we only need to allocate extra excitation signals from which there are two vertex disjoint paths to $\{w_3, w_7\}$, and the two paths should be vertex disjoint with $e \rightarrow w_4$. As in step 5, the potential locations to allocate excitation signals is $\bar{\mathcal{W}} = \{w_1, w_2, w_3, w_4, w_5, w_7\}$, which satisfies that \mathcal{D} remains a disconnecting set from $\bar{\mathcal{W}}$ to $\mathcal{W}_7^- \setminus \{w_3\}$. After removing path $e \rightarrow w_4$ as in step 6, we choose $\mathcal{W}_{\text{exp}} = \{w_1, w_5\} \subseteq \bar{\mathcal{W}}$ to be excited by r_1 and r_5 , as shown in Figure 4.3(b).

According to Theorem 4.1, $G_{73}(q)$ is indeed generically identifiable in Figure 4.3(b): There exists a disconnecting set $\mathcal{D} = \{w_4, w_7\}$ from $\mathcal{X}_7 = \{r_1, r_5, e\}$ to $\mathcal{W}_7^- \setminus \{w_3\} = \{w_4, w_6, w_8\}$ such

that $b_{\mathcal{X}_7 \rightarrow \mathcal{D} \cup \{w_3\}} = 3$, i.e. there are maximally three vertex disjoint paths from \mathcal{X}_7 to $\mathcal{D} \cup \{w_3\}$, as indicated by the blue paths in Figure 4.3(b). Note that in this example, the choice of excitation locations, i.e. the set \mathcal{W}_{exp} , is not unique, e.g., choosing $\mathcal{W}_{\text{exp}} = \{w_3, w_7\}$ to be excited can also achieve the generic identifiability of $G_{73}(q)$.

When the generic identifiability of a subset of modules with different outputs is of interest, i.e. the modules in $G_{j\mathcal{W}_j}(q)$ for some $j \in \{1, \dots, L\}$, Algorithm 1 can be applied recursively to achieve the generic identifiability of $G_{j\mathcal{W}_j}$ for each j . If the generic identifiability of the full network is concerned, a more compact graphical approach for signal allocation can be developed in the following sections.

4.4 DISJOINT PSEUDOTREE COVERING

The synthesis approaches in the previous sections can naturally be extended to address the generic identifiability of a full network, by applying the synthesis algorithm to each local MISO subsystem such that $G_{j\mathcal{W}_j}(q)$ is generically identifiable for every j . However, such a local procedure may allocate redundant excitation signals and increase the experimental cost for the synthesis of a full network, since each MISO subsystem is considered independently and the connection between different MISO subsystems is overlooked.

To develop a synthesis tool that does not require the above vertex-wise procedure, we will first introduce a novel graph concept in this section, called *pseudotrees*, and relevant results on disjoint pseudotree covering. Then in Section 4.5, a new characterization of generic identifiability will be presented based on disjoint pseudotrees, which further leads to an excitation signal allocation approach for the generic identifiability of a full network.

We make the result of this section self-contained and independent of the signal allocation problem of dynamic networks. Some basic graphical notations used in the pseudotree-related results are first introduced. Given a directed graph \mathcal{G} , we denote $\mathcal{V}(\mathcal{G})$ and $\mathcal{E}(\mathcal{G})$ as the vertex set and edge set of \mathcal{G} , respectively. The union of two graphs \mathcal{G}_1 and \mathcal{G}_2 is denoted by $\mathcal{G} \triangleq \mathcal{G}_1 \cup \mathcal{G}_2$, where $\mathcal{V}(\mathcal{G}) = \mathcal{V}(\mathcal{G}_1) \cup \mathcal{V}(\mathcal{G}_2)$ and $\mathcal{E}(\mathcal{G}) = \mathcal{E}(\mathcal{G}_1) \cup \mathcal{E}(\mathcal{G}_2)$. The sources and sinks of \mathcal{G} are collected by sets $\mathcal{S}_{\text{ou}}(\mathcal{G})$ and $\mathcal{S}_{\text{in}}(\mathcal{G})$, respectively.

In this section, a novel graph concept called *directed pseudotree* is introduced.

Definition 4.1. *A connected simple directed graph \mathcal{T} , with $|\mathcal{V}(\mathcal{T})| \geq 2$, is called a (directed) **pseudotree** if any vertex in \mathcal{T} has at most one in-neighbor.*

The above concept of pseudotrees is an extension of its definition in the undirected case, in which they are also referred to as *unicyclic graphs*, see e.g., [44, 108]. Particularly, we exclude a singleton vertex being a pseudotree. Analogous to directed tree graphs, the following terminologies are used.

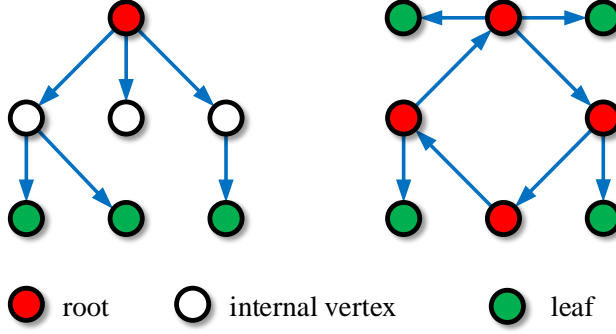


Figure 4.4: Typical examples of pseudotrees, in which roots, internal vertices and leaves are labeled with different colors. Note that a pseudotree may have multiple roots.

Definition 4.2. In a directed pseudotree \mathcal{T} , a vertex is called a **root** if there is exactly one directed path from this vertex to every other vertex in \mathcal{T} . Furthermore, a vertex is called a **leaf** of \mathcal{T} if it has no out-neighbors in \mathcal{T} , and a vertex is an **internal vertex** of \mathcal{T} if it is neither a root nor a leaf. We denote $\Upsilon(\mathcal{T})$ as the set that collects all the roots of a pseudotree \mathcal{T} .

The notion of internal vertices is used with abuse of notation when pseudotrees are concerned. In Figure 4.4, typical examples of pseudotrees are presented, in which the definitions of roots, internal vertices, and leaves are illustrated. Note that the class of directed pseudotrees also includes all directed rooted trees. However, different from the standard definition of trees, a pseudotree can allow for multiple roots, which form a directed circle with all the edges being oriented in the same direction, and outgoing branches from any vertex on this circle are also possible, see the right subplot in Figure 4.4.

Similar to the concept of vertex-disjoint paths, disjoint pseudotrees are defined as follows.

Definition 4.3 (Disjoint pseudotrees). Consider two pseudotrees \mathcal{T}_1 and \mathcal{T}_2 as subgraphs of a directed graph \mathcal{G} . \mathcal{T}_1 and \mathcal{T}_2 are called **disjoint** in \mathcal{G} if the following two conditions hold.

1. $\mathcal{E}(\mathcal{T}_1) \cap \mathcal{E}(\mathcal{T}_2) = \emptyset$;
2. either $\mathcal{E}_j \subseteq \mathcal{E}(\mathcal{T}_1)$ or $\mathcal{E}_j \subseteq \mathcal{E}(\mathcal{T}_2)$, $\forall j \in \mathcal{V}(\mathcal{T}_1) \cup \mathcal{V}(\mathcal{T}_2)$, where $\mathcal{E}_j \triangleq \{(j, i) \in \mathcal{E}(\mathcal{T}_1) \cup \mathcal{E}(\mathcal{T}_2) \mid i \text{ is an out-neighbor of } j\}$.

The first condition means that \mathcal{T}_1 and \mathcal{T}_2 do not share any edges, while the second condition means that for each vertex, all its outgoing edges in the two pseudotrees are contained in one and the same pseudotree. As a special case, if both \mathcal{T}_1 and \mathcal{T}_2 are directed rooted trees, then \mathcal{T}_1 and \mathcal{T}_2 do not share the same root or any common internal vertex. We illustrate the concept of disjoint pseudotrees in Definition 4.3 with the following example.

Example 4.3. In Figure 4.5, we illustrate the conditions for disjoint pseudotrees. In (a) and (b), we decompose the directed graph into two pseudotrees, which do not share any common edges. However,

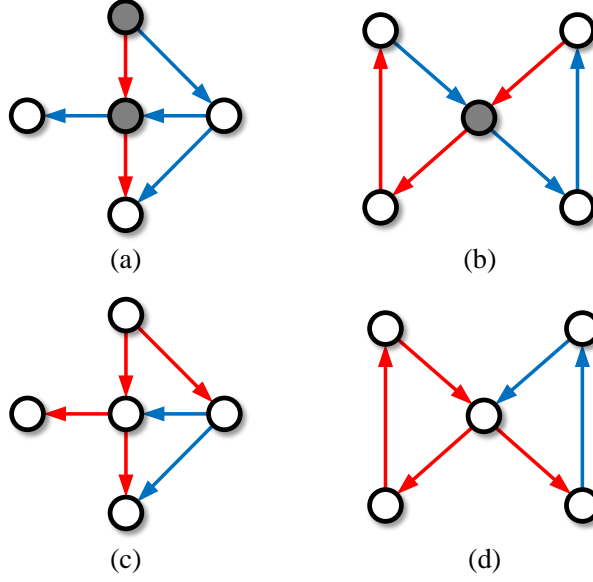


Figure 4.5: Illustration of disjoint pseudotrees, in which the different pseudotrees are induced by the edges with distinct colors. In (a) and (b), the pseudotrees are not disjoint, since the out-going edges of the gray vertices are assigned to different pseudotrees. In contrast, the pseudotrees in (c) and (d) are characterized as disjoint pairs.

they are not disjoint. In (a) and (b), the two outgoing edges of the internal vertex in the center have been assigned to different pseudotrees, which violates the second condition in Definition 4.3. In contrast, we take a different decomposition of the two networks in (c) and (d), and then the two pseudotrees obtained in (c) and (d) become disjoint.

It is worth noting that the notion of disjoint pseudotrees is closely related to that of vertex-disjoint paths. Consider \mathcal{T}_1 and \mathcal{T}_2 as two disjoint pseudotrees in \mathcal{G} . For any $i \in \mathcal{V}(\mathcal{T}_1) \cap \mathcal{V}(\mathcal{T}_2)$, if i has two or more in-neighbors, then there exist two in-neighbors of i located in \mathcal{T}_1 and \mathcal{T}_2 separately. Then, due to the fact that distinct pseudotrees cannot share any common root or internal vertex, we can find two vertex-disjoint paths in the union $\mathcal{T}_1 \cup \mathcal{T}_2$ starting from two roots in \mathcal{T}_1 and \mathcal{T}_2 , respectively, to the two distinct in-neighbors of i , and each pseudotree contains exactly one path.

Next, the concept of disjoint-edge covering for a directed graph is introduced.

Definition 4.4. Consider a directed graph \mathcal{G} , and let $\Pi := \{\mathcal{T}_1, \mathcal{T}_2, \dots, \mathcal{T}_n\}$ be a collection of connected subgraphs of \mathcal{G} . The edges in a set $\mathcal{E} \subseteq \mathcal{E}(\mathcal{G})$ are covered by Π , if $\mathcal{E} \subseteq \mathcal{E}(\mathcal{T}_1) \cup \mathcal{E}(\mathcal{T}_2) \cup \dots \cup \mathcal{E}(\mathcal{T}_n)$, and Π is called a **covering** of \mathcal{E} . Moreover, if all the elements in Π are pseudotrees, which are disjoint to each other, then Π is a **disjoint pseudotree covering** of \mathcal{E} .

The concept of connectedness of the subgraphs is defined in Section 2.4. Relating to the definition of disjoint pseudotree coverings, the following two lemmas are given.

Lemma 4.1. *For a directed simple graph \mathcal{G} with $|\mathcal{V}(\mathcal{G})| \geq 2$, there always exists a set of disjoint pseudotrees that cover all the edges in $\mathcal{E}(\mathcal{G})$ or any subset of $\mathcal{E}(\mathcal{G})$.*

Proof. To prove this statement, we consider each vertex $j \in \mathcal{V}(\mathcal{G}) \setminus \mathcal{S}_{\text{in}}(\mathcal{G})$, with $\mathcal{S}_{\text{in}}(\mathcal{G})$ the set of all the sinks of \mathcal{G} . Starting from j , we can construct a directed star tree (a special type of pseudotrees) with j as the single root and all its out-neighbors as the leaves. Then, $|\mathcal{V}(\mathcal{G}) \setminus \mathcal{S}_{\text{in}}(\mathcal{G})|$ pseudotrees are formed as a covering of $\mathcal{E}(\mathcal{G})$, which are disjoint, since any two trees do not share a common root or any common internal vertex. For any subset of $\mathcal{E}(\mathcal{G})$, its disjoint pseudotree covering can be found using the similar approach. \square

Let us define a *minimal* pseudotree, which only contains one root and all the out-neighbors of this root. By the proof of Lemma 4.1, the maximal number of disjoint pseudotrees that coexist in \mathcal{G} is $|\mathcal{V}(\mathcal{G}) \setminus \mathcal{S}_{\text{in}}(\mathcal{G})|$. Then, the following lemma holds.

Lemma 4.2. *Let \mathcal{G} be a simple directed graph. If there exist k_1 disjoint pseudotrees covering $\mathcal{E}(\mathcal{G})$, with $k_1 < |\mathcal{V}(\mathcal{G}) \setminus \mathcal{S}_{\text{in}}(\mathcal{G})|$, then there also exist k_2 disjoint pseudotrees, for any $k_1 < k_2 \leq |\mathcal{V}(\mathcal{G}) \setminus \mathcal{S}_{\text{in}}(\mathcal{G})|$, that cover $\mathcal{E}(\mathcal{G})$.*

Proof. The maximal number of disjoint pseudotrees that coexist in \mathcal{G} does not exceed $|\mathcal{V}(\mathcal{G}) \setminus \mathcal{S}_{\text{in}}(\mathcal{G})|$, where $\mathcal{S}_{\text{in}}(\mathcal{G})$ is the set of the sinks in \mathcal{G} . It then requires $k_1 < |\mathcal{V}(\mathcal{G}) \setminus \mathcal{S}_{\text{in}}(\mathcal{G})|$, implying that in the k_1 disjoint pseudotrees, there exists at least one pseudotree \mathcal{T}_k which contains at least one internal vertex or contains multiple roots. In both cases, we will show that \mathcal{T}_k can be decomposed into two disjoint pseudotrees.

Suppose \mathcal{T}_k contains internal vertices. We can always find an internal vertex i with all its out-neighbors being the leaves of \mathcal{T}_k . Define a directed tree T_a with i as the root and all its out-neighbors as the leaves. Thereby, \mathcal{T}_k is decomposed into two a directed tree T_a and a pseudotree \mathcal{T}_b , where $R(T_b) := \Upsilon(\mathcal{T}_k)$, $\mathcal{V}(\mathcal{T}_b) \subseteq (\mathcal{T}_k)$, and $\mathcal{E}(T_b) := \mathcal{E}(\mathcal{T}_k) \setminus \mathcal{E}(T_a)$. Note that T_a and \mathcal{T}_b are disjoint by Definition 4.3. Moreover, since T_a and \mathcal{T}_b are subgraphs of \mathcal{T}_k , which is disjoint to the other trees, T_a and \mathcal{T}_b are also disjoint to the other pseudotrees. Next, suppose \mathcal{T}_k does not contain any internal vertex but multiple roots, i.e., $|\Upsilon(\mathcal{T}_k)| \geq 2$. In this case, we define the directed tree T_a , which is rooted at one of $\Upsilon(\mathcal{T}_k)$ and includes all the out-neighbors of this root as the leaves of T_a . Then, similar to the previous case, we can partition \mathcal{T}_k into two disjoint pseudotrees, which are disjoint to the other pseudotrees in \mathcal{G} . Therefore, in the above cases, \mathcal{E} can be covered by $k_1 + 1$ disjoint pseudotrees. The statement of this lemma follows by iteratively applying the above reasoning for all $k_2 \geq k_1 + 1$. \square

The above result will be used to design an iterative synthesis approach for signal allocation, as shown in Section 4.5.2 and [38].

4.5 SIGNAL ALLOCATION FOR FULL NETWORK IDENTIFIABILITY

On the basis of disjoint pseudotree covering, we present a novel approach for the allocation of excitation signals such that the generic identifiability of a full network model set \mathcal{M} is achieved, i.e. all modules are generically identifiable. The key step relies on a partitioning of \mathcal{G} associated with \mathcal{M} into a minimal number of disjoint pseudotrees.

4.5.1 GENERIC IDENTIFIABILITY: A PSEUDOTREE CHARACTERIZATION

From Section 4.4, we notice that there is a clear connection between vertex disjoint paths and disjoint pseudotrees. Thus, a novel characterization for the generic identifiability of a full network is developed using the concept of disjoint pseudotrees, which is used as the theoretical foundation for the follow-up synthesis method. To this end, we first define a new graph associated with a model set \mathcal{M} .

Definition 4.5. *Given a network model set \mathcal{M} and its associated graph \mathcal{G} . Let $\bar{\mathcal{G}}$ be a graph obtained from \mathcal{G} by removing all the known out-going edges of the vertices in \mathcal{X} and after that, removing the vertices in \mathcal{X} which have no out-going edge.*

The removal of the known edges from \mathcal{G} in the above definition is because these known edges do not need to be covered by the pseudotree covering. The definition of $\bar{\mathcal{G}}$ is equivalent to the so-called extended network in [38], where only the entries in $G(q)$ and the unknown entries in $R(q)$ and $H(q)$ are represented as directed edges.

Recall that an internal signal is said to be directly excited by an external signal if there exists one directed edge from the external signal to the internal signal in \mathcal{G} associated with \mathcal{M} . An external signal is also considered to be directly excited by itself.

Theorem 4.4. *Consider a network model set \mathcal{M} that satisfies Assumptions 3.1, 3.2, 3.4, 3.5 and its associated graph $\bar{\mathcal{G}}$ in Definition 4.5. Then the network model set \mathcal{M} is generically identifiable from (w, r) if there exists a disjoint pseudotree covering of $\mathcal{E}(\bar{\mathcal{G}})$, denoted by $\Pi = \{\mathcal{T}_1, \mathcal{T}_2, \dots, \mathcal{T}_n\}$, such that any pseudotree \mathcal{T}_k in this covering satisfies at least one of the following two conditions:*

- \mathcal{T}_k contains a root that is directly excited in \mathcal{M} by an external signal, and this external signal is distinct from the ones that excite the roots of other pseudotrees;
- For any internal signal in $\mathcal{V}(\mathcal{T}_k)$, denoted by w_j , it holds in \mathcal{M} that

$$b_{\mathcal{X} \rightarrow \mathcal{W}_j^-} = |\mathcal{W}_j^-|. \quad (4.7)$$

The above conditions become also necessary when \mathcal{M} is additionally a non-parametric model set.

Proof. We first prove the ‘if’ statement. Let $\Pi = \{\mathcal{T}_1, \mathcal{T}_2, \dots, \mathcal{T}_n\}$ be a set of pseudotrees that cover all the edges in $\bar{\mathcal{G}}$. Note that the disjointness of the pseudotrees in Definition 4.3 implies that the paths in different disjoint pseudotrees are vertex-disjoint, if they have no common starting or ending nodes, and, for any internal signal w_j in $\bar{\mathcal{G}}$, the edges from \mathcal{W}_j^- and $\mathcal{X} \setminus \mathcal{X}_j$ to w_j should belong to distinct pseudotrees. Furthermore, any two disjoint pseudotrees cannot share a common root node.

Now define $\bar{\mathcal{V}} := \mathcal{V}(\mathcal{T}_{m+1}) \cup \dots \cup \mathcal{V}(\mathcal{T}_n)$ that collects the pseudotrees satisfying the second condition, and thus all the in-coming edges of each internal signal $w_j \in V(\bar{\mathcal{G}}) \setminus \bar{\mathcal{V}}$ belong to distinct pseudotrees in $\{\mathcal{T}_1, \dots, \mathcal{T}_m\}$. Combining the first condition and the disjointness of the pseudotrees, (4.7) holds for any $w_j \in V(\bar{\mathcal{G}}) \setminus \bar{\mathcal{V}}$. Finally, for any vertex $w_j \in \bar{\mathcal{V}}$, (4.7) is guaranteed by the second condition, and thus (4.7) holds for any internal signal of $\bar{\mathcal{G}}$ and thus of \mathcal{G} . Then according to Theorem 3.4, the full network (and thus all modules) is generically identifiable.

Next, the ‘only if’ statement is proven. Let the network model set \mathcal{M} be generically identifiable, and we will show that a disjoint pseudotree covering exists and satisfies the condition in this theorem. It is obtained from Lemma 4.1 that we can always find a disjoint pseudotree covering of $\mathcal{E}(\bar{\mathcal{G}})$, denoted by $\Pi = \{\mathcal{T}_1, \mathcal{T}_2, \dots, \mathcal{T}_n\}$, with $n = |V(\bar{\mathcal{G}}) \setminus \mathcal{S}_{\text{in}}(\bar{\mathcal{G}})|$, where each pseudotree is only composed of a node as its root and all its out-neighbors as leaves. In these pseudotrees, there must exist a set of pseudotrees $\Pi_r \subseteq \Pi$, with $|\Pi_r| = m$ and $0 \leq m \leq n$, in which every pseudotree has its root that is directly excited by a distinct vertex in \mathcal{X} . Then, we only need to prove that the path condition $b_{\mathcal{X} \rightarrow \mathcal{W}_j^-} = |\mathcal{W}_j^-|$ holds, for every internal signal $w_j \in \Pi \setminus \Pi_r$. This is guaranteed by Theorem 3.4 when the generic identifiability of all the modules is concerned. That completes the proof. \square

Note that in the first condition of Theorem 4.4, the pseudotree covering is constructed according to the graph $\bar{\mathcal{G}}$; however, the verification of the excitation sources for the roots of the pseudotrees should be conducted in the model set \mathcal{M} , i.e., the removed external signals in $\bar{\mathcal{G}}$ from \mathcal{G} should still be considered.

Theorem 4.4 states that the generic identifiability of a full network can be guaranteed, if a pseudotree covering of the graph $\bar{\mathcal{G}}$ exists where a subset of these pseudotrees has their roots excited, while for the pseudotree without excited roots, their vertices should satisfy the path-based identifiability condition in (4.7). A special case of this theorem is when all the pseudotrees satisfy the second condition, and then generic identifiability is ensured by (4.7). This path-based condition (4.7) is a special case of the condition in Theorem 3.4 with $\bar{\mathcal{W}}_j = \mathcal{W}_j^-$. However, the more interesting case is when all the pseudotrees satisfy the first condition in Theorem 4.4, which leads to the following sufficient condition for generic identifiability.

Corollary 4.6. *Consider the setting of Theorem 4.4. Then the network model set \mathcal{M} is generically identifiable from (r, w) if there exists a set of disjoint pseudotrees covering of $\mathcal{E}(\bar{\mathcal{G}})$, and each pseudotree contains a root that is directly excited by a distinct external signal.*

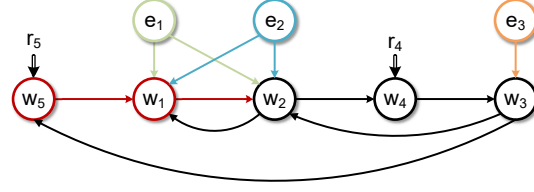


Figure 4.6: Consider $\bar{\mathcal{G}}$ defined in Definition 4.5 of a model set with all the internal signals measured. r_5 and r_4 are not represented as vertices according to the definition of $\bar{\mathcal{G}}$ because all their out-going edges are known (double-lined edges). $\bar{\mathcal{G}}$ is decomposed into 5 disjoint pseudotrees, which are highlighted with different colors. Since each pseudotree contains a root that is excited by a distinct external signal, this model set is generically identifiable.

The above condition is sufficient for the generic identifiability of a full network and obtained from the first condition in Theorem 4.4. The second condition in Theorem 4.4 is needed when we have more disjoint pseudotrees in a covering than necessary, such that only a subset of pseudotrees need their roots to be directly excited. Then the vertices in the remaining pseudotrees only need to satisfy (4.7).

Corollary 4.6 is related to the graphical conditions for structural controllability of linear state-space models [42, 87], where to achieve controllability, the graph of a state-space model needs to be covered by paths from inputs to states and cycles. However, we should note that controllability and the identifiability concept of this work are essentially different properties of different models, which consequently leads to different graphical conditions. These graphical conditions have similarities as all of them are derived based on rank tests.

Corollary 4.6 is illustrated in Example 4.4.

Example 4.4. Consider a five-vertex model set whose associated graph $\bar{\mathcal{G}}$, that is defined in Definition 4.5, is depicted in Figure 4.6. The graph $\bar{\mathcal{G}}$ can be covered by five disjoint pseudotrees. Observe that each pseudotree has a root that is directly excited by a distinct external signal. For example, e_1 , as a root of one pseudotree, is excited by itself. Similarly, the root w_5 in the red pseudotree is excited by r_5 . Thus, the condition in Corollary 4.6 is satisfied, and we conclude that the dynamic network model set \mathcal{M} in Figure 4.6 is generically identifiable.

While Theorem 3.4 can also be used to test the generic identifiability of a full network by verifying the path-based condition (4.7) for each vertex, Corollary 4.6 provide a more integrated condition for characterizing the generic identifiability of a full network. The major advantage of this pseudotree covering condition in Corollary 4.6 over the path-based condition in Theorem 3.4 is that, rather than providing a vertex-wise analysis, it has the potential for the synthesis problem that we are interested in.

Corollary 4.6 clearly suggests an approach to address the synthesis problem by finding the minimal number of disjoint pseudotrees in the network that cover all the edges in $\bar{\mathcal{G}}$. At this point, we relate the synthesis problem to a combinatorial optimization problem. Then if the

roots of a subset of those pseudotrees are not excited, additional excitation signals can be allocated to excite these roots.

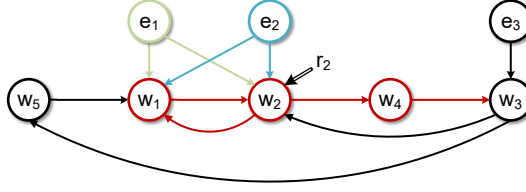


Figure 4.7: Consider $\bar{\mathcal{G}}$ in Figure 4.6 without excitation signals r_4 and r_5 . The goal is to allocate extra r signals to achieve the generic identifiability of the full network. Four disjoint pseudotrees are needed to cover all the edges of this graph. Thus, in addition to the white noise excitations e_1, e_2 and e_3 , only one external excitation signal is required to achieve the generic identifiability of the network, and assigning this excitation signal to either vertex w_1 or w_2 will lead to this result, e.g., a signal r_2 is allocated at w_2 .

For a simple network consisting of only a few vertices, we may immediately obtain the minimal number of disjoint pseudotrees and then allocate excitation signals such that the generic identifiability of the full network is achieved, see Figure 4.7. However, when a more complicated graph is considered, a systematic approach is required to decompose a graph into a set of disjoint pseudotrees, or ideally, a minimum number of pseudotrees. Thus, in the next subsection, we discuss such an algorithmic procedure.

4.5.2 EXCITATION ALLOCATION: A PSEUDOTREE MERGING APPROACH

In this section, we briefly discuss one algorithmic procedure to decompose a network into disjoint pseudotrees and then to allocate additional excitation signals such that the generic identifiability of all modules can be achieved. One more advanced algorithm and the relevant details can be found in [38].

To find a set of disjoint pseudotrees that covers all the edges in $\bar{\mathcal{G}}$, we devise a simple graph merging algorithm. Lemma 4.1 indicates that for any directed graph $\bar{\mathcal{G}}$, we can always find a disjoint minimal pseudotree covering,

$$\Pi_0 = \{\mathcal{T}_1^{(0)}, \mathcal{T}_2^{(0)}, \dots, \mathcal{T}_{|\Pi_0|}^{(0)}\}, \quad (4.8)$$

where each minimal pseudotree is rooted at a vertex in $V(\bar{\mathcal{G}}) \setminus \mathcal{S}_{\text{in}}(\bar{\mathcal{G}})$, with \mathcal{S}_{in} the set of sinks in $\bar{\mathcal{G}}$. Here, $|\Pi_0| = |V(\bar{\mathcal{G}})| - |\mathcal{S}_{\text{in}}(\bar{\mathcal{G}})|$. In other words, each vertex, besides the sinks, is the root of its own pseudotree, consisting of all its out-going edges. The proposed approach starts with Π_0 as the initial disjoint pseudotree covering, and we then implement a specific strategy to recursively merge the pseudotrees to reduce the number of pseudotrees, until there are no mergeable pseudotrees in a covering. As a relevant and necessary concept, the *mergeability* of pseudotrees is defined as follows.

Definition 4.6 (Mergeability). *Consider two disjoint pseudotrees \mathcal{T}_1 and \mathcal{T}_2 and $\mathcal{V}(\mathcal{T}_1) \cap \mathcal{V}(\mathcal{T}_2) \neq \emptyset$. We say that \mathcal{T}_1 is mergeable to \mathcal{T}_2 if*

1. *the union of \mathcal{T}_1 and \mathcal{T}_2 , i.e., $(\mathcal{V}(\mathcal{T}_1) \cup \mathcal{V}(\mathcal{T}_2), \mathcal{E}(\mathcal{T}_1) \cup \mathcal{E}(\mathcal{T}_2))$, is also a pseudotree,*
2. *and there is a directed path from every root of \mathcal{T}_2 to every vertex in \mathcal{T}_1 .*

If \mathcal{T}_1 is mergeable to \mathcal{T}_2 then the roots of \mathcal{T}_2 remain the roots of the merged pseudotree. The mergeability of a pseudotree \mathcal{T}_1 to \mathcal{T}_2 requires that \mathcal{T}_1 and \mathcal{T}_2 do not share any common leaf and internal vertex. As a result, merging \mathcal{T}_1 and \mathcal{T}_2 yields a new pseudotree \mathcal{T}_3 , where the roots of \mathcal{T}_2 remain roots in \mathcal{T}_3 . Note that \mathcal{T}_1 being mergeable to \mathcal{T}_2 does not necessarily mean that \mathcal{T}_2 is also mergeable to \mathcal{T}_1 . We say \mathcal{T}_1 and \mathcal{T}_2 are mergeable if \mathcal{T}_1 is mergeable to \mathcal{T}_2 or \mathcal{T}_2 is also mergeable to \mathcal{T}_1 .

Then an algorithm can be introduced to merge the pseudotrees in the initial covering Π_0 , such that the number of pseudotrees and thus the required excitation signals for allocation are reduced. Here we consider a simple greedy procedure, where we randomly start with a pseudotree in Π_0 , e.g. $\mathcal{T}_1^{(0)}$, and then merge it with other mergeable pseudotrees recursively, until merging is not possible. Then another pseudotree can be chosen to repeat the above procedure until there is no pseudotree in the covering that can be further merged. This will lead to a final set of disjoint pseudotrees Π .

Finally, for each pseudotree in Π , we can test if there exists a root that is excited by an initially present external signal. If not, an additional excitation signal can be allocated at one root of the pseudotree. It is clear that the above procedure can lead to a generically identifiable model set, according to Corollary 4.6.

The above procedure is an illustrative example of an algorithm for obtaining a pseudotree covering and then allocating excitation signals. This approach may not lead to a minimum number of disjoint pseudotrees and thus a minimum number of allocated excitation signals. A more advanced merging algorithm is developed in [38], where an attractive algebraic implementation of the algorithm is also obtained*.

It is noted that a subsequent procedure can be taken after signal allocation according to the pseudotree covering, that is to perform the vertex-wise tests in Theorem 3.4 to check if the full network remains generically identifiable when an allocated excitation signal is removed. This procedure can remove the redundant excitation signals and further decrease the experimental cost, see the details in [38].

*The algebraic implementation of the merging algorithm in [38] is not presented here for ease of discussion. Consequently, [38, Lemma 5], which is contributed by the author of this thesis and is an important step for the algebraic implementation, is not discussed here.

4.6 CONCLUSIONS

In this chapter, the sub-question 2 in Section 1.5, i.e. where to allocate excitation signals such that subnetworks and a full network become generically identifiable, is investigated in the special setting where all the internal signals are measured. For the synthesis problem for subnetworks, a novel analysis result is obtained by exploiting the concept of disconnecting sets. Compared to the path-based condition, the disconnecting-set-based condition explicitly states which signals should be excited. With the above information, a synthesis approach is developed to allocate excitation signals such that the generic identifiability of subnetworks can be achieved. In contrast to the experimental setup in [59] where excitation signals need to be directly allocated at the inputs of the target modules, the developed synthesis approach allows for the extra freedom to allocate the excitation signals elsewhere in the network and consequently, it can achieve an experimental setup with fewer excitation signals than the setup in [59].

When the synthesis problem for a full network is concerned, the novel graphical concept of pseudotree is developed and exploited. Firstly, an analysis result based on pseudotrees is obtained, which shows that the generic identifiability of a full network is ensured if all the edges are covered by disjoint pseudotrees whose roots are excited. Based on the above result, a pseudotree merging algorithm is developed to decompose a dynamic network into a set of disjoint pseudotrees and then allocate excitation signals to achieve generic identifiability. In contrast to the results in [13], the developed approach can be applied to general network topologies in the situation where all the internal signals are measured.

4.7 APPENDIX

4.7.1 PROOF OF THEOREM 4.1

Theorem 4.1 is established by two graphical results.

Lemma 4.3. *In a simple directed graph, given a set \mathcal{P} of vertex disjoint paths from vertex set \mathcal{V}_1 to a vertex set \mathcal{V}_2 , there exists a set \mathcal{P}_{new} of vertex disjoint paths from \mathcal{V}_1 to \mathcal{V}_2 such that $|\mathcal{P}_{new}| = |\mathcal{P}|$ and the paths in \mathcal{P}_{new} are internally vertex disjoint with $\mathcal{V}_1 \cup \mathcal{V}_2$.*

Proof. We prove the lemma by showing that there always exists a \mathcal{P}_{new} by modifying the paths in \mathcal{P} . Let $w_i \rightarrow w_j$ be an arbitrary path in \mathcal{P} which contains an internal vertex in $\mathcal{V}_1 \cup \mathcal{V}_2$, then we can always replace $w_i \rightarrow w_j$ by its subpath which contains a starting vertex in \mathcal{V}_1 and an ending vertex in \mathcal{V}_2 , while the other vertices in the subpath are not in $\mathcal{V}_1 \cup \mathcal{V}_2$. This includes the special case that the obtained subpath has no internal vertex. Applying the above modification to all the paths in \mathcal{P} which contain internal vertices in $\mathcal{V}_1 \cup \mathcal{V}_2$, we obtain \mathcal{P}_{new} , with $|\mathcal{P}_{new}| = |\mathcal{P}|$, in which all the paths are still vertex disjoint. \square

In a second lemma, a new graphical result is presented to reformulate the path-based condition in Theorem 3.4 in terms of disconnecting sets.

Lemma 4.4. *Consider a simple directed graph $\mathcal{G} = (\mathcal{V}, \mathcal{E})$ and its any two vertex sets $\mathcal{V}_1, \mathcal{V}_2$ with a subset $\bar{\mathcal{V}}_2 \subseteq \mathcal{V}_2$. The following statements are equivalent:*

1. $b_{\mathcal{V}_1 \rightarrow \bar{\mathcal{V}}_2} = |\bar{\mathcal{V}}_2|$ and $b_{\mathcal{V}_1 \rightarrow \mathcal{V}_2} = b_{\mathcal{V}_1 \rightarrow \bar{\mathcal{V}}_2} + b_{\mathcal{V}_1 \rightarrow \mathcal{V}_2 \setminus \bar{\mathcal{V}}_2}$;
2. *there exists a $\mathcal{V}_1 - \mathcal{V}_2 \setminus \bar{\mathcal{V}}_2$ disconnecting set \mathcal{D} such that*

$$b_{\mathcal{V}_1 \rightarrow \mathcal{D} \cup \bar{\mathcal{V}}_2} = |\mathcal{D}| + |\bar{\mathcal{V}}_2|; \quad (4.9)$$

3. *there exist $\bar{\mathcal{V}}_1 \subseteq \mathcal{V}_1$ and a $\bar{\mathcal{V}}_1 - \mathcal{V}_2 \setminus \bar{\mathcal{V}}_2$ disconnecting set \mathcal{D} such that*

$$b_{\bar{\mathcal{V}}_1 \rightarrow \bar{\mathcal{V}}_2 \cup \mathcal{D}} = |\mathcal{D}| + |\bar{\mathcal{V}}_2|.$$

Proof. We first prove that (1) holds if and only if (2) holds. Based on Lemma 4.3, let $\mathcal{B}_{\mathcal{V}_1 \rightarrow \mathcal{V}_2}$ denote a set of maximum number of vertex disjoint paths from \mathcal{V}_1 to \mathcal{V}_2 that are internally vertex disjoint with $\mathcal{V}_1 \cup \mathcal{V}_2$.

If (2) holds, there exist $\mathcal{B}_{\mathcal{V}_1 \rightarrow \bar{\mathcal{V}}_2}$ with cardinality $|\bar{\mathcal{V}}_2|$ and $\mathcal{B}_{\mathcal{V}_1 \rightarrow \mathcal{D}}$ with cardinality of $|\mathcal{D}|$, and the paths in the above two sets are vertex disjoint. A new set $\mathcal{B}_{\mathcal{D} \rightarrow \mathcal{V}_2 \setminus \bar{\mathcal{V}}_2}$ can also be introduced and is vertex disjoint with both $\mathcal{B}_{\mathcal{V}_1 \rightarrow \bar{\mathcal{V}}_2}$ and $\mathcal{B}_{\mathcal{V}_1 \rightarrow \mathcal{D}}$, because if not vertex disjoint, a path from \mathcal{V}_1 to $\mathcal{V}_2 \setminus \bar{\mathcal{V}}_2$ will exist and do not intersect with \mathcal{D} , contradicting \mathcal{D} as a disconnecting set. Thus, a set of maximum number of vertex disjoint paths $\mathcal{B}_{\mathcal{V}_1 \rightarrow \mathcal{V}_2 \setminus \bar{\mathcal{V}}_2}$ can be formulated by linking a subset of paths in $\mathcal{B}_{\mathcal{V}_1 \rightarrow \mathcal{D}}$ and all paths in $\mathcal{B}_{\mathcal{D} \rightarrow \mathcal{V}_2 \setminus \bar{\mathcal{V}}_2}$. Such concatenation is always feasible as $|\mathcal{B}_{\mathcal{V}_1 \rightarrow \mathcal{D}}| = |\mathcal{D}|$, and the obtained $\mathcal{B}_{\mathcal{V}_1 \rightarrow \mathcal{V}_2 \setminus \bar{\mathcal{V}}_2}$ is also vertex disjoint with $\mathcal{B}_{\mathcal{V}_1 \rightarrow \bar{\mathcal{V}}_2}$. Since $b_{\mathcal{V}_1 \rightarrow \mathcal{V}_2} \leq b_{\mathcal{V}_1 \rightarrow \bar{\mathcal{V}}_2} + b_{\mathcal{V}_1 \rightarrow \mathcal{V}_2 \setminus \bar{\mathcal{V}}_2}$ always holds, $\mathcal{B}_{\mathcal{V}_1 \rightarrow \bar{\mathcal{V}}_2}$ with cardinality $|\bar{\mathcal{V}}_2|$ and $\mathcal{B}_{\mathcal{V}_1 \rightarrow \mathcal{V}_2 \setminus \bar{\mathcal{V}}_2}$ together form a set of maximum number of vertex disjoint paths from \mathcal{V}_1 to \mathcal{V}_2 , which proves (1).

If (1) holds, let \mathcal{D} be a minimum $\mathcal{V}_1 - \mathcal{V}_2 \setminus \bar{\mathcal{V}}_2$ disconnecting set, and we have $\mathcal{B}_{\mathcal{V}_1 \rightarrow \bar{\mathcal{V}}_2}$ with cardinality $|\bar{\mathcal{V}}_2|$ and $\mathcal{B}_{\mathcal{V}_1 \rightarrow \mathcal{D}}$ with cardinality $|\mathcal{D}|$ which are vertex disjoint. Thus the above two sets together form a set of vertex disjoint paths from \mathcal{V}_1 to $\bar{\mathcal{V}}_2 \cup \mathcal{D}$, which leads to

$$b_{\mathcal{V}_1 \rightarrow \bar{\mathcal{V}}_2 \cup \mathcal{D}} \geq |\mathcal{D}| + |\bar{\mathcal{V}}_2|.$$

As $b_{\mathcal{V}_1 \rightarrow \bar{\mathcal{V}}_2 \cup \mathcal{D}}$ is upper bounded by $|\mathcal{D}| + |\bar{\mathcal{V}}_2|$, it then holds that $b_{\mathcal{V}_1 \rightarrow \bar{\mathcal{V}}_2 \cup \mathcal{D}} = |\mathcal{D}| + |\bar{\mathcal{V}}_2|$, which leads to (1) \iff (2).

Then we show that (2) is equivalent to (3). The implication (2) \implies (3) is straightforward by letting $\bar{\mathcal{V}}_1 = \mathcal{V}_1$. For (3) \implies (2), if (3) holds, then $\mathcal{D}_1 = \mathcal{D} \cup (\mathcal{V}_1 \setminus \bar{\mathcal{V}}_1)$ becomes a $\mathcal{V}_1 - \mathcal{V}_2 \setminus \bar{\mathcal{V}}_2$ disconnecting set, and $b_{\mathcal{V}_1 \rightarrow \mathcal{D}_1 \cup \bar{\mathcal{V}}_2} = |\mathcal{D}_1| + |\bar{\mathcal{V}}_2|$ holds since a single vertex can be regarded to have a path to itself, which concludes the proof. \square

Eventually, based on Lemma 4.4 and Theorem 3.4, Theorem 4.1 is obtained.

4.7.2 PROOF OF THEOREM 4.2

According to Lemma 2.1, the disconnecting set separates all the vertices in the graph into three disjoint sets as $\mathcal{V} = \mathcal{S} \cup \mathcal{D} \cup \mathcal{P}$, while there is no directed edge from \mathcal{S} to \mathcal{P} . In addition, each set may contain both internal signals and external signals, i.e. $\mathcal{S} = \mathcal{S}_x \cup \mathcal{S}_w$, $\mathcal{D} = \mathcal{D}_x \cup \mathcal{D}_w$ and $\mathcal{P} = \mathcal{P}_x \cup \mathcal{P}_w$, and it holds that $\bar{\mathcal{X}} \subseteq \mathcal{S}_x \cup \mathcal{D}_x$ and $\bar{\mathcal{W}} \subseteq \mathcal{D}_w \cup \mathcal{P}_w$. Algebraically, the above statements mean that there exist permuted network matrices such that

$$G = \begin{bmatrix} G_{\mathcal{S}_w \mathcal{S}_w} & G_{\mathcal{S}_w \mathcal{D}_w} & G_{\mathcal{S}_w \mathcal{P}_w} \\ G_{\mathcal{D}_w \mathcal{S}_w} & G_{\mathcal{D}_w \mathcal{D}_w} & G_{\mathcal{D}_w \mathcal{P}_w} \\ 0 & G_{\mathcal{P}_w \mathcal{D}_w} & G_{\mathcal{P}_w \mathcal{P}_w} \end{bmatrix}, \quad X = \begin{bmatrix} X_{\mathcal{S}_w \mathcal{S}_x} & X_{\mathcal{S}_w \mathcal{D}_x} & X_{\mathcal{S}_w \mathcal{P}_x} \\ X_{\mathcal{D}_w \mathcal{S}_x} & X_{\mathcal{D}_w \mathcal{D}_x} & X_{\mathcal{D}_w \mathcal{P}_x} \\ 0 & X_{\mathcal{P}_w \mathcal{D}_x} & X_{\mathcal{P}_w \mathcal{P}_x} \end{bmatrix},$$

$$T_{\mathcal{W}\mathcal{X}} = \begin{bmatrix} T_{\mathcal{S}_w \mathcal{S}_x} & T_{\mathcal{S}_w \mathcal{D}_x} & T_{\mathcal{S}_w \mathcal{P}_x} \\ T_{\mathcal{D}_w \mathcal{S}_x} & T_{\mathcal{D}_w \mathcal{D}_x} & T_{\mathcal{D}_w \mathcal{P}_x} \\ T_{\mathcal{P}_w \mathcal{S}_x} & T_{\mathcal{P}_w \mathcal{D}_x} & T_{\mathcal{P}_w \mathcal{P}_x} \end{bmatrix}, \quad (4.10)$$

where, for example, $T_{\mathcal{S}_w \mathcal{D}_x}$ denotes the mapping from \mathcal{D}_x to \mathcal{S}_w . Based on the above structure and the equation $(I - G)T_{\mathcal{W}\mathcal{X}} = X$, our goal is to find a proper matrix K such that $T_{\bar{\mathcal{W}}\bar{\mathcal{X}}} = KT_{\mathcal{D}\bar{\mathcal{X}}}$.

Firstly, considering the division of the sets \mathcal{D} and $\bar{\mathcal{X}}$, the mapping $T_{\mathcal{D}\bar{\mathcal{X}}}$ can be re-written as

$$T_{\mathcal{D}\bar{\mathcal{X}}} = \begin{bmatrix} T_{\mathcal{D}_w \bar{\mathcal{X}}_S} & T_{\mathcal{D}_w \bar{\mathcal{X}}_D} \\ 0 & I \\ 0 & 0 \end{bmatrix}, \quad (4.11)$$

where $\bar{\mathcal{X}}_S = \bar{\mathcal{X}} \cap \mathcal{S}_x$, $\bar{\mathcal{X}}_D = \bar{\mathcal{W}} \cap \mathcal{D}_x$, and the identity matrix is the mapping $T_{\bar{\mathcal{X}}_D \bar{\mathcal{X}}_D}$. Note that the rows of the bottom block matrices in (4.11) correspond to the vertices in $\mathcal{D}_x \setminus \bar{\mathcal{X}}_D$. In addition, $T_{\bar{\mathcal{W}}\bar{\mathcal{X}}}$ can be written as

$$T_{\bar{\mathcal{W}}\bar{\mathcal{X}}} = \begin{bmatrix} T_{\bar{\mathcal{W}}_P \bar{\mathcal{X}}} \\ T_{\bar{\mathcal{W}}_D \bar{\mathcal{X}}} \end{bmatrix}, \quad (4.12)$$

where $\bar{\mathcal{W}}_P = \bar{\mathcal{W}} \cap \mathcal{P}_w$ and $\bar{\mathcal{W}}_D = \bar{\mathcal{W}} \cap \mathcal{D}_w$. Thus, it is clear that

$$T_{\bar{\mathcal{W}}_D \bar{\mathcal{X}}} = C \begin{bmatrix} T_{\mathcal{D}_w \bar{\mathcal{X}}_S} & T_{\mathcal{D}_w \bar{\mathcal{X}}_D} \end{bmatrix}, \quad (4.13)$$

where C is a selection matrix that extracts the rows of $\begin{bmatrix} T_{\mathcal{D}_w \bar{\mathcal{X}}_S} & T_{\mathcal{D}_w \bar{\mathcal{X}}_D} \end{bmatrix}$ corresponding to $\bar{\mathcal{W}}_D$.

In addition, from the permuted matrices and the equation $(I - G)T_{\mathcal{W}\mathcal{X}} = X$, it holds that

$$T_{\mathcal{P}_w \mathcal{S}_x} = (I - G_{\mathcal{P}_w \mathcal{P}_w})^{-1} G_{\mathcal{P}_w \mathcal{D}_w} T_{\mathcal{D}_w \mathcal{S}_x},$$

where $I - G_{\mathcal{P}_w \mathcal{P}_w}$ is invertible and inversely proper because $I - G_{\mathcal{P}_w \mathcal{P}_w}$ is proper and the network is well-posed, i.e. $\lim_{z \rightarrow \infty} \det(I - G_{\mathcal{P}_w \mathcal{P}_w}(z)) \neq 0$. The above equation leads to

$$T_{\bar{\mathcal{W}}_P \bar{\mathcal{X}}_S} = \bar{K} T_{\mathcal{D}_w \bar{\mathcal{X}}_S}, \quad (4.14)$$

where $\bar{K} = [(I - G_{\mathcal{P}_w \mathcal{P}_w})^{-1}]_{\bar{\mathcal{W}}_P \star} G_{\mathcal{P}_w \mathcal{D}_w}$. Then combining the above equation with (4.11), (4.12) and (4.13) leads to

$$\begin{aligned} T_{\bar{\mathcal{W}} \bar{\mathcal{X}}} &= \begin{bmatrix} T_{\bar{\mathcal{W}}_P \bar{\mathcal{X}}_S} & T_{\bar{\mathcal{W}}_P \bar{\mathcal{X}}_D} \\ T_{\bar{\mathcal{W}}_D \bar{\mathcal{X}}_S} & T_{\bar{\mathcal{W}}_D \bar{\mathcal{X}}_D} \end{bmatrix} = \begin{bmatrix} \bar{K} & T_{\bar{\mathcal{W}}_P \bar{\mathcal{X}}_D} - \bar{K} T_{\mathcal{D}_w \bar{\mathcal{X}}_D} & 0 \\ C & 0 & 0 \end{bmatrix} \\ &\times \begin{bmatrix} T_{\mathcal{D}_w \bar{\mathcal{X}}_S} & T_{\mathcal{D}_w \bar{\mathcal{X}}_D} \\ 0 & I \\ 0 & 0 \end{bmatrix} = K T_{\mathcal{D} \bar{\mathcal{X}}}. \end{aligned}$$

The formulation of the above K matrix can be further simplified. Based on the permuted matrices and the equation $(I - G)T_{\mathcal{W}\mathcal{X}} = X$, it holds

$$(I - G_{\mathcal{P}_w \mathcal{P}_w}) T_{\mathcal{P}_w \mathcal{D}_x} - G_{\mathcal{P}_w \mathcal{D}_w} T_{\mathcal{D}_w \mathcal{D}_x} = X_{\mathcal{P}_w \mathcal{D}_x}.$$

Thus, we can conclude that

$$K = \begin{bmatrix} \bar{K} & [(I - G_{\mathcal{P}_w \mathcal{P}_w})^{-1}]_{\bar{\mathcal{W}}_P \star} X_{\mathcal{P}_w \bar{\mathcal{X}}_D} & 0 \\ C & 0 & 0 \end{bmatrix}, \quad (4.15)$$

where \bar{K} is defined in (4.14); C is defined in (4.13) and its rows correspond to $\bar{\mathcal{W}}_D$; the columns of the last block column in (4.15) correspond to $\mathcal{D}_x \setminus \bar{\mathcal{X}}_D$. Note that certain block matrices in K may disappear depending on if the corresponding set of signals is empty.

4.7.3 PROOF OF PROPOSITION 4.1

Before proving the proposition, we first prove that there exists a directed path from w_i to $\mathcal{W}_j^- \setminus \{w_i\}$ if and only if there exist a parallel path from w_i to w_j or a cycle around the output w_j . Note that \mathcal{G} is a simple graph, i.e. there is no self-loop such as (w_i, w_i) , and no parallel directed edges from one vertex to another vertex. For “if” part, if there exists a parallel path from w_i to w_j , this parallel path must intersect with $\mathcal{W}_j^- \setminus \{w_i\}$. Then we can find a directed path from w_i to one vertex in $\mathcal{W}_j^- \setminus \{w_i\}$ as a subpath of the parallel path. If a cycle around w_j exists, it must also intersect with $\mathcal{W}_j^- \setminus \{w_i\}$, and thus the cycle contains a subpath from w_j to one vertex in

$\mathcal{W}_j^- \setminus \{w_i\}$. Linking this subpath and the edge (w_i, w_j) leads to a path from w_i to $\mathcal{W}_j^- \setminus \{w_i\}$.

For “only if” part, for any directed path from w_i to $w_k \in \mathcal{W}_j^- \setminus \{w_i\}$, if the path does not contain edge (w_i, w_j) , then combining the path and the edge (w_k, w_j) will create a parallel path. If the path contains (w_i, w_j) , then combining the path and the edge (w_k, w_j) while excluding (w_i, w_j) will lead to a cycle around w_j . This concludes the relationship between the parallel paths, the cycles around the output and the paths from w_i to $\mathcal{W}_j^- \setminus \{w_i\}$.

Then based on the above result, the “only if” of the proposition is straightforward. For the “if” part, if we collect an internal vertex from each parallel path and a vertex from cycles around the output into \mathcal{D} , \mathcal{D} then must disconnect from w_i to $\mathcal{W}_j^- \setminus \{w_i\}$.

莫思身外无穷事，且尽生前有限杯。

杜甫（唐）

*Don't brood on the endless troubles beyond the immediate, and finish the
limited number of cups in the time while you're alive.*

Fu Du (Tang dynasty)

5

Identifiability with partial measurement and excitation

5.1 INTRODUCTION

In Chapters 3 and 4, the identifiability analysis and synthesis have been addressed in the setting where all the internal signals are measured, and only a subset of them is excited. However, in some practical situations, it is not feasible to measure all the internal signals, which motivates the study in this chapter on the identifiability analysis and synthesis in a more general setting, where not all internal signals are measured and not all of them are excited, also referred to as the partial measurement and partial excitation setting.

The identifiability concept concerns the uniqueness of network modules given the available external-to-internal mappings, where the availability is decided by the scheme of excitation and measurement in the dynamic network. Therefore, the main challenge of the identifiability study in the partial measurement and excitation setting is to decide which signals to measure or to excite, such that the available external-to-internal mappings can lead to unique network modules. Compared to the full measurement case where the mappings from the external signals to all the internal signals are available, only the mappings from the external signals to a subset of internal

The material of this chapter is based on the results in [142, 143].

signals, i.e. the measured internal signals, are available in the current setting.

To the best of the author's knowledge, [13, 83] are the only works considering identifiability in this setting so far. Preliminary results for local identifiability are presented in [83]; however, systematic graphical analysis has not been developed, and local identifiability is a weaker notion than generic identifiability. Sufficient conditions for generic identifiability are developed in [13], which require a sufficient number of excitation signals to achieve generic identifiability. However, only measured excitation signals are considered in [13], while the contribution of the unmeasured noise signals is not exploited as excitation sources for identifiability as done in [169] and Theorem 3.4 for the full measurement case. In addition, the main result in [13] is not fully graphical as it also requires the availability of certain mappings from excitation signals to node signals, and thus the conditions cannot be tested solely based on the network topology. Special network structures, i.e. trees and loops, are then considered in [13] such that the required mappings are obtainable; however, how to handle networks with more general topology is not considered yet.

In this chapter the concept of generic identifiability in Definition 3.4 and the concept of global identifiability in Remark 3.2 are considered. We generalize the results in [169] and the previous chapters significantly from the full measurement setting to the setting with partial measurement and partial excitation. In particular, we focus on the identifiability of a single module, and then the results can be extended trivially to a subset of modules. We also address the limitations of [13] by exploiting unmeasured noises as excitation sources and by developing fully graphical identifiability conditions. Additionally, the model sets considered are allowed to contain a priori known/fixed modules.

In Section 5.3 we show how unmeasured noise signals can serve as excitation sources for identifiability analysis. This is done by introducing a concept of equivalence between network models and by developing a novel network model structure. Due to the excitation contributed by the noise signals, a smaller number of measured excitation signals is needed for network identifiability, compared to the result in [13].

More importantly, with the developed model structure, this work develops a series of novel graphical sufficient conditions to analyze both global and generic identifiability of a single module with different excitation and measurement schemes in Sections 5.4, 5.5 and 5.6. With the obtained conditions, single module identifiability can be checked by only inspecting the topology of the dynamic network. It is worth emphasizing that the conditions presented in this chapter cover all possible cases in identifying a single module in a network. In addition, the graphical conditions further lead to comprehensive synthesis approaches in Section 5.7, for excitation and sensor allocation to achieve identifiability, and indirect identification methods for single module estimation in Section 5.8. All the above results also extend to multiple modules, i.e. sub-networks, from the same MISO or SIMO subsystem of the network. *The proofs of the technical results are collected in Section 5.10.*

5.2 PROBLEM FORMULATION

Identifiability conditions of network modules typically require a sufficient number of r signals as excitation sources. Moreover, it is shown in Proposition 3.1 that when all the internal signals are measured, i.e. $C = I$ in (2.1), the spectrum matrix $\Phi(z)$ in (2.9) admits a unique spectral factor $T(q)H(q)$ under Assumptions 3.1 and 3.2 [169]. In this case, implication (3.5) can be equivalently simplified by considering $(T(q)R, T(q)H(q))$ in the left-hand side (LHS) instead of $(T(q)R, \Phi(z))$, as shown in Corollary 3.2. Since the mapping from the noises to the internal signals is used for identifiability analysis, the noises play the same role as $r(t)$ for the identifiability analysis, and the appearance of e signals can compensate for a lack of r signals to achieve identifiability.

However, in the setting with partial excitation and measurement, where only a subset of internal signals is excited by r signals and only a subset of internal signals is measured, i.e. $C \neq I$ in (2.1), the above result does not apply anymore as only the submatrix $C\Phi(z)C^\top$ of $\Phi(z)$ is taken as a starting point for the identifiability analysis. Thus, the first question is to investigate how noise signals can be used as excitation sources for the identifiability analysis in the current setting.

More importantly, this work further aims to develop graphical conditions to verify global and generic identifiability of modules by only inspecting the graph of the model set. In these graphical conditions, both r and unmeasured noise signals can be used as excitation sources for identifiability tests.

Note that throughout this chapter, we consider that each r signal influences a single internal signal, and R in the network model (2.1) is a binary selection matrix that decides which internal signals are influenced by $r(t)$, i.e. R contains a subset of columns of an $L \times L$ identity matrix. Thus, by post-multiplying a matrix A by R , i.e. AR , a subset of columns in A can be extracted. Then it is clear that $T_{\mathcal{WR}}(q) = T(q)R$ in (2.13) consists of a subset of columns in $T(q)$. In addition, we consider the situation where the measured internal signals are affected by a full-rank process noise.

Assumption 5.1. *The power spectrum $C\Phi(z)C^\top$ has full rank.*

Recall from Section 2.1 that set \mathcal{Z} contains all the unmeasured internal signals, and without loss of generality, in this chapter w in (2.1) is considered to be ordered as

$$w = \begin{bmatrix} w_{\mathcal{C}} \\ w_{\mathcal{Z}} \end{bmatrix},$$

where $w_{\mathcal{C}}$ and $w_{\mathcal{Z}}$ are vectors that contain the measured internal signals and the unmeasured ones, respectively. Accordingly, C in (2.1) is partitioned as $C = \begin{bmatrix} I & 0 \end{bmatrix}$.

5.3 EQUIVALENT NETWORK FOR NOISE EXCITATION

Identifiability in Definition 3.4 concerns the uniqueness of a single module given the mapping $CT(q)R$ and the spectrum $C\Phi(z)C^\top$. In this section, in order to exploit the noise signals as excitation sources, we introduce a novel network model structure to model the data without loss of generality. With this model structure, $C\Phi(z)C^\top$ admits a unique spectral factor $CT(q)\tilde{H}(q)$ for a transformed noise model $\tilde{H}(q)$. Therefore, implication (3.5) can be equivalently simplified by considering the uniqueness of a single module given $(CT(q)R, CT(q)\tilde{H}(q))$ instead of $(CT(q)R, C\Phi(z)C^\top)$, which means that the unmeasured noises can act as excitation sources for the identifiability analysis.

5.3.1 NOISE SPECTRUM ANALYSIS AND EQUIVALENT NETWORKS

We introduce the novel model structure by exploiting a concept of network equivalence. The objects $CT(q)Rr(t)$ and $C\Phi(z)C^\top$ reflect the mean and the power spectral density of the measured process w_C . These objects encode all the stochastic properties of interest, i.e. the first and the second moments, for the measured processes (w_C, r) . Therefore, this motivates the concept of network equivalence by extending [168, Definition 4] to the setting with partial measurement.

Definition 5.1. *Two network models M_1 and M_2 are said to be (observationally) equivalent if it holds that*

$$C_1T_1(q)R_1 = C_2T_2(q)R_2, \text{ and } C_1\Phi_1(z)C_1^\top = C_2\Phi_2(z)C_2^\top,$$

and this equivalence is denoted by $M_1 \sim M_2$.

The above concept of equivalence characterizes two network models that can be used to model the same measured processes (w_C, r) , because given measured r , the stochastic process w_C in two equivalent models has the same mean $CT(q)Rr$ and power spectrum $C\Phi(z)C^\top$. Thus, a network model M can be replaced by an equivalent network model to represent the same measured processes. Note that $G_1(q)$ and $G_2(q)$ from two equivalent models may have different dimensions, e.g. a model M and its immersed network where w_Z is eliminated [48, 168], and thus, the matrices C_1 and R_1 can also be different from C_2 and R_2 .

Furthermore, it can be found that any network model admits the following equivalent model with the same $G(q)$, R and C matrices, by exploiting the noise spectrum $C\Phi(z)C^\top$.

Theorem 5.1. *For any network model $M = (G(q), R, H(q), C, \Lambda)$, there exists an equivalent network model as*

$$\tilde{M} \triangleq (G(q), R, [\tilde{H}^*(q) \quad 0]^\star, C, \tilde{\Lambda}), \quad (5.1)$$

where $\tilde{H}(q) \in \mathbb{R}(q)^{m \times m}$, with m denoting the number of measured internal signals, is minimum phase and monic; $\tilde{\Lambda} \in \mathbb{R}^{m \times m}$ is positive semi-definite. In addition,

- if M satisfies Assumption 5.1, $(\tilde{H}(q), \tilde{\Lambda})$ is unique with positive definite $\tilde{\Lambda}$;

Based on the above result, the measured process (w_C, r) that is modeled by M can be equivalently modeled by \tilde{M} in (5.1), which has the same matrices $G(q)$, R , C , and the structure of the noise model in \tilde{M} implies that the unmeasured internal signals are noise-free in \tilde{M} . In addition, \tilde{M} has a transformed white noise signal \tilde{e} with the covariance matrix $\tilde{\Lambda}$. This noise model is simpler than the one in M , and more importantly, \tilde{M} keeps the $G(q)$ matrix invariant as in M . This invariance is important for the identifiability analysis and the identification of network modules.

The equivalence between M and \tilde{M} is obtained due to the freedom in transforming the unmeasured internal signals and modeling the noises, since $CT(q)R$ and $C\Phi(z)C^\top$ only reflect the properties of the measured processes. Therefore, \tilde{M} may describe different unmeasured processes from w_Z in M due to the possible change in its stochastic properties. However, for the simplicity of notation, we still use w_Z and \mathcal{X} to denote the unmeasured internal signals and the external signals in \tilde{M} , respectively.

Furthermore, in the equivalent model \tilde{M} obtained from M , its noise model $\tilde{H}(q)$ admits a block diagonal structure if a particular noise model is chosen for M by employing the following spectral factorization of the disturbance spectrum $\Phi_v(z)$ in (2.2):

$$\Phi_v(z) = H(z)H(z)^*, \quad (5.2)$$

where $H(z)$ has dimension $L \times p$ with p denoting the rank of $\Phi_v(z)$ [60]. The above spectral factorization suggests a noise model for M with $H(q)$ having dimension $L \times p$ and an identity covariance matrix with dimension p , i.e. $\Lambda = I$.

Given a network model M with the above noise model, the noise model $\tilde{H}(q)$ of its equivalent network \tilde{M} also has a special block diagonal structure, if the signal vector w_C is ordered according to the so-called confounding variables in the graph associated with M [122].

Definition 5.2. In a dynamic network, a noise signal e_k is called a confounding variable of w_i and w_j if e_k has directed paths to w_i and w_j via only unmeasured internal vertices or with length one. In this case, w_i and w_j are also said to be confounded by e_k .

Without loss of generality, the measured internal signal vector w_C in M can be ordered such that the measured internal signals confounded by the same noise signals are grouped together: All the measured internal signals are divided into disjoint subsets as $\mathcal{C} = \cup_{i=1}^k \mathcal{S}_i$ such that two measured internal signals from two different disjoint sets are not confounded by the same noise signal. Then if w_C is ordered as

$$w_C = \begin{bmatrix} w_{\mathcal{S}_1} \\ \vdots \\ w_{\mathcal{S}_k} \end{bmatrix}, \quad (5.3)$$

the noise model $\tilde{H}(q)$ has a block diagonal structure as follows.

Corollary 5.1. *Consider any network model M with its covariance matrix $\Lambda = I \in \mathbb{R}^{p \times p}$ and the noise model $H(q)$ of dimension $L \times p$ as in (5.2). If the measured internal signal vector w_C in M is ordered according to (5.3), then M admits an equivalent network \tilde{M} as in (5.1), whose $\tilde{H}(q)$ and noise covariance matrix $\tilde{\Lambda}$ have a block diagonal structure as*

$$\tilde{H}(q) = \text{diag}(\tilde{H}_{S_1}(q), \dots, \tilde{H}_{S_k}(q)), \text{ and } \tilde{\Lambda} = \text{diag}(\tilde{\Lambda}_{S_1}, \dots, \tilde{\Lambda}_{S_k}),$$

where $\tilde{H}_{S_i}(q) \in \mathbb{R}(q)^{|S_i| \times |S_i|}$ and $\tilde{\Lambda}_{S_i} \in \mathbb{R}^{|S_i| \times |S_i|}$.

In addition to the result in Theorem 5.1, Corollary 5.1 provides a direct connection between the sparsity pattern of the noise model in \tilde{M} and the network topology of M under the special noise model suggested by (5.2).

5.3.2 EQUIVALENT NETWORK FOR HANDLING NOISE EXCITATION

Since a network M and its equivalent model \tilde{M} in (5.1) contain the same $G(q)$ matrix, both of them can be used to model the same data set, i.e. the measured (w_C, r) , for the identification of modules in the dynamic network (2.1). In the previous section, it is discussed that \tilde{M} in (5.1) can potentially be a better option due to its simpler noise model. In this section, we further show that the particular noise model of \tilde{M} is also beneficial for the identifiability analysis.

From now on, we use \mathcal{M} to specifically refer to a set of models in the form of (5.1) in this chapter. It can be found that the implication (3.5) for \mathcal{M} can be further simplified under mild conditions.

Proposition 5.1. *For a network model set \mathcal{M} that satisfies Assumptions 3.2 and 5.1, implication (3.5) for \mathcal{M} can be equivalently formulated as*

$$CT_{\mathcal{W}\mathcal{X},0}(q) = CT_{\mathcal{W}\mathcal{X},1}(q) \Rightarrow G_{ji,0}(q) = G_{ji,1}(q), \quad (5.4)$$

for all $M_1 \in \mathcal{M}$.

The above result indicates that both the mappings from r and \tilde{e} to the measured internal signals can be used for analyzing identifiability in \mathcal{M} , and thus the unmeasured noise signal \tilde{e} plays the same role as the measured $r(t)$ for the identifiability analysis. In this case, we say that \tilde{e} signals act as excitation sources for the identifiability analysis. Proposition 5.1 is an extension of Proposition 3.1 to the partial measurement and partial excitation setting.

Proposition 5.1 shows another advantage of \tilde{M} over a general network model M in network identification with partial measurement and partial excitation. These two models are equivalent to describe the same data and contain the same modules; however, the set \mathcal{M} of models in the form of \tilde{M} allows us to exploit the noise spectral density through Proposition 5.1, such that the noise signals can act as excitation signals for identifiability analysis. In contrast, identifiability in

a model set of models in the form of \mathcal{M} involves $C\Phi C^\top$ and the mapping from r to w_C , i.e. only r signals can be used as excitation signals, as also considered in [13, 69]. Therefore, in this chapter, we regard $\tilde{\mathcal{M}}$ as the standard model for network identification in the partial measurement and partial excitation setting.

5.4 NECESSARY GRAPHICAL CONDITIONS

From now on, we focus on the development of graphical conditions for identifiability in \mathcal{M} that contains models in the form of $\tilde{\mathcal{M}}$. Particularly, we focus on the identifiability of a single module.

Necessary and sufficient graphical conditions for the generic identifiability of a single module are obtained in [69] for the full excitation case and in Chapter 3 for the full measurement case. When the setting with partial measurement and partial excitation is considered, the existing necessary conditions from the above works for the full measurement or full excitation setting naturally remain necessary conditions for the current setting. Recall the notations in Section 2.5 and that the necessity of the graphical conditions can be achieved by non-parametric model sets as in Theorem 3.4. Then the necessary conditions are as follows.

Lemma 5.1. *Consider a non-parametric model set \mathcal{M} that satisfies Assumptions 3.2, 3.4, 3.5 and 5.1. Then module $G_{ji}(q)$ is generically identifiable from (w_C, r) only if the following conditions are satisfied:*

1. $b_{\mathcal{X}_j \rightarrow \mathcal{W}_j^-} = 1 + b_{\mathcal{X}_j \rightarrow \mathcal{W}_j^- \setminus \{w_i\}}$;
2. $b_{\mathcal{W}_i^+ \rightarrow \mathcal{C}} = 1 + b_{\mathcal{W}_i^+ \setminus \{w_j\} \rightarrow \mathcal{C}}$;
3. Each signal in $\{w_i, w_j\}$ is measured or is directly excited by a vertex in \mathcal{X} .

Proof. Condition 1 is obtained from the necessity in Theorem 3.4 when $\bar{\mathcal{W}}_j = \{w_i\}$, and the second condition is the dual result as investigated in [69]. The final condition is analogous to [13, Theorem III.2]. \square

Lemma 5.1 implies a necessary number of measured signals and external signals, including r and \tilde{e} , for identifiability. This is because the scheme of measurement and excitation decides the sparsity pattern of matrices $C, R, H(q)$, and thus further influences the mapping $CT(q)X(q)$ in Proposition 5.1. The formulation of set \mathcal{X}_j indicates that the noises, which have unknown directed edges to w_j , are not helpful for the identifiability of $G_{ji}(q)$. Note that compared to Theorem 3.4, Assumption 3.1, which requires the noise model to be structured such that its upper block is minimum-phase and monic, is dropped in Lemma 5.1, since the noise model of $\tilde{\mathcal{M}}$ under Assumption 5.1 already satisfies Assumption 3.1.

The graphical conditions can be easily tested using graphical algorithms to compute the maximum number of vertex disjoint paths. However, the conditions are not suitable for designing

synthesis approaches for excitation and sensor allocation, since they do not specify explicitly which signals are necessary to be excited and measured. Thus, following the results in Chapter 4, the above path-based conditions can be equivalently formulated in terms of disconnecting sets.

Lemma 5.2. *Consider the setting of Lemma 5.1,*

1. *condition 1 holds if and only if there exists a $\mathcal{X}_j - \mathcal{W}_j^- \setminus \{w_i\}$ disconnecting set \mathcal{D} such that $b_{\mathcal{X}_j \rightarrow \{w_i\} \cup \mathcal{D}} = |\mathcal{D}| + 1$;*
2. *condition 2 holds if and only if there exists a $\mathcal{W}_i^+ \setminus \{w_j\} - \mathcal{C}$ disconnecting set \mathcal{D}_c such that $b_{\{w_j\} \cup \mathcal{D}_c \rightarrow \mathcal{C}} = |\mathcal{D}_c| + 1$.*

Proof. The first result follows from Lemma 4.4 and condition (1) of Lemma 5.1. The last result is the dual situation. \square

In the above lemma, the first result shows that the signals in $\{w_i\} \cup \mathcal{D}$ are necessary to be excited by r and \tilde{e} directly or indirectly. In addition, the second result specifies that the signals in $\{w_j\} \cup \mathcal{D}_c$ should be either measured or indirectly measured, i.e. they are not measured but have vertex disjoint paths to measured internal signals.

However, the necessary conditions in Lemma 5.1 are not sufficient to verify identifiability. This also means that the requirements on excitation signals and on measured internal signals are not separable for identifiability, i.e. first allocating excitation signals according to the results for the full measurement case and then selecting measured signals according to the results for the full excitation case are not sufficient for the identifiability in the current setting.

5.5 SUFFICIENT CONDITIONS: BOTH INPUT AND OUTPUT MEASURED OR EXCITED

In this section, sufficient graphical conditions are developed to verify global and generic identifiability of a single module in \mathcal{M} for the situation, where the input and the output of the target module are both measured or both directly excited. As shown in Proposition 5.1, identifiability concerns the uniqueness of network modules given $CT_{\mathcal{W}\mathcal{X}}(q)$. In the special cases where $C = I$ or $R = I$, identifiability of modules relates to the rank of submatrices in $T_{\mathcal{W}\mathcal{X}}(q)$ as shown in [14, 69] and Chapter 3. Consider the case where $C = I$ as an example, and recall from Section 2.5 that

$$T_{\mathcal{W}\mathcal{X}}(q) \triangleq [I - G(q)]^{-1}X(q).$$

Then the rank condition is analyzed on the basis of the relation

$$[I - G(q)]T_{\mathcal{W}\mathcal{X}}(q) = X(q), \quad (5.5)$$

based on which, the identifiability of modules in $G(q)$ can be formulated as the uniqueness of solutions for entries in $G(q)$ given matrix $T_{\mathcal{W}\mathcal{X}}(q)$, which is thus connected to $T_{\mathcal{W}\mathcal{X}}(q)$'s rank and can also be tested using the following graphical rank tests.

Lemma 5.3. *Consider a network model set \mathcal{M} that satisfies Assumptions 3.4 and 3.5, and let $T_{\bar{\mathcal{W}}\bar{\mathcal{X}}}(q)$ denote a submatrix of $T_{\mathcal{W}\mathcal{X}}(q)$ with its rows and columns corresponding to $\bar{\mathcal{W}} \subseteq \mathcal{W}$ and $\bar{\mathcal{X}} \subseteq \mathcal{X}$, respectively. It holds that*

1. $\text{rank}[T_{\bar{\mathcal{W}}\bar{\mathcal{X}}}(q)] = b_{\bar{\mathcal{X}} \rightarrow \bar{\mathcal{W}}}$ generically;
2. $\text{rank}[T_{\bar{\mathcal{W}}\bar{\mathcal{X}}}(q)] = b_{\bar{\mathcal{X}} \rightarrow \bar{\mathcal{W}}}$ globally if the set of maximum number of vertex disjoint paths from $\bar{\mathcal{X}}$ to $\bar{\mathcal{W}}$ is unique, and the transfer functions contained in these paths are non-zero for all models in \mathcal{M} .

Proof. The first result is from Theorem 3.2 for non-parametric model sets and from Proposition 3.3 for parametric model sets. The global rank has been investigated in [157] in terms of the unique (constrained) set of vertex disjoint paths. Note that the assumption for non-zero transfer functions is implicit in [157]. \square

In the above result, when a parametric model set is considered, the genericity should be understood as the genericity notion in the parameter space, that is either based on the Lebesgue measure or the open and dense sets, as shown in Section 3.5.2. The above result shows that the generic and the global rank of $T_{\mathcal{W}\mathcal{X}}(q)$ in \mathcal{M} can be found by counting the maximum number of vertex disjoint paths. In addition, we define a new notation $\bar{b}_{\bar{\mathcal{X}} \rightarrow \bar{\mathcal{W}}}$ for the global rank test in Lemma 5.3, i.e. the equality $\bar{b}_{\bar{\mathcal{X}} \rightarrow \bar{\mathcal{W}}} = a$ implies that $b_{\bar{\mathcal{X}} \rightarrow \bar{\mathcal{W}}} = a$, and the set of maximum number of vertex disjoint paths is unique, while the transfer functions contained in those paths are non-zero for all the models in the set.

In contrast to (5.5), when $C \neq I$ and $R \neq I$, we have $T_{C\mathcal{X}}(q) = C[I - G(q)]^{-1}X(q)$ instead, where $[I - G(q)]^{-1}$ cannot be moved to the LHS to obtain a system of linear equations as in (5.5) in general. Thus in this work, we consider identifiability of a single module in several special situations, depending on whether its input or output is measured. For each situation, identifiability conditions can still be connected to the rank of $T_{\mathcal{W}\mathcal{X}}(q)$ and further to the graphical rank tests in Lemma 5.3.

Even if each of the considered cases is limited to a specific situation and these cases cannot be combined into a single result, they together cover all the situations for single module identification in the partial measurement and partial excitation setting.

5.5.1 MEASURED INPUT AND OUTPUT

A sufficient condition is first derived for the verification of single module identifiability in the situation where both the input and the output of $G_{ji}(q)$ are measured.

Recall $T_{\mathcal{W}\mathcal{X}}(q) \triangleq [I - G(q)]^{-1}X(q)$ where $X(q) \triangleq \begin{bmatrix} R(q) & H(q) \end{bmatrix}$. Then consider the equation $[I - G(q)]T_{\mathcal{W}\mathcal{X}}(q) = X(q)$, whose j th row can be permuted to obtain

$$\begin{bmatrix} -G_{ji} & -G_{j\mathcal{N}_j^-\setminus\{w_i\}} & 1 & 0 \end{bmatrix} \begin{bmatrix} T_{i\mathcal{X}} \\ T_{\mathcal{N}_j^-\setminus\{w_i\}\mathcal{X}} \\ T_{j\mathcal{X}} \\ \star \end{bmatrix} = X_{j\star}, \quad (5.6)$$

where for simplicity we omit its dependency on q , $X_{j\star}$ denotes the j th row vector of X , and set \mathcal{N}_j^- contains the in-neighbors of w_j in \mathcal{W} for now and will be formally defined later. The modules contained in the j th row of $G(q)$ are shown as blue blocks in Figure 5.1. Identifiability of $G_{ji}(q)$ concerns the uniqueness of $G_{ji}(q)$ in (5.6) given the mappings in $CT_{\mathcal{W}\mathcal{X}}(q)$.

If all internal signals are measured, i.e. $C = I$, all the external-to-internal mappings in (5.6) are given by $T_{\mathcal{W}\mathcal{X}}(q) = CT_{\mathcal{W}\mathcal{X}}(q)$, and thus in (5.6), we can analyze the uniqueness for $G_{ji}(q)$ given $T_{\mathcal{W}\mathcal{X}}(q)$, as investigated in Chapter 3. However, when only a subset of internal signals is measured, $CT_{\mathcal{W}\mathcal{X}}(q)$ only consists of a subset of rows in $T_{\mathcal{W}\mathcal{X}}(q)$. Although $T_{i\mathcal{X}}(q)$ and $T_{j\mathcal{X}}(q)$ in (5.6) are submatrices of $CT_{\mathcal{W}\mathcal{X}}(q)$ due to measured w_i and w_j , the mapping $T_{\mathcal{N}_j^-\setminus\{w_i\}\mathcal{X}}(q)$ may not be directly available, i.e. it may not be a submatrix of $CT_{\mathcal{W}\mathcal{X}}(q)$, because the signals in $\mathcal{N}_j^- \setminus \{w_i\}$ may not be measured.

To address the unavailability of $T_{\mathcal{N}_j^-\setminus\{w_i\}\mathcal{X}}(q)$, the following result is instrumental, which is an extension of Theorem 4.2.

Lemma 5.4. *For any network model set \mathcal{M} that satisfies Assumptions 3.4, 3.5 with a disconnecting set $\mathcal{D} \subseteq \mathcal{W} \cup \bar{\mathcal{X}}$ from any $\bar{\mathcal{X}} \subseteq \mathcal{X}$ to any $\bar{\mathcal{W}} \subseteq \mathcal{W}$, there exists a proper transfer matrix $K(q)$ such that*

$$T_{\bar{\mathcal{W}}\bar{\mathcal{X}}}(q) = K(q)T_{\mathcal{D}\bar{\mathcal{X}}}(q). \quad (5.7)$$

In addition, it holds that

- $K(q)$ is full column rank generically if $b_{\mathcal{D} \rightarrow \bar{\mathcal{W}}} = |\mathcal{D}|$;
- $K(q)$ is full column rank globally if $\bar{b}_{\mathcal{D} \rightarrow \bar{\mathcal{W}}_1} = |\mathcal{D}|$ for some $\bar{\mathcal{W}}_1 \subseteq \bar{\mathcal{W}}$.

The above result shows that if an appropriate disconnecting set \mathcal{D} from \mathcal{X} to $\mathcal{N}_j^- \setminus \{w_i\}$ is chosen, as in Figure 5.1, $T_{\mathcal{N}_j^-\setminus\{w_i\}\mathcal{X}}(q)$ can be factorized into $K(q)T_{\mathcal{D}\mathcal{X}}(q)$ for some $K(q)$. This factorization together with (5.6) leads to

$$\begin{bmatrix} G_{ji} & G_{j\mathcal{W}_j^-\setminus\{w_i\}}K \end{bmatrix} \begin{bmatrix} T_{i\mathcal{X}} \\ T_{\mathcal{D}\mathcal{X}} \end{bmatrix} = T_{j\mathcal{X}} - X_{j\star}, \quad (5.8)$$

and thus the uniqueness of $G_{ji}(q)$ is ensured if $\begin{bmatrix} T_{i\mathcal{X}}(q) \\ T_{\mathcal{D}\mathcal{X}}(q) \end{bmatrix}$ is full row rank and the signals in

$\mathcal{D} \cup \{w_i, w_j\}$ are measured, i.e. the mappings $T_{i\mathcal{X}}$, $T_{D\mathcal{X}}$ and $T_{j\mathcal{X}}$ are submatrices of $CT_{\mathcal{W}\mathcal{X}}$ and thus available. This shows that only the signals in $\mathcal{D} \cup \{w_i, w_j\}$ need to be measured for the identifiability of G_{ji} , instead of measuring all the internal signals as in Chapters 3 and 4.

The above requirement for full row rank can be reformulated into a path-based condition using Lemma 5.3, i.e. \mathcal{D} is indirectly excited by a set $\bar{\mathcal{X}}$ of external signals as in Figure 5.1. In addition, the requirement for measuring \mathcal{D} can be further relaxed by the indirect measurement of \mathcal{D} , i.e. \mathcal{D} has paths to a set $\bar{\mathcal{C}}$ of measured internal signals as in Figure 5.1.

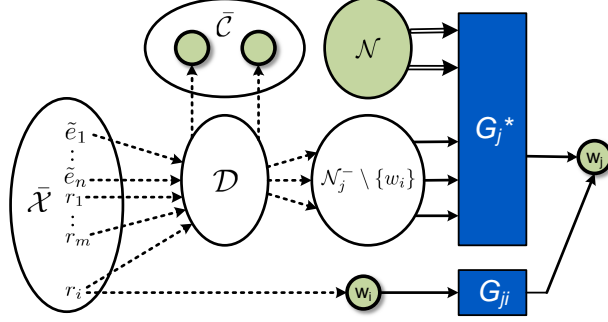


Figure 5.1: Visualization of a situation where G_{ji} is generically identifiable. G_j^* represents the other in-coming modules of w_j , and the dashed edges represent directed paths. The set \mathcal{N} contains all the measured internal signals that have known directed edges (double-lined edges) to the output w_j .

The above reasoning for identifiability analysis can be generalized. Before introducing this result, we first define an important set of signals:

- Let set \mathcal{N}_j^- contain the signals in \mathcal{W}_j^- and additionally the *unmeasured* internal signals that have *known* directed edges to w_j .

As shown in Figure 5.1, \mathcal{N}_j^- contains a subset of in-neighbors of w_j . When all the non-zero modules are unknown, we have $\mathcal{N}_j^- = \mathcal{W}_j^-$ which simply contains all the incoming internal signals of w_j .

Then the following graphical result can be obtained from the generalization of the reasoning in (5.8).

Theorem 5.2. *Consider a model set \mathcal{M} that satisfies Assumptions 3.2, 3.4, 3.5 and 5.1. Then $G_{ji}(q)$ is generically identifiable in \mathcal{M} from (w_c, r) if for some $\bar{\mathcal{X}} \subseteq \mathcal{X}_j$ and $\bar{\mathcal{C}} \subseteq \mathcal{C} \setminus \{w_i\}$, there exists a $\bar{\mathcal{X}} - (\mathcal{N}_j^- \setminus \{w_i\}) \cup \bar{\mathcal{C}}$ disconnecting set $\mathcal{D} \subseteq \mathcal{W}$ such that*

1. $b_{\bar{\mathcal{X}} \rightarrow \{w_i\} \cup \mathcal{D}} = |\mathcal{D}| + 1$;
2. $b_{\mathcal{D} \rightarrow \bar{\mathcal{C}}} = |\mathcal{D}|$.
3. w_i and w_j are in \mathcal{C} .

The above result is visualized in Figure 5.1 for the special case where $w_j \notin \bar{\mathcal{C}}$, for simplicity. It shows that to identify $G_{ji}(q)$, instead of measuring and exciting all the inputs of the MISO subsystem that contains $G_{ji}(q)$, we only need to indirectly excite and measure the signals in $\mathcal{D} \cup \{w_i\}$. The difficulty in applying the above result may arise from the need to search for the subsets $\bar{\mathcal{X}}$ and $\bar{\mathcal{C}}$, which, however, cannot be avoided due to the coupling between the excitation signals and the measured signals that are relevant to the identifiability of $G_{ji}(q)$.

Compared to Theorem 4.1 where the signals in $\{w_i\} \cup \mathcal{D}$ are excited when all the internal signals are measured, Theorem 5.2 provides a generalization which only requires the signals in $\{w_i, w_j\} \cup \mathcal{D}$ to be measured. Moreover, \mathcal{D} can also be measured indirectly as in condition (2), i.e. \mathcal{D} itself is not measured but has vertex disjoint paths to the measured signals in $\bar{\mathcal{C}}$.

This indirect measurement of \mathcal{D} also appears in the network identification method of [123]. For the consistent estimation of $G_{ji}(q)$, the method requires the indirect measurement of the signals that block the so-called parallel paths from w_i to w_j and the loops around w_j , while these signals actually coincide with \mathcal{D} as shown in Proposition 4.1. Thus, the considered experimental setup in [123] matches the one in Theorem 5.2.

Remark 5.1. *Based on the connection between the unique set of vertex disjoint paths and the global rank of transfer matrices as formulated in Lemma 5.3, Theorem 5.2 can be modified to address global identifiability by considering $\bar{b}_{\bar{\mathcal{X}} \rightarrow \{w_i\} \cup \mathcal{D}}$ and $\bar{b}_{\mathcal{D} \rightarrow \bar{\mathcal{C}}}$ instead.*

Theorem 5.2 has a potential application for signal and sensor allocation, as it explicitly states that the signals in $\{w_i\} \cup \mathcal{D}$ should be (indirectly) excited as in condition (1), and the signals in \mathcal{D} should be (indirectly) measured as in condition (2). However, it can be difficult to analyze a given model set as it needs to search for a disconnecting set. Thus, an equivalent path-based version of Theorem 5.2 is developed.

Proposition 5.2. *Consider a model set \mathcal{M} that satisfies Assumptions 3.2, 3.4, 3.5 and 5.1. $G_{ji}(q)$ is generically identifiable in \mathcal{M} from $(w_{\mathcal{C}}, r)$ if for some $\bar{\mathcal{X}} \subseteq \mathcal{X}_j$ and $\bar{\mathcal{C}} \subseteq \mathcal{C} \setminus \{w_i\}$, it holds that*

1. $b_{\bar{\mathcal{X}} \rightarrow \mathcal{N}_j^- \cup \bar{\mathcal{C}}} = b_{\bar{\mathcal{X}} \rightarrow (\mathcal{N}_j^- \setminus \{w_i\}) \cup \bar{\mathcal{C}}} + 1;$
2. $b_{\bar{\mathcal{X}} \rightarrow (\mathcal{N}_j^- \setminus \{w_i\}) \cup \bar{\mathcal{C}}} = b_{\bar{\mathcal{X}} \rightarrow \bar{\mathcal{C}}};$
3. w_i and w_j are in \mathcal{C} .

Compared to Theorem 5.2, the above result avoids the search for a disconnecting set and thus is easier for analyzing identifiability. However, it is less informative than Theorem 5.2 since it does not specify explicitly where to allocate excitation signals and sensors for single module identifiability. The results in this subsection are illustrated in the following example.

Example 5.1. *Consider a model set \mathcal{M} in Figure 5.2 with the target module $G_{21}(q)$ and the measured internal signals $\mathcal{C} = \{w_1, w_2, w_3, w_6\}$. It can be found that $\mathcal{N}_2^- = \{w_1, w_4\}$, which does*

not include the in-neighbor w_3 of w_2 since w_3 is measured and has a known edge to w_2 . In addition, we have $\mathcal{X}_2 = \{\tilde{e}_1, r_4, r_5\}$ because these external signals do not have an unknown edge to w_2 . The goal is then to verify the generic and global identifiability of $G_{21}(q)$ using the graphical conditions.

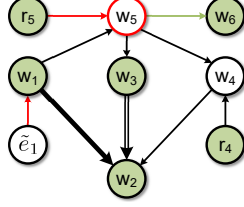


Figure 5.2: Identifiable $G_{21}(q)$ (thick edge) with only green internal signals measured and one known module $G_{23}(q)$ (double-lined edge).

By taking $\bar{\mathcal{X}} = \{\tilde{e}_1, r_5\}$ and $\bar{\mathcal{C}} = \{w_6\}$, it holds that $\{w_5\} = \mathcal{D}$ is a $\bar{\mathcal{X}} - (\mathcal{N}_2^- \setminus \{w_1\}) \cup \bar{\mathcal{C}}$ disconnecting set, as indicated by a red vertex in Figure 5.2. Thus, condition (1) of Theorem 5.2 is satisfied as there are two vertex disjoint paths $\tilde{e}_1 \rightarrow w_1$ and $r_5 \rightarrow w_5$, indicated by the red arrows in Figure 5.2. In addition, condition (2) also holds because of the green path $w_5 \rightarrow w_6$. Then based on Theorem 5.2, $G_{21}(q)$ is generically identifiable. The conditions in Proposition 5.2 can be verified similarly with the chosen $\bar{\mathcal{X}}$ and $\bar{\mathcal{C}}$.

If the transfer functions are non-zero in all the models of the model set, $G_{21}(q)$ is also globally identifiable as the set of maximum number of vertex disjoint paths from $\{\tilde{e}, r_5\}$ to $\{w_1, w_5\}$ and the one from w_5 to w_6 are unique.

Next, we extend the result in Proposition 5.2 from a single module to a subnetwork, i.e. a subset of in-coming modules of w_j .

Corollary 5.2. Consider a model set \mathcal{M} that satisfies Assumptions 3.2, 3.4, 3.5 and 5.1, and any subset $\bar{\mathcal{W}}_j \subseteq \mathcal{W}_j^-$. Then $G_{j\bar{\mathcal{W}}_j}(q)$ is generically identifiable in \mathcal{M} from (w_c, r) if for some $\bar{\mathcal{X}} \subseteq \mathcal{X}_j$ and $\bar{\mathcal{C}} \subseteq \mathcal{C} \setminus \bar{\mathcal{W}}_j$, it holds that

1. $b_{\bar{\mathcal{X}} \rightarrow \mathcal{N}_j^- \cup \bar{\mathcal{C}}} = b_{\bar{\mathcal{X}} \rightarrow (\mathcal{N}_j^- \setminus \bar{\mathcal{W}}_j) \cup \bar{\mathcal{C}}} + b_{\bar{\mathcal{X}} \rightarrow \bar{\mathcal{W}}_j}$ and $b_{\bar{\mathcal{X}} \rightarrow \bar{\mathcal{W}}_j} = |\bar{\mathcal{W}}_j|$;
2. $b_{\bar{\mathcal{X}} \rightarrow (\mathcal{N}_j^- \setminus \bar{\mathcal{W}}_j) \cup \bar{\mathcal{C}}} = b_{\bar{\mathcal{X}} \rightarrow \bar{\mathcal{C}}}$.
3. $\bar{\mathcal{W}}_j \cup \{w_j\}$ is a subset of \mathcal{C} .

Proof. The proof is analogous to the proof of Proposition 5.2 and can be based on the proof of Theorem 5.2. In this case, we only need to replace G_{ji} with $G_{j\bar{\mathcal{W}}_j}$ and $T_{i\bar{\mathcal{X}}}$ with $T_{\bar{\mathcal{W}}_j\bar{\mathcal{X}}}$ in (5.19). Then the rank condition implied by the first path-based condition leads to a unique solution for $G_{j\bar{\mathcal{W}}_j}$. \square

The above result is a generalization of Theorem 3.4 to the partial measurement setting. In addition, Corollary 5.2 is related to [13, Theorem IV.4] which also specifies sufficient conditions

for the generic identifiability of $G_{j\bar{w}_i}(q)$, in a setting without known non-zero modules and with only r signals as excitation sources for identifiability analysis. In addition, the theorem in [13] not only contains a graphical condition but also requires the prior knowledge for certain submatrices of $T_{\mathcal{W}\mathcal{X}}(q)$. When all the non-zero modules are unknown and only r signals are considered as excitation sources for the identifiability analysis, the graphical condition there is equivalent to the first condition in Corollary 5.2, while the corollary further specifies the graphical conditions, under which the required submatrices of [13, Theorem IV.4] can be obtained.

5.5.2 EXCITED INPUT AND OUTPUT

In the previous section, it is assumed that both the input and the output of a module are measured, which may not be feasible in some practical situations. This motivates us to consider the situation where the input or the output can be unmeasured, with the cost that they are directly excited.

In this case, instead of starting with the equation $[I - G(q)]T_{\mathcal{W}\mathcal{X}}(q) = X(q)$ as in (5.6), we analyze identifiability using the i -th column of $C = T_{\mathcal{C}\mathcal{W}}(q)[I - G(q)]$, where $T_{\mathcal{C}\mathcal{W}}(q) = CT(q)$. Unlike (5.6) which treats $G_{ji}(q)$ in the corresponding MISO subsystem, we take a dual perspective now and analyze $G_{ji}(q)$ in the corresponding SIMO subsystem, as shown in Figure 5.3, where the two blue blocks denote the module $G_{ji}(q)$ and the other out-going modules of w_i . Thus, a dual result of Lemma 5.4 can be obtained.

Lemma 5.5. *For any network model set \mathcal{M} that satisfies Assumptions 3.4, 3.5 with a disconnecting set $\mathcal{D} \subseteq \mathcal{W}$ from any $\bar{\mathcal{X}} \subseteq \mathcal{X}$ to any $\bar{\mathcal{W}} \subseteq \mathcal{W}$, there exists a proper transfer matrix $K(q)$ such that*

$$T_{\bar{\mathcal{W}}\bar{\mathcal{X}}}(q) = T_{\bar{\mathcal{W}}\mathcal{D}}(q)K(q). \quad (5.9)$$

Additionally, it holds that

- $K(q)$ is full row rank generically if $b_{\bar{\mathcal{X}} \rightarrow \mathcal{D}} = |\mathcal{D}|$;
- $K(q)$ is full row rank globally if $\bar{b}_{\bar{\mathcal{X}}_1 \rightarrow \mathcal{D}} = |\mathcal{D}|$ for some $\bar{\mathcal{X}}_1 \subseteq \bar{\mathcal{X}}$.

In view of analyzing the generic identifiability of $G_{ji}(q)$ when its input and output are directly excited, the above result allows us to find an appropriate disconnecting set \mathcal{D} , as shown in Figure 5.3. It can then be found that $G_{ji}(q)$ is generically identifiable, if the signals in \mathcal{D} are indirectly excited by a set $\bar{\mathcal{X}}$ of external signals and indirectly measured, i.e. \mathcal{D} has vertex disjoint paths to a set $\bar{\mathcal{C}}$ of measured signals. This is illustrated in Figure 5.3 and can be formalized as follows.

To introduce the identifiability results, we first define an important set:

- Let \mathcal{N}_i^+ contain the signals in \mathcal{W}_i^+ , defined in Section 2.5, and additionally the internal signals, to which w_i have *known* directed edges *and* that are *not* directly excited by vertices in \mathcal{X} whose out-degree is one and the only out-going edge is known.

measure and excite the signals in $\mathcal{D} \cup \{w_j\}$ indirectly. The existence of x_i and x_j in Theorem 5.3 requires the input w_i and the output w_j of the target module to be directly excited, by either r signals or e signals that only have one known out-going edge. The above direct excitation for w_i and w_j ensures that the mappings T_{C_i} and T_{C_j} , which are required for the identifiability analysis, can be obtained from $CT(q)X(q)$.

Theorem 5.3 is also a dual result of Theorem 5.2: while Theorem 5.3 considers the input and the output to be directly excited, Theorem 5.2 assumes them to be measured; in addition, the graphical conditions of the two results have a similar structure. The result can also be extended to address global identifiability by requiring that the sets of maximum number of vertex disjoint paths are unique. In addition, a path-based formulation of Theorem 5.3 can also be obtained, which is analogous to Proposition 5.2.

Proposition 5.3. *For a model set \mathcal{M} that satisfies Assumptions 3.2, 3.4, 3.5 and 5.1, $G_{ji}(q)$ is generically identifiable in \mathcal{M} from (w_C, r) if two vertices x_i and x_j exist in \mathcal{X} , which have out-degree 1 and known directed edges to w_i and w_j respectively, and for some $\bar{\mathcal{X}} \subseteq \mathcal{X} \setminus \{x_j\}$ and $\bar{\mathcal{C}} \subseteq \mathcal{C}$, it holds that*

1. $b_{\mathcal{N}_i^+ \cup \bar{\mathcal{X}} \rightarrow \bar{\mathcal{C}}} = b_{\mathcal{N}_i^+ \setminus \{w_j\} \cup \bar{\mathcal{X}} \rightarrow \bar{\mathcal{C}}} + 1$;
2. $b_{\mathcal{N}_i^+ \setminus \{w_j\} \cup \bar{\mathcal{X}} \rightarrow \bar{\mathcal{C}}} = b_{\bar{\mathcal{X}} \rightarrow \bar{\mathcal{C}}}$.

While Proposition 5.3 is a dual result of Proposition 5.2, it allows us to analyze identifiability in a completely different setting, as illustrated in the following example.

Example 5.2. *Consider the identifiability of $G_{21}(q)$ in \mathcal{M} as shown in Figure 5.4, where only the r signals, w_4 , w_5 , and w_7 are measured, while $\{w_1, w_2\}$ is directly excited by $\{r_1, \tilde{e}_2\}$. It holds that $\mathcal{N}_1^+ = \{w_2, w_3, w_5\}$, and furthermore, we can choose $\bar{\mathcal{X}} = \{\tilde{e}_5, r_6\}$ and $\bar{\mathcal{C}} = \{w_4, w_5, w_7\}$.*

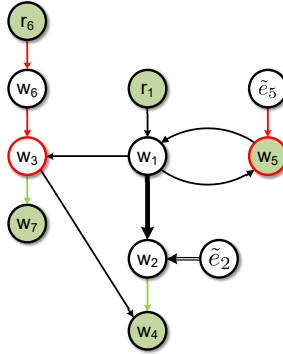


Figure 5.4: Identifiability of $G_{21}(q)$ is considered (thick line) in \mathcal{M} with both input and output unmeasured, while w_2 is directly excited by \tilde{e}_2 via a known edge (double-arrow edge)

It can be found that $\{w_3, w_5\} = \mathcal{D}$ is a $(\mathcal{N}_1^+ \setminus \{w_2\}) \cup \bar{\mathcal{X}} - \bar{\mathcal{C}}$ disconnecting set, as indicated by the red vertices in Figure 5.4. In addition, condition (1) of Theorem 5.3 is satisfied since

there are three vertex disjoint paths, including $w_3 \rightarrow w_7$, $w_2 \rightarrow w_4$, and w_5 itself, indicated by the green edges in Figure 5.4. Condition (2) is then satisfied because there are two vertex disjoint paths indicated by the red edges, including $r_6 \rightarrow w_3$ and $\tilde{e}_5 \rightarrow w_5$, which concludes the generic identifiability of $G_{21}(q)$. Note that r_6 excites w_3 indirectly through a path.

Since the above sets of maximum number of vertex disjoint paths are unique, $G_{21}(q)$ is also globally identifiable.

Remark 5.2. When the identifiability of multiple modules $G_{\bar{W}_i}(q)$ from one SIMO subsystem is considered, where $\bar{W}_i \subseteq W_i^+$, the results in this subsection can be extended in a straightforward way by considering \bar{W}_i instead of the single output w_j , which is similar to the extension in Corollary 5.2

The above remark leads to a graphical result that is related to [13, Theorem IV.2], which also considers the identifiability of multiple modules from one SIMO model. However, [13, Theorem IV.2] is not fully graphical as it requires the availability of certain mappings, and it considers neither known modules nor the excitation contributed by unmeasured noises.

5.6 SUFFICIENT CONDITIONS: MEASURED INPUT OR OUTPUT WITH INDIRECT EXCITATION

Even if Proposition 5.3 considers the most general measurement scheme, it requires w_i and w_j to be directly excited. When w_i (or w_j) is measured, it is not necessary to directly excite w_i (or w_j), as shown in the last condition of Lemma 5.1. In this section, we develop graphical identifiability conditions for the situation where either w_i or w_j is measured and not directly excited.

We first consider the case where the input w_i is unmeasured and the output w_j is measured, and the measured w_j may not be directly excited by r or \tilde{e} . As in (5.6), the mapping $T_{i\mathcal{X}}(q)$ is not a submatrix of $CT(q)X(q)$ as w_i is unmeasured, and thus $T_{i\mathcal{X}}(q)$ needs to be represented by available mappings via an appropriately chosen disconnecting set, which can be motivated by the following example:

Example 5.3. Consider the network model set in Figure 5.5(a) where the identifiability of $G_{21}(q)$ is of interest while w_1 is unmeasured. Since the mapping from r_1 to w_1 is known to be 1, $G_{21}(q)$ can be uniquely recovered from the available external-to-internal mapping from r_1 to w_2 .

In Figure 5.5(b) there is a loop around w_1 , and the mapping from r_1 to w_2 is

$$T_{w_2 r_1}(q) = \frac{G_{21}(q)}{1 - G_{13}(q)G_{31}(q)},$$

and thus $G_{21}(q)$ cannot be recovered from $T_{w_2 r_1}(q)$ alone as in Figure 5.5(a). However, the loop



Figure 5.5: Two network model sets with $G_{21}(q)$ as the target module and w_1 unmeasured. $G_{21}(q)$ is generically and globally identifiable in both cases under measured signals (green).

transfer can be found as

$$T_{w_3 r_3}(q) = \frac{1}{1 - G_{13}(q)G_{31}(q)},$$

and thus $G_{21}(q) = T_{w_2 r_1}(q)T_{w_3 r_2}^{-1}(q)$, where both mappings are available because w_3 and w_2 are measured.

As shown in the above example, it is important to measure and excite the vertices in the loops around the unmeasured input, in order to achieve the identifiability of the module under consideration. This observation can be generalized as follows.

Theorem 5.4. *For a model set \mathcal{M} that satisfies Assumptions 3.2, 3.4, 3.5 and 5.1, suppose that w_j is measured but w_i cannot be measured. Let set \mathcal{N}_i^* contain all the in-neighbors of w_i in \mathcal{W} . Module $G_{ji}(q)$ is generically identifiable in \mathcal{M} from (w_C, r) if a vertex $x_i \in \mathcal{X}_j$ exists, which has out-degree one and a known edge to w_i , and for some $\bar{\mathcal{X}} \subseteq \mathcal{X}_j \setminus \{x_i\}$ and $\bar{\mathcal{C}} \subseteq \mathcal{C}$, there exists a $\bar{\mathcal{X}} \cup \{x_i\} - \mathcal{N}_i^* \cup (\mathcal{N}_j^- \setminus \{w_i\}) \cup \bar{\mathcal{C}}$ disconnecting set $\mathcal{D} \subseteq \mathcal{W}$ such that*

1. $b_{\bar{\mathcal{X}} \cup \{x_i\} \rightarrow \mathcal{D} \cup \{w_i\}} = 1 + |\mathcal{D}|$;
2. $b_{\mathcal{D} \rightarrow \bar{\mathcal{C}}} = |\mathcal{D}|$.

In the above result, the disconnecting set intersects with the paths from x_i to \mathcal{N}_i^* , which implies that all the loops around w_i are blocked by the disconnecting set \mathcal{D} , matching the observation from Example 5.3. Therefore, this result is an extension of Theorem 5.2 to the setting with unmeasured input by additionally blocking all the loops around the unmeasured input.

In addition, both Theorem 5.3 and Theorem 5.4 can be used to analyze the identifiability of $G_{ji}(q)$ with unmeasured input and measured output, while Theorem 5.4 provides the extra freedom that w_j does not need to be directly excited.

Then the corresponding path-based formulation of Theorem 5.4 can also be derived.

Corollary 5.3. *For a model set \mathcal{M} that satisfies Assumptions 3.2, 3.4, 3.5 and 5.1, suppose that w_j is measured but w_i cannot be measured. Module $G_{ji}(q)$ is generically identifiable if a vertex*

$x_i \in \mathcal{X}_j$ exists, which has out-degree one and a known edge to w_i , and for some $\bar{\mathcal{X}} \subseteq \mathcal{X}_j \setminus \{x_i\}$ and $\bar{\mathcal{C}} \subseteq \mathcal{C}$, the following conditions hold:

1. $b_{\bar{\mathcal{X}} \cup \{x_i\} \rightarrow \mathcal{N}_i^* \cup \mathcal{N}_j \cup \bar{\mathcal{C}}} = 1 + b_{\bar{\mathcal{X}} \cup \{x_i\} \rightarrow \mathcal{N}_i^* \cup (\mathcal{N}_j^- \setminus \{w_i\}) \cup \bar{\mathcal{C}}}$;
2. $b_{\bar{\mathcal{X}} \cup \{x_i\} \rightarrow \mathcal{N}_i^* \cup (\mathcal{N}_j^- \setminus \{w_i\}) \cup \bar{\mathcal{C}}} = b_{\bar{\mathcal{X}} \cup \{x_i\} \rightarrow \bar{\mathcal{C}}}$.

The above result can also be extended trivially to a subset of in-coming modules of w_j , which is similar to the extension in Corollary 5.2.

For the situation where the input w_i is measured while the output w_j is unmeasured, the requirement for the direct excitation for w_i in Theorem 5.3 can also be relaxed. Here we start with the analysis in a SIMO problem as in Section 5.5.2. When the direct excitation for w_i is not present, the mapping $T_{C_i}(q)$ is thus not given by $CT_{\mathcal{W}\mathcal{X}}(q)$. However, based on Lemma 5.5, we can simply require a disconnecting set \mathcal{D} from $\{w_i\}$ to \mathcal{C} , and then $T_{C_i}(q)$ is represented by $T_{\mathcal{C}\mathcal{D}}(q)K(q)$ for some $K(q)$, where $T_{\mathcal{C}\mathcal{D}}(q)$ can be obtained in certain way.

Theorem 5.5. *For a model set \mathcal{M} that satisfies Assumptions 3.2, 3.4, 3.5 and 5.1, suppose that for module $G_{ji}(q)$, its input w_i is measured while output w_j is unmeasured. Then $G_{ji}(q)$ is generically identifiable in \mathcal{M} from (w_c, r) if a vertex $x_j \in \mathcal{X}$ exists, which has out-degree one and a known edge to w_j , and for some $\bar{\mathcal{X}} \subseteq \mathcal{X} \setminus \{x_j\}$ and $\bar{\mathcal{C}} \subseteq \mathcal{C}$ with $w_i \in \bar{\mathcal{C}}$, there exists a $(\mathcal{N}_i^+ \setminus \{w_j\}) \cup \bar{\mathcal{X}} \cup \{w_i\} - \bar{\mathcal{C}}$ disconnecting set $\mathcal{D} \subseteq \mathcal{W}$ such that*

1. $b_{\{w_j\} \cup \mathcal{D} \rightarrow \bar{\mathcal{C}}} = |\mathcal{D}| + 1$;
2. $b_{\bar{\mathcal{X}} \rightarrow \mathcal{D}} = |\mathcal{D}|$.

Note that since $w_i \in \bar{\mathcal{C}}$, the disconnecting set in the above result must contain w_i . This result generalizes Theorem 5.3 to address the situation where the input is measured but has an indirect excitation source, while the input needs to be directly excited in Theorem 5.3. The above generalization is achieved by additionally blocking the paths from w_i to $\bar{\mathcal{C}}$ using the disconnecting set, compared to Theorem 5.3. Furthermore, the result in Theorem 5.5 can be extended to analyzing global identifiability as in Remark 5.1 and the identifiability of a subnetwork, i.e. a subset of out-going modules of w_i in this case, as in Remark 5.2. A path-based formulation of Theorem 5.5 can be also obtained analogously as in Corollary 5.3,

5.7 ACTUATOR AND SENSOR ALLOCATION FOR IDENTIFIABILITY

The results in the previous sections provide analysis results for verifying identifiability for a given configuration of measured and excited signals. In order to extend these results for addressing the synthesis problem, i.e. allocating sensors and actuators to achieve identifiability, we extend the reasoning in Section 4.3 as follows.

Depending on whether the input or the output of a module is measured, Theorems 5.2, 5.3, 5.4 and 5.5 explicitly require the signals in the disconnecting sets to be excited and measured to guarantee single module identifiability. Therefore, the idea is to first compute a disconnecting set and then allocate actuators and sensors accordingly. However, the disconnecting sets in the theorems cannot be computed before the excitation signals $\bar{\mathcal{X}}$ and the measured signals $\bar{\mathcal{C}}$ are specified. Thus, we first provide necessary conditions for the disconnecting sets that do not rely on external and measured signals.

Corollary 5.4. *For a model set \mathcal{M} that Assumptions 3.2, 3.4, 3.5 and 5.1,*

- *if it satisfies the conditions in Theorem 5.2 with disconnecting set \mathcal{D}_1 , then \mathcal{D}_1 is also a $\{w_i\} - \mathcal{N}_j^- \setminus \{w_i\}$ disconnecting set;*
- *if it satisfies the conditions in Theorem 5.3 with disconnecting set \mathcal{D}_2 , then \mathcal{D}_2 is also a $\mathcal{N}_i^+ \setminus \{w_j\} - \{w_j\}$ disconnecting set;*
- *if it satisfies the conditions in Theorem 5.4 with disconnecting set \mathcal{D}_3 , then \mathcal{D}_3 is also a $\{w_i\} - \mathcal{N}_i^* \cup (\mathcal{N}_j^- \setminus \{w_i\})$ disconnecting set;*
- *if it satisfies the conditions in Theorem 5.5 with disconnecting set \mathcal{D}_4 , then \mathcal{D}_4 is also a $(\mathcal{N}_i^+ \setminus \{w_j\}) \cup \{w_i\} - \{w_i, w_j\}$ disconnecting set;*

Proof. The proof is analogous to the proof of Corollary 4.3. □

After the above disconnecting sets are computed, excitation signals and sensors can be allocated to achieve the identifiability of $G_{ji}(q)$. Following the theorems, we illustrate the synthesis approaches in Table 5.1 for different cases depending on whether the input or the output can be measured. For each situation, we specify how the disconnecting set is constructed and which signals are to be excited or measured.

Taking Case 2 in Table 5.1 as an example, a $\mathcal{N}_i^+ \setminus \{w_j\} - \{w_j\}$ disconnecting set \mathcal{D} that satisfies $w_j \notin \mathcal{D}$ is first computed. Then for actuator and sensor allocation, each signal in $\mathcal{D} \cup \{w_i, w_j\}$ is directly excited by a distinct r signal, and all signals in \mathcal{D} are measured. In addition, the output w_j is indirectly measured, which is also required in Case 4.

The indirect measurement of w_j in Cases 2 and 4 means that w_j has a path to a measured vertex w_k , and more importantly, based on Theorems 5.3 and 5.5, we choose w_k in the following way: $w_k \in \mathcal{C} \setminus \{w_j\}$ is an internal signal such that the computed \mathcal{D} is also a $\mathcal{N}_i^+ \setminus \{w_i\} - \{w_k\}$ disconnecting set in Case 2 or a $(\mathcal{N}_i^+ \setminus \{w_j\}) \cup \{w_i\} - \{w_k\}$ disconnecting set in Case 4; in addition, there exists a path from w_j to w_k that is vertex disjoint with \mathcal{D} .

The synthesis approaches can be justified in the following result.

Theorem 5.6. *For a model set \mathcal{M} that satisfies Assumptions 3.2, 3.4, 3.5 and 5.1, consider each case in Table 5.1. If the disconnecting set \mathcal{D} is formulated and the excitation signals and sensors are allocated according to Table 5.1, module $G_{ji}(q)$ is generically identifiable.*

Table 5.1: Different synthesis approaches for identifiability of $G_{ji}(q)$.

	Case 1: Measured w_i and w_j	Case 2: Excited w_i and w_j	Case 3: unmeasured w_i and measured w_j	Case 4: measured w_i and unmeasured w_j
Disconnecting set \mathcal{D}	$\{w_i\} - \mathcal{N}_j^- \setminus \{w_i\}$ with $w_i \notin \mathcal{D}$	$\mathcal{N}_i^+ \setminus \{w_j\} - \{w_j\}$ with $w_j \notin \mathcal{D}$	$\{w_i\} - \mathcal{N}_i^* \cup (\mathcal{N}_j^- \setminus \{w_i\})$ with $w_i \notin \mathcal{D}$	$(\mathcal{N}_i^+ \setminus \{w_j\}) \cup \{w_i\} - \{w_i, w_j\}$ with $w_j \notin \mathcal{D}$
Excitation allocation	Directly excite $\mathcal{D} \cup \{w_i\}$ with r	Directly excite $\mathcal{D} \cup \{w_i, w_j\}$ with r	Directly excite $\mathcal{D} \cup \{w_i\}$ with r	Directly excite $\mathcal{D} \cup \{w_j\}$ with r
Sensor allocation	Measure $\mathcal{D} \cup \{w_i, w_j\}$	Measure \mathcal{D} and indirectly measure w_j	Measure $\mathcal{D} \cup \{w_j\}$	Measure \mathcal{D} and indirectly measure w_j

Proof. In Case 1, the allocated r signals form a set $\bar{\mathcal{X}}$, and \mathcal{D} forms a set $\bar{\mathcal{C}}$. It is straightforward that the obtained $\bar{\mathcal{X}}$, $\bar{\mathcal{C}}$ and \mathcal{D} together satisfy the conditions in Theorem 5.2. In Case 2, the r signals that directly excite \mathcal{D} form the set $\bar{\mathcal{X}}$, and $\mathcal{D} \cup \{w_k\}$ forms the set $\bar{\mathcal{C}}$ where w_k is the indirect measurement of w_j . Then due to the chosen w_k and the direct excitation and measurement of \mathcal{D} , the conditions of Theorem 5.3 are satisfied. The proofs for the other two cases follow analogously and thus are omitted. \square

When computing the disconnecting set in the above approaches, a minimum disconnecting set can be found by standard graphical algorithms [135]. Also note that in the obtained model set in Cases 1 and 3, module $G_{ji}(q)$ is globally identifiable as all the relevant signals are directly excited and measured, and thus Theorems 5.3 and 5.4 are satisfied with the unique sets of the maximum number of vertex disjoint paths. Global identifiability of $G_{ji}(q)$ in the other two cases depends on the chosen indirect measurement w_k for w_j .

Example 5.4. Consider the target module $G_{21}(q)$ in the network model set in Figure 5.6(a), where there is one known module $G_{41}^0(q)$, and w_4 is excited by a noise signal e_4 through a known edge. Assuming that the input w_1 and the output w_2 of the target module cannot be measured, i.e. Case 2 in Table 5.1, the goal is to allocate additional r signals and sensors to achieve the generic identifiability of $G_{21}(q)$.

Firstly, it can be found that $\mathcal{N}_1^+ = \{w_3, w_2\}$ according to the definition of \mathcal{N}_1^+ in Section 5.5.2, since w_4 is directly excited by e_4 . Then based on Case 2 in Table 5.1, a $\mathcal{N}_1^+ \setminus \{w_2\} - \{w_2\}$ disconnecting set can be constructed as $\mathcal{D} = \{w_3\}$, indicated by the red vertex in Figure 5.6(b). Then the target module $G_{21}(q)$ becomes generically identifiable, if the input w_1 , the output w_2 and \mathcal{D} are excited, and an indirect measurement of w_2 exists, i.e. w_5 in this case since w_2 only has a path to w_5 . The obtained experimental setup is shown in Figure 5.6(b).

Furthermore, like the extension made in Corollary 5.2, the synthesis approaches for Cases 1 and 3 can be extended trivially to deal with a subset of in-coming modules of w_j ; and the ones for Cases 2 and 4 can also be extended to consider a subset of out-going modules of w_i , as noted in Remark 5.2.

For simplicity, the developed synthesis approaches in this section do not take advantage of the initially present external signals, while these signals may also contribute to the identifiability of

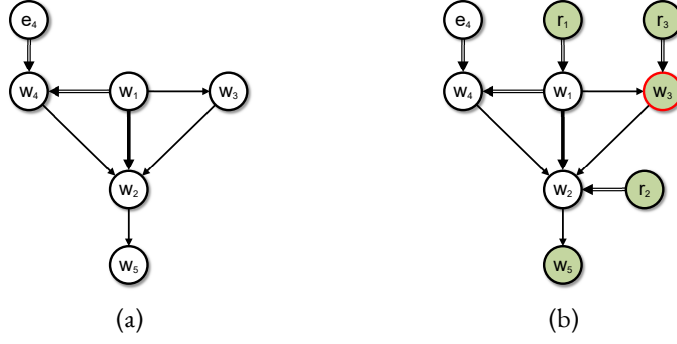


Figure 5.6: The target module $G_{21}(q)$ in (a) becomes generically identifiable after the additional actuators and sensors are allocated as in (b).

$G_{ji}(q)$ and thus reduce the number of additional signals required for the allocation. In addition, the r signals are directly allocated at the signals in the disconnecting sets in Table 5.1; however, the freedom of allocating these r signals elsewhere such that they have vertex disjoint paths to the disconnecting sets is not exploited. This limitation could be addressed by extending the synthesis approaches in Table 5.1 to more advanced approaches similar to Algorithm 1 for the full measurement case. The difficulty of the above extension lies in the interdependence between the excitation signals and the measured signals.

5.8 INDIRECT IDENTIFICATION METHODS

The disconnecting-set-based results in Theorems 5.2, 5.3, 5.4 and 5.5 also suggest several indirect identification methods through which the module of interest $G_{ji}(q)$ can actually be estimated in the situation that the identifiability conditions are satisfied through external excitation signals r only. r signals are required for the indirect identification because the mappings from the r signals to the measured internal signals can be estimated consistently.

The identification algorithms can be retrieved from the following result, where all the non-zero modules are assumed to be unknown for simplicity.

Proposition 5.4. *For \mathcal{M} with all the fixed modules being zeros,*

- *if it satisfies the conditions in Theorems 5.2 with $w_j \notin \mathcal{D}$ and $\bar{\mathcal{X}}$ having no directed edge to w_j , then for \mathcal{M} , it holds generically that*

$$G_{ji}(q) = T_{j\bar{\mathcal{X}}}(q) \begin{bmatrix} T_{i\bar{\mathcal{X}}}(q) \\ T_{\bar{\mathcal{C}}\bar{\mathcal{X}}}(q) \end{bmatrix}^\dagger \begin{bmatrix} 1 \\ 0 \end{bmatrix}; \quad (5.10)$$

- if it satisfies the conditions in Theorem 5.3 with $w_i \notin \mathcal{D} \cup \bar{\mathcal{C}}$, it holds generically that

$$G_{ji}(q) = \begin{bmatrix} 1 & 0 \end{bmatrix} \begin{bmatrix} T_{\bar{\mathcal{C}}j}(q) & T_{\bar{\mathcal{C}}\bar{\mathcal{X}}}(q) \end{bmatrix}^\dagger T_{\bar{\mathcal{C}}i}(q); \quad (5.11)$$

- if it satisfies the conditions in Theorem 5.4 with $w_j \notin \mathcal{D}$, $\bar{\mathcal{X}}$ having no directed edge to w_j , and $x_i \in \mathcal{R}$, then it holds generically that

$$G_{ji}(q) = T_{j\bar{\mathcal{X}}}(q) \begin{bmatrix} \mathbf{e}_{x_i} \\ T_{\bar{\mathcal{C}}(\bar{\mathcal{X}} \cup \{x_i\})}(q) \end{bmatrix}^\dagger \begin{bmatrix} 1 \\ 0 \end{bmatrix}, \quad (5.12)$$

where \mathbf{e}_{x_i} is a standard basis vector which denotes the mapping from $(\bar{\mathcal{X}} \cup \{x_i\})$ to x_i ;

- if it satisfies the conditions in Theorem 5.5, it holds generically that

$$G_{ji}(q) = \begin{bmatrix} 1 & 0 \end{bmatrix} \begin{bmatrix} T_{\bar{\mathcal{C}}j}(q) & T_{\bar{\mathcal{C}}\bar{\mathcal{X}}}(q) \end{bmatrix}^\dagger C_{\bar{\mathcal{C}}i}, \quad (5.13)$$

where $C_{\bar{\mathcal{C}}i}$ is the submatrix of C whose rows and columns correspond to $\bar{\mathcal{C}}$ and w_i , respectively.

Proof. (5.10) is obtained from (5.19) where $P = T_{j\bar{\mathcal{X}}}$ under the assumptions that $\bar{\mathcal{X}}$ has no directed edge to w_j and there is no known module, and (5.11) is a dual result of (5.10). Similarly, (5.12) is derived from (5.23), and combining (5.24) and (5.25) leads to (5.13). \square

The four expressions in the above proposition show opportunities to estimate $G_{ji}(q)$ when the set \mathcal{X}_j consists of only measured r signals. In this case, all the involved mappings, including $T_{\bar{\mathcal{C}}\bar{\mathcal{X}}}(q)$, $T_{\bar{\mathcal{C}}i}(q)$ and $T_{\bar{\mathcal{C}}j}(q)$, are mappings from measured r signals to measured internal signals, and thus, they can be estimated consistently using the standard open-loop identification methods [90]. Consequently, $G_{ji}(q)$ can also be estimated consistently on the basis of the above expressions. Taking (5.11) as an example, it shows that an estimate of $G_{ji}(q)$ can be obtained from dividing the mapping from x_i to $\bar{\mathcal{C}}$ by the mapping from $\{x_j\} \cup \bar{\mathcal{X}}$ to $\bar{\mathcal{C}}$, as visualized in Figure 5.3. Note that these methods can also be generalized to identify multiple modules, which is similar to the extensions in Corollary 5.2 and Remark 5.2.

The methods cover all the possible situations for single module identification depending on whether the input or the output is measured. The particularly interesting case is (5.11) which leads to a method that can estimate $G_{ji}(q)$ even when both its input and output are unmeasured. The methods also do not require measuring the inputs of the MISO subsystem that contains $G_{ji}(q)$, which is a typical choice in the literature such that the MISO subsystem can be estimated to obtain the module estimate [59].

The obtained indirect methods can address significantly more general settings than the existing network identification methods [48, 59, 88, 123, 140] which are typically limited to a specific measurement scheme, e.g., both the input and output are measured [48, 59, 123, 140]; or the

input is unmeasured but the output is measured [59, 88]. However, the indirect methods in this chapter require measured r signals as excitation sources, which can lead to a higher experimental cost than some of the existing methods, e.g., the direct method in [48].

5.9 CONCLUSIONS

The identifiability conditions for verifying single module identifiability, i.e. sub-question 1 as formulated in Chapter 2, and the synthesis approaches for allocating actuators and sensors to achieve single module identifiability, i.e. sub-question 2 in Chapter 2, are investigated in this chapter in the setting with partial measurement and partial excitation.

For the single module identifiability analysis, in order to exploit the noise excitation for the identifiability tests, the concept of network equivalence is introduced and a novel network model structure is developed. This model structure has a simple noise model and allows us to explore the noise excitation for the identifiability tests.

More importantly, graphical conditions for verifying both the global and generic identifiability of a single module are developed in the case of partial measurement and partial excitation. Given the developed model structure, the graphical conditions regard both measured reference signals and unmeasured noises as excitation sources for the identifiability analysis. It is also shown that disconnecting sets provide the important information regarding which signals should be excited or measured to achieve identifiability. The above information further leads to synthesis approaches, for excitation allocation and sensor allocation to achieve identifiability, and indirect methods for estimating network modules.

Open questions include the extension of the synthesis approaches to take advantage of the initially present external signals and to gain extra freedom to allocate actuators and sensors, since in the current approaches r signals are directly allocated at the signals in the disconnecting set. In addition, the extension of the pseudotree-based synthesis approaches in Chapter 4 to the partial measurement and partial excitation setting may provide more efficient synthesis approaches for the full network identifiability. This extension has been preliminarily considered in [37] for acyclic dynamic networks. It is also attractive to investigate how the identifiability results connect to the existing identification methods, e.g., the ones in [48, 120, 152], which are typically less dependent on the presence of r signals than the indirect methods developed in this chapter.

5.10 APPENDIX

5.10.1 PROOF OF THEOREM 5.1

We first exploit the spectrum $C\Phi C^\top$ of M . Based on the measured signals w_C , an immersed network model, which only represents the behavior of the measured signals, can be obtained by

eliminating the unmeasured signals (called immersion or Kron reduction) [48]. To introduce the immersed network, we first define

$$\begin{aligned}\bar{G} &= G_{\mathcal{C}\mathcal{C}} + G_{\mathcal{C}\mathcal{Z}}(I - G_{\mathcal{Z}\mathcal{Z}})^{-1}G_{\mathcal{Z}\mathcal{C}} \\ \bar{H} &= H_{\mathcal{C}} + G_{\mathcal{C}\mathcal{Z}}(I - G_{\mathcal{Z}\mathcal{Z}})^{-1}H_{\mathcal{Z}},\end{aligned}$$

and \bar{R} similarly, where, for example, $G_{\mathcal{C}\mathcal{Z}}$ represents the submatrix of G that has its rows and columns corresponding to the signals in \mathcal{C} and \mathcal{Z} , respectively. Then the immersed network model after the elimination of unmeasured internal signals has the following form:

$$w_{\mathcal{C}} = \bar{G}w_{\mathcal{C}} + \bar{R}r(t) + \bar{H}e(t).$$

Note that the above model may have non-zero diagonal entries in \bar{G} , and $(I - \bar{G})$ has a proper inverse because of Assumption 2.1(b) and consequently $(I - \bar{G}^\infty)$ being full rank. This model further leads to an external-to-internal mapping:

$$w_{\mathcal{C}} = (I - \bar{G})^{-1}\bar{R}r(t) + (I - \bar{G})^{-1}\bar{H}e(t). \quad (5.14)$$

Based on (2.6) and (5.14), it can be found that

$$C\Phi C^\top = (I - \bar{G})^{-1}\bar{H}\Lambda\bar{H}^*(I - \bar{G})^{-*}, \quad (5.15)$$

where it holds that

$$C(I - G)^{-1}C^\top = (I - \bar{G})^{-1}. \quad (5.16)$$

In addition, $\bar{H}\Lambda\bar{H}^*$ can be re-factorized into $\tilde{H}\tilde{\Lambda}\tilde{H}^*$ [60], where $(\tilde{H}, \tilde{\Lambda})$ satisfies the properties of this theorem. Note that $(\tilde{H}, \tilde{\Lambda})$ is unique and $\tilde{\Lambda}$ is full rank if Assumption 5.1 is satisfied. This together with (5.15) and (5.16) leads to

$$C\Phi C^\top = C(I - G)^{-1} \begin{bmatrix} \tilde{H} \\ 0 \end{bmatrix} \tilde{\Lambda} \begin{bmatrix} \tilde{H}^* & 0 \end{bmatrix} (I - G)^{-*} C^\top.$$

The above equation implies that the external-to-output mapping of (5.1), i.e.

$$w_{\mathcal{C}} = C(I - G)^{-1}Rr + C(I - G)^{-1} \begin{bmatrix} \tilde{H} \\ 0 \end{bmatrix} \tilde{e},$$

leads to the same object $(CTR, C\Phi C^\top)$ as M , which concludes that $\tilde{M} \sim M$.

5.10.2 PROOF OF COROLLARY 5.1

The existence of the equivalent network model \tilde{M} follows from the proof of Theorem 5.1. In addition, with the ordering of $w_{\mathcal{C}}$, \bar{H} in (5.15) has a block diagonal structure, and each block corresponds to a set \mathcal{S}_i , based on the proof of Theorem 1 in [123]. As Λ is an identity matrix, $\bar{H}\Lambda\bar{H}^*$ is block diagonal, and thus the spectral factorization of each block matrix in $\bar{H}\Lambda\bar{H}^*$ leads to block diagonal $\tilde{H}(q)$ and $\tilde{\Lambda}$.

5.10.3 PROOF OF PROPOSITION 5.1

For any network model, it holds that

$$C\Phi_v(\theta)C^\top = C(I - G)^{-1}H_p\tilde{\Lambda}H_p^*(I - G)^{-*}C^\top,$$

where $H_p \triangleq \begin{bmatrix} \tilde{H} \\ 0 \end{bmatrix}$, \tilde{H} is monic and $C = [I \ 0]$. Then the proposition is proved by showing that $C(I - G)^{-1}H_p$ and $\tilde{\Lambda}$ can be found uniquely given CTR and $C\Phi C^\top$ under Assumption 3.2, and then the two implications are trivially equivalent.

If G is strictly proper under Assumption 3.2(a), $C(I - G)^{-1}H_p$ is also monic. Since $C\Phi_v C^\top$ admits a unique factorization as

$$C\Phi_v C^\top = L\Lambda_p L^*,$$

where L is monic [58], it holds that $C(I - G)^{-1}H_p = L$ and $\tilde{\Lambda} = \Lambda_p$. Thus, the uniqueness of Λ and $C(I - G)^{-1}H_p$ is guaranteed given $C\Phi_v C^\top$, which concludes the proof under Assumption 3.2(a).

If Assumption 3.2(b) holds, there exists a permutation matrix P such that

$$C\Phi_v C^\top = (CP^\top)F(PH_p)\tilde{\Lambda}(H_p^*P^\top)F^*(PC^\top),$$

where $F \triangleq [I - PG^\infty P^\top]^{-1}$ and F is lower unitriangular. As CP^\top contains the first $|\mathcal{C}|$ rows of P^\top , there exists another permutation matrix \bar{P} such that $\bar{P}CP^\top$ is in row echelon form. Note that pre-multiplying a square matrix by $\bar{P}CP^\top$ extracts a subset of rows in the matrix without re-ordering them. Based on the above facts, consider

$$\bar{P}C\Phi_v C^\top \bar{P}^\top = (\bar{P}CP^\top)F(PH_p\bar{P}^\top)\bar{P}\tilde{\Lambda}\bar{P}^\top(\bar{P}H_p^*P^\top)F^*(PC^\top\bar{P}^\top),$$

where

$$(\bar{P}CP^\top)F(PH_p\bar{P}^\top)$$

is lower unitriangular because the pre- and post-multiplication of F leads to a submatrix of F with rows and columns corresponding to the same indexes. As $\bar{P}C\Phi_v C^\top \bar{P}^\top$ admits a unique

LDL^* decomposition as

$$\bar{P}C\Phi_v C^\top \bar{P}^\top = \bar{L}\Lambda_p \bar{L}^*,$$

where \bar{L} is lower unitriangular, $(\bar{P}C\bar{P}^\top)F(PH_p\bar{P}^\top)$ and $\bar{P}\tilde{\Lambda}\bar{P}^\top$ can be uniquely determined as

$$(\bar{P}C\bar{P}^\top)F(PH_p\bar{P}^\top) = \bar{L}, \quad \bar{P}\tilde{\Lambda}\bar{P}^\top = \Lambda_p.$$

Therefore, $C(I - G)^{-1}H_p$ and $\tilde{\Lambda}$ can also be uniquely found given the spectrum matrix, which proves the proposition under Assumption 3.2(b).

5.IO.4 PROOF OF LEMMA 5.4

The existence of K is proven in Theorem 4.2. As now \mathcal{D} is a subset of $\mathcal{W} \cup \bar{\mathcal{X}}$, K has the following form according to Theorem 4.2:

$$K = \begin{bmatrix} [(I - G_{\mathcal{P}\mathcal{P}})^{-1}]_{\mathcal{W}_1\star} G_{\mathcal{P}\mathcal{D}_1} & [(I - G_{\mathcal{P}\mathcal{P}})^{-1}]_{\mathcal{W}_1\star} X_{\mathcal{P}\mathcal{D}_2} \\ C & 0 \end{bmatrix},$$

for some $\mathcal{P} \subseteq \mathcal{W}$ and $\mathcal{W}_1 \subseteq \mathcal{P}$, and some disjoint sets \mathcal{D}_1 and \mathcal{D}_2 such that $\mathcal{D}_1 \cup \mathcal{D}_2 = \mathcal{D}$; C is a selection matrix that extracts the rows corresponding to \mathcal{W}_2 from a matrix whose rows correspond to \mathcal{D}_1 , where $\mathcal{W}_2 = \bar{\mathcal{W}} \cap \mathcal{D}_1$.

Note that the K matrix equals the external-to-internal mapping from \mathcal{D} to \mathcal{P} in a subgraph of \mathcal{G} , where the vertices in \mathcal{D} are the external signals with all in-coming edges of \mathcal{D} removed, and the signals in \mathcal{P} are internal signals. This characterization of K is clearly seen from its formulation: $(I - G_{\mathcal{P}\mathcal{P}})^{-1} \begin{bmatrix} G_{\mathcal{P}\mathcal{D}_1} & X_{\mathcal{P}\mathcal{D}_2} \end{bmatrix}$ has the same structure as $T_{\mathcal{W}\mathcal{X}}$ in (2.13); and the block row $[C \ 0]$ in K represents the mapping from \mathcal{D} to \mathcal{W}_2 , as C is the mapping from \mathcal{D}_1 to $\mathcal{W}_2 \subseteq \mathcal{D}_1$, and the zero entries indicate that there is no path between any two distinct vertices in \mathcal{D} when the vertices in \mathcal{D} are external signals. Thus, the full column rank of K can be evaluated based on Lemma 5.3 for this subgraph.

5.IO.5 PROOF OF THEOREM 5.2

The proof is to show that a unique G_{ji} can be found given $T_{\bar{\mathcal{C}}\bar{\mathcal{X}}}$, $T_{i\bar{\mathcal{X}}}$ and $T_{j\bar{\mathcal{X}}}$. Note that by condition (1), $w_i \notin \mathcal{D}$ holds. Let set \mathcal{N} contain the remaining in-coming internal signals of w_j which are not in \mathcal{N}_j^- , i.e. \mathcal{N} contains the ones that are measured and have known directed edges to w_j . When $w_j \notin \mathcal{D}$, recall the row of $(I - G)T_{\mathcal{W}\mathcal{X}} = X$ corresponding to w_j , and after

permutation we have

$$\begin{bmatrix} -G_{ji} & -G_{j\mathcal{N}_j^- \setminus \{w_i\}} K_1 & 1 & 0 \end{bmatrix} \begin{bmatrix} T_{i\bar{\mathcal{X}}} \\ T_{\mathcal{D}\bar{\mathcal{X}}} \\ T_{j\bar{\mathcal{X}}} \\ \star \end{bmatrix} = \bar{X} + G_{j\mathcal{N}} T_{\mathcal{N}\bar{\mathcal{X}}}, \quad (5.17)$$

where \bar{X} is a row vector with its columns corresponding to the signals in $\bar{\mathcal{X}}$ and thus is known; $G_{j\mathcal{N}} T_{\mathcal{N}\bar{\mathcal{X}}}$ is also given as the modules in $G_{j\mathcal{N}}$ are known and \mathcal{N} is measured; K_1 satisfies $K_1 T_{\mathcal{D}\bar{\mathcal{X}}} = T_{\mathcal{N}_j^- \setminus \{w_i\}\bar{\mathcal{X}}}$ based on Lemma 5.4. Furthermore, there exists K_2 such that $K_2 T_{\mathcal{D}\bar{\mathcal{X}}} = T_{\bar{\mathcal{C}}\bar{\mathcal{X}}}$, and K_2 is full column rank generically by condition (2) and Lemma 5.4. This generically leads to

$$T_{\mathcal{D}\bar{\mathcal{X}}} = K_2^\dagger T_{\bar{\mathcal{C}}\bar{\mathcal{X}}}, \quad (5.18)$$

where $()^\dagger$ denotes the matrix's left inverse. Then combining the above equation and (5.17) leads to

$$\begin{bmatrix} -G_{ji} & -G_{j\mathcal{N}_j^- \setminus \{w_i\}} K_1 K_2^\dagger \end{bmatrix} \begin{bmatrix} T_{i\bar{\mathcal{X}}} \\ T_{\bar{\mathcal{C}}\bar{\mathcal{X}}} \end{bmatrix} = P, \quad (5.19)$$

where $P = \bar{X} - T_{j\bar{\mathcal{X}}} + G_{j\mathcal{N}} T_{\mathcal{N}\bar{\mathcal{X}}}$, and the above equation holds generically. In addition, due to conditions (1) and (2), it holds that

$$b_{\bar{\mathcal{X}} \rightarrow \{w_i\} \cup \bar{\mathcal{C}}} = 1 + b_{\bar{\mathcal{X}} \rightarrow \bar{\mathcal{C}}},$$

and thus

$$\text{rank}(T_{(\{w_i\} \cup \bar{\mathcal{C}})\bar{\mathcal{X}}}) = 1 + \text{rank}(T_{\bar{\mathcal{C}}\bar{\mathcal{X}}}), \quad (5.20)$$

which implies that (5.19) has a unique solution for G_{ji} generically based on Theorem 3.1 and thus also implies the generic identifiability of G_{ji} .

When $w_j \in \mathcal{D}$, the j th row of $(I - G)T_{\mathcal{W}\bar{\mathcal{X}}} = X$ can be written as follows after permutation:

$$\begin{bmatrix} -G_{ji} & -G_{j(\{w_j\} \cup \mathcal{N}_j^- \setminus \{w_i\})} \bar{K}_1 & 0 \end{bmatrix} \begin{bmatrix} T_{i\bar{\mathcal{X}}} \\ T_{\mathcal{D}\bar{\mathcal{X}}} \\ \star \end{bmatrix} = \bar{X} + G_{j\mathcal{N}} T_{\mathcal{N}\bar{\mathcal{X}}},$$

where $\bar{K}_1 T_{\mathcal{D}\bar{\mathcal{X}}} = T_{(\{w_j\} \cup \mathcal{N}_j^- \setminus \{w_i\})\bar{\mathcal{X}}}$ for some \bar{K}_1 . Note that for the above equation in the special case where $\mathcal{N} = \emptyset$, $G_{j\mathcal{N}} T_{\mathcal{N}\bar{\mathcal{X}}}$ disappears and \bar{X} becomes non-zero, because $\bar{\mathcal{X}}$ must have a directed edge to $w_j \in \mathcal{D}$; otherwise, there exists a path from $\bar{\mathcal{X}}$ to $\mathcal{N}_j^- \setminus \{w_i\}$ which does not intersect with \mathcal{D} based on condition (1) and thus contradicts that \mathcal{D} is a disconnecting set. Finally, combining the above equation and (5.18) leads to unique G_{ji} generically given $CT_{\mathcal{W}\bar{\mathcal{X}}}$ and the first two conditions.

5.10.6 PROOF OF PROPOSITION 5.2

We prove this result by showing that the conditions are equivalent to the conditions of Theorem 5.2. Firstly, based on Lemma 4.4, condition (1) is equivalent to condition (1) of Theorem 5.2, and both conditions are satisfied by choosing \mathcal{D} to be a minimum $\bar{\mathcal{X}} - (\mathcal{N}_j^- \setminus \{w_i\}) \cup \bar{\mathcal{C}}$ disconnecting set. With this choice, $b_{\bar{\mathcal{X}} \rightarrow (\mathcal{N}_j^- \setminus \{w_i\}) \cup \bar{\mathcal{C}}} = |\mathcal{D}|$ by the Menger's theorem, and \mathcal{D} is also a $\bar{\mathcal{X}} - \bar{\mathcal{C}}$ disconnecting set. Then if condition (2) is satisfied, it holds that

$$|\mathcal{D}| = b_{\bar{\mathcal{X}} \rightarrow \bar{\mathcal{C}}},$$

which implies that \mathcal{D} is a minimum $\bar{\mathcal{X}} - \bar{\mathcal{C}}$ disconnecting set by the Menger's theorem, and thus $b_{\mathcal{D} \rightarrow \bar{\mathcal{C}}} = |\mathcal{D}|$, i.e. condition (2) in Theorem 5.2. On the other hand, if condition (2) in Theorem 5.2 holds, there are maximally $|\mathcal{D}|$ vertex disjoint paths from $\bar{\mathcal{X}}$ via \mathcal{D} to $\bar{\mathcal{C}}$, collected into set \mathcal{P} . As \mathcal{D} is a minimum $\bar{\mathcal{X}} - (\mathcal{N}_j^- \setminus \{w_i\}) \cup \bar{\mathcal{C}}$ disconnecting set, all the paths from $\bar{\mathcal{X}}$ to $(\mathcal{N}_j^- \setminus \{w_i\})$ should intersect with the paths in \mathcal{P} , which implies condition (2) of this result and thus concludes the proof.

5.10.7 PROOF OF LEMMA 5.5

The proof is analogous to the proof of Lemma 5.4 with some non-trivial differences that are presented here. Let \mathcal{S} contain all the vertices that is reachable by $\bar{\mathcal{X}}$ without intersecting \mathcal{D} , and $\mathcal{P} = \mathcal{V} \setminus (\mathcal{D} \cup \mathcal{S})$. As $\mathcal{D} \subseteq \mathcal{W}$, $\bar{\mathcal{X}} \subseteq \mathcal{S}$ and $\bar{\mathcal{W}} \subseteq \mathcal{D} \cup \mathcal{P}$ hold. By the definition of the above sets, no edge from \mathcal{S} to \mathcal{P} exists, and thus the submatrix $G_{\mathcal{P}_w \mathcal{S}_w} = 0$, where $\mathcal{P}_w = \mathcal{P} \cap \mathcal{W}$ and $\mathcal{S}_w = \mathcal{S} \cap \mathcal{W}$. Combining the above fact and $T(I - G) = I$ implies that

$$T_{(\mathcal{P}_w \cup \mathcal{D})(\mathcal{S}_w \cup \mathcal{D})} = T_{(\mathcal{P}_w \cup \mathcal{D})\mathcal{D}} \begin{bmatrix} G_{\mathcal{D}\mathcal{S}_w} (I - G_{\mathcal{S}_w \mathcal{S}_w})^{-1} & I \end{bmatrix}, \quad (5.21)$$

where the inverse exists and is proper by Assumption 2.1(b).

As $\bar{\mathcal{X}} \subseteq \mathcal{S}$ only has edges to the internal signals in $\mathcal{S}_w \cup \mathcal{D}$, it holds that for any $\tilde{\mathcal{W}} \subseteq \mathcal{W}$,

$$\begin{aligned} T_{\tilde{\mathcal{W}}\bar{\mathcal{X}}} &= (I - G)_{\tilde{\mathcal{W}}\star}^{-1} X_{\star\bar{\mathcal{X}}} \\ &= (I - G)_{\tilde{\mathcal{W}}(\mathcal{S}_w \cup \mathcal{D})}^{-1} X_{(\mathcal{S}_w \cup \mathcal{D})\bar{\mathcal{X}}} = T_{\tilde{\mathcal{W}}(\mathcal{S}_w \cup \mathcal{D})} X_{(\mathcal{S}_w \cup \mathcal{D})\bar{\mathcal{X}}}. \end{aligned}$$

Denote $\bar{\mathcal{X}} = X_{(\mathcal{S}_w \cup \mathcal{D})\bar{\mathcal{X}}}$, and thus based on the above equation and (5.21), it holds that

$$T_{(\mathcal{P}_w \cup \mathcal{D})\bar{\mathcal{X}}} = T_{(\mathcal{P}_w \cup \mathcal{D})\mathcal{D}} \begin{bmatrix} G_{\mathcal{D}\mathcal{S}_w} (I - G_{\mathcal{S}_w \mathcal{S}_w})^{-1} & I \end{bmatrix} \bar{\mathcal{X}}.$$

As $\bar{\mathcal{W}} \subseteq \mathcal{D} \cup \mathcal{P}$, the above equation implies (5.9) with

$$K = \begin{bmatrix} G_{\mathcal{D}\mathcal{S}_w} (I - G_{\mathcal{S}_w \mathcal{S}_w})^{-1} & I \end{bmatrix} \bar{\mathcal{X}}.$$

Regarding the rank result, the term K denotes an external-to-internal mapping in a subgraph (sub-network) of \mathcal{G} : Consider a subgraph $\bar{\mathcal{G}}$ of \mathcal{G} with only vertices $\bar{\mathcal{X}} \cup \mathcal{S}_w \cup \mathcal{D}$, and the edges among these vertices are kept as in G , while all the out-going edges of \mathcal{D} are removed. The network matrix \bar{G} of $\bar{\mathcal{G}}$ is given as

$$\bar{G} = \begin{bmatrix} G_{\mathcal{S}_w \mathcal{S}_w} & 0 \\ G_{\mathcal{D} \mathcal{S}_w} & 0 \end{bmatrix},$$

where the zero block matrices appear as \mathcal{D} has no out-going edges in $\bar{\mathcal{G}}$. Then we have the mapping in $\bar{\mathcal{G}}$ from $\bar{\mathcal{X}}$ to $\mathcal{S}_w \cup \mathcal{D}$ as

$$\bar{T} = (I - \bar{G})^{-1} \bar{X} = \begin{bmatrix} \star & \star \\ G_{\mathcal{D} \mathcal{S}_w} (I - G_{\mathcal{S}_w \mathcal{S}_w})^{-1} & I \end{bmatrix} \bar{X},$$

which shows that K is a submatrix of \bar{T} and represents the mapping from $\bar{\mathcal{X}}$ to \mathcal{D} in the sub-network $\bar{\mathcal{G}}$. Therefore, we have $\text{rank}(K) = b_{\bar{\mathcal{X}} \rightarrow \mathcal{D}}$ generically in $\bar{\mathcal{G}}$. In addition, as \mathcal{D} is a $\bar{\mathcal{X}} - \bar{\mathcal{W}}$ disconnecting set, it holds that $b_{\bar{\mathcal{X}} \rightarrow \mathcal{D}}$ in the subgraph equals $b_{\bar{\mathcal{X}} \rightarrow \mathcal{D}}$ in \mathcal{G} , and thus by Lemma 5.3, K is full row rank generically if $b_{\bar{\mathcal{X}} \rightarrow \mathcal{D}} = |\mathcal{D}|$ in \mathcal{G} or globally full row rank if $\bar{b}_{\bar{\mathcal{X}}_1 \rightarrow \mathcal{D}} = |\mathcal{D}|$ in \mathcal{G} for some $\bar{\mathcal{X}}_1 \subseteq \bar{\mathcal{X}}$.

5.10.8 PROOF OF THEOREM 5.4

When $w_i \notin \mathcal{D}$, as the conditions imply the first two conditions in Theorem 5.2 with $\bar{\mathcal{X}} \cup \{x_i\}$, we can use part of the proof for Theorem 5.2, while the differences start from (5.19) by replacing $\bar{\mathcal{X}}$ in (5.19) with $\tilde{\mathcal{X}}$, where $\tilde{\mathcal{X}} = \bar{\mathcal{X}} \cup \{x_i\}$. In addition, it can be found that $\mathcal{D} \cup \{x_i\}$ is a $\tilde{\mathcal{X}} - \{w_i\}$ disconnecting set, and thus for some proper K_i , it holds

$$T_{i\tilde{\mathcal{X}}} = K_i \begin{bmatrix} \mathbf{e}_{x_i} \\ T_{\mathcal{D}\tilde{\mathcal{X}}} \end{bmatrix}, \quad (5.22)$$

where \mathbf{e}_{x_i} is a row vector contains one entry as 1 and zeros elsewhere, and it denotes the mapping from $\tilde{\mathcal{X}}$ to w_i since $x_i \in \tilde{\mathcal{X}}$. Moreover, following the proof of Lemma 5.4, K_i is the external-to-internal mapping of a sub-network, where $\mathcal{D} \cup \{x_i\}$ are external signals, and all the in-coming edges of \mathcal{D} are removed. As $\mathcal{D} \cup \{x_i\}$ intersects with all the paths from w_i to \mathcal{N}_i^* in \mathcal{G} , the sub-network does not contain any loop around w_i . This indicates that K_i has a special structure as

$$K_i = \begin{bmatrix} \bar{H} & \bar{K}_i \end{bmatrix},$$

where \bar{H} is the *known* module from x_i to w_i in the sub-network, and note that $\bar{H} = 1$ if x_i is a measured excitation signal. Combining the above equation, (5.22), (5.18) and (5.19) leads to

$$\begin{bmatrix} -G_{ji}\bar{H} & (-G_{ji}\bar{K}_i - G_{j\mathcal{N}_j^+ \setminus \{w_i\}}K_1)K_2^\dagger \end{bmatrix} \begin{bmatrix} \mathbf{e}_{x_i} \\ T_{\bar{\mathcal{C}}\tilde{\mathcal{X}}} \end{bmatrix} = P, \quad (5.23)$$

where $\begin{bmatrix} \mathbf{e}_{x_i} \\ T_{\bar{\mathcal{C}}\tilde{\mathcal{X}}} \end{bmatrix}$ denotes the mapping from $\tilde{\mathcal{X}}$ to $\bar{\mathcal{C}} \cup \{x_i\}$. Following a similar reasoning as in the proof of Lemma 5.4, it can be obtained from the two path-based conditions that generically, $G_{ji}\bar{H}$ and thus G_{ji} are obtained uniquely since \bar{H} is known. The proof for the case where $w_j \in \mathcal{D}$ can be shown analogously.

5.10.9 PROOF OF THEOREM 5.5

Firstly, it holds that $w_i \in \mathcal{D}$ since $\bar{\mathcal{C}}$ contains w_i , and let \mathcal{N} denote the out-neighbors of w_i that are not in \mathcal{N}_i^+ . Considering the column of $C = T_{C\mathcal{W}}(I - G)$ corresponding to w_i , and since \mathcal{D} is a $(\mathcal{N}_i^+ \setminus \{w_j\}) \cup \{w_i\} - \bar{\mathcal{C}}$ disconnecting set, we have

$$\begin{bmatrix} T_{\bar{\mathcal{C}}j} & T_{\bar{\mathcal{C}}\mathcal{D}}\bar{K}_1 \end{bmatrix} \begin{bmatrix} -G_{ji} \\ -G_{\mathcal{N}_i^+ \setminus \{w_j\}i} \\ 1 \end{bmatrix} = P, \quad (5.24)$$

where $T_{\bar{\mathcal{C}}\mathcal{D}}\bar{K}_1 = T_{\bar{\mathcal{C}}(\mathcal{N}_i^+ \setminus \{w_j\}) \cup \{w_i\}}$ for some \bar{K}_1 based on Lemma 5.5; and $P = C_{\bar{\mathcal{C}}i} + T_{\bar{\mathcal{C}}\mathcal{N}}G_{\mathcal{N}i}$ where P is known and $C_{\bar{\mathcal{C}}i}$ is now non-zero because $w_i \in \bar{\mathcal{C}}$. Note that $T_{\bar{\mathcal{C}}j}$ is given by $CT_{\mathcal{W}\mathcal{X}}$ due to the existence of x_j . In addition, it holds that for some \bar{K}_2

$$T_{\bar{\mathcal{C}}\mathcal{D}} = T_{\bar{\mathcal{C}}\tilde{\mathcal{X}}}\bar{K}_2^\dagger, \quad (5.25)$$

based on Lemma 5.5. Combining the above equation and (5.24), and following the analysis of Theorem 5.2 analogously conclude that unique G_{ji} is guaranteed generically.

故乡篱下菊，今日几花开。

江总（南北朝）

*The chrysanthemum under the fence of hometown, how many flowers
bloom today?*

Zong Jiang (Northern and Southern dynasties)

6

Bayesian topology identification

6.1 INTRODUCTION

The topological analysis and synthesis for network identifiability in the previous chapters rely on the pre-specified network topology for a network model set. While this topological information can come from the user's modeling assumptions or prior knowledge, in many practical situations it is attractive to estimate the network topology from data. This topology identification problem itself is also an important subject of study, e.g., in systems biology [68] and social science [181].

This chapter concerns the topology identification problem, i.e. the estimation of the sparsity pattern of $G(q)$ matrix, of a dynamic network in (2.1), when all the internal signals are measured, i.e. $C = I$, and there is no measured excitation signals, i.e., only the observational data is considered. This is an important special case of the general dynamic network model as considered in many applications [68, 181].

Several methods using measures in the frequency domain, e.g. the coherence, can be found in [95, 96, 147]. The approach in [95] uses the coherence function and is built on the idea that nodes that are adjacent in a network should have a higher correlation than nodes that are more distant. However, this approach is restricted to undirected tree structures only. A follow-up can be found in [96], where zero entries in a multivariate Wiener filter estimate of the dynamics are

The material of this chapter is based on [138].

used to infer the topology. This method is further extended in [147] to address the appearance of feedthrough terms and correlated noises.

Another way to approach the topology identification problem is to formulate it into a sparse estimation problem, where the parameters of the dynamic networks are estimated with sparsity-induced regularization. Then the non-zero parameters show which modules in $G(q)$ are non-zero and thus represent the network topology. Typical regularization strategies exploit the l_0 norm penalty [137] or the grouped version of the l_1 norm penalty [27, 179] on the parameter vector. In addition, search algorithms have also been employed to estimate the topology. An iterative algorithm known as *block orthogonal matching pursuit* in compressed sensing employs a forward search procedure [81].

The common challenge in all the above methods is to choose certain tuning parameters, e.g. the threshold value in the frequency-domain methods [96], the regularization parameter that reflects the degree of penalty in the regularized regression [27, 179], and the number of non-zero parameters in the ground truth [81]. These tuning parameters decide how sparse the obtained topology estimate is and thus are critical for the algorithms to achieve good performance. Even if there are recent works that address the choice of the tuning parameters for particular methods, e.g. the regularization parameter in Lasso for independent data [99], this problem remains open for many methods and dynamic systems. In many cases these parameters are chosen in an ad hoc manner.

To avoid the above issue, there are also approaches that are free of tuning parameters. The approach in [40] uses the Bayesian information criterion (BIC) coupled with a greedy search algorithm to estimate the topology of Bayesian networks, where the BIC does not require any tuning parameter. However, this method is designed for independent data and thus not suited for dynamic systems. A Bayesian approach formulated for dynamic networks can be found in [41], where the impulse responses of the modules in the network are modeled as Gaussian processes whose kernel is parameterized by hyperparameters; these hyperparameters are modeled as random variables whose probability density aims at enforcing the sparsity of the network. However, this approach is designed for the joint estimation of topology and dynamics and thus consists of multiple stages and is very complex.

Inspired by [40, 41] and the recent interests in Gaussian processes in the system identification community [117], a Bayesian model selection approach [75, 166] is exploited in this chapter to solve the topology identification problem. While in [41] focus was on the joint estimation of topology and dynamics, our aim is to develop a Bayesian approach for topology identification, without estimating the dynamics. In addition, compared to the approach in [40] which uses the BIC, the Bayesian model selection makes use of the marginal likelihood that allows for the incorporation of the prior knowledge.

The approach in this chapter employs a Bayesian measure, i.e. the marginal likelihood of the network topology, coupled with a forward and backward search algorithm to select the topology

which optimizes the measure. To obtain the measure, the infinite impulse responses of the modules in dynamic networks are modeled as Gaussian processes with hyperparameters. In addition, we take an empirical Bayesian approach where the hyperparameters are modeled as deterministic variables and estimated by maximizing the marginal likelihood using a computationally attractive instance of the expectation-maximization (EM) algorithm; this is a major difference from the approach in [41] where the hyperparameters are modeled as random variables instead. In addition, compared to [41], in this chapter the topology is modeled as a random variable, which permits to incorporate structural prior information and to exploit the uncertainty of the topology estimate when required by specific applications. The important benefit of the developed approach is that no tuning effort is required from the user, and the prior knowledge regarding the stability of the modules can be incorporated into the method.

This chapter is organized as follows. In Section 6.2, the problem of topology identification is formulated. In Section 6.3, the Bayesian model selection is introduced and then extended to a new algorithm for the problem of this chapter in Section 6.4. The group Lasso estimator and its new variant are introduced in Section 6.5 to compare with the Bayesian approach. The numerical results are shown in Section 6.6 and the conclusion completes the chapter.

6.2 PROBLEM FORMULATION

We consider a special form of the dynamic network as

$$w_j(t) = \sum_{i \in \mathcal{I} \setminus j} G_{ji}(q)w_i(t) + H_j(q)e_j(t), \quad j \in \mathcal{I}, \quad (6.1)$$

where $\mathcal{I} = \{1, \dots, L\}$ is the index set, and the notation w_I will be used to denote the set $\{w_j | j \in \mathcal{I}\}$. With some abuse of notation, $w_j(t)$ denotes both a random variable and its realization.

Compared to the general network model in (2.1), the model (6.1) in this chapter has a diagonal and square $H(q)$, and all the internal signals are measured. In addition, there are no r signals, which corresponds to the observational data where no external excitation is provided by the user. Combining (6.1) into a matrix form, the full model can be written as

$$w(t) = G(q)w(t) + H(q)e(t), \quad (6.2)$$

where $w(t) = [w_1(t), \dots, w_L(t)]^\top$, $e(t) = [e_1(t), \dots, e_L(t)]^\top$ and $H(q)$ is a diagonal matrix containing $H_j(q)$ for $j \in \mathcal{I}$. The matrix $G(q)$ contains $G_{ji}(q)$ and has zero entries on its main diagonal.

Besides Assumption 2.1 on the general network model, we consider a simpler model structure that additionally satisfies the following assumptions throughout this chapter:

- All entries in $G(q)$ are strictly proper and stable;

- $H_j(q)$ is monic and minimum-phase for all j ;
- The covariance matrix of $e(t)$ is diagonal, and for all $j \in \mathcal{I}$, $e_j(t)$ follows a Gaussian distribution with an unknown standard deviation σ_j : $e_j(t) \sim \mathcal{N}(0, \sigma_j^2)$.

For the considered model structure, since the noise model $H(q)$ is diagonal and there is no r signal, the network topology is completely determined by the sparsity pattern of $G(q)$. Therefore, we consider a simpler definition of network topology throughout this chapter where only the non-zero entries in $G(q)$ are represented by directed edges, compared to the general definition in Section 2.4.2 where the entries in both $G(q)$ and $H(q)$ are represented by directed edges.

Definition 6.1. *The network topology \mathcal{G} associated with (6.1) is defined as $\mathcal{G} = (\mathcal{V}, \mathcal{E})$, where $\mathcal{V} = \{w_1, \dots, w_L\}$ and $\mathcal{E} = \{(i, j) | G_{ji}(q) \neq 0, i, j \in \mathcal{I}\}$.*

Given the number of internal signals L , the set of vertices \mathcal{V} in \mathcal{G} is given. Then \mathcal{G} is completely determined by the edge set \mathcal{E} , and thus \mathcal{G} and \mathcal{E} are used interchangeably throughout this chapter. When an edge (i, j) exists in \mathcal{E} , we denote $(i, j) \in \mathcal{E}$ or $(i, j) \in \mathcal{G}$.

The problem of topology identification is then to estimate \mathcal{G} of the data generation system, given the measurements of $w_j(t)$ for all $t \in \{0, \dots, N\}$ and all $j \in \mathcal{I}$. We shall denote such a set of measurements by D .

Note that in (6.1), each internal signal is influenced by a distinct white noise. Then when a model set that contains models of the type (6.1) is considered, $G(q)$ is generically identifiable in the model set from the measured internal signals according to Theorem 3.4.

6.3 BAYESIAN MODEL SELECTION

To identify the topology, we need to define a measure that distinguishes two candidate structures on the basis of data. In this chapter, a Bayesian model selection approach [166] is employed by modeling the topology as a random variable and using measure $P(\mathcal{G}_1|D)/P(\mathcal{G}_2|D)$ to compare two candidates, where $P(\mathcal{G}_i|D)$ is the posterior probability of \mathcal{G}_i given the data. Using the Bayes' theorem, the measure can be further formulated as

$$\frac{P(\mathcal{G}_1|D)}{P(\mathcal{G}_2|D)} = \frac{P(D|\mathcal{G}_1)P(\mathcal{G}_1)}{P(D|\mathcal{G}_2)P(\mathcal{G}_2)} = \frac{P(D|\mathcal{G}_1)}{P(D|\mathcal{G}_2)}, \quad (6.3)$$

where $P(D|\mathcal{G})$ is the marginal likelihood, and the second equality holds when there is no prior knowledge on the topology and thus $P(\mathcal{G}_i) = P(\mathcal{G}_j)$. In this chapter, we will assume that the second equality in (6.3) holds, and for the reader who is interested in the structure prior, an example of a structure prior can be found in [172]. Thus, we will use $P(D|\mathcal{G}_1)/P(D|\mathcal{G}_2)$ which is also called the *Bayes factor* [75]. Taking the logarithm of $P(D|\mathcal{G})$, we can obtain an objective function whose maximization yields the topology with the highest marginal likelihood. Note that the BIC is an approximation of $\log P(D|\mathcal{G})$ with a bounded error when $N \rightarrow \infty$ [75].

When the network modules are parameterized by a vector θ , the marginal likelihood in (6.3) can be obtained as

$$P(D|\mathcal{G}) = \int P(D|\theta, \mathcal{G})P(\theta|\mathcal{G})d\theta, \quad (6.4)$$

where $P(D|\theta, \mathcal{G})$ is the likelihood and $P(\theta|\mathcal{G})$ is the parameter prior distribution. Following the Bayesian approach, the topology that maximizes $\log P(D|\mathcal{G})$ is the solution of the problem under study, which leads to the following problem:

$$\max_{\mathcal{G} \in \mathcal{G}_{\text{set}}} \log P(D|\mathcal{G}), \quad (6.5)$$

where \mathcal{G}_{set} denotes the set of all possible graphs. To solve (6.5), we need to address i) the choice of $P(\theta|\mathcal{G})$, ii) the calculation of the integration in (6.4), and iii) the solver to select the topology when there are a large number of candidates. These issues are discussed in the next section.

Remark 6.1. *The criterion $\log P(D|\mathcal{G})$ in (6.5) can be replaced by standard model selection criteria, e.g., the BIC or the Akaike information criterion (AIC); however, $\log P(D|\mathcal{G})$ has the additional capability to incorporate the prior knowledge $P(\theta|\mathcal{G})$ as in (6.4).*

6.4 BAYESIAN TOPOLOGY IDENTIFICATION

6.4.1 REFORMULATION OF THE PROBLEM

Model (6.1) can be reformulated as

$$w_j(t) = \hat{w}_j(t) + e_j(t), \quad (6.6)$$

where $\hat{w}_j(t)$ is the one-step ahead predictor [90], namely

$$\hat{w}_j(t) = [1 - H_j^{-1}(q)]w_j(t) + \sum_{i \in \mathcal{I} \setminus \{j\}} \frac{G_{ji}(q)}{H_j(q)} w_i(t), \quad (6.7)$$

and under the assumptions that $G_{ji}(z)$ is stable and $H_j(z)$ is minimum-phase, it holds [90] that

$$\frac{G_{ji}(q)}{H_j(q)} = \sum_{k=1}^{\infty} \theta_{ji,k} q^{-k}, \quad 1 - H_j^{-1}(q) = \sum_{k=1}^{\infty} \theta_{jj,k} q^{-k}. \quad (6.8)$$

In this chapter we consider the non-parametric model in (6.6) where we directly work with the impulse responses in (6.8). However, since in practice the infinite-order impulse responses in (6.8) need to be truncated to a finite-order n , we focus our discussion on the following finite-

order approximation of (6.6) that contains measurements up to time N :

$$w_j^N = \sum_{i \in \mathcal{I}} A_{ji} \theta_{ji} + e_j^N, \quad j \in \mathcal{I} \quad (6.9)$$

where $w_j^N = [w_j(1), \dots, w_j(N)]^\top$, $\theta_{ji} = [\theta_{ji,1}, \dots, \theta_{ji,n}]^\top$, $e_j^N = [e_j(1), \dots, e_j(N)]^\top$, and

$$A_{ji} = \begin{bmatrix} w_i(0) & w_i(-1) & \cdots & w_i(-n+1) \\ w_i(1) & w_i(0) & \cdots & w_i(-n+2) \\ \vdots & \ddots & \ddots & \vdots \\ w_i(N-1) & w_i(N-2) & \cdots & w_i(N-n) \end{bmatrix}.$$

Equation (6.9) can also be written as

$$w_j^N = A_j \theta_j + e_j^N,$$

where $A_j = [A_{j1}, \dots, A_{jL}]$ and $\theta_j = [\theta_{j1}^\top, \dots, \theta_{jL}^\top]^\top$. In the above model θ_j contains the impulse response coefficients in (6.8), and with some abuse of notation, it is also referred to as parameters even if the impulse response functions in (6.8) are not parameterized.

Equivalently, the problem considered in this chapter can also be formulated based on (6.9) as the identification of the set $\bar{\mathcal{G}} = \{(i,j) | \theta_{ji} \neq 0, i, j \in \mathcal{I}\}$. Note that $\bar{\mathcal{G}}$ is defined on the predictor model (6.6) while \mathcal{G} is defined on (6.1). It can be found from (6.7) that \mathcal{G} is equivalent to $\bar{\mathcal{G}}$ after the self-loops in $\bar{\mathcal{G}}$, e.g., (j,j) , are removed. Even if the algorithm is designed to recover $\bar{\mathcal{G}}$, the notation \mathcal{G} is still used in place of $\bar{\mathcal{G}}$ and the self-loops are made implicit to improve the readability.

Remark 6.2. For simplicity, no measured excitation signal, i.e. the $r(t)$ signal in (2.1), is considered in (6.2) and (6.9). However, the developed approach extends trivially to the case where r signals appear, i.e. the following model class

$$w(t) = G(q)w(t) + R(q)r(t) + H(q)e(t),$$

where $H(q)$ is diagonal, and $e(t)$ is Gaussian and has a diagonal covariance matrix. In this case, the predictor model (6.7) also has the extra r signals as inputs and still leads to a linear regression model of type (6.9). The appearance of r signals does not change the methodology of the developed Bayesian approach, but it may increase the signal-to-noise ratio and thus improve the accuracy of the topology estimation.

6.4.2 DECOMPOSITION OF THE OBJECTIVE FUNCTION

In this section, we show that the objective function $\log P(D|\mathcal{G})$ can be decomposed into a set of independent terms corresponding to MISO subsystems, where each MISO topology identification problem can be solved independently.

Based on (6.4), $P(D|\mathcal{G})$ can be factorized by decomposing $P(D|\theta, \mathcal{G})$ and $P(\theta|\mathcal{G})$ as follows. According to Theorem 2.2, it holds that the likelihood can be factorized as

$$P(D|\theta, \mathcal{G}) = \prod_{j=1}^L \prod_{t=1}^N P(w_j(t)|\hat{w}_j(t)).$$

In addition, we assume that the prior $P(\theta|\mathcal{G})$ in (6.4) satisfies

$$P(\theta|\mathcal{G}) = \prod_{j=1}^L P(\theta_j|\mathcal{G}_j), \quad (6.10)$$

where \mathcal{G}_j and θ_j denote the topology and the parameter vector of one MISO model, respectively. Thus, given (6.1) and the parameter independence assumption, the marginal likelihood in (6.5) can be decomposed into L independent terms as $\log P(D|\mathcal{G}) = \sum_{j=1}^L \log P(D_j|\mathcal{G}_j)$, where D_j denotes the data relevant to a single MISO problem of the type (6.9) and

$$\log P(D_j|\mathcal{G}_j) \triangleq \log \int \prod_{t=1}^N P(w_j(t)|\hat{w}_j(t)) P(\theta_j|\mathcal{G}_j) d\theta_j. \quad (6.11)$$

Since each term is a function of the MISO topology, the search algorithm for the MISO topology can then be parallelized to obtain the overall network topology.

6.4.3 OBJECTIVE FUNCTION: PARAMETER PRIOR AND INTEGRATION

Due to the independence among the MISO problems, we describe the developed algorithm for a single MISO model of the type (6.9) in this section.

Firstly, we need to specify the dependence of $P(D_j|\theta_j, \mathcal{G}_j)$ and $P(\theta_j|\mathcal{G}_j)$ on one particular structure \mathcal{G}_j . Given one topology $\mathcal{G}_j = \{(i_1, j), \dots, (i_p, j)\}$, $P(\theta_j|\mathcal{G}_j)$ considers the distribution of the parameter vector formulated based on \mathcal{G}_j , i.e.

$$\theta_j|\mathcal{G}_j = \begin{bmatrix} \theta_{ji_1}^\top & \cdots & \theta_{ji_p}^\top \end{bmatrix}^\top,$$

where with some abuse of notation, $\theta_j|\mathcal{G}_j$ denotes a vector formulated based on the edges in \mathcal{G}_j . In addition, the likelihood function $P(D_j|\theta_j, \mathcal{G}_j)$ is calculated based on the model

$$w_j^N = (A_j|\mathcal{G}_j) \cdot (\theta_j|\mathcal{G}_j) + e_j^N,$$

where $A_j|\mathcal{G}_j = \begin{bmatrix} A_{ji_1} & \cdots & A_{ji_p} \end{bmatrix}$.

PARAMETER PRIOR

Following the kernel-based approach for system identification [116], the impulse response coefficients are modeled as Gaussian processes. Since the prior knowledge that the impulse responses should decay with time is available, the parameter prior $P(\theta_j|\mathcal{G}_j)$ is chosen from [117] as

$$\theta_j|\mathcal{G}_j \sim \mathcal{N}(0, K_j), \quad (6.12)$$

where K_j is a block diagonal matrix structured as

$$K_j = \text{diag}(\lambda_{ji_1} \bar{K}(\beta_{ji_1}), \dots, \lambda_{ji_p} \bar{K}(\beta_{ji_p})),$$

where $\bar{K}(\beta_{ji})$ is an $n \times n$ matrix that depends on an unknown scalar hyperparameter β_{ji} , and the (k, m) entry of $\bar{K}(\beta_{ji})$ is defined by $\beta_{ji}^{\max(k, m)}$. It is also required that $\lambda_{ji} > 0$ and $\beta_{ji} \in [0, 1)$. For this choice of kernel, β_{ji} regulates the rate of decay of the impulse responses to zero. Therefore, the module priors depend on the unknown hyperparameter vectors, i.e. $\lambda_j|\mathcal{G}_j = [\lambda_{ji_1} \cdots \lambda_{ji_p}]^\top$ and $\beta_j|\mathcal{G}_j = [\beta_{ji_1} \cdots \beta_{ji_p}]^\top$. Since every MISO problem will be assigned an independent parameter prior as (6.12), equation (6.10) is satisfied.

INTEGRATION

Denote $\eta_j = [\sigma_j^2 \quad \lambda_j^\top \quad \beta_j^\top]^\top$, where the dependencies of λ_j and β_j on \mathcal{G}_j are implicit. Based on (6.9) and (6.12), given one particular \mathcal{G}_j , (6.11) can be obtained in a closed form because of the chosen Gaussian distributions. After scaling and removing a constant term, we can obtain that

$$\begin{aligned} J(\mathcal{G}_j; \eta_j) &= 2 \log P(D_j|\mathcal{G}_j; \eta_j) - \text{constant term} \\ &= - (w_j^N)^\top \Gamma_j^{-1} w_j^N - \log \det \Gamma_j, \end{aligned} \quad (6.13)$$

where $\Gamma_j = \sigma_j^2 I_N + A_j K_j A_j^\top$, and the dependencies of A_j and K_j on a particular topology \mathcal{G}_j are implicit. Note that Γ_j is also a function of η_j . Since η_j is unknown, an estimate of η_j has to be computed first and then we can use $J(\mathcal{G}_j; \hat{\eta}_j)$ as the objective function for the topology estimation problem.

ESTIMATION OF HYPERPARAMETERS

To obtain an estimate of $\hat{\eta}_j$, we first estimate the hyperparameter vector associated with the complete MISO graph, where all the other internal signals have directed edges to w_j . The obtained

estimate is denoted by η_j^{full} . Then, given a graph \mathcal{G}_j , the corresponding hyperparameter vector $\hat{\eta}_j$ associated to that graph can be obtained by neglecting those hyperparameters in η_j^{full} associated to zero modules (i.e., missing edges in the graph). This procedure avoids the re-estimation of η_j for all different graphs and reduces the computational cost. The hyperparameter vector η_j^{full} is estimated by solving the following marginal likelihood problem:

$$\hat{\eta}_j^{full} = \operatorname{argmax}_{\eta_j^{full}} \log P(D_j | \mathcal{G}_j^{full}; \eta_j^{full}), \quad (6.14)$$

where \mathcal{G}_j^{full} is a complete MISO graph, i.e. $\mathcal{G}_j^{full} = \{(1j), \dots, (Lj)\}$. A local optimum of this problem can be found by the EM algorithm [28].

Assuming that an estimate $\hat{\eta}_j^{(k)}$ of η_j^{full} is available at the k -th iteration of the EM algorithm, an updated estimate is obtained by the following steps:

(E-step) Compute

$$Q(\eta_j, \hat{\eta}_j^{(k)}) = E_{P(\theta_j | w_j^N; \hat{\eta}_j^{(k)})} [\log P(\theta_j, w_j^N; \eta_j)]; \quad (6.15)$$

(M-step) Compute

$$\hat{\eta}_j^{(k+1)} = \operatorname{argmax}_{\eta_j \in \mathcal{V}} Q(\eta_j, \hat{\eta}_j^{(k)}). \quad (6.16)$$

Note that for a MISO problem, the input and the graph are regarded as fixed and thus implicit in (6.15).

Proposition 6.1. *Denote $\hat{\eta}^{(k)}$ as the estimate of the hyperparameter vector at the k th iteration of the EM algorithm used to solve (6.14). Then according to (6.15) and (6.16), $\hat{\eta}^{(k+1)}$ is obtained with the following update rules:*

- The hyperparameter $\hat{\sigma}_j^{(k+1)}$ is obtained as

$$\hat{\sigma}_j^{(k+1)} = \sqrt{\frac{M^{(k)}}{N}}, \quad (6.17)$$

where

$$\begin{aligned} M^{(k)} &= (w_j^N)^\top w_j^N - 2(w_j^N)^\top A_j \hat{C}_j^{(k)} w_j^N + \operatorname{tr}[A_j^\top A_j \hat{\Delta}_j^{(k)}], \\ \hat{C}_j^{(k)} &= [\hat{\sigma}_j^{(k)}]^{-2} [\hat{\Sigma}_j^{(k)}]^{-1} A_j^\top, \\ \hat{\Sigma}_j^{(k)} &= [\hat{\sigma}_j^{(k)}]^{-2} A_j^\top A_j + [K_j(\hat{\lambda}_j^{(k)}, \hat{\beta}_j^{(k)})]^{-1}, \\ \hat{\Delta}_j^{(k)} &= [\hat{\Sigma}_j^{(k)}]^{-1} + \hat{C}_j^{(k)} w_j^N (w_j^N)^\top [\hat{C}_j^{(k)}]^\top. \end{aligned}$$

- The hyperparameter $\hat{\beta}_{ji}^{(k+1)}$, $i = 1, \dots, L$, is obtained as

$$\hat{\beta}_{ji}^{(k+1)} = \arg \min_{\beta_{ji} \in [0, 1]} n \log[\text{tr}(\bar{K}^{-1}(\beta_{ji}) \hat{\Delta}_j^{(k)}[i])] + \log \det \bar{K}(\beta_{ji}), \quad (6.18)$$

where $\hat{\Delta}_j^{(k)}[i]$ is a square sub-matrix obtained from $\hat{\Delta}_j^{(k)}$ by the $[(i-1)n+1]$ -th row and column until the (in) -th row and column of $\hat{\Delta}_j^{(k)}$.

- The hyperparameter $\hat{\lambda}_{ji}^{(k+1)}$, $i = 1, \dots, L$, is obtained as

$$\hat{\lambda}_{ji}^{(k+1)} = \frac{1}{n} \text{tr}[\bar{K}^{-1}(\hat{\beta}_{ji}^{k+1}) \hat{\Delta}_j^{(k)}[i]]. \quad (6.19)$$

The proof of the above proposition is presented in Section 6.8. It can be found that (6.14) is decomposed into a set of optimization problems with scalar optimization variables for estimating β and closed-form solutions for estimating σ and λ . The computational speed and the numerical robustness of the above algorithm can be further improved by exploiting the factorization of \bar{K} [31] [28] such that its inverse can be more easily computed, which is also implemented in the algorithm.

6.4.4 ALGORITHM FOR OPTIMIZATION

The objective function of problem (6.5) has been reformulated in (6.13), where $J(\mathcal{G}_j; \hat{\eta}_j)$ is used to replace $\log P(D_j | \mathcal{G}_j)$ and $\hat{\eta}_j$ is obtained as $\hat{\eta}_j = \hat{\eta}_j^{\text{full}} | \mathcal{G}_j$. The next step is to design a solver for the optimization problem.

Since the number of all possible directed graphs in \mathcal{G}_{set} is 2^{L^2-L} , it is infeasible to consider all the candidates when L is large. Following [40], a forward-backward greedy search algorithm is implemented to find a local optimum of (6.5). Recall that the graph of the predictor model is considered here so that self-loops are always present. The algorithm initializes a graph with only self-loops and then starts an iterative edge-addition procedure, where at each iteration, the edge, whose existence leads to the largest increase in the objective value, is added to the graph from the previous iteration. The iteration stops when the objective function cannot be further increased by adding edges.

Given the resulting graph from the edge-addition phase, the algorithm then starts an iterative edge-deletion phase, where at each iteration, one edge is removed from the graph of the previous iteration if such deletion leads to the largest increase in the objective function comparing to the removal of other edges. The final output of the algorithm is obtained when no improvement in the objective value can be made by deleting any edge.

As mentioned earlier, due to the decomposition in (6.11), the search algorithm can be applied to every MISO problem separately, merging the outcomes to obtain the network topology.

6.4.5 FINAL ALGORITHM

Algorithm 2 Bayesian search (BS) algorithm

INPUT: Measurements $w_I(t)$ for all $t \in \{1, \dots, N\}$;

OUTPUT: Graph estimate $\hat{\mathcal{G}}$

```

1: Obtain  $\hat{\eta} = \max_{\eta} \log p(D|\mathcal{G}_{full}; \eta)$  by EM algorithm;
2: Initialize  $\hat{\mathcal{G}}^{(0)} = \{(j, j)\}$  and  $Edge = \{(1, j), \dots, (L, j)\}$ 
3: for  $b = 1 : L - 1$  (Edge-addition phase) do
4:    $Edge = Edge \setminus \hat{\mathcal{G}}^{(b-1)}$ ;
5:    $(i, j) = \operatorname{argmax}_{(i, j) \in Edge} J(\{\hat{\mathcal{G}}^{(b-1)}, (i, j)\}; \hat{\eta})$ 
6:   if  $J(\{\hat{\mathcal{G}}^{(b-1)}, (i, j)\}; \hat{\eta}) - J(\hat{\mathcal{G}}^{(b-1)}; \hat{\eta}) > \tau$  then
7:      $\hat{\mathcal{G}}^{(b)} = \{\hat{\mathcal{G}}^{(b-1)}, (i, j)\}$ 
8:   else
9:     Break
10:  end if
11: end for
12: Initialize for the second phase:  $\hat{\mathcal{G}}^{(0)} = \hat{\mathcal{G}}_{FinalAddition}$ , where  $\hat{\mathcal{G}}_{FinalAddition}$  is the output of the
    previous step
13: for  $d = 1 : |\hat{\mathcal{G}}^{(0)}|$  (Edge-deletion phase) do
14:    $(i, j) = \operatorname{argmax}_{(i, j) \in \hat{\mathcal{G}}^{(d-1)}} J(\hat{\mathcal{G}}^{(d-1)} \setminus (i, j); \hat{\eta})$ 
15:   if  $J(\hat{\mathcal{G}}^{(d-1)} \setminus (i, j); \hat{\eta}) - J(\hat{\mathcal{G}}^{(d-1)}; \hat{\eta}) > \tau$  then
16:      $\hat{\mathcal{G}}^{(d)} = \hat{\mathcal{G}}^{(d-1)} \setminus (i, j)$ 
17:   else
18:     Break
19:   end if
20: end for

```

After the formulation of the objective function and the greedy search algorithm, the algorithm is now complete and summarized in this section. Firstly, recall that $\hat{\eta}_j^{full}$ obtained in the previous step is for a full graph and thus, given a structure \mathcal{G}_j , $\hat{\eta}_j$ should be reformulated as $\hat{\eta}_j^{full}|\mathcal{G}_j = \left[\hat{\sigma}_j \quad (\hat{\lambda}_j^{full}|\mathcal{G}_j)^\top \quad (\hat{\beta}_j^{full}|\mathcal{G}_j)^\top \right]^\top$. To simplify the notation, the index j is dropped in the algorithm. The final algorithm is presented in Algorithm 2*.

The tolerance τ in Algorithm 2, determining whether an edge should be added or removed, is chosen to be zero as the default value; its suggested range is $[0, 10]$, see [75]. Note that varying the value of τ is not necessary if the topology with the maximum marginal likelihood is desired. In this case, Algorithm 2 has no tuning parameter, except the initialization values for the EM algorithm.

Remark 6.3. To empirically validate the choice of using the estimate of $\hat{\eta}^{full}$ under the full graph, the BS algorithm is compared with its variant using an iterative EM approach, which re-estimates

*The Matlab code of Algorithm 2 can be found in <https://codeocean.com/capsule/3224411/tree/v1>.

$\hat{\eta}$ by the EM algorithm under every iteration of the search algorithm. We call this procedure the iterative-EM BS algorithm.

Comparing to the approach in [41], the main difference of the BS algorithm is that the hyperparameters are modeled as deterministic variables and then estimated by the EM algorithm. By contrast, in [41], the hyperparameters are modeled as random variables, and a prior distribution of the hyperparameters is also used. The choice of modeling also the hyperparameters as random variables requires designing their prior distribution, which usually needs additional hyper-hyperparameters that may be difficult to estimate.

6.5 KERNEL-BASED GROUP LASSO

The performance of the BS algorithm is compared with the group Lasso (GLasso) estimator [179], which is formulated on the basis of (6.9) as

$$\min_{\theta_j} \frac{1}{2} \|w_j^N - A_j \theta_j\|_2^2 + \delta_j \sum_{i=1}^L \sqrt{\theta_{ji}^\top \Lambda_j \theta_{ji}}, \quad (6.20)$$

where Λ_j is an identity matrix. Here, the topology estimation problem is also divided into independent MISO problems. It is also of interest to see if the performance of (6.20) can be improved by incorporating the covariance matrix in (6.12) into the regularization term. This kernel-based GLasso can be formulated by setting $\Lambda_j = \bar{K}(\beta_j)^{-1}$. To reduce the computational complexity, we choose to have the same hyperparameters β_j for all modules of each MISO problem. To select δ_j and β_j , cross-validation can be employed. After having the estimated parameters, the topology can be obtained by checking if the l_2 norm of the parameter vector corresponding to one module is zero.

6.6 NUMERICAL RESULTS

The performance of the algorithms is evaluated in extensive simulation studies. To quantify the performance of the algorithm, an existing edge in the network is labeled as one positive instance; its absence is labeled as one negative instance. Let P denote the total number of positives and Z denote the total number of negatives in the ground truth. In addition, for the outcome of the algorithm, if the algorithm outputs one edge that does exist in the ground truth, it scores a true positive (TP). If the algorithm outputs one edge that does not exist in the ground truth, it scores a false positive (FP). The behavior of the algorithms is studied by using the receiver operating characteristic (ROC) curve [92], i.e. TP rate (TPR) vs FP rate (FPR) over different choices of

their tuning parameters, where

$$TPR = \frac{TP}{P}, \quad FPR = \frac{FP}{Z},$$

which are further averaged over the number of Monte Carlo experiments.

The tuning parameter for the (iterative-EM) BS algorithm is $\tau \in \{0, 1, \dots, 10\}$, while the tuning parameters of GLasso and the kernel-based GLasso are $\delta_j \in \{0, 10, 20, \dots, 2000\}$ and $\beta_j = \{0.1, \dots, 0.9\}$. To build ROC curves for the two GLasso estimators, δ_j and β_j are kept the same for all MISO problems to reduce the number of tuning parameters. The $(0, 1)$ point in the ROC plot denotes the ideal performance without any error. Thus, the points on ROC curves of different methods can be compared based on their closeness to the $(0, 1)$ point, i.e. computing

$$dis = \sqrt{FPR^2 + (1 - TPR)^2}.$$

A smaller dis value implies better performance.

We consider randomly generated dynamic networks with 6 nodes, and three experiment conditions with different data length N and model order n are considered: $N = 2000$ and $n = 100$; $N = 500$ and $n = 100$; $N = 50$ and $n = 50$. Note that in the final study, the number of the postulated unknown parameters in the algorithm is larger than the number of the measurements. For each experiment condition, 50 different data-generating systems and thus independent data sets are randomly generated as follows. For each data-generating system, its topology is generated by assigning a discrete uniform distribution to the existence of each edge and then we assign a random transfer function to every existing edge by using *drmodel* function in Matlab. The orders of generated G_{ji} and H_j are randomly selected from 2 to 5 with a uniform distribution. To guarantee a reasonable signal-to-noise ratio, G_{ji} is further normalized by its own l_2 norm. Finally, the data of the resulting system is obtained by injecting white Gaussian noises with zero mean and $\sigma_j(t) = 1$, for all j and t .

For each data set, to initialize the hyperparameter vector for the EM algorithm, we set $\hat{\beta}_{ji}^{(0)} = 0.5$, $\hat{\lambda}_{ji}^{(0)} = 0.5$ for all modules and $\hat{\sigma}_j^{(0)}(t)$ is the same for all j and t , which is drawn from a normal distribution with mean 1 and standard deviation 0.2.

The obtained ROC curves are shown in Figure 6.1. For the kernel-based GLasso, only the ROC curves corresponding to $\beta_j = 0.7$ are shown since $\beta_j = 0.7$ typically provides the best performance. It can be found that in all tests, the two search algorithms perform better than the two GLasso estimators because the ROC curves of the search algorithms are closer to the $(0, 1)$ point for every value of τ . To compare the performance of the iterative-EM BS and the BS algorithm, the following measure is used:

$$V = \left[\sum_{i=1}^{11} \frac{dis_{iter-EMBS,i} - dis_{BS,i}}{dis_{BS,i}} \right] \div 11 \times 100\%,$$

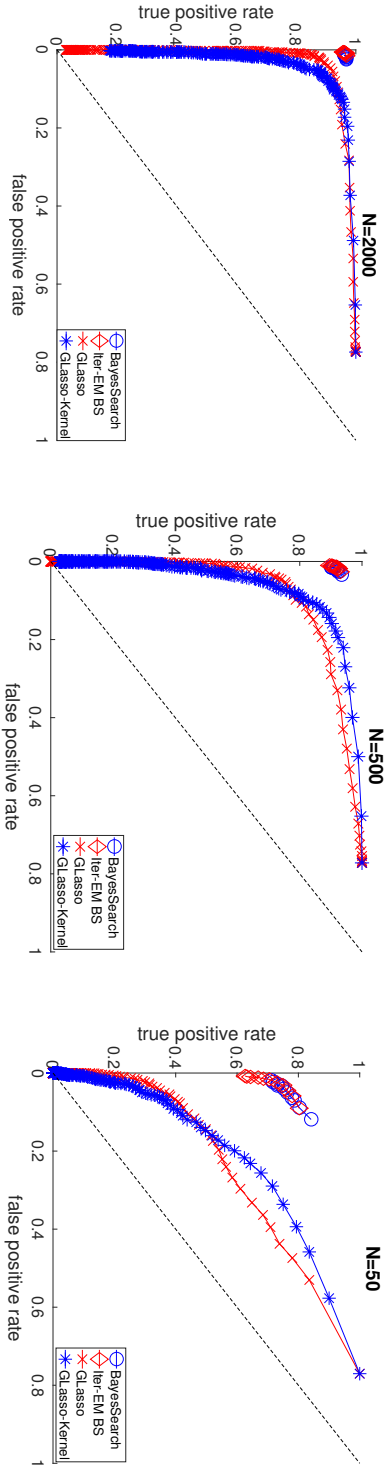


Figure 6.1: TPR vs FPR of the four algorithms over tuning parameters, i.e. $\hat{\tau}$ in the Bayesian algorithms and $\hat{\delta}_j$ in the group Lasso, for different data length: $N = 2000$ (left), $N = 500$ (middle), $N = 50$ (right). $(0, 1)$ is the ideal point which indicates that the estimate makes no error compared to the ground truth. For each algorithm, each point in the figure associates with a particular threshold value and denotes the (FPR, TPR) averaged over 50 Monte Carlo experiments.

where i denotes the i th value of τ in $\{0, 1, \dots, 10\}$. Given one value of τ , one point on the ROC curve is correspondingly selected and thus $dis_{BS,i}$ can be calculated based on Figure 6.1. Note that a positive value of V implies a worse performance of the iterative-EM algorithm. It can then be found that $V = -4\%$ when $N = 2000$, $V = 1\%$ when $N = 500$ and $V = 18\%$ when $N = 50$. Thus, the iterative-EM BS algorithm performs better than the BS algorithm when N is large while it has worse performance when the sample size is relatively small. Intuitively, this can be explained by the fact that the iterative-EM algorithm relies more on the data because it adjusts the parameter prior given every different graph during the search procedure, leading to a larger error when the data length is limited. The computational speed of the iterative-EM algorithm is also around 10 times slower than the BS algorithm in this 6-node example. Thus, it is suggested to use the BS algorithm when N is small and faster computation is preferred.

The performance of the algorithms is also compared when cross-validation is employed for the two GLasso estimators while τ equals the default value, i.e. $\tau = 0$, for the two BS algorithms. For the cross-validation, the training data contains the data up to time $2(N+1)/3$, and the data left is kept for validation. The tuning parameter that provides the smallest root-mean-square error in predicting the validation data is selected. Note that in this case, the tuning parameters of the two GLasso estimators are allowed to be different over the MISO problems. The final results contain one (FPR, TPR) point for every algorithm, and their distance to $(0, 1)$ is summarized in Table 6.1.

Table 6.1: Distance of the results of the algorithms to $(0, 1)$ with the cross-validated or the default tuning parameter

	BS	Iter-EM BS	GLasso	K-GLasso
$N = 2000$	0.04	0.04	0.59	0.64
$N = 500$	0.07	0.07	0.37	0.60
$N = 50$	0.20	0.22	0.52	0.47

No significant difference is observed between the BS and the iterative-EM BS algorithm, while the two search algorithms outperform the two GLasso estimators due to their smaller distance to $(0, 1)$. This is because the cross-validation is designed for obtaining the tuning parameters corresponding to the best prediction performance, which typically leads to a model with more positives to improve the prediction. Instead, the Bayes factor typically favors simpler models, which may lead to a model with poorer prediction performance. This difference in the design purpose between BIC, which is an asymptotic approximation of the Bayes factor, and cross-validation is also mentioned in [56].

6.7 CONCLUSIONS

The topology identification problem of dynamic networks is considered in this chapter, in the special setting where noises are uncorrelated and there are no external measured excitation signals. A Bayesian model selection approach for topology identification of networks of transfer

functions is explored. It uses the Bayes factor coupled with a forward-backward search algorithm. The Bayes factor is obtained by modeling the infinite impulse responses of the modules as Gaussian processes, where the hyperparameters of the Gaussian prior are estimated by the EM algorithm. Numerical results demonstrate the effectiveness of the algorithm, which shows better performance compared to the group Lasso estimator.

Some open questions can be investigated for future research. For example, little is known regarding the theoretical properties of the developed Bayesian method, e.g., whether the method can estimate the true network topology with probability 1 when the data length approaches infinity. While there are results about Bayes factor consistency [39], these results are typically limited to the independent data and static models. Non-trivial extensions of the existing theoretical results need to be made to address dynamic systems and time series. In addition, the Bayesian approach in this chapter can be extended to address the setting with correlated noises and reduced-rank noises [170], where there are fewer noise sources than the internal signals.

6.8 APPENDIX

6.8.1 PROOF OF PROPOSITION 6.1

Recall the notations defined in (6.17). The proof contains two steps, including the E-step and the M-step of the EM algorithm.

E-step: Firstly, note that

$$\log P(\theta_j, w_j^N; \eta_j) = \log P(w_j^N | \theta_j; \eta_j) + \log P(\theta_j; \eta_j),$$

where $\log P(w_j^N | \theta_j; \eta_j)$ is the likelihood function given by the model and $\log P(\theta_j; \eta_j)$ is the parameter prior of the full graph given by (6.12). Thus, it can be found that

$$\begin{aligned} \log P(\theta_j, w_j^N; \eta_j) = & \text{constant} - \frac{1}{2} \sum_{i=1}^L \log \det(\lambda_{ji} \bar{K}(\beta_{ji})) \\ & - \frac{1}{2} \log \det(\sigma_j^2 I_N) - \frac{1}{2\sigma_j^2} (w_j^N)^\top w_j^N \\ & - \frac{1}{2} \theta_j^\top \Sigma_j \theta_j + \frac{1}{\sigma_j^2} (w_j^N)^\top A_j \theta_j, \end{aligned}$$

where Σ_j is formulated as in (6.17) given η_j .

$Q(\eta_j, \hat{\eta}_j^{(k)})$ can then be obtained by calculating the expectation of $\log P(\theta_j, w_j^N; \eta_j)$ over the posterior distribution of θ_j given the data and $\hat{\eta}_j^{(k)}$. Due to the Gaussian noise and the parameter prior (6.12), it follows that the posterior distribution of the parameter also has a Gaussian

distribution as

$$\theta_j | w_j \sim \mathcal{N}(\hat{C}_j^{(k)} w_j^N, (\hat{\Sigma}_j^{(k)})^{-1}).$$

Thus, the E-step can be finalized as

$$Q(\eta_j, \hat{\eta}_j^{(k)}) = Q_1(\sigma_j, \hat{\eta}_j^{(k)}) + \sum_{i=1}^L Q_2(\lambda_{ji}, \beta_{ji}, \hat{\eta}_j^{(k)}) + \text{constant}, \quad (6.21)$$

where

$$Q_1(\sigma_j, \hat{\eta}_j^{(k)}) = -N \log \sigma_j - \frac{1}{2\sigma_j^2} M^{(k)}, \quad (6.22)$$

$$Q_2(\lambda_{ji}, \beta_{ji}, \hat{\eta}_j^{(k)}) = -\frac{1}{2} \log \det[\lambda_{ji} \bar{K}(\beta_{ji})] - \frac{1}{2} \text{tr}[(\lambda_{ji} \bar{K}(\beta_{ji}))^{-1} \hat{\Delta}_j^{(k)}[i]], \quad (6.23)$$

where $M^{(k)}$ is formulated as shown in (6.17).

It can be found that Q is decomposed into two parts, including Q_1 as a function of σ_j and Q_2 as a function of the parameters from the parameter prior. Thus, the optimization of Q can be solved by considering Q_1 and Q_2 independently. The constant term in (6.21) will be ignored because it does not influence the optimization result.

M-step: It can be found that (6.22) is maximized by (6.17) assuming that $M^{(k)} > 0$.

To maximize $Q_2(\lambda_{ji}, \beta_{ji}, \hat{\eta}_j^{(k)})$, set the derivative of (6.23) over λ_{ji} to be zero, which leads to the solution of λ_{ji} as

$$\lambda_{ji}^* = \frac{1}{n} \text{tr}[\bar{K}^{-1}(\beta_{ji}) \hat{\Delta}_j^{(k)}[i]], \quad (6.24)$$

which is a function of β_{ji} . Plugging (6.24) back into (6.23), one obtains that

$$Q_2(\lambda_{ji}^*, \beta_{ji}, \eta^{(k)}) = -\frac{n}{2} \log[\text{tr}(\bar{K}^{-1}(\beta_{ji}) \hat{\Delta}_j^{(k)}[i])] - \frac{1}{2} \log \det \bar{K}(\beta_{ji}) + \text{constant},$$

which can be maximized by minimizing (6.18). After having $\hat{\beta}_{ji}^{(k+1)}$, $\hat{\lambda}_{ji}^{(k+1)}$ can be found by (6.19). Thus, Q_1, Q_2 have been optimized independently and M-step is proved.

出其东门，有女如云。虽则如云，匪我思存。

诗经

*At the great gate to the East. Mix crowds. Be girls like clouds. Who cloud
not my thought in the least.*

Shijing; Translated by Ezra Pound

7

Topology identification of brain networks for detecting the Mozart effect

7.1 INTRODUCTION

While the topology identification approach developed in Chapter 6 estimates the network topology given a single data set, it is further extended in this chapter to consider a group of data sets. This extension is of practical importance since there can be multiple data sets from the subjects in experimental studies. More importantly, we will focus on applying the above method to a study on brain networks, in order to reveal the topological changes in brain networks after the subjects in the study listen to Mozart's music intensively.

In the last decade, the effects of music on the brain have been an active topic of research [24, 77, 173]. In particular, one piece of classical music, Mozart's Sonata K448, has been claimed to have unique effects on the brain, besides the general effects caused by listening to music. One of the original studies in [124] reported that listening to Mozart music increased spatial and temporal reasoning skills in healthy subjects, but this effect did not last beyond a 15-minute testing period. Moreover, a strong effect specific to Mozart music was unable to be replicated

The material of this chapter is based on [156]. This chapter is a joint work with other coauthors, and the contribution of the author of this thesis to this chapter is specified in Section 1.6.

in repeated studies [115]. In another study, neural activity was measured through the spectral analysis of electroencephalogram (EEG) data [161]. After listening to Mozart music, an increase in brain wave activity linked to memory, cognition, and problem solving was observed in adults.

Besides these effects, listening to Mozart music was reported as being effective as a medicine. First of all, the authors in [43] reported that the consistent exposure to Mozart music for 15 days caused a reduction in the frequency of epileptic seizures in children with epilepsy and in some cases led to a complete recession of seizures. Furthermore, the effects persisted even after the exposure to Mozart music was stopped. Another study [26] reported similar positive results in adults with epilepsy. Finally, in a study of the influence of Mozart music therapy on schizophrenia patients [175], Mozart music was found to have effects on the functional connectivity of patients, which was inferred from functional magnetic resonance imaging (fMRI) data.

However, no well-established theories exist on the neural dynamics in the brain that are responsible for the Mozart effect found in these studies. Moreover, research into the existence of a Mozart effect does not focus on inferring effective connectivity between brain networks from time series. Therefore, in this work, we will focus on methods that can infer how brain networks are connected and interact, using fMRI blood-oxygen-level-dependent (BOLD) time series that describe the dynamic neural activity of those brain networks.

The brain is a dynamic system; cognition and consciousness arise from not just the static correlations between brain networks, i.e. functional connectivity, but also through the dynamic behavior of the brain. Therefore, the inference of dynamic interactions of brain networks, i.e. effective connectivity, is an important aspect in the analysis of the brain as it reveals how brain networks dynamically influence each other. In this work, we focus on the inference of effective connectivity using resting-state fMRI BOLD measurements. We could infer connectivity directly from voxel BOLD measurements [17] or from the mean BOLD signals in brain networks defined by an atlas [129]. Instead, we will follow an approach that uses independent component analysis (ICA) [15, 72] to find active brain networks and their corresponding ICA time series. These ICA time series are then used as indications of the dynamic behavior of the brain regions [21, 49, 91, 125].

7.1.1 LITERATURE REVIEW OF RELATED ESTIMATION METHODS

By far the most popular method for the inference of effective connectivity is the Granger-causality analysis [61, 63]. While the method originated in the field of economics, it has been used in the past for the inference of brain connectivity using EEG [12] and fMRI data of the brain [21]. Its strength is the potential as an exploratory method to assess the effective connectivity between a large number of brain networks of interest, as effective connectivity can be assessed pairwise between brain networks. Despite the popularity of this method, it is not without flaws. Most importantly, care must be taken when performing the Granger-causality analysis on fMRI data, as the low sampling rate of fMRI measurements can make the method unreliable [136].

The dynamic causal modeling (DCM) [55] is a modeling approach designed to model neural activity [30] and effective connectivity using specialized state-space models. For example, in [94], excitatory and inhibitory states are used, which is in line with how populations of neurons function in the brain. DCM allows for much more biologically accurate modeling of the neural activity compared to Granger-causality analysis, but the estimation of an accurate DCM model can be computationally expensive and is often limited to modeling the interactions between a small number of brain networks. In addition, DCM typically requires prior knowledge regarding network connectivity, while this prior knowledge may not always be available [163]. For this reason, DCM is often not used as an exploratory method to assess effective connectivity and is thus also problematic for inferring the existence of a Mozart effect, as we do not have the prior knowledge about how and where the effective connectivity might be affected by listening to Mozart music.

The methods based on regularized regression [17, 165] penalize the model parameters of the connections in the effective connectivity and force a subset of parameters to zero, which leads to a sparse estimate of the effective connectivity. These methods estimate the effective connectivity of the complete brain networks, instead of the pairwise approach of the Granger-causality analysis. Although these methods scale very well with large dynamic networks, they often have many tuning parameters that must be carefully chosen to achieve a good estimate of the effective connectivity.

Furthermore, there exist non-parametric approaches, such as the method detailed in [96]. This method can potentially be used to estimate the effective connectivity pairwise between brain networks. It calculates a Wiener filter estimate of the dynamics of one connection to infer whether the connection exists in the dynamic network. The Wiener filter requires a lot of data to compute accurate estimates of effective connectivity. The Mozart study uses fMRI measurements and the data length is relatively short. Thus, it is unlikely that we will get good Wiener filter estimates given this short data length.

Finally, in this chapter we will consider the method in Chapter 6, which employs a Bayesian model selection approach to estimate the connectivity of a dynamic network. The main advantage of this approach is the ability to incorporate a prior probability distribution of the model, and thus the Bayesian method performs well even when not a lot of data is available. This is very useful in combination with fMRI data and the ICA procedure, where the data length is short. The Bayesian method uses a non-parametric model, and unlike the Wiener filter, it determines the effective connectivity of the complete network. By making use of Gaussian processes, the model order can be increased beyond what is possible with parametrized models, like those used by the Granger-causality analysis, without the risk of overfitting. This can lead to a more accurate estimate of effective connectivity.

7.1.2 CHAPTER STRUCTURE

Our first research question is to investigate whether Bayesian topology identification in Chapter 6 can be used as an alternative to the Granger-causality analysis for the inference of the effective connectivity using fMRI data. First, we investigate if there is a significant difference in the performances of the two methods in a simulation setup. Then since the Bayesian method was originally developed to infer the graph estimate of a single data set, we extend the Bayesian method such that we can draw conclusions on the connectivity of groups of data sets, which is beneficial in the inference of the Mozart effect.

After we extend the Bayesian approach, our second research question is to investigate the influence of listening to Mozart's Sonata K448 on effective connectivity through fMRI data of healthy adults. Both the Granger-causality analysis and the Bayesian approach are applied in the Mozart effect study to consolidate the findings. Here, we put more emphasis on the results obtained from the approach that performs better in the simulation study. Furthermore, we will investigate if the length of time that subjects listened to Mozart music leads to different conclusions on the effective connectivity.

This chapter is structured as follows: first, a model is introduced to describe the dynamic interactions between brain regions. Second, we describe the existing Granger-causality analysis and how we can infer connectivity using fMRI data. Third, we detail the Bayesian topology identification method and extend it such that it can infer effective connectivity changes between two groups of subjects. Then the performances of the Granger-causality analysis and the Bayesian method are compared using simulated data. Finally, we will apply the two methods to fMRI data and infer whether intensively listening to Mozart's Sonata K448 has an effect on the effective connectivity of the subjects in the study.

7.2 THEORY

To infer the brain effective connectivity using the fMRI measurements of the neurodynamics of the brain, we will first define a modeling framework wherein the dynamic interactions between brain networks can be modeled appropriately.

7.2.1 DYNAMIC NETWORK MODEL OF BRAIN NETWORK CONNECTIVITY

The effective connectivity between brain networks, using fMRI measurements to describe neural activity, can be described by linear models [136]. Furthermore, in general the causal relationship between two brain networks can be described by an infinite impulse response (IIR) filter, as long as the hemodynamics [109] can be considered as an invertible filter [136]. The neural activity of brain networks is described by L time series $w_j(t)$, $j = 1, \dots, L$, i.e. one ICA time series for each brain network found by an ICA decomposition of the fMRI measurements from

a subject. A brief introduction for the above ICA decomposition can be found in Section 7.3.2. Then the dynamic interactions between brain networks can be modeled as in Chapter 6:

$$\begin{aligned} w_j(t) &= \sum_{i \in \mathcal{I}} G_{ji}(q) w_i(t) + e_j(t), \quad j \in \mathcal{I}, \\ G_{ji}(q) &= \sum_{k=1}^{\infty} \theta_{ji,k} q^{-k}, \end{aligned} \quad (7.1)$$

where q is the shift operator, i.e. $q^{-1}w_j(t) = w_j(t-1)$, $\mathcal{I} = \{1, \dots, L\}$, $\theta_{ji,k}$ indicates one coefficient of $G_{ji}(q)$ and $e_j(t)$ denotes the background noise of brain network j . The full model is written in matrix form as:

$$w(t) = G(q)w(t) + e(t), \quad (7.2)$$

where $G(q)$ is an $L \times L$ matrix, and

$$\begin{aligned} w(t) &= [w_1(t), \dots, w_L(t)]^T, \\ e(t) &= [e_1(t), \dots, e_L(t)]^T. \end{aligned}$$

Note that $G(q)$ is not hollow here, and thus (7.2) actually corresponds to the predictor model in (6.6).

Some assumptions are made on the components of the model in (7.1):

1. $G_{ji}(q)$ is stable, i.e. $\sum_{k=1}^{\infty} |\theta_{ji,k}| < \infty$, for all j, i ;
2. $[I - G(q)]^{-1}$ is stable;
3. $e_j(t)$ is Gaussian distributed with zero mean and unknown variance σ_j^2 , and $e(t)$ has a diagonal covariance matrix.

Each IIR transfer operator $G_{ji}(q)$ can be approximated by a finite-order impulse response of order m , and the approximation is written as an autoregressive (AR) model of order m :

$$w_j(t) = \sum_{i=1}^L \sum_{k=1}^m w_i(t-k) \theta_{ji,k} + e_j(t),$$

and written in matrix form as in (6.9) for the measurements up to time N :

$$w_j^N = \sum_{i \in \mathcal{I}} A_{ji} \theta_{ji} + e_j^N. \quad (7.3)$$

The model (7.3) will be used in the inference of Granger-causality and furthermore, will form the modeling framework on which the Bayesian topology identification method relies.

7.2.2 DIRECTED GRAPH

We can also define a graphic representation of model (7.1) that encodes the effective connectivity between brain networks. Since (7.2) has a simpler model structure than the general model in (2.1) due to the absence of r signals and the simple noise model, the graphical representation can be defined in a simpler way.

A directed graph of model (7.1) is denoted as $\mathcal{G} = (\mathcal{V}, \mathcal{E})$, where $\mathcal{V} = \{w_1, \dots, w_L\}$ is the set of all nodes and \mathcal{E} is the set of all directed edges in the graph. Node $w_j \in \mathcal{V}$ in the graph represents a particular brain network, defined by the ICA procedure, and its dynamic behavior is described by the corresponding ICA times series $w_j(t)$. Thus the cardinality of \mathcal{V} equals the total number of ICA time series. A directed edge from w_i to w_j exists, denoted as $(i, j) \in \mathcal{E}$ or $(i, j) \in \mathcal{G}$, if and only if $G_{ji}(q)$ in (7.1), or θ_{ji} in (7.3) equivalently, is non-zero, which indicates a causal connection from node w_i to w_j . Note that the self loops of type (i, i) may be present in \mathcal{G} ; however, we do not show these edges explicitly in figures, as they do not contain information regarding interconnections among different brain networks.

In this chapter, we also denote the set of all incoming edges to w_j as \mathcal{N}_j or \mathcal{G}_j . Now, a graph \mathcal{G} indicates the effective connectivity between brain networks.

7.3 MATERIALS

7.3.1 SIMULATION DATA GENERATION

Before being applied to the fMRI data, which typically suffers from low sampling rates and measurement noises, the methods for the inference of effective connectivity should at least show a reasonable performance for the simulated data generated in an ideal setting, i.e. without the above complexities. Since the data generation model is known in simulation, the goal of the simulation study is to test how well the estimated connectivity of one method approximates the true connectivity.

In this work, in order to evaluate the relative performances of the Granger-causality analysis and the Bayesian topology identification, we test them in a controlled environment using the simulated data, which is generated by models as defined in (7.1). Since the model (7.1) in this chapter is the same as the model (6.1) in Chapter 6, we will use the same method as the one in Section 6.6 to generate random networks and the simulation data. In the data generation process, the node time series $w_j(t)$ are generated from a model (7.1), where some random directed edges are chosen to form the ground-truth connectivity \mathcal{G}_0 , and for each edge (i, j) which exists in \mathcal{G}_0 , its corresponding $G_{ji}(q)$ is a random transfer function such that the resulting dynamic network adheres to the IIR model assumptions. The noise $e_j(t)$ in (7.1) is randomly sampled from a Gaussian distribution for each node in the simulation model. More details of the data generation can be found in Section 6.6 and Section 7.4.3.

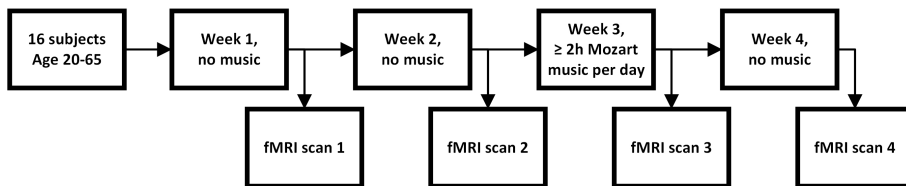


Figure 7.1: Flowchart of Mozart music experiment.

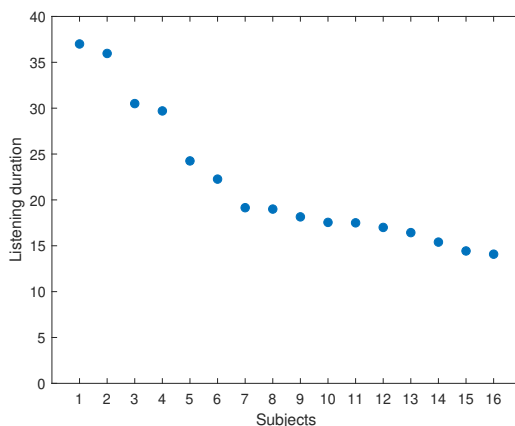


Figure 7.2: Listening duration in hours of all 16 subjects ordered from the longest to shortest listening duration.

7.3.2 MOZART EFFECT STUDY

Sixteen volunteers (11 females, 5 males) without a medical history of neurological or psychiatric diseases, aged 20-65 (mean 43.3), participated in the experiment. This number of subjects was chosen to be comparable with the one in [43]. To prevent bias, subjects with a variety of tastes in music were selected, and no subjects were selected who already consistently (2 hours or more per day) listened to Mozart music. Informed consent of the experiment and scans was obtained from each subject. The scanning of healthy volunteers was approved by the Medical Ethical Committee of the Academic Center for Epilepsy Kempenhaeghe (Heeze, The Netherlands).

MOZART'S SONATA K448 EXPERIMENT

Four resting-state fMRI scans were collected for each subject in the study, and the experimental procedure is summarized in Figure 7.1. Each of the four scans was taken one week apart in time. In the week between scans 1 and 2, subjects were instructed not to listen to Mozart's Sonata K448 for any amount of time. Then, the subjects were instructed to listen for a minimum of 14 hours to Mozart's Sonata K448 during the week between scans 2 and 3 and to listen for at least 2 hours each day unless this was not possible due to unavoidable circumstances. This listening

duration was chosen to be consistent with the duration in [43]. The listening duration of each subject during the week of music exposure was recorded by the subjects themselves. In Figure 7.2 we can see the spread of total listening duration across all 16 subjects. After the third scan subjects were once again instructed to stop listening to Mozart music, and then the final scan was taken one week after the subjects stopped listening to Mozart's Sonata K448. From the first scan to the fourth scan, subjects were also instructed to avoid listening to any other music, but limited exposure to music in public places could in some cases not be avoided. Other auditory stimuli, for example from entertainment on television or the internet, could also affect brain activity and bias the results. However, the first two scans establish a baseline of the regular brain activity and thus should rule out the effect of most regularly present auditory stimuli, when we compare the baseline activity to the brain activity after the subjects listened to Mozart music.

ACQUISITION

Imaging was performed using a 3T Philips Achieva MRI scanner. A T1-weighted reference scan was recorded using a 3D spoiled gradient-echo sequence (T1TFE), TR/TE: 8.3/3.5ms. The matrix size was $240 \times 240 \times 180$ with isotropic voxels of 1mm^3 . Total T1 scan duration was 600s. Second, a multi-echo time fMRI scan was recorded using a gradient-echo EPI sequence with TR/TE/ES: 2000/12/23ms. 26 slices with a width of 4.5mm (0mm gap) were recorded. The data were acquired with $3.5 \times 3.5\text{mm}$ in-plane resolution, final in-plane resolution was also $3.5 \times 3.5\text{mm}$ (64×64). SENSE [118] acceleration was used with SENSE factor of 2.7 in the read-out direction. The total multi-echo scan time was 608s.

During all the scans, the subjects were asked to remain still with their eyes open and to focus on a projected dark-blue cross. Physiology data (heart and respiratory rate) were recorded using a standard scanner setup.

PREPROCESSING

In preprocessing, the ICA decomposition [16] is an essential step and thus is first briefly explained here. The ICA decomposition is motivated by the hypothesis that a large amount of fMRI data is generated by fewer unmeasured and independent source signals. The goal of the ICA decomposition is to recover these unmeasured source signals from the fMRI data. Let X be a data matrix consisting of a single fMRI data set, i.e. $X = \begin{bmatrix} x_1 & \cdots & x_z \end{bmatrix}$, where

$$x_i = \begin{bmatrix} x_i(1) & \cdots & x_i(N) \end{bmatrix}^\top$$

contains the measurements of the i -th voxel in the fMRI scan. The ICA procedure assumes that the measured data matrix X can be represented by a matrix of ICA times series $W \in \mathbb{R}^{N \times L}$ with

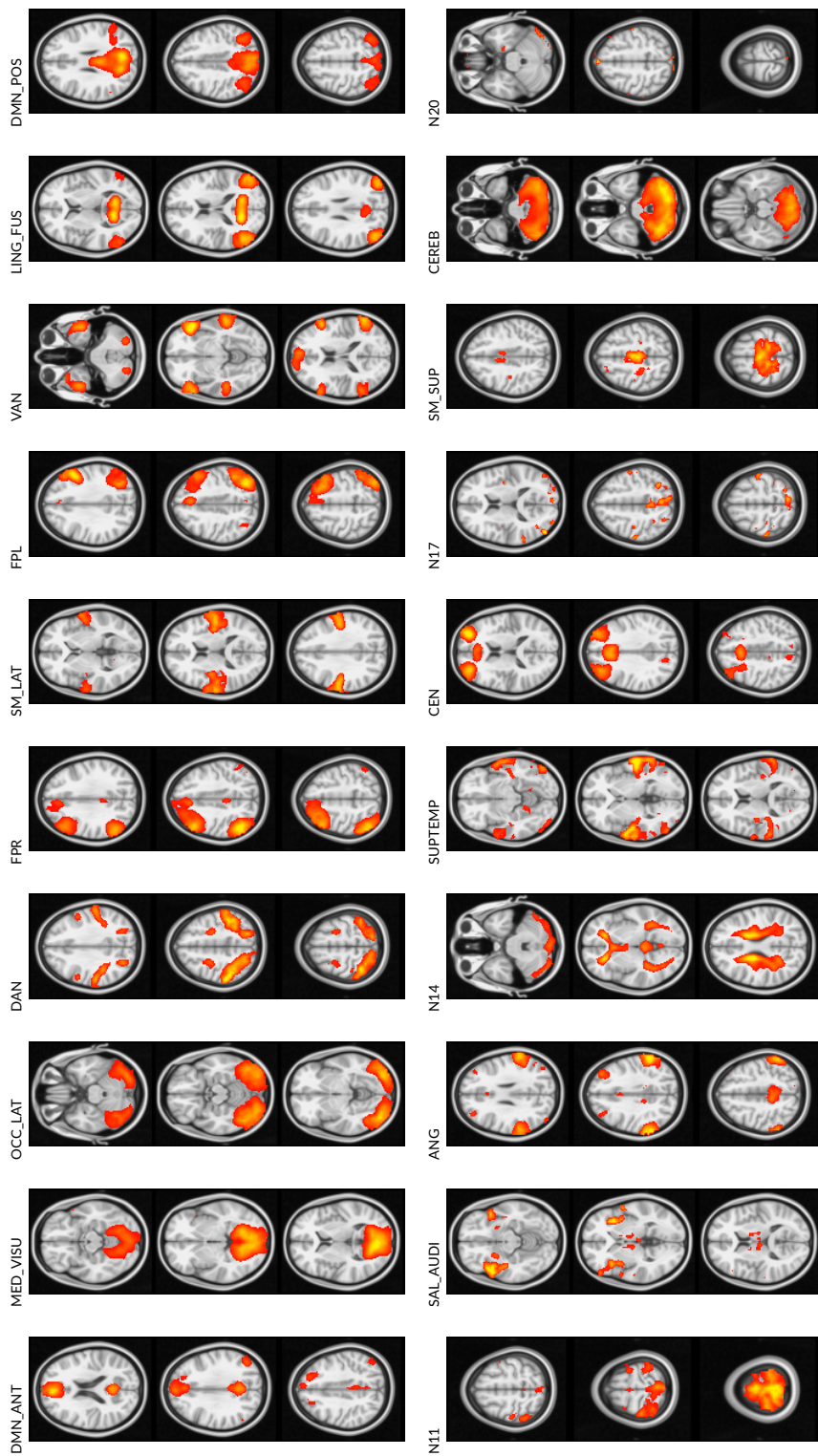


Figure 7.3: Spatial maps of the 20 active brain networks found through the ICA decomposition. Each image consists of 3 relevant horizontal slices of the brain, where the spatial map is indicated by the red color scale.

L components and $L < z$, a matrix of spatial processes S and a matrix of noise processes E :

$$X = WS + E, \quad (7.4)$$

where the j -th column of W contains the ICA time series $w_j(t)$ from time 1 to N , and the j -th row of S represents the spatial map, i.e. the voxels in the fMRI scan, that corresponds to $w_j(t)$. Under the assumption that the rows of S are statistically independent, the ICA aims to estimate W and S given the measured X , and the uniqueness of W and S can be guaranteed by some additional assumptions on (7.4) [16]. The j -th column of the estimated W leads to the ICA time series $w_j(t)$ used in model (7.3), and the significant entries in the j -th row of S show the spatial map, i.e. the voxels, corresponding to $w_j(t)$.

In this study, non-BOLD signals of the fMRI data caused by physiological effects such as movement, breathing, and pulse were first removed by multi-echo ICA [80]. Then, using FM-RIB Software Library [15] (v5.0, <https://fsl.fmrib.ox.ac.uk/fsl/fslwiki/>), all 64 data sets were temporally concatenated and a group ICA was performed to identify 20 ICA time series and the corresponding 20 independent spatial maps. The spatial maps are listed in Table 7.1 and are also visualized in Figure 7.3. Next, dual regression [15] was performed to obtain individual spatial maps and time series for each fMRI scan of the subjects, where each ICA time series consists of $N = 300$ data points.

Table 7.1: List of all brain networks found in the group ICA decomposition.

#	Shorthand	Description
1	DMN_ANT	default mode network, anterior
2	MED_VISU	medial visual cortex
3	OCC_LAT	occipetal & lateral visual cortex
4	DAN	dorsal attention network
5	FPR	fronto-parietal right network
6	SM_LAT	sensori-motor, lateral network
7	FPL	fronto-parietal left network
8	VAN	ventral attention network
9	LING_FUS	lingual fusiform cortex
10	DMN_POS	default mode network, posterior
11	N11	noise
12	SAL_AUDI	salience auditory network
13	ANG	angular gyrus
14	N14	White matter
15	SUPTEMP	superior temporal gyrus
16	CEN	central executive network
17	N17	noise
18	SM_SUP	sensori motor medial superior
19	CEREB	cerebellum
20	N20	borders and movements

7.4 METHODS

This section is divided into two parts. In the first part, we briefly discuss both the Granger-causality analysis and the Bayesian topology identification from Chapter 6. Next, we detail how we apply both methods to the simulation data. Then the Bayesian method is extended to incorporate multiple data sets. In the second part, we first validate the use of AR models to model the ICA time series. Then we will apply the extended Bayesian topology identification and the Granger-causality analysis to the ICA time series of the Mozart effect study.

7.4.1 GRANGER-CAUSALITY ANALYSIS

Here we briefly describe the well-established Granger-causality analysis, which will be used as a reference to compare with the Bayesian topology identification. The Granger-causality analysis is based on the concept that if θ_{ji} in (7.3) is significantly non-zero for given j and i , then setting parameter vector θ_{ji} to 0 will significantly increase the size of the residual $e_j(t)$, where with some abuse of notation, $e_j(t)$ represents both the white noise in (7.3) and the residual signal of the model (7.3). To relate this change in the residual to a real connection between two brain networks and not from a shared influence from other regions, we will infer connectivity only using the conditional Granger-causality analysis.

The existence of a connection (i, j) is inferred by fitting two different AR models to the measurement data and comparing the residuals. The first AR model includes all L node time series in the regression as in (7.3). In the second AR model, A_{ji} corresponding to connection (i, j) is excluded:

$$w_j^N = \sum_{k \in \mathcal{T} \setminus i} A_{jk} \cdot \theta_{jk} + \bar{e}_j^N, \quad (7.5)$$

where \bar{e}_j^N denotes the residual vector of the above model. The model order m , i.e. the length of parameter vectors θ_{ji} , is selected by AIC [4] to model the data without overfitting, as overfitting can make the Granger-causality analysis unreliable [11].

Then the Granger-value \mathcal{F}_{ji} corresponding to connection (i, j) is defined as the logarithm of the ratio of the residuals' variances:

$$\mathcal{F}_{ji} = \log \frac{\text{var}[\bar{e}_j(t)]}{\text{var}[e_j(t)]}, \quad (7.6)$$

where $\bar{e}_j(t)$ and $e_j(t)$ denote the residual signals in (7.5) and (7.3) respectively, with some abuse of notation. The Granger-value \mathcal{F}_{ji} is the degree to which the addition of connection (i, j) helps predict w_j and as such, a significantly non-zero \mathcal{F}_{ji} indicates the existence of connection (i, j) . Furthermore, \mathcal{F}_{ji} asymptotically follows a χ^2 distribution as data length $N \rightarrow \infty$, and thus we can perform a statistical test to infer if \mathcal{F}_{ji} is significantly non-zero [11]. Furthermore, the Granger-value is equivalent to the transfer entropy [10, 74, 134], a measurement of the rate of

information transfer between two time series. As such, \mathcal{F}_{ji} can be interpreted as a measurement of the connectivity strength. Therefore, a change in the Granger-value of a connection between two fMRI scans of a subject indicates a difference in the connectivity strength of that connection, and we can use a paired t-test to test for differences in connectivity strength between two fMRI scans.

For the simulation study, since the effective connectivity of the data-generation systems is known, our goal is to quantify the quality of \mathcal{F}_{ji} as a measurement of connectivity. To be able to compare the quality of the estimates of both methods on simulated data, we will use an F-test to determine a graph estimate, because the Bayesian method also infers a graph estimate, and the paired t-test cannot lead to a graph estimate. Even though we consider the paired t-test on the experimental data instead of the F-test, the F-test in the simulation study still gives us an indication of the reliability of \mathcal{F}_{ji} as a measurement of connectivity. As such, we will infer an estimate $\hat{\mathcal{G}}$ of the ground truth connectivity \mathcal{G}_0 by testing the significance of \mathcal{F}_{ji} for all connections (i, j) and adding the connection to $\hat{\mathcal{G}}$ if the statistical test is significant. To calculate the reduced regression in (7.5), the Granger-values in (7.6) and the significance of the Granger-values, we will use the MVGC MATLAB toolbox [11] (version 1.0, <https://users.sussex.ac.uk/~lionelb/MVGC/>).

7.4.2 BAYESIAN TOPOLOGY IDENTIFICATION

The Bayesian method in Chapter 6 is a machine learning method that infers from node time series data $D = \{w_1(1), \dots, w_1(N), \dots, w_L(N)\}$ an estimate $\hat{\mathcal{G}}$ of \mathcal{G}_0 , the connectivity of the dynamic network. As shown in (6.5), this method aims to find the graph estimate $\hat{\mathcal{G}}$ that maximizes the following marginal likelihood:

$$p(D|\mathcal{G}) = \int p(D|\theta, \mathcal{G})p(\theta|\mathcal{G})d\theta, \quad (7.7)$$

where $p(D|\theta, \mathcal{G})$ is the likelihood under model parameters θ and a graph \mathcal{G} , and $p(\theta|\mathcal{G})$ is the prior distribution of θ given \mathcal{G} .

In the context of this study, the parameter θ in the parameter prior $p(\theta|\mathcal{G})$ contains the set of all θ_{ji} of an AR model as defined in (7.3), where the parameter vectors θ_{ji} are modeled as Gaussian random vectors. The covariance matrices of these random vectors are parametrized with some hyperparameters, which encode the assumption of stability. The hyperparameters of random parameter vectors θ_{ji} and the variance σ_j^2 of e_j are estimated using the EM algorithm [23] in Chapter 6. Because the θ_{ji} s are modeled as random vectors, we can simply set model order m in (7.3) to some large number at most equal to the data length N , instead of determining an optimal model order, as the estimated hyperparameters will determine the relevance of each of the m parameters.

Now, under the assumption of Gaussian distributed noise, $p(D|\theta, \mathcal{G})$ can be computed based

on (7.3):

$$p(D|\theta, \mathcal{G}) = \prod_{j=1}^L \mathcal{N} \left(\sum_{i \in C} A_{ji} \theta_{ji}, \sigma_j^2 I_N \right),$$

where $C = \{k|(k, j) \in \mathcal{G}\}$. Given this parametrization, the integral in (7.7) has a closed form solution as shown in Chapter 6, and thus we can avoid a numerical integration, which could be computationally costly.

The graph \mathcal{G} with the maximum marginal likelihood $p(D|\mathcal{G})$ is chosen as the connectivity estimate $\hat{\mathcal{G}}$. This maximum can be found by comparison of the marginal likelihoods of all possible graphs. To avoid the combinatorial problem of comparing all possible graphs, a greedy search algorithm is employed that efficiently finds a graph estimate $\hat{\mathcal{G}}$, as shown in Chapter 6.

To perform the Bayesian topology identification, the implementation from Chapter 6 is used (version 1.0, <https://codeocean.com/capsule/3224411/tree/v1>).

7.4.3 EVALUATION OF METHODS IN SIMULATION

To motivate the use of the Bayesian topology identification for the inference of brain network connectivity, we will evaluate whether the Bayesian approach has any advantages over Granger-causality analysis in the estimation of the connectivity using simulation data. Recall that the true effective connectivity of the simulation model \mathcal{G}_0 is known. The graph estimates $\hat{\mathcal{G}}$ of both methods are compared to \mathcal{G}_0 and the quality of the estimate is quantified using the TPR and the FPR:

$$\begin{aligned} \text{TPR} &= \text{TP} / \text{P}, \\ \text{FPR} &= \text{FP} / \text{Z}, \end{aligned} \tag{7.8}$$

where recall from Chapter 6 that the TPR is the number of edges in $\hat{\mathcal{G}}$ that also exist in \mathcal{G}_0 , denoted as TP, over the total number of edges in \mathcal{G}_0 , denoted as P. The FPR is the number of edges in $\hat{\mathcal{G}}$ that do not exist in \mathcal{G}_0 , denoted as FP, divided by the total number of edges that do not exist in \mathcal{G}_0 , denoted as Z. To avoid uncertainties in the conclusion on the relative performance of the two methods given certain design parameters for the simulation, i.e. a particular data length N and certain network size in terms of number of nodes, 50 random simulation models with random \mathcal{G}_0 are generated, and then TPR and FPR are calculated by averaging the results of the 50 estimates. The random simulation models are generated by selecting random parameters for each transfer for which the connection exists in \mathcal{G}_0 , such that the transfer is stable. This process is repeated until $(I - G(q))^{-1}$ is stable according to our modeling assumptions in (7.2).

The design parameters for the simulation are chosen as follows. First, to test how the performances of both methods vary with the data length, we consider three different data lengths with $N \in \{50, 300, 2000\}$ for six-node dynamic networks. Second, to evaluate how the number of nodes in the network affects the estimation performance, we compare the TPR and FPR of the methods between six and twelve node networks, with $N = 2000$. Third, for each of the pre-

vious evaluations, we will assess the performance of the Granger-causality analysis over a range of thresholds, determined by a range of significance levels $\alpha \in \{0.005, 0.05, \dots, 0.95\}$ of the F-test, which are corrected for multiple comparisons using the false discovery rate (FDR) correction [70] in the MVGC MATLAB toolbox. This latter evaluation is performed to rule out the differences in the performance of the methods caused by a specific choice of significance threshold. Note that the Bayesian method requires no tuning threshold, and thus no such variation in threshold is needed. Finally, as mentioned in Section 7.4.2, the model order m of the Bayesian method should be chosen to be some large number at most N . In practice we set it to $m \in \{50, 100, 100\}$ for $N \in \{50, 300, 2000\}$ respectively, as higher m does not visibly increase performance.

7.4.4 BAYESIAN GROUP HYPOTHESIS TEST

The Bayesian topology identification method is designed to obtain a graph estimate of the effective connectivity from a single fMRI scan, which can be used in simulation to compare with the true connectivity. However, it is not directly applicable to the Mozart effect study using multiple data sets from groups of subjects. In the Mozart effect study, there are 4 groups of data sets from the subjects, where each group refers to one of the four scans in the four consecutive weeks. To investigate the Mozart effect, we want to infer how the overall brain network connectivity of the subjects changes over the weeks. Using the Bayesian method, changes in effective connectivity can be measured through a change in the presence of a connection in the graphs of the subjects. For a group of subjects, we define for each connection separately the following hypotheses:

\mathcal{H}_1 : Connection (i, j) is present in the group.

\mathcal{H}_0 : Connection (i, j) is absent in the group.

To infer if changes in the overall brain network connectivity occurred over the four weeks, we first find the most likely hypothesis for each week separately. If the hypotheses change between the weekly scans, this indicates an overall change in the effective connectivity of this connection.

The procedure is summarized in Figure 7.4, and to find the more likely hypothesis for one group (one scan as in Figure 7.1), the preliminary step is to compute the Bayesian selection frequency of every connection, i.e. the number of subjects whose graph estimates include this connection. It will first allow us to choose a small number of connections that are potentially of interest, which is useful because the analysis of all the 380 possible connections in the Mozart study can require weeks or months to complete, while many of those connections are actually not be of interest. For a given group, if the selection frequency of one connection is close to 0, we expect that the most likely hypothesis for this connection to be \mathcal{H}_0 , i.e., this connection is absent in the effective connectivity of all the subjects. However, if the selection frequency is close to 16, i.e. the connection is present in almost all the subjects, we expect that the most likely hypothesis

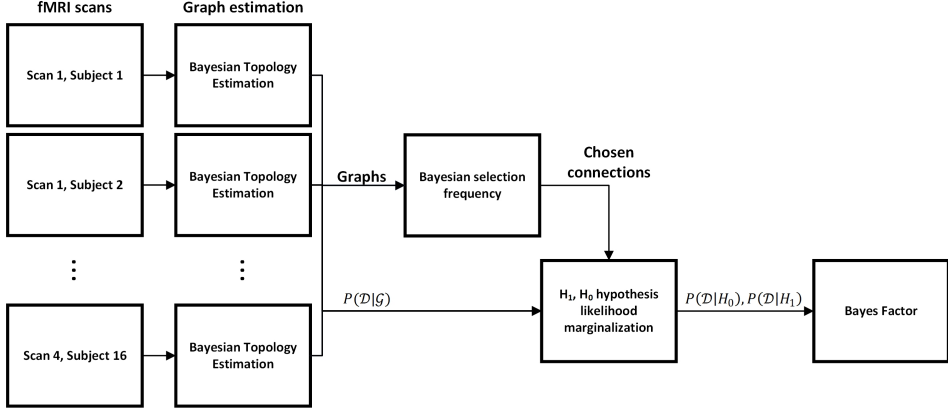


Figure 7.4: In this figure the procedure of the extended Bayesian method is summarized.

will be \mathcal{H}_1 . The Bayesian selection frequency can be easily reported for every connection from the graph estimates of each subject over the four weeks.

To evaluate which of the two hypotheses is actually more likely than the other for a given connection in one week, we will calculate the likelihood of the two hypotheses:

$$\begin{aligned}
 p(\mathcal{D}|\mathcal{H}_1) &= \prod_{k \in S} p(D^k|(i,j)), \\
 p(\mathcal{D}|\mathcal{H}_0) &= \prod_{k \in S} p(D^k|\neg(i,j)),
 \end{aligned} \tag{7.9}$$

where with some abuse of notation (i,j) indicates the existence of the connection, D^k indicates the data from subject k , S is the index set of all subjects and \mathcal{D} is defined as the collection of data D^k from each subject in the group. The likelihoods $p(D^k|(i,j))$, $p(D^k|\neg(i,j))$ in (7.9) of each subject are not yet known and must be calculated from the marginal likelihood in (7.7), which is calculated by the Bayesian method. The likelihoods in (7.9) can be calculated through the marginalization of $p(D|\mathcal{G})$ over all graphs for which the hypothesis is true. As an example we use hypothesis \mathcal{H}_1 here, but the calculation is similar for \mathcal{H}_0 :

$$p(D^k|(i,j)) = \sum_{\mathcal{G} \in \mathcal{P}_1} p(\mathcal{G})p(D^k|\mathcal{G}), \tag{7.10}$$

where

$$\begin{aligned}
 \mathcal{P}_1 &= \{\mathcal{G} | (i,j) \in \mathcal{G}\}, \\
 \mathcal{P}_0 &= \{\mathcal{G} | (i,j) \notin \mathcal{G}\}.
 \end{aligned} \tag{7.11}$$

This marginalization over graphs can be seen as averaging out the effects that other connections have on the likelihood of the connection in the hypothesis. The calculation of $p(D^k|(i,j))$ in (7.10) can be further simplified. The simplification of the marginalization is detailed in Sec-

tion 7.8.1.

Then we can calculate the hypothesis likelihoods in (7.9) and find the optimal hypothesis by comparison of the likelihoods of the two hypotheses:

$$\text{BF} = 2 \log \frac{p(\mathcal{D}|\mathcal{H}_1)}{p(\mathcal{D}|\mathcal{H}_0)}. \quad (7.12)$$

This log-likelihood ratio is the Bayes factor (BF) [75], which represents the strength of evidence of one hypothesis against the other and can also be interpreted as the evidence of the edge (i, j) in the data set. In [75], a scale for BF is proposed, which we will use to interpret the size of the Bayes factor. If BF is larger than 0, the optimal hypothesis is \mathcal{H}_1 , and thus connection (i, j) is likely to be present in the group. If BF is smaller than 0, the alternative hypothesis \mathcal{H}_0 is more likely, and thus the connection is likely to be absent in the group.

7.4.5 VALIDATION OF ICA TIME SERIES AR MODELS

Both the Granger-causality analysis and the Bayesian method rely on the assumption that the data is approximately generated by an AR model as defined in (7.3). If the dynamics of the ICA time series cannot be modeled by the AR model sufficiently well, the two methods become less reliable for the inference of brain network connectivity. To assess the goodness of the model fit, we estimate an AR model using all the 20 ICA time series from one fMRI scan for each of the 64 scans in the study. The model parameters are calculated using ordinary least squares. Then, we perform a whiteness (auto-correlation) test [90] of the residuals of each VAR model, to test whether the AR models can sufficiently model the dynamics in the ICA time series. For model order $m = 3$, 96.5% of the AR model residuals are white, which increases to 99.4% for $m = 5$. Therefore, the results of the tests are satisfactory.

7.4.6 INFERENCE OF THE EXISTENCE OF A MOZART EFFECT

In our search for a Mozart effect, we will first choose connections with potential effects using the Bayesian selection frequency. Then we will apply the extended Bayesian method and the Granger-causality analysis to the ICA time series of the chosen connections. Based on other studies of the Mozart effect [26, 124, 161, 175], we hypothesize that there will be changes in the connections of effective connectivity related to cognitive processing. Furthermore, due to the exposure of the subjects to music, we expect to find changes in connectivity between brain networks involved in auditory processing and possibly motor regions.

In the Mozart effect study, the scans in weeks 1 and 2 are used to infer the natural variability in the brain network connectivity of the subjects. If a connection has a low variability in effective connectivity in these weeks, it is more likely that any change in the connectivity of subjects between week 2 and week 3 is due to listening to Mozart music. Finally, for the connections

of which the connectivity change between weeks 2 and 3, we can compare their connectivity of weeks 3 and 4 to see if the effect lasts even into week 4 or if it was only of short duration.

Given the criteria described above, we illustrate for each method when a change in effective connectivity is considered to take place as a result of listening to Mozart music. For the Bayesian hypothesis test, we determine the optimal hypothesis for each week, and a change in connectivity is indicated if the optimal hypotheses over the four weeks have the following feature. For weeks 1 and 2, the optimal hypotheses should be the same for both weeks. Then in week 3, the optimal hypothesis should be the opposite of weeks 1 and 2. The optimal hypothesis in week 4 indicates whether the change between weeks 2 and 3 lasts into week 4. Finally, for the Granger-causality analysis and if there is a change in the effective connectivity of one connection, a significant difference in Granger-values of the connection should only be found between weeks 2 and 3, and possibly between weeks 3 and 4, depending on if the change lasts into week 4.

7.4.7 INFERENCE BASED ON LISTENING DURATION

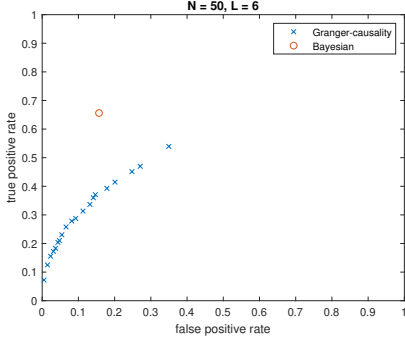
We will perform one more analysis of the data, by dividing the subjects' weekly scans into two subgroups based on their listening duration of Mozart music between weeks 2 and 3. We rank the subjects based on listening time and choose the 8 longest listeners as the first subgroup, and the remaining 8 subjects form the second subgroup. The first subgroup of longer listeners listened for $27:14 \pm 7:07$ hours on average to Mozart music and the second subgroup $16:19 \pm 1:31$ hours on average. We perform both the Bayesian hypothesis test and the paired t-test of the Granger-values for both subgroups to assess if effects are influenced by the listening duration of the subjects.

7.4.8 DATA AND CODE AVAILABILITY

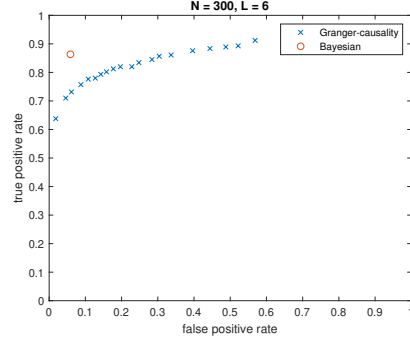
The data supporting the findings of this study can be made available upon request, with a formal data-sharing agreement. The developed code and the simulation data of this study have been made available online [155].

7.5 RESULTS

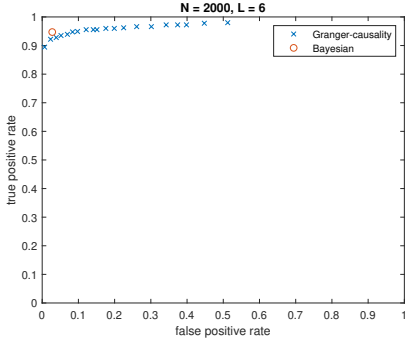
In this section, we first evaluate the performance of the Bayesian topology identification against Granger-causality analysis on simulation data. Then we apply both methods to the Mozart music ICA time series to infer changes in connectivity caused by listening to Mozart music. Finally, we apply our methods on two subgroups of 8 subjects, divided based on listening duration, to assess if listening duration affects the possible detection of effects.



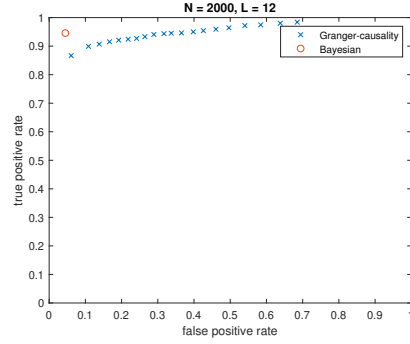
(a) TPR vs FPR for $\alpha \in \{0.005, 0.05, \dots, 0.95\}$, $N = 50$ and $L = 6$.



(b) TPR vs FPR for $\alpha \in \{0.005, 0.05, \dots, 0.95\}$, $N = 300$ and $L = 6$.



(c) TPR vs FPR for $\alpha \in \{0.005, 0.05, \dots, 0.95\}$, $N = 2000$ and $L = 6$.



(d) TPR vs FPR for $\alpha \in \{0.005, 0.05, \dots, 0.95\}$, $N = 2000$ and $L = 12$.

Figure 7.5: Average FPR vs TPR of the Bayesian method and Granger-causality analysis over 50 Monte Carlo experiments. One blue cross indicates the TPR and FPR of the Granger-causality analysis for a given threshold α . As α increases, the TPR and FPR of the Granger-causality analysis increases. The TPR and FPR of the Bayesian topology identification is indicated with a red circle. Only a single circle exists in each figure as the Bayesian method does not rely on a threshold to determine the graph estimate.

7.5.1 EVALUATION OF METHODS IN SIMULATION

The optimal performance in Figures 7.5a-d is when $\text{TPR} = 1$ and $\text{FPR} = 0$, which implies $\hat{\mathcal{G}} = \mathcal{G}_0$. The closer a (FPR,TPR) point to (0,1) the better the performance of the method. In Figures 7.5a-c, we see that the performance of the Bayesian method improves as the data length increases. Note that the Bayesian method does not rely on thresholding, unlike the Granger method. We can also observe that the performance of the Granger method improves as the data length increases, where the optimal significance threshold differs over different data lengths. Finally, it is clearly visible that in Figures 7.5a-7.5c, the (FPR,TPR) of the Bayesian approach is always closer to the optimal point than the Granger method.

From Figures 7.5a-c, we notice that the Bayesian method outperforms the Granger-causality analysis for all three data lengths over all different thresholds. From Figures 7.5c to 7.5d, there is barely any change in performance for the Bayesian method when the number of nodes in the

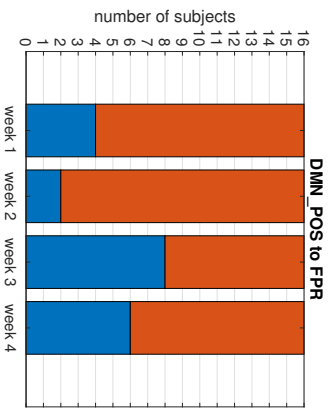
dynamic network is increased, as the TPR stays the same and the FPR becomes only slightly larger. However, for the Granger-causality analysis, the TPR of almost all thresholds decreases. Furthermore, we also notice a clear increase in the FPR of the Granger-causality analysis for all thresholds. Lastly, one more important detail is that in 7.5a-c for the Granger-causality analysis, the optimal performance for each of the figures does not belong to the same threshold, instead, it depends on the data length N . But based on the change in performance for each threshold as N becomes large, it appears the 5% threshold will be the optimal threshold for large N .

7.5.2 INFERENCE OF THE MOZART EFFECT

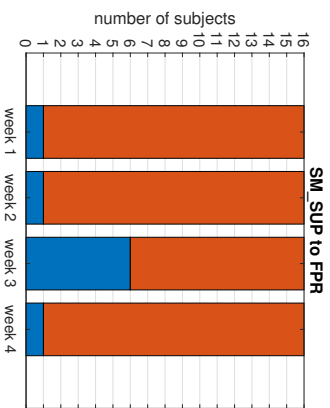
From the initial search for the Mozart effect using the Bayesian selection frequency of the connections over the four weeks, we have chosen six connections, whose selection frequencies indicate that there might be a change in the optimal hypothesis of these connections between weeks 2 and 3, i.e. before and after the subjects listened to Mozart music. The Bayesian selection frequencies of these connections are reported in Figure 7.6.

In Figure 7.6a and 7.6b, we find two connections inbound to the fronto-parietal right network, and in Figure 7.6f, we see the connection from the anterior default mode network to the dorsal attention network. These connections are of interest because the default mode networks and the fronto-parietal right network are involved in cognitive processing [93, 119]. In Figure 7.6c, we see the selection frequency of a connection that involves the central executive network, which is also related to cognitive processing [101]. Then in Figure 7.6d, we show the selection frequency of the connection from the sensori-motor, lateral network to the superior temporal gyrus. Figure 7.6d is of special interest because first of all, it has the largest selection frequency in week 3 among all the connections, with 12 out of 16 subjects showing positive evidence of this connection. Furthermore, it has a relatively small drop in selection frequency in week 4 relative to week 3. Both of the brain networks involved in this connection are involved in auditory processing in the brain [32, 77]. Finally, in Figure 7.6e, we show a connection from the dorsal attention network to the angular gyrus. This connection is of interest because large selection frequencies are detected in weeks 1 and 2 with low variability over these two weeks, which then almost completely disappears in week 3 and does not increase in week 4. This could indicate that effective connectivity of connections can decrease as a result of listening to Mozart music. In summary, through our analysis of the selection frequency, we have found a small number of connections that show potential Mozart effects. However, while we see some changes in the selection frequencies between weeks 2 and 3, the effects are far from universal across all subjects.

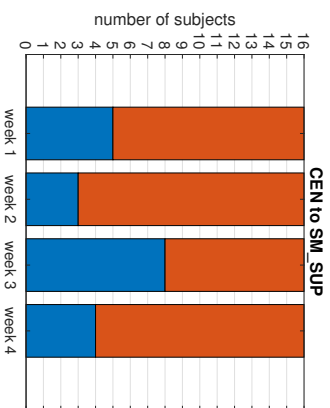
Then for each week, we assess the optimal group hypothesis of the six connections in Figure 7.6. In Table 7.2, we report the optimal hypothesis and the associated Bayes Factor of each connection for each week. Consider the connection from the posterior default mode network to the fronto-parietal right network and the connection from the central executive network to the sensori-motor superior network. For these two connections, the optimal hypotheses in weeks 1



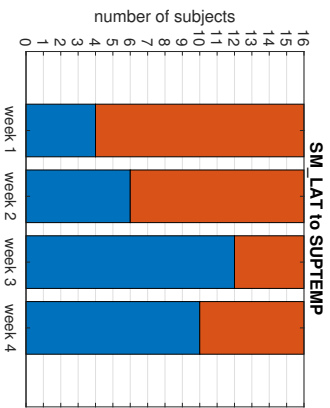
(a) Connection from the posterior default mode network to the fronto-parietal right network.



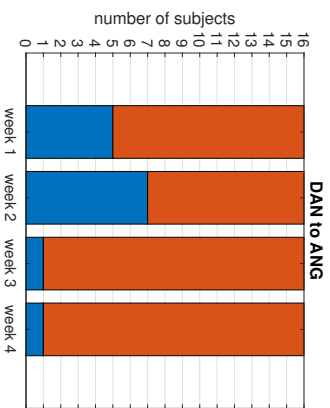
(b) Connection from the sensori-motor superior network to the fronto-parietal right network.



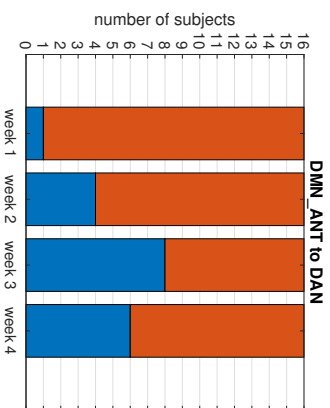
(c) Connection from the central executive network to the sensori-motor superior network.



(d) Connection from the lateral sensori-motor network to the superior temporal gyrus.



(e) Connection from the dorsal attention network to the angular gyrus.



(f) Connection from the anterior default mode network to the dorsal attention network.

Figure 7.6: Selection frequencies of six connections with possible effects of interest. Here, red indicates the number of subjects that did not have the connection in that week, and blue indicates the number of subjects that did have the connection.

Connections	week 1		week 2		week 3		week 4	
	\mathcal{H}_{opt}	BF	\mathcal{H}_{opt}	BF	\mathcal{H}_{opt}	BF	\mathcal{H}_{opt}	BF
DMN_ANT to DAN	\mathcal{H}_0	-40.08	\mathcal{H}_0	-33.62	\mathcal{H}_0	-7.305	\mathcal{H}_0	-29.65
DMN_POS to FPR	\mathcal{H}_0	-41.26	\mathcal{H}_0	-44.80	\mathcal{H}_1	1.890	\mathcal{H}_0	-45.07
CEN to SM_SUP	\mathcal{H}_0	-38.88	\mathcal{H}_0	-47.75	\mathcal{H}_1	8.266	\mathcal{H}_0	-27.03
SM_LAT to SUPTEMP	\mathcal{H}_0	-20.78	\mathcal{H}_1	37.46	\mathcal{H}_1	237.7	\mathcal{H}_1	72.34
DAN to ANG	\mathcal{H}_0	-24.73	\mathcal{H}_0	-39.28	\mathcal{H}_0	-109.5	\mathcal{H}_0	-74.87
SM_SUP to FPR	\mathcal{H}_0	-53.55	\mathcal{H}_0	-70.83	\mathcal{H}_0	-53.21	\mathcal{H}_0	-86.71

Table 7.2: Results of the extended Bayesian method on the ICA time series in the Mozart effect study. The results are summarized for each of the four weeks, where we indicate for each week the optimal hypothesis and the Bayes factor (BF).

Connections	week 1		week 2		week 3		week 4	
	\mathcal{H}_{opt}	BF	\mathcal{H}_{opt}	BF	\mathcal{H}_{opt}	BF	\mathcal{H}_{opt}	BF
DMN_ANT to DAN	\mathcal{H}_0	-15.09	\mathcal{H}_0	-25.46	\mathcal{H}_1	2.43	\mathcal{H}_0	-28.49
DMN_POS to FPR	\mathcal{H}_0	-21.37	\mathcal{H}_0	-56.62	\mathcal{H}_1	13.77	\mathcal{H}_0	-10.76

Table 7.3: Results of the inference based on the listening duration of subjects from the Bayesian method. The results are summarized for the four weeks, where we show the optimal hypothesis and the Bayes factor (BF) of each week. Only two connections are shown here, and both of them only show a change for the subgroup with the longer listening duration. The evidence and optimal hypotheses of the shorter listening subgroup is not shown as they show no effects of interest.

and 2 are \mathcal{H}_0 , and the optimal hypothesis in week 3 becomes \mathcal{H}_1 , indicating a change in effective connectivity of these connections after the subjects listened to Mozart music. Furthermore, in both connections, the change did not last into week 4, as the optimal hypothesis is once again \mathcal{H}_0 . The brain networks involved in the above two connections, which undergo potential changes after listening to Mozart music, have been visualized in Figure 7.7.

Next, we note in Table 7.2 that the connection from the sensori motor lateral network to the superior temporal gyrus shows strong evidence in favor of \mathcal{H}_1 in week 3, however, the optimal hypotheses in weeks 1 and 2 change from \mathcal{H}_0 to \mathcal{H}_1 . Therefore, we conclude that the natural variability of this connection before listening to Mozart music is too large to detect any change in effective connectivity caused by the Mozart music. Finally, for the other three connections, the optimal hypotheses for both weeks 1 and 2 do not change, but there is also no change in optimal hypotheses between weeks 2 and 3, which implies that there is no significant change in the effective connectivity of the connections for the 16 subjects.

Finally, for all the six connections in Figure 7.6, no significant difference is found in Granger-values between weeks 1 and 2. Then the Granger-values of weeks 2 and 3 are compared, and the significance of the paired t-test is found only for the connection from the anterior default mode network to the dorsal attention network with $p = 0.035$. In addition, for this connection, no significant difference of the Granger values between weeks 3 and 4 is found, indicating that the effective connectivity change persists into week 4.

INFERENCE BASED ON LISTENING DURATION

In our final test, the subjects are divided into two subgroups of 8 subjects. The subjects in group 1 listened for $27:14 \pm 7:07$ hours on average to Mozart music between weeks 2 and 3, and the subjects in group 2 listened for $16:19 \pm 1:31$ hours on average to Mozart music. Both the Bayesian approach and the Granger-causality analysis are applied to the new subgroups.

Using the Bayesian hypothesis test on both subgroups, we find two connections that show a change only for the subgroup with the longer listening duration. These two connections are presented in Table 7.3. We only show the BF and optimal hypotheses for the subgroup with the longer listening duration, as no change in optimal hypotheses is found between weeks 2 and 3 for the subgroup with the shorter listening duration. The other connections, which are previously selected in Figure 7.6, are not favored by one of the subgroups and are therefore also not presented here.

The first connection in Table 7.3, from the anterior default mode network to the dorsal attention network, shows no change in optimal hypotheses between weeks 2 and 3 for the complete group of 16 subjects; however, it shows positive evidence in favor of \mathcal{H}_1 in week 3 for the subgroup of longer listeners. As such, there is a change in optimal hypotheses between weeks 2 and 3 for the longer listening subgroup. The change in optimal hypotheses between weeks 2 and 3 does not last in week 4, which implies that this effect is of short duration. The second connec-

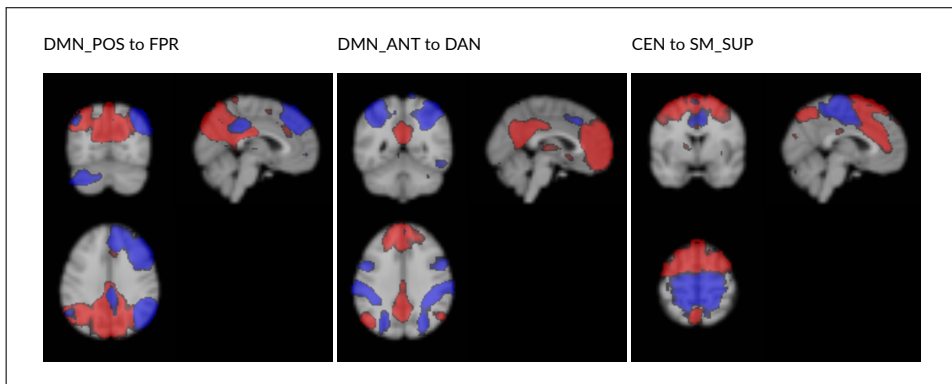


Figure 7.7: Brain networks in which the connections which were found to have the strongest evidence of a change in effective connectivity after subjects (full group or long listening subgroup) listened to Mozart music (see row 1-3 in Table 7.2 and in Table 7.3; Figure 7.6a, 7.6c and 7.6f). Here, the direction of the connection is from the red network to the blue network.

tion in Table 7.3, from the posterior default mode network to the fronto-parietal right, shows a change in optimal hypotheses between weeks 2 and 3, with a strong evidence in favor of \mathcal{H}_1 in week 3 for the subgroup with the longer listening duration. Therefore, the change in optimal hypotheses of this connection between weeks 2 and 3 in the full group of 16 subjects is also predominantly caused by the subjects with the longer listening duration. Similar to the result for the full group of 16 subjects, the change of this connection in optimal hypotheses between weeks 2 and 3 does not last into week 4, and thus the effect is of short duration. A visualization of the networks involved in these connections can be found in Figure 7.7.

Finally, no results are found for the significance of Granger-values for both groups. All comparisons between weeks for both long and short listeners do not show significant changes in the effective connectivity of the selected connections in Figure 7.6.

7.6 DISCUSSION

In this study, we illustrate, using simulation data, that the Bayesian approach outperforms the Granger-causality analysis, especially when not much data is available. The Bayesian method is extended to enable it to test hypotheses on the existence of a connection for each week separately. The optimal hypotheses of different weeks are combined to draw conclusions on the changes in the effective connectivity over the weeks in the Mozart study. Then we apply the extended Bayesian method and the Granger-causality analysis to the Mozart effect data and find a number of connections with changes in effective connectivity after the subject listened to Mozart music. Finally, we split the subjects into two subgroups based on the listening duration and find that for two connections, a change in effective connectivity can be detected in the subgroup with the longer listening duration.

7.6.1 SIMULATIONS

The Bayesian approach is compared with the Granger-causality analysis for the inference of brain network connectivity. The methods are compared through their performance in estimating a graph of the effective connectivity using simulated data with a known ground truth connectivity. The performance evaluations in Figure 7.5 show that the Bayesian method performs better than the Granger-causality analysis for short data lengths. As the data length increases, the performance of the Granger-causality analysis matches that of the Bayesian method more closely. Thus, for the study of the Mozart effect, where the data is limited due to the slow sampling rate, it seems that the Bayesian method has a distinct advantage in the inference of brain network connectivity over the Granger-causality analysis.

7.6.2 MOZART EFFECT STUDY

In the study of the Mozart effect, we apply both the Bayesian method and the Granger-causality analysis to the ICA time series of the subjects. Here, we focus on the Bayesian method as it performs better than the Granger-causality analysis in simulation. First, using the Bayesian hypothesis test, changes in the effective connectivity of multiple connections are observed after subjects listened to Mozart music intensively. For the full group of 16 subjects, we find a change in the connection from the central executive network to the dorsal attention network, which is of short duration. The central executive network is involved in maintaining and manipulating working memory, and performing goal-oriented decision making [101]. Therefore, this change in effective connectivity could be an indication of a change in cognition.

Then the connection from the posterior default mode network to the fronto-parietal right network also shows an increase in effective connectivity after listening to music as reported by the Bayesian method, although the evidence is only weak. When we split the subjects into subgroups based on the listening duration, it becomes apparent that the effect predominantly occurs in subjects with a longer listening duration and is also of short duration. The default mode network is involved in emotional processing, self-referential mental activity, and the posterior default mode network involves the recollection of past experiences [119]. The fronto-parietal right network is involved in cognitive control [93]. This change in effective connectivity between the two networks involved in cognitive processing is an interesting result as it could indicate the existence of the Mozart effect.

Finally, for the whole group of 16 subjects, the connection from the anterior default mode network to the dorsal attention network is detected to have a significant change between weeks 2 and 3 by the Granger-causality analysis. For the Bayesian method, a change of this connection is detected for the subgroup of subjects with a longer listening duration. However, the two methods disagree on whether the effect is of short duration, and thus we cannot draw any strong conclusion on the duration of this change. We have mentioned the functionality of the

default mode network already above. Furthermore, the dorsal attention network is involved in the orientation of attention to external stimuli [164]. Thus the brain networks involved in this connection are related to cognitive processing. The change of this connection caused by Mozart music, detected by both methods, could indicate the evidence of the Mozart effect.

7.6.3 LIMITATIONS AND FUTURE WORK

Firstly, compared to the Granger value, which is a measurement of connectivity strength and for which statistical tests exist to infer a difference in this value, the extended Bayesian method can only test binary hypotheses. In the future development of the Bayesian method, one of our goals is to extend the Bayesian method to provide a quantitative measure of the connectivity strength. This could help us draw conclusions on effective connectivity changes in the connection from the sensori-motor lateral network to the superior temporal gyrus. Even if for this connection, the optimal hypotheses are \mathcal{H}_1 in both weeks 2 and 3, a very large increase in BF is observed from week 2 to week 3. However, with the current binary hypotheses on effective connectivity, we cannot confirm if this indicates a change in effective connectivity.

Secondly, the listening duration of the subjects appears to be insufficient to cause changes in the effective connectivity of all the subjects. The listening duration in another related study is at least 2 hours per day for 15 days [43]. In [26], patients were exposed to Mozart music for a year. Therefore, in future work, we would like to increase the minimum listening duration of subjects, to verify whether the Mozart effects is more universal across subjects.

Finally, we consider this study to be exploratory, and potential future work can consider an increased number of subjects, now that the insight of this work has been obtained.

7.7 CONCLUSIONS

This is an exploratory study of the Mozart effect by inferring changes in brain effective connectivity using ICA time series from fMRI data. As far as we are aware, this study is the first of its kind in measuring effective connectivity changes caused by Mozart's Sonata K448. Furthermore, it is the first time that the Bayesian topology identification algorithm is applied to fMRI data. We have found changes in cognitive processing in subjects, some of which are predominantly in the subjects with a longer listening duration. More effects are hinted at by the Bayesian selection frequencies in Figure 7.6, but can not ultimately be detected through the Bayesian hypothesis test. We are hopeful that in future studies, with increased listening duration and more subjects, more changes in the effective connectivity caused by Mozart music will be found.

7.8 APPENDIX

7.8.1 SIMPLIFICATION OF LIKELIHOOD MARGINALIZATION

First of all, based on the definition of our model in (7.3) and $p(D|\mathcal{G})$ in (7.7), the marginalization in (7.10) can be decomposed into L separate marginalizations. Then we only need to marginalize over \mathcal{G}_j , i.e. the subgraph which contains connection (i, j) :

$$p(D^k|(i, j)) \propto \sum_{\mathcal{G}_j \in \mathcal{P}_{j,1}} p(\mathcal{G}_j) p(D^k|\mathcal{G}_j), \quad (7.13)$$

where $\mathcal{P}_{j,1} = \{\mathcal{G}_j | (i, j) \in \mathcal{G}_j\}$. Note that $p(D^k|(i, j))$ is only proportional to the marginalization, which will still result in the correct log-likelihood ratio since we use the proportional marginals from (7.13) to calculate BF in (7.12).

山重水复疑无路，柳暗花明又一村。

陆游（宋）

*After endless mountains and rivers that leave doubt whether there is a
path out, amid the shade of willows and bright flowers a village appears.*

You Lu (Song dynasty)

8

Conclusions and future work

8.1 CONCLUSIONS

This thesis has focused on the topological aspects of identifiability and identification in linear dynamic networks. In particular, the topological analysis and synthesis for network identifiability have been addressed. Moreover, the problem of topology identification has been considered.

Since there are situations where different network models can generate the same data, the concept of network identifiability was introduced in the literature as an ability to distinguish different network models given the same data set. We have mainly focused on a particular version of network identifiability, i.e. the so-called generic identifiability, since given the topological information of the dynamic network, the concept of generic identifiability allows for the attractive graphical analysis of identifiability.

Graphical conditions on the topology of dynamic networks have been developed in Chapter 3 to verify generic identifiability, in the special setting where all the node signals are measured. It has been found that the generic identifiability of network modules depends on the interconnection structure of subsystems in the network, the correlation and the location of noise signals, and the location of measured excitation signals. Path-based conditions have been developed to verify generic identifiability, and these conditions are less conservative than the existing ones since they incorporate the presence of noises and possibly prior known components in the network. While

the path-based conditions are sufficient for the generic identifiability of modules in parametric model sets, it has been found that these conditions become also necessary when non-parametric, i.e. infinite-dimensional, model sets are considered instead.

With the above path-based conditions, the synthesis problem, i.e. the question where to allocate actuators and sensors to achieve the identifiability of network modules as formulated in subquestion 2 of Chapter 1, has been considered in Chapter 4 for the situation where all the node signals are measured. The goal is to develop synthesis approaches for excitation signal allocation such that the generic identifiability of a subnetwork or a full network can be achieved. To this end, it has been found that the path-based conditions can be reformulated into disconnecting-set-based conditions and pseudotree-based conditions, which explicitly state which internal signals should be excited for generic identifiability. With these new graphical conditions, novel synthesis procedures have been developed, where excitation signals are allocated according to the computed disconnecting sets for the generic identifiability of a subnetwork or according to the computed pseudotrees for the generic identifiability of a full network.

The above results for identifiability have also been generalized to a more flexible setting with partial measurement and partial excitation in Chapter 5. Novel graphical conditions have been developed in this chapter, which shows that disconnecting sets provide important information regarding the question which signals should be measured or excited for generic identifiability. These conditions also lead to new synthesis approaches, which can allocate sensors and actuators to achieve identifiability, and novel indirect identification methods, which can estimate network modules consistently.

The analysis and synthesis questions for network identifiability require the interconnection structure of subsystems in dynamic networks. The problem of identifying this topological information from data has been investigated in Chapter 6. It has been found that the topology identification problem can be formulated into a model selection problem. In order to take advantage of the available prior knowledge about the stability of network modules, the Bayesian model selection approach has been employed to select the (local) optimal topology. Furthermore, the EM algorithm provides an efficient way to estimate the hyperparameters, such that the final topology identification algorithm does not require any tuning effort from the user. The developed method shows a promising performance, especially when the number of data is limited compared to the network size.

While the Bayesian approach is developed to infer a topology estimate from a single data set, it has been further extended in Chapter 7 to consider multiple data sets from groups of subjects. With the above extension, the inference of the effective connectivity in brain networks has been investigated, which has revealed new insights into the changes in brain networks caused by intensively listening to Mozart's music, a topic that is of interest in the neuroscience community.

8.2 FUTURE WORK

8.2.1 SYNTHESIS FOR IDENTIFIABILITY

The developed synthesis approaches in Chapter 5 concern the allocation of actuators and sensors such that modules in a network become generically identifiable. However, the approaches do not take advantage of the initially present excitation signals and measured signals, and the r signals are directly allocated at the disconnecting sets, while it is possible to allocate the r signals elsewhere such that they have vertex disjoint paths to the disconnecting sets. The above limitations can be addressed to obtain more advanced synthesis approaches.

In addition, in the situation of partial measurement and partial excitation, the focus of Chapter 5 has been put on local modules in a network. While the pseudotree covering in Chapter 4 provides effective means to achieve full network identifiability when all the node signals are measured, the extension of this approach to the setting with partial measurement and excitation is still an open problem. Preliminary efforts have been made in [37] to address the above extension for acyclic graphs.

Furthermore, the synthesis approaches for identifiability in this thesis concern only the allocation of actuators and sensors. An interesting research direction is to investigate synthesis approaches that modify the network topology, e.g., via adding/deleting edges or removing nodes. The last action is typically referred to as knockout experiments in the inference of biological networks [151].

8.2.2 FROM IDENTIFIABILITY TO IDENTIFICATION

In Section 5.8, it has been shown that identifiability results directly lead to generalized forms of indirect identification methods that can estimate modules consistently. However, these indirect methods rely on a strong presence of measured external excitation signals and thus require more “expensive” experiments. Therefore, it is attractive to investigate whether the identifiability results can also lead to direct identification methods, which typically impose less conservative conditions on the measured excitation signals than the indirect methods [152]. The first step towards this direction can be to investigate the connections between the identifiability results in this thesis and the existing direct methods in, e.g., [48, 122, 123].

8.2.3 ANALYSIS AND ERROR CONTROL IN TOPOLOGY IDENTIFICATION

The Bayesian search algorithm developed in Chapter 6 has shown a very good performance in the extensive simulation study. However, little is known regarding its theoretical properties, for example, the frequentist consistency. The consistency of Bayes factor and Bayesian model selection has been extensively studied in the Bayesian statistics literature [39, 106, 110] for static

models and data-independent priors. However, the analysis of the method in Chapter 6 requires additional extensions of the existing theoretical results such that dynamic systems and data-dependent priors can be addressed.

In addition, how to ensure an upper bound on the error of the topology estimate is still an open question. The topology estimation problem is essentially a multiple hypothesis testing problem, where we compare the following two hypotheses:

$$\mathcal{H}_0 : G_{ji}(q) = 0 \text{ versus } \mathcal{H}_1 : G_{ji}(q) \neq 0,$$

for all j and i . The typical error criterion considered for the above problem is the false discovery rate (FDR), which is the expected ratio of the false discoveries (positives) over all the discoveries [19]. The question how to bound the FDR in the topology identification problem, which is also referred to as a variable selection problem, has been studied in statistics [99], but typically for independent data. The FDR criterion and the corresponding error control procedure have not yet been considered in the system identification community, where the data is generated by dynamic systems and thus highly correlated.

References

- [1] A. Aalto, L. Viitasaari, P. Ilmonen, L. Mombaerts, and J. Gonçalves. Gene regulatory network inference from sparsely sampled noisy data. *Nat. Commun.*, 11(1):1–9, 2020.
- [2] M. J. Ablowitz, A. S. Fokas, and A. S. Fokas. *Complex variables: introduction and applications*. Cambridge University Press, 2003.
- [3] J. Adebayo, T. Southwick, V. Chetty, E. Yeung, Y. Yuan, J. Gonçalves, J. Grose, J. Prince, G.-B. Stan, and S. Warnick. Dynamical structure function identifiability conditions enabling signal structure reconstruction. In *Proc. 51st IEEE Conf. Decis Control (CDC)*, pages 4635–4641. IEEE, 2012.
- [4] H. Akaike. A new look at the statistical model identification. *IEEE Trans. Autom. Control*, 19(6):716–723, 1974.
- [5] M. Alam, J. Ferreira, and J. Fonseca. Introduction to intelligent transportation systems. In *Intelligent Transportation Systems*, pages 1–17. Springer, 2016.
- [6] D. Alberer, H. Hjalmarsson, and L. Del Re. System identification for automotive systems: Opportunities and challenges. *Identification for Automotive Systems*, pages 1–10, 2012.
- [7] B. D. O. Anderson, M. Deistler, E. Felsenstein, B. Funovits, L. Koelbl, and M. Zamani. Multivariate AR systems and mixed frequency data: G-identifiability and estimation. *Econometric Theory*, 32(4):793–826, 2016.
- [8] O. Ardakanian, V. W. S. Wong, R. Dobbe, S. H. Low, A. von Meier, C. J. Tomlin, and Ye Yuan. On identification of distribution grids. *IEEE Trans. Control. Netw.*, 6(3):950–960, 2019.
- [9] M. T. Asif, N. Mitrovic, J. Dauwels, and P. Jaillet. Matrix and tensor based methods for missing data estimation in large traffic networks. *IEEE Trans. Intell. Transp. Syst.*, 17(7):1816–1825, 2016.
- [10] L. Barnett, A. B. Barrett, and A. K. Seth. Granger causality and transfer entropy are equivalent for Gaussian variables. *Phys. Rev. Lett.*, 103(23), 2009.
- [11] L. Barnett and A. K. Seth. The MVGC multivariate granger causality toolbox: A new approach to granger-causal inference. *J. Neurosci. Methods*, 223:50–68, 2014.
- [12] A. B. Barrett, M. Murphy, M. A. Bruno, Q. Noirhomme, M. Boly, and S. Laureys. Granger causality analysis of steady-state electroencephalographic signals during propofol-induced anaesthesia. *PLoS ONE*, 2012.

- [13] A. S. Bazanella, M. Gevers, and J. M. Hendrickx. Network identification with partial excitation and measurement. In *Proc. 58th IEEE Conf. Decis Control (CDC)*, pages 5500–5506. IEEE, 2019.
- [14] A. S. Bazanella, M. Gevers, J. M. Hendrickx, and A. Parraga. Identifiability of dynamical networks: which nodes need be measured? In *Proc. 56th IEEE Conf. Decis Control (CDC)*, pages 5870–5875. IEEE, 2017.
- [15] C. F. Beckmann, C. E. Mackay, N. Filippini, and S. M. Smith. Group comparison of resting-state fMRI data using multi-subject ICA and dual regression. *Neuroimage*, 47, 2009.
- [16] C. F. Beckmann and S. M. Smith. Probabilistic independent component analysis for functional magnetic resonance imaging. *IEEE transactions on medical imaging*, 23(2):137–152, 2004.
- [17] J. C. Beer, H. J. Aizenstein, S. J. Anderson, and R. T. Krafty. Incorporating prior information with fused sparse group lasso: Application to prediction of clinical measures from neuroimages. *Biometrics*, pages 1–11, 2019.
- [18] M. N. Belur and H. L. Trentelman. Stabilization, pole placement, and regular implementability. *IEEE Trans. Autom. Control*, 47(5):735–744, 2002.
- [19] Y. Benjamini and Y. Hochberg. Controlling the false discovery rate: a practical and powerful approach to multiple testing. *J. R. Stat. Soc. Ser. B Methodol.*, 57(1):289–300, 1995.
- [20] J. Berberich, J. Köhler, M. A. Müller, and F. Allgöwer. Data-driven model predictive control with stability and robustness guarantees. *IEEE Trans. Autom. Control*, 66(4):1702–1717, 2020.
- [21] A. Bernas, E. M. Barendse, A. P. Aldenkamp, W. H. Backes, P. A. M. Hofman, M. P. H. Hendriks, R. P. C. Kessels, F. M. J. Willems, P. H. N. de With, S. Zinger, and J. F. A. Jansen. Brain resting-state networks in adolescents with high-functioning autism: analysis of spatial connectivity and temporal neurodynamics. *Brain and Behaviour*, 8, 2018.
- [22] B. Bhattacharya and A. Sinha. Intelligent fault analysis in electrical power grids. In *2017 IEEE 29th International Conference on Tools with Artificial Intelligence (ICTAI)*, pages 985–990. IEEE, 2017.
- [23] C. M. Bishop. *Pattern recognition and machine learning*. Springer, 2009.
- [24] A. J. Blood, J. Zatorre, P. Bermudez, and A. C. Evans. Emotional responses to pleasant and unpleasant music correlate with activity in paralimbic brain regions. *Nat. Neurosci.*, 2:382–387, 1999.
- [25] S. Boccaletti, V. Latora, Y. Moreno, M. Chavez, and D. -U. Hwang. Complex networks: Structure and dynamics. *Phys. Rep.*, 424(4-5):175–308, 2006.
- [26] M. Bodner, R. P. Turner, J. Schwacke, C. Bowers, and C. Norment. Reduction of seizure occurrence from exposure to auditory stimulation in individuals with neurological handicaps: A randomized controlled trial. *PLoS One*, 7(10), 2012.

- [27] A. Bolstad, B. D. Van Veen, and R. Nowak. Causal network inference via group sparse regularization. *IEEE Trans. Signal Process.*, 59(6):2628–2641, 2011.
- [28] G. Bottegal, A. Y. Aravkin, H. Hjalmarsson, and G. Pillonetto. Robust EM kernel-based methods for linear system identification. *Automatica*, 67:114–126, 2016.
- [29] F. Bullo. *Lectures on network systems*. Kindle Direct Publishing, 2020.
- [30] R. B. Buxton, E. C. Wong, and L. R. Frank. Dynamics of blood flow and oxygenation changes during brain activation: The balloon model. *Magn. Reson. Med.*, 39(6):855–864, 1998.
- [31] F. P. Carli. On the maximum entropy property of the first-order stable spline kernel and its implications. In *Control Applications (CCA), 2014 IEEE Conference on*, pages 409–414. IEEE, 2014.
- [32] J. L. Chen, V. B. Penhune, and R. J. Zatorre. Listening to musical rhythms recruits motor regions of the brain. *Cerebral Cortex*, 18:2844–2854, 2008.
- [33] X. Cheng, Y. Kawano, and J. M. A. Scherpen. Reduction of second-order network systems with structure preservation. *IEEE Trans. Autom. Control*, 62(10):5026–5038, 2017.
- [34] X. Cheng, Y. Kawano, and J. M. A. Scherpen. Model reduction of multiagent systems using dissimilarity-based clustering. *IEEE Trans. Autom. Control*, 64(4):1663–1670, 2018.
- [35] X. Cheng and J. M. A. Scherpen. Model reduction methods for complex network systems. *Annu. Rev. Control Robot. Auton. Syst.*, 4(1), 2021.
- [36] X. Cheng, S. Shi, and P. M. J. Van den Hof. Allocation of excitation signals for generic identifiability of dynamic networks. In *Proc. 58th IEEE Conf. Decis Control (CDC)*, pages 5507–5512, 2019.
- [37] X. Cheng, S. Shi, and P. M. J. Van den Hof. Identifiability in dynamic acyclic networks with partial excitation and measurement. 2021. Accepted abstract in *20th European Control Conference (ECC)*.
- [38] X. Cheng, S. Shi, and P. M. J. Van den Hof. Allocation of excitation signals for generic identifiability of linear dynamic networks. *IEEE Trans. Autom. Control*, 67(2), 2022. To appear.
- [39] S. Chib and T. A. Kuffner. Bayes factor consistency. *arXiv preprint arXiv:1607.00292*, 2016.
- [40] D. M. Chickering. Optimal structure identification with greedy search. *J. Mach. Learn. Res.*, 3(Nov):507–554, 2002.
- [41] A. Chiuso and G. Pillonetto. A Bayesian approach to sparse dynamic network identification. *Automatica*, 48(8):1553–1565, 2012.
- [42] C. Commault. Structural controllability of networks with dynamical structured nodes. *IEEE Trans. Autom. Control*, 65(6):2736–2742, 2019.

- [43] G. Coppola, A. Toro, F. F. Operto, S. Pisano, A. Viggiano, and A. Verrotti. Mozart’s music in children with drug-refractory epileptic encephalopathies. *Epilepsy and Behavior*, 50:18–22, 2015.
- [44] D. Cvetković and P. Rowlinson. Spectra of unicyclic graphs. *Graphs and Combinatorics*, 3(1):7–23, 1987.
- [45] R. D’Andrea and G. E. Dullerud. Distributed control design for spatially interconnected systems. *IEEE Trans. Autom. Control*, 48(9):1478–1495, 2003.
- [46] A. G. Dankers. System identification in dynamic networks. *PhD dissertation*, 2014. Delft University of Technology.
- [47] A. G. Dankers, P. M. J. Van den Hof, X. Bombois, and P. S. C. Heuberger. Errors-in-variables identification in dynamic networks—consistency results for an instrumental variable approach. *Automatica*, 62:39–50, 2015.
- [48] A. G. Dankers, P. M. J. Van den Hof, X. Bombois, and P. S. C. Heuberger. Identification of dynamic models in complex networks with prediction error methods: Predictor input selection. *IEEE Trans. Autom. Control*, 61(4):937–952, 2016.
- [49] O. Demirci, M. C. Stevens, N. C. Andreasen, A. Michael, J. Liu, T. White, G. D. Pearson, V. P. Clark, and V. D. Calhoun. Investigation of relationships between fMRI brain networks in the spectral domain using ICA and Granger causality reveals distinct differences between schizophrenia patients and healthy controls. *Neuroimage*, 46(2):419–431, 2009.
- [50] M. Eichler. Graphical modelling of multivariate time series. *Probab. Theory Relat. Fields*, 153(1-2):233–268, 2012.
- [51] C. Englund, L. Chen, J. Ploeg, E. Semsar-Kazerooni, A. Voronov, H. H. Bengtsson, and J. Didoff. The grand cooperative driving challenge 2016: boosting the introduction of cooperative automated vehicles. *IEEE Wirel. Commun.*, 23(4):146–152, 2016.
- [52] N. Everitt, G. Bottegal, and H. Hjalmarsson. An empirical Bayes approach to identification of modules in dynamic networks. *Automatica*, 91:144–151, May 2018.
- [53] S. Fonken, M. Ferizbegovic, and H. Hjalmarsson. Consistent identification of dynamic networks subject to white noise using weighted null-space fitting. In *Proc. 21st IFAC World Congress*, 2020.
- [54] K. J. Friston, L. Harrison, and W. Penny. Dynamic causal modelling. *Neuroimage*, 19(4):1273–1302, 2003.
- [55] K. J. Friston, L. Harrison, and W. Penny. Dynamic causal modelling. *Neuroimage*, 19(4):1273–1302, 2003.
- [56] A. Gelman, J. Hwang, and A. Vehtari. Understanding predictive information criteria for bayesian models. *Stat. Comput*, 24(6):997–1016, 2014.
- [57] M. Gevers. A personal view of the development of system identification: A 30-year journey through an exciting field. *IEEE Control systems magazine*, 26(6):93–105, 2006.

- [58] M. Gevers and B. D. O. Anderson. Representations of jointly stationary stochastic feed-back processes. *Int. J. Control*, 33(5):777–809, 1981.
- [59] M. Gevers, A. S. Bazanella, and G. V. da Silva. A practical method for the consistent identification of a module in a dynamical network. *IFAC-PapersOnLine*, 51(15):862–867, 2018.
- [60] M. Gevers, A. S. Bazanella, and G. A. Pimentel. Identifiability of dynamical networks with singular noise spectra. *IEEE Trans. Autom. Control*, 64(6):2473–2479, 2019.
- [61] J. Geweke. Measures of conditional linear dependence and feedback between time series. *J. Am. Stat. Assoc.*, 79(388):907–915, 1984.
- [62] J. Gonçalves and S. Warnick. Necessary and sufficient conditions for dynamical structure reconstruction of LTI networks. *IEEE Trans. Autom. Control*, 53(7):1670–1674, August 2008.
- [63] C. W. J. Granger. Investigating causal relations by econometric models and cross-spectral methods. *Econometrica*, pages 424–438, 1969.
- [64] R. C. Gunning and H. Rossi. *Analytic functions of several complex variables*, volume 368. American Mathematical Society, 2009.
- [65] R. Gupta, A. Stincone, P. Antczak, S. Durant, R. Bicknell, A. Bikfalvi, and F. Falciani. A computational framework for gene regulatory network inference that combines multiple methods and datasets. *BMC systems biology*, 5(1):1–14, 2011.
- [66] A. Haber and M. Verhaegen. Subspace identification of large-scale interconnected systems. *IEEE Trans. Autom. Control*, 59(10):2754–2759, 2014.
- [67] D. Hayden, Y. H. Chang, J. Goncalves, and C. J. Tomlin. Sparse network identifiability via compressed sensing. *Automatica*, 68:9–17, 2016.
- [68] M. Hecker, S. Lambeck, S. Toepfer, E. Van Someren, and R. Guthke. Gene regulatory network inference: data integration in dynamic models—a review. *Biosystems*, 96(1):86–103, 2009.
- [69] J. M. Hendrickx, M. Gevers, and A. S. Bazanella. Identifiability of dynamical networks with partial node measurements. *IEEE Trans. Autom. Control*, 64(6):2240–2253, 2019.
- [70] Y. Hochberg and A. C. Tamhane. *Multiple comparison procedures*. Wiley, New York, 1987.
- [71] Z. S. Hou and Z. Wang. From model-based control to data-driven control: Survey, classification and perspective. *Information Sciences*, 235:3–35, 2013.
- [72] A. Hyvärinen, J. Karhunen, and E. Oja. *Independent Component Analysis*. Wiley, New York, 2001.
- [73] R. Jategaonkar, D. Fischenberg, and W. von Gruenhagen. Aerodynamic modeling and system identification from flight data-recent applications at DLR. *Journal of Aircraft*, 41(4):681–691, 2004.

- [74] A. Kaiser and T. Schreiber. Information transfer in continuous processes. *Physica D: Nonlinear Phenomena*, 166(1–2):43–62, 2002.
- [75] R. E. Kass and A. E. Raftery. Bayes factors. *J. Am. Stat. Assoc.*, 90(430):773–795, 1995.
- [76] E. M. M. Kivits and P. M. J. Van den Hof. A dynamic network approach to identification of physical systems. In *Proc. 58th IEEE Conf. Decis Control (CDC)*, pages 4533–4538. IEEE, 2019.
- [77] S. Koelsch, T. Fritz, K. Schulze, D. Alsop, and G. Schlaug. Adults and children processing music: An fMRI study. *Neuroimage*, 25(4):1068–1076, 2005.
- [78] D. Koller and N. Friedman. *Probabilistic graphical models: principles and techniques*. MIT Press, 2009.
- [79] B. D. Kroposki. Basic research needs for autonomous energy grids: Summary report of the workshop on autonomous energy grids: September 13-14, 2017. Technical report, National Renewable Energy Lab.(NREL), Golden, CO (United States), 2017.
- [80] P. Kundu, S. J. Inati, J. W. Evans, W. Luh, and P. A. Bandettini. Differentiating BOLD and non-BOLD signals in fMRI time series using multi-echo EPI. *Neuroimage*, 60:1759–1770, 2012.
- [81] P. Kuppinger, Y. C. Eldar, and H. Bölcskei. Block-sparse signals: Uncertainty relations and efficient recovery. *IEEE Trans. Signal Process*, 58(6), 2010.
- [82] S. L. Lauritzen. *Graphical models*, volume 17. Clarendon Press, 1996.
- [83] A. Legat and J. M. Hendrickx. Local network identifiability with partial excitation and measurement. In *Proc. 59th IEEE Conf. Decis Control (CDC)*, pages 4342–4347, 2020.
- [84] B. Li. Stochastic modeling for vehicle platoons (i): Dynamic grouping behavior and on-line platoon recognition. *Transportation Research Part B: Methodological*, 95:364–377, 2017.
- [85] Z. Li, Z. Duan, G. Chen, and L. Huang. Consensus of multiagent systems and synchronization of complex networks: a unified viewpoint. *IEEE Trans. Circuits Syst. I: Regul. Pap.*, 57(1):213–224, 2010.
- [86] F. L. Lian, J. Moyne, and D. Tilbury. Network design consideration for distributed control systems. *IEEE Trans. Control Syst. Technol.*, 10(2):297–307, 2002.
- [87] C. T. Lin. Structural controllability. *IEEE Trans. Autom. Control*, 19(3):201–208, 1974.
- [88] J. Linder and M. Enqvist. Identification and prediction in dynamic networks with unobservable nodes. *IFAC-PapersOnLine*, 50(1):10574–10579, 2017.
- [89] L. Ljung. Convergence analysis of parametric identification methods. *IEEE Trans. Autom. Control*, 23(5):770–783, 1978.
- [90] L. Ljung. *System Identification: Theory for the User*. Prentice-hall, 1999.
- [91] A. Londei, A. D’Ausilio, D. Basso, and M. O. Belardinelli. A new method for detecting causality in fMRI data of cognitive processing. *Cognitive Processes*, 7(1):42–52, 2006.

- [92] D. Marbach, J. C. Costello, R. Küffner, N. M. Vega, R. J. Prill, D. M. Camacho, K. R. Allison, M. Kellis, J. J. Collins, and G. Stolovitzky. Wisdom of crowds for robust gene network inference. *Nature methods*, 9(8):796–804, 2012.
- [93] S. Marek and N. U. F. Dosenbach. The frontoparietal network: function, electrophysiology, and importance of individual precision mapping. *Dialogues Clin. Neurosci.*, 20(2):133–140, 2018.
- [94] A. C. Marreiros, S. J. Kiebel, and K. J. Friston. Dynamic causal modelling for fMRI: a two-state model. *Neuroimage*, 39(1):269–278, 2008.
- [95] D. Materassi and G. Innocenti. Topological identification in networks of dynamical systems. *IEEE Trans. Autom. Control*, 55(8):1860–1871, 2010.
- [96] D. Materassi and M. V. Salapaka. On the problem of reconstructing an unknown topology via locality properties of the wiener filter. *IEEE Trans. Autom. Control*, 57(7):1765–1777, 2012.
- [97] D. Materassi and M. V. Salapaka. Identification of network components in presence of unobserved nodes. In *Proc. 54th IEEE Conf. Decis Control (CDC)*, pages 1563–1568, 2015.
- [98] D. Materassi and M. V. Salapaka. Signal selection for estimation and identification in networks of dynamic systems: A graphical model approach. *IEEE Trans. Autom. Control*, 65(10):4138–4153, 2020.
- [99] N. Meinshausen and P. Bühlmann. Stability selection. *J. R. Stat. Soc. Ser. B Methodol.*, 72(4):417–473, 2010.
- [100] M. Mesbahi and M. Egerstedt. *Graph Theoretic Methods in Multiagent Networks*. Princeton University Press, 2010.
- [101] E. K. Miller and J. D. Cohen. An integrative theory of prefrontal cortex function. *Annual Review of Neuroscience*, 24:167–202, 2001.
- [102] B. Mityagin. The zero set of a real analytic function. *arXiv preprint arXiv:1512.07276*, 2015.
- [103] F. Morelli, X. Bombois, H. Hjalmarsson, L. Bako, and K. Colin. Optimal experiment design for the identification of one module in the interconnection of locally controlled systems. In *2019 18th European Control Conference (ECC)*, pages 363–368. IEEE, 2019.
- [104] K. P. Murphy and S. Russell. Dynamic Bayesian networks: representation, inference and learning. 2002.
- [105] S. Nabavi and A. Chakraborty. A graph-theoretic condition for global identifiability of weighted consensus networks. *IEEE Trans. Autom. Control*, 61(2):497–502, 2015.
- [106] N. N. Narisetty. Bayesian model selection for high-dimensional data. *Principles and Methods for Data Science*, 43:207, 2020.
- [107] G. J. L. Naus, R. P. A. Vugts, J. Ploeg, M. J. G. van de Molengraft, and M. Steinbuch. String-stable CACC design and experimental validation: A frequency-domain approach. *IEEE Trans. Veh. Technol.*, 59(9):4268–4279, 2010.

- [108] J. Nikiel. *Topologies on Pseudo-trees and Applications*, volume 416. American Mathematical Society, 1989.
- [109] S. Ogawa, T.M. Lee, A. R. Kay, and D. W. Tank. Brain magnetic resonance imaging with contrast dependent on blood oxygenation. *Proceedings of the National Academy of Sciences*, 87(24):9868–9872, 1990.
- [110] A. O’Hagan and J. J. Forster. *Kendall’s advanced theory of statistics, volume 2B: Bayesian inference*, volume 2. Arnold, 2004.
- [111] T. Oomen, R. van Herpen, S. Quist, M. van de Wal, O. Bosgra, and M. Steinbuch. Connecting system identification and robust control for next-generation motion control of a wafer stage. *IEEE Trans. Control Syst. Technol.*, 22(1):102–118, 2013.
- [112] W. Ott and J. Yorke. Prevalence. *Bull. Am. Math. Soc.*, 42(3):263–290, 2005.
- [113] J. Pearl. *Causality*. Cambridge University Press, 2009.
- [114] J. Peters, D. Janzing, and B. Schölkopf. Causal inference on time series using restricted structural equation models. *Advances in Neural Information Processing Systems*, 26:154–162, 2013.
- [115] J. Pietschnig, M. Voracek, and A. K. Formann. Mozart effect-shmozart effect: A meta-analysis. *Intelligence*, 38(3), 2010.
- [116] G. Pillonetto and G. De Nicolao. A new kernel-based approach for linear system identification. *Automatica*, 46(1):81–93, 2010.
- [117] G. Pillonetto, F. Dinuzzo, T. Chen, G. De Nicolao, and L. Ljung. Kernel methods in system identification, machine learning and function estimation: A survey. *Automatica*, 50(3):657–682, 2014.
- [118] K. P. Pruessmann, M. Weiger, M. B. Scheidegger, and P. Boesiger. SENSE: sensitivity encoding for fast MRI. *Magn. Reson. Med.*, 42(5):952–962, 1999.
- [119] M. E. Raichle. The brain’s default mode network. *Annual Review of Neuroscience*, 38:433–447, 2015.
- [120] K. R. Ramaswamy, G. Bottegal, and P. M. J. Van den Hof. Local module identification in dynamic networks using regularized kernel-based methods. In *Proc. 57th IEEE Conf. Decis Control (CDC)*, pages 4713–4718. IEEE, 2018.
- [121] K. R. Ramaswamy, G. Bottegal, and P. M. J. Van den Hof. Learning linear modules in a dynamic network using regularized kernel-based methods. *Automatica*, 129:109591, 2021.
- [122] K. R. Ramaswamy and P. M. J. Van den Hof. A local direct method for module identification in dynamic networks with correlated noise. *IEEE Trans. Autom. Control*, 66(11), November 2021.
- [123] K. R. Ramaswamy, P. M. J. Van den Hof, and A. G. Dankers. Generalized sensing and actuation schemes for local module identification in dynamic networks. In *Proc. 58th IEEE Conf. Decis Control (CDC)*, pages 5519–5524, 2019.

- [124] F. H. Rauscher, G. L. Shaw, and C. N. Ky. Music and spatial task performance. *Nature*, 365(611), 1993.
- [125] M. F. Regner, N. Saenz, K. Maharajh, D. J. Yamamoto, B. Mohl, K. Wylie, J. Tregellas, and J. Tanabe. Top-down network effective connectivity in abstinent substance dependent individuals. *PLoS One*, 11(10), 2016.
- [126] W. Ren, R. W. Beard, and E. M. Atkins. A survey of consensus problems in multi-agent coordination. In *Proc. the 2005 American Control Conference (ACC)*, pages 1859–1864. IEEE, 2005.
- [127] A. Roebroeck, E. Formisano, and R. Goebel. Mapping directed influence over the brain using granger causality and fMRI. *Neuroimage*, 25(1):230–242, 2005.
- [128] D. Romeres, F. Dörfler, and F. Bullo. Novel results on slow coherency in consensus and power networks. In *Proc. 2013 European Control Conference*, pages 742–747. IEEE, 2013.
- [129] M. J. Rosa, L. Portugal, T. Hahn, A. J. Fallgatter, M. I. Garrido, J. Shawe-Taylor, and J. Mourao-Miranda. Sparse network-based models for patient classification using fMRI. *Neuroimage*, 105:493–506, 2015.
- [130] B. Rynne and M. A. Youngson. *Linear functional analysis*. Springer Science & Business Media, 2013.
- [131] C. Scherer. Theory of robust control. *Delft University of Technology*, pages 1–160, 2001.
- [132] T. B. Schön, A. Wills, and B. Ninness. System identification of nonlinear state-space models. *Automatica*, 47(1):39–49, 2011.
- [133] M Schoukens and P. M. J. Van den Hof. Detecting nonlinear modules in a dynamic network: A step-by-step procedure. *IFAC-PapersOnLine*, 51(15):593–597, 2018.
- [134] T. Schreiber. Measuring information transfer. *Phys. Rev. Lett.*, 85(2), 2000.
- [135] A. Schrijver. Disjoint paths. In *Combinatorial optimization: polyhedra and efficiency*, pages 131–132. Springer Science & Business Media, 2003.
- [136] A. K. Seth, P. Chorley, and C. Barnett. Granger causality analysis of fMRI BOLD signals is invariant to hemodynamic convolution but not downsampling. *Neuroimage*, 65:540–555, 2012.
- [137] S. Shahrampour and V. M. Preciado. Topology identification of directed dynamical networks via power spectral analysis. *IEEE Trans. Autom. Control*, 60(8):2260–2265, 2015.
- [138] S. Shi, G. Bottegal, and P. M. J. Van den Hof. Bayesian topology identification of linear dynamic networks. In *2019 18th European Control Conference (ECC)*, pages 2814–2819, 2019.
- [139] S. Shi, X. Cheng, and P. M. J. Van den Hof. Excitation allocation for generic identifiability of a single module in dynamic networks: A graphic approach. In *Proc. 21st IFAC World Congress*, 2020.

- [140] S. Shi, X. Cheng, and P. M. J. Van den Hof. Generic identifiability of subnetworks in a linear dynamic network: the full measurement case. *arXiv preprint arXiv:2008.01495*, 2020.
- [141] S. Shi, X. Cheng, and P. M. J. Van den Hof. On the genericity concept in identifiability of linear dynamic networks. Technical report, Eindhoven University of Technology, 2020.
- [142] S. Shi, X. Cheng, and P. M. J. Van den Hof. Single module identifiability in linear dynamic networks with partial excitation and measurement. *arXiv preprint arXiv:2012.11414*, 2020.
- [143] S. Shi, X. Cheng, and P. M. J. Van den Hof. Exploiting unmeasured disturbance signals in identifiability of linear dynamic networks with partial measurement and partial excitation. 2021. Accepted abstract in *17th IFAC Symposium on System Identification*.
- [144] T. A. B. Snijders. The statistical evaluation of social network dynamics. *Sociological methodology*, 31(1):361–395, 2001.
- [145] T. Steffen. *Control reconfiguration of dynamical systems: linear approaches and structural tests*, volume 320. Springer Science & Business Media, 2005.
- [146] S. Sun, C. Zhang, and G. Yu. A bayesian network approach to traffic flow forecasting. *IEEE Trans. Intell. Transp. Syst.*, 7(1):124–132, 2006.
- [147] S. Talukdar, D. Deka, H. Doddi, D. Materassi, M. Chertkov, and M. V. Salapaka. Physics informed topology learning in networks of linear dynamical systems. *Automatica*, 112:108705, 2020.
- [148] K. Tchoń. On generic properties of linear systems: An overview. *Kybernetika*, 19(6):467–474, 1983.
- [149] R. S. Tsay. *Multivariate time series analysis: with R and financial applications*. John Wiley & Sons, 2013.
- [150] A. Tsiamis and G. J. Pappas. Finite sample analysis of stochastic system identification. In *Proc. 58th IEEE Conf. Decis Control (CDC)*, pages 3648–3654. IEEE, 2019.
- [151] S. M. M. Ud-Dean and R. Gunawan. Optimal design of gene knockout experiments for gene regulatory network inference. *Bioinformatics*, 32(6):875–883, 2016.
- [152] P. M. J. Van den Hof, A. G. Dankers, P. S. C. Heuberger, and X. Bombois. Identification of dynamic models in complex networks with prediction error methods basic methods for consistent module estimates. *Automatica*, 49(10):2994–3006, 2013.
- [153] A. J. van der Schaft and B. M. Maschke. Port-Hamiltonian systems on graphs. *SIAM Journal on Control and Optimization*, 51(2):906–937, 2013.
- [154] J. W. van der Woude. A graph-theoretic characterization for the rank of the transfer matrix of a structured system. *Math. Control Signals Syst.*, 4(1):33–40, 1991.
- [155] R. J. C. van Esch. Code and simulation data for: A Bayesian method for inference of effective connectivity in brain networks for detecting the Mozart effect. <https://data.mendeley.com/datasets/n9yh7t4bxv/1>, 2020.

- [156] R. J.C. van Esch, S. Shi, A. Bernas, S. Zinger, A. P. Aldenkamp, and P. M. J. Van den Hof. A Bayesian method for inference of effective connectivity in brain networks for detecting the Mozart effect. *Comput. Biol. Med.*, page 104055, 2020.
- [157] H. J. van Waarde, P. Tesi, and M. K. Camlibel. Necessary and sufficient topological conditions for identifiability of dynamical networks. *IEEE Trans. Autom. Control*, 65(11):4525–4537, 2019.
- [158] H. J. van Waarde, P. Tesi, and M. K. Camlibel. Topology reconstruction of dynamical networks via constrained Lyapunov equations. *IEEE Trans. Autom. Control*, 64(10):4300–4306, 2019.
- [159] H. J. van Waarde, P. Tesi, and M. K. Camlibel. Topology identification of heterogeneous networks: Identifiability and reconstruction. *Automatica*, 123:109331, 2021.
- [160] A. Venkitaraman, H. Hjalmarsson, and B. Wahlberg. Learning sparse linear dynamic networks in a hyper-parameter free setting. *arXiv preprint arXiv:1911.11553*, 2019.
- [161] W. Verrusio, E. Ettorre, E. Vicenzini, N. Vanacore, M. Cacciafesta, and O. Mecarelli. The mozart effect: a quantitative EEG study. *Consciousness and Cognition*, 35:150–155, 2015.
- [162] R. Vershynin. *High-dimensional probability: An introduction with applications in data science*, volume 47. Cambridge University Press, 2018.
- [163] R. Vicente, M. Wibral, M. Lindner, and G. Pipa. Transfer entropy—a model-free measure of effective connectivity for the neurosciences. *Journal of Computational Neuroscience*, 30(1):45–67, 2011.
- [164] S. Vossel, J. J. Geng, and G. R. Fink. Dorsal and ventral attention systems. *Neuroscientist*, 20(2):150–159, 2014.
- [165] Y. Wang, M. Sznaiar, and O. Camps. A super-atomic norm minimization approach to identifying sparse dynamical graphical models. In *American Control Conference (ACC)*, pages 1962–1967. IEEE, 2016.
- [166] L. Wasserman. Bayesian model selection and model averaging. *J. Math. Psychol.*, 44(1):92–107, 2000.
- [167] H. H. M. Weerts, A. G. Dankers, and P. M. J. Van den Hof. Identifiability in dynamic network identification. *IFAC-PapersOnLine*, 48-28:1409–1414, 2015. Proc. 17th IFAC Symposium on System Identification, Beijing, China.
- [168] H. H. M. Weerts, J. Linder, M. Enqvist, and P. M. J. Van den Hof. Abstractions of linear dynamic networks for input selection in local module identification. *Automatica*, 117:108975, July 2020.
- [169] H. H. M. Weerts, P. M. J. Van den Hof, and A. G. Dankers. Identifiability of linear dynamic networks. *Automatica*, 89:247–258, 2018.
- [170] H. H. M. Weerts, P. M. J. Van den Hof, and A. G. Dankers. Prediction error identification of linear dynamic networks with rank-reduced noise. *Automatica*, 98:256–268, 2018.

- [171] H. H. M. Weerts, P. M. J. Van den Hof, and A. G. Dankers. Single module identifiability in linear dynamic networks. In *Proc. 57th IEEE Conf. Decis Control (CDC)*, pages 4725–4730. IEEE, 2018.
- [172] A. V. Werhli and D. Husmeier. Reconstructing gene regulatory networks with bayesian networks by combining expression data with multiple sources of prior knowledge. *Stat. Appl. Genet. Mol. Biol.*, 6(1), 2007.
- [173] J. C. Whitehead and J. L. Armony. Singing in the brain: Neural representation of music and voice as revealed by fMRI. *Human Brain Mapping*, 39(12), 2018.
- [174] J. C. Willems. The behavioral approach to open and interconnected systems. *IEEE control systems magazine*, 27(6):46–99, 2007.
- [175] M. Yang, H. He, M. Duan, X. Chen, X. Chang, Y. Lai, J. Li, T. Liu, C. Luo, and D. Yao. The effects of music intervention on functional connectivity strength of the brain in schizophrenia. *Neural Plasticity*, 2018, 2018.
- [176] M. Yazdani and A. Mehrizi-Sani. Distributed control techniques in microgrids. *IEEE Trans. Smart Grid*, 5(6):2901–2909, 2014.
- [177] C. Yu, J. Chen, and M. Verhaegen. Subspace identification of individual systems in a large-scale heterogeneous network. *Automatica*, 109:108517, 2019.
- [178] C. Yu and M. Verhaegen. Subspace identification of individual systems operating in a network (SI²ON). *IEEE Trans. Autom. Control*, 63(4):1120–1125, April 2018.
- [179] M. Yuan and Y. Lin. Model selection and estimation in regression with grouped variables. *J. Royal Stat. Soc.*, 68(1):49–67, 2006.
- [180] Z. Yue, J. Thunberg, W. Pan, L. Ljung, and J. Gonçalves. Linear dynamic network reconstruction from heterogeneous datasets. *IFAC-PapersOnLine*, 50(1):10586–10591, 2017.
- [181] D. D. Zhang, H. F. Lee, C. Wang, B. Li, Q. Pei, J. Zhang, and Y. An. The causality analysis of climate change and large-scale human crisis. *Proc. Natl. Acad. Sci.*, page 201104268, 2011.
- [182] N. Zhou, X. Cheng, Z. Sun, and Y. Xia. Fixed-time cooperative behavioral control for networked autonomous agents with second-order nonlinear dynamics. *IEEE Trans. Cybern.*, 2021.
- [183] N. Zhou, J. W. Pierre, and J. F. Hauer. Initial results in power system identification from injected probing signals using a subspace method. *IEEE Trans. Power Syst.*, 21(3):1296–1302, 2006.
- [184] Y. Zhu. *Multivariable system identification for process control*. Elsevier, 2001.
- [185] M. Zorzi and A. Chiuso. Sparse plus low rank network identification: a nonparametric approach. *Automatica*, 76:355–366, 2017.

List of Symbols

$G(q), G(z)$	A matrix of transfer operators and its corresponding transfer matrix.
$G(q)^*, G(z)^*$	$G^\top(q^{-1})$ and $G^\top(z^{-1})$.
$M, M(\theta)$	A dynamic network model and a parameterized network model with the parameter θ .
$P(x), p(x)$	Probability distribution and probability density function of a random vector x .
$\Phi_v(z)$	Power spectral density matrix of the discrete-time signal $v(t)$.
\mathcal{M}	A set of dynamic network models.
(w_i, w_j)	A directed edge from vertex w_i to vertex w_j .
D	A data set.
$E(x)$	The expected value of a random variable x .
$T_{\bar{\mathcal{W}}\bar{\mathcal{X}}}$	The mapping from the external signals in $\bar{\mathcal{X}} \subseteq \mathcal{X}$ to the internal signals in $\bar{\mathcal{W}} \subseteq \mathcal{W}$.
Π	A set of subgraphs of a directed graph.
$\Upsilon(\mathcal{T})$	The set of all the roots in a pseudotree \mathcal{T} .
$\Xi_v(\tau)$	Auto-covariance function of signal $v(t)$.
$\mathcal{B}(x, r)$	An open ball with center x and radius r .
\mathcal{C}	The set of all the measured internal signals.
\mathcal{D}	A disconnecting set in a directed graph.
\mathcal{E}	A set of directed edges in a directed graph.
\mathcal{G}	A directed graph.
\mathcal{H}	A hypothesis.
\mathcal{M}_Θ	A set of parameterized network models with the parameter space Θ .
\mathcal{N}_i^+	The set that contains the signals in \mathcal{W}_i^+ and additionally the internal signals, to which w_i has known direct edges <i>and</i> that are not directly excited by the vertices in \mathcal{X} , whose out-degree is one and the only out-going edge is known.

\mathcal{N}_j^-	The set that contains the signals in \mathcal{W}_j^- and additionally all the unmeasured internal signals that are in-neighbors of w_j .
\mathcal{R}	The set of all the measured excitation signals.
$\mathcal{S}_{in}(\mathcal{G})$	The set of all the sinks in graph \mathcal{G} .
$\mathcal{S}_{ou}(\mathcal{G})$	The set of all the sources in graph \mathcal{G} .
\mathcal{T}	A pseudotree.
\mathcal{V}	A set of vertices in a directed graph.
\mathcal{W}	The set of all the internal signals.
\mathcal{W}_i^+	The set of internal signals to which w_i has unknown directed edges.
\mathcal{W}_j^-	The set of the internal signals that have unknown directed edges to w_j .
\mathcal{X}	The set of all the external signals, including the measured excitation signals and the white noises.
\mathcal{X}_j	The set of external signals that do not have any unknown edge to w_j .
\mathcal{Z}	The set of all the unmeasured internal signals.
$\ \bullet\ _\infty$	H_∞ norm.
$b_{\mathcal{V}_1 \rightarrow \mathcal{V}_2}$	The maximum number of vertex disjoint paths from a vertex set \mathcal{V}_1 to a vertex set \mathcal{V}_2 in a directed graph.

List of Abbreviations

AEG	Autonomous energy grid.
AIC	Akaike information criterion.
AR	Autoregressive.
BF	Bayes factor.
BIC	Bayesian information criterion.
BOLD	Blood-oxygen-level-dependent.
BS	Bayesian search.
DBN	Dynamic Bayesian network.
DCM	Dynamic causal modeling.
EEG	Electroencephalography.
EM	Expectation-maximization.
FDR	False discovery rate.
fMRI	Functional magnetic resonance imaging.
FP	False positive.
FPR	False positive rate.
GLasso	Group least absolute shrinkage and selection operator.
ICA	Independent component analysis.
IIR	Infinite impulse response.
ITS	Intelligent transportation system.
LHS	Left-hand side.
MIMO	Multiple-input-multiple-output.
MISO	Multiple-input-single-output.
PEM	Prediction-error method.
PGM	Probabilistic graphical model.

RHS	Right-hand side.
ROC	Receiver operating characteristic.
SEM	Structural equation model.
SIMO	Single-input-multiple-output.
TP	True positive.
TPR	True positive rate.
VAR	Vector autoregressive.

Acknowledgments

This four-year Ph.D. project was an inspiring and fruitful journey for me, during which I had opportunities to learn new knowledge and train my skills for critical thinking. I appreciate particularly the open environment during my Ph.D. project, where there were always opportunities for discussions and debates. This openness could not be achieved without all the colleagues and friends I had inside and outside the research group.

I would like to thank my supervisor Prof. Paul Van den Hof for giving me the opportunity to start this 4-year journey and for introducing me to the interesting topics on system identification and dynamic networks. I learned a lot from my discussions with him about writing, problem formulation and general methodologies for conducting research. His feedback, typically written in red ink, provided important guidance during my research.

I want to express my gratitude to all the colleagues who contributed to the content of this thesis. Xiaodong helped me a lot in developing the graph-theoretical tools of this thesis and in providing feedback on the thesis writing. I always enjoyed the frequent discussions with him using the whiteboard. Giulio helped me build up my background in system identification, and my special thanks go to him for using his personal time for discussions and questions. In addition, I want to thank Rik, Antoine, Sveta and Bert for their efforts on the brain network project. Job and Dana also helped me develop some of the ideas in this thesis through my cooperation with them on their student projects.

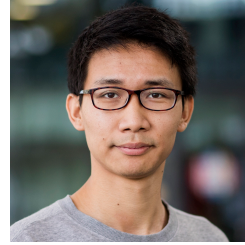
I am grateful to all my friends and colleagues in the Control Systems group for the good moments we had together. I want to thank my officemates Karthik, Lizan, Mannes, and Tom for the nice discussions and chats we had. It was a great pleasure to have interesting conversations and to attend conferences, workshops with Amritam, Constantijn, Carlos, Daming, Giuseppe, Harm, Jurre, Mircea, Maarten, Pepijn, Ruxandra, Ruben, Siep, Sofie, Tom Bloemers, Yanin, Yutao and many others. My special thanks go to Mircea and Will for my wonderful teaching assistance experience and to Diana and Hiltje for their help in many administration processes.

I would like to thank my friends Avinash, Changjie, Fei, Handian, Hongxu, Xuming, Yanming, Yang, Yi, Yizhou and Zhe for our time together since our master study. It is hard to imagine how my life abroad would look without their company.

Finally, I express my deepest gratitude to my family who has always been very supportive of my study and research. My father, Jun, encouraged me to pursue my study further since I was a kid, and my mother, Wei, could always cheer me up with her positive attitude towards life. My grandparents, Quanqi and Mincheng, always cared about my life abroad. My grandfather Xueming, who is a self-taught researcher and is still working intensively on writing books, has always been a role model for me. I also would like to thank my girlfriend Jiaen for her warm company and the technical discussions we had. I was lucky enough to meet her, with whom not only can I share my daily life but also discuss my work and research.

Curriculum Vitae

Shengling Shi was born in Sichuan, China, in 1992. He received the B.Sc. degree in Automotive Engineering from the Harbin Institute of Technology, China, in 2013. From 2014 to 2017, he followed the M.Sc. program in Automotive Technology at the Eindhoven University of Technology (TU/e), the Netherlands, and he graduated with distinction (great appreciation) in 2017. His M.Sc. thesis was titled “Decentralized and distributed model predictive control of vehicle platoons”. During his M.Sc. program, he did a 5-month research internship on the battery modeling for vehicle energy management at the Institute for Dynamic Systems and Control of ETH Zurich.



In 2017, he started his Ph.D. project in the Control Systems Group of TU/e. His Ph.D. project was on topological aspects in identifiability and identification of linear dynamic networks under the supervision of Prof. dr. ir. P. M. J. Van den Hof. During the period 2017 - 2020, he took graduate courses at the Dutch Institute of Systems and Control (DISC) and received the DISC certificate. He was a member of the research student council of DISC (Unit DISC) during the period 2018 - 2021.

Due to advances in current technology, many engineering systems are becoming increasingly complex and encompass numerous sub-systems that are spatially interconnected. Such systems are typically referred to as dynamic networks. Modeling dynamic networks is an important task for designing, analyzing, and controlling these systems. Due to the ability for data collection from dynamic networks, this thesis focuses on the data-driven modeling of dynamic networks by exploiting the network topology and graph-theoretical analysis. Network identifiability is first addressed in this thesis, which reflects the ability to distinguish different network models based on data and thus is a prerequisite for the data-driven modeling of dynamic networks. To verify network identifiability, graph-theoretical tools are developed to inspect the network topology and the locations of the excitation signals and the noises in the network. If a dynamic network is not identifiable, graphical synthesis approaches are also developed to allocate additional actuators and sensors such that network identifiability can be achieved, by exploiting the graphical concepts of disconnecting sets and pseudotrees. Furthermore, due to the importance of the topological information of dynamic networks, a novel Bayesian identification method is developed to estimate the network topology from data. This method is then applied to the inference of brain networks to investigate the effect of intensively listening to Mozart's music on brain connectivity, a topic that is of interest in neuroscience.

